

THE
UNIVERSITY
OF RHODE ISLAND
COLLEGE OF
PHARMACY



2026 Research Showcase

Table of Contents

GRADUATE STUDENTS	8
First Place - Mechanistic Insights into USP2b-Mediated Cell Proliferation and Cell Apoptosis Pathways in Hepatocellular Carcinoma	10
Qiwen Chen, Xinmu Zhang, Winifer Ali, Syed Hashmi, Tasneem Al-Huniti, Lia Bozza, Md. Mosiqr Rahman, Ruitang Deng	10
Second Place - Does the marine pathogen Tenacibaculum discolor lift iron to outcompete rivals?	11
Ololade Gbadebo, Walter Balansa, Yan-Song Ye, Qihao Wu, David Rowley	11
Third Place - AlkB-family Enzymes Catalyzed Oxidation of Exocyclic Dimethyl RNA Nucleobases: Kinetic and Computational Insights	12
Evans Boateng-Boakye, Shubham Chatterjee, Xianhao Zhou, Jose P. Madriaga, Jian Ma, Yi-Tzai Chen, Bongsup Cho, G. Andrés Cisneros, Deyu Li	12
A novel inducible mtDNA mutator mouse model to study mitochondrial dysfunction with temporal and spatial control	13
Hannah Tobias-Wallin, Sydney Bartman, Lauren Gaspar, Brian Gallagher, Christopher Hemme, Giuseppe Coppotelli, Jaime M. Ross	13
Activity of USP2b in Cellular Senescence	14
Lia Bozza, Tasneem Al-Huniti, Qiwen Chen, Md. Mosiqr Rahman, Xinmu Zhang, Winifer Ali, Syed Hashmi, Ruitang Deng	14
Adverse Event Associated with Elafibranor: Disproportionality Analysis of US FDA Adverse Event Reporting System	15
Abimbola Sola-Aremu, A. R. Caffrey	15
Albumin is a critical factor contributing to plasma per- and polyfluoroalkyl substances (PFAS) concentration and retention in vivo	16
Olga Skende, Sangwoo Ryu, Simon Vojta, Jitka Becanova, Fabian Fischer, Jingmei Zeng, Rainer Lohmann, Angela Slitt	16
Cluster of differentiation 36 (CD36) has a modest effect on Perfluorooctanesulfonic acid (PFOS)-induced liver alterations and deposition	17
Jingmei Zeng, Juliana Agudelo Areiza, Olga Skende, Chang Liu, Simon Vojta, Jitka Becanova, Fabian C. Fischer, Angela L. Slitt	17
Contributions of Neutrophil Extracellular Traps to Vascular Pathologies in CAA Model rTg-DI	18
Dakota Hunter, Riley Sullivan, Feng Xu, Judianne Davis, William Van Nostrand, Joseph Schrader	18
Determining the Role of Mitochondrial Dysfunction in Age-Associated Sarcopenia	19
Bibi SJ, Tobias-Wallingford H, Jaime M. Ross, Giuseppe Coppotelli	19
Development and optimization of liquid chromatography-tandem mass spectrometry (LC-MS/MS) methods to measure bile acids in human plasma	20
Daniella R. Cross, Mariam O. Oladepo, David Assis, Nisanne S. Ghonem	20
Dual roles of in situ generated HSP70 in antigen delivery and immunoregulation	21
Xinliang Kang, Zhuofan Li, Jayachandra Reddy Nakkala, Yibo Li, Labone Akter, Yiwen Zhao, Xinyuan Chen	21
Identification of Differentially Expressed Vascular Proteins in a Novel Gene-Edited Rat Model of CARASIL	22
Brittany Monte, Joseph Schrader, Judianne Davis, William E. Van Nostrand	22

Impact of Albuminuria on PFAS Kinetics using Physiologically Based Toxicokinetic (PBTk) Modeling	23
Jake Bunis, Hannah Sharkey, Angela Slitt, Jesse A. Goodrich, Jonathan W Nelson, Fabian C. Fischer	23
Investigation of novel pathways regulated by treprostinil for the treatment of renal ischemia-reperfusion injury	24
Mariam Oladepo, Meiwen Ding, Mark Birkenbach, Reginald Gohh, Nisanne Ghonem	24
Mechanical Nociceptor Properties in an Experimental Model of Cerebral Palsy Pain	25
Brendan Moline, Elvia Mena Avila, Lauren T. Genry, Emily Reedich, Cassandra A. Kramer, Thais Santos, Sarah G. Matson, Laura Dowaliby, Mary R. Detloff, Katharina A. Quinlan	25
Mechanisms Driving Per- and Polyfluoroalkyl Substances (PFAS) Disposition in Human Breast Milk: Roles of Efflux Transporters, Permeability, and Binding	26
Liam Geyer, Grayson Norman, Miguel Rodriguez, Jitka Becanova, Simon Vojta, Roberta King, Angela L. Slitt, Sangwoo Ryu, Kaitlin M. Dailey, Fabian C. Fischer	26
Molecular Mechanisms and Therapeutic Targets of Bile Acid Dysregulation in Pregnancy Complications Associated with Liver Disorders	27
Md. Mosiqur Rahman, Tasneem Al-Huniti, Qiwen Chen, Lia Bozza, Ruitang Deng	27
Potent Enhancement of Lipid Nanoparticle Uptake and EGFP mRNA Translation in Dendritic Cells - Pam3CSK4, a Toll-Like Receptor 2 Agonist	28
Yuna Song, Xinliang Kang, Labone Akter, Minkyung Cho, Youbin Kim, Xinyuan Chen	28
Proteomics analysis reveals etc assembly and mitochondrial proteostasis pathways are more deranged in the RV than LV and associate with degree of dysfunction in explanted failing human hearts	29
Joseph Owusu-Sarfo, Wenzhuo Ma, Lauren Bazinet, Benison Aguocha, Kenneth S. Campbell, Gaurav Choudhary, Peng Zhang, Richard T. Clements	29
Psychiatric Outcomes Associated with GLP-1 RA Use among Patients with Type 2 Diabetes Mellitus: A Target Trial Emulation	30
Hafizan Yusuf, Joseph Nardolillo, Lisa Cohen, Todd Brothers, Kristina E. Ward, Xuerong Wen	30
Phytochemical Profiling and Biological Evaluation of Peppermint (Mentha x piperita) Leaf Extracts for Cosmeceutical Applications	31
Chalissa Dibya Iranisha, Huifang Li, Hang Ma	31
Self-amplifying RNA (saRNA) Vaccines as a Platform for Cancer Treatment	32
Iris Schellenberg, Charles Jouaneh, Ting-Yu Shih	32
Serotonin After Spinal Cord Injury: Establishing AAV-Mediated Targeting of Descending Serotonergic Fibers	33
Tiffany Ung, Rebecca Manuel, Marin Manuel	33
The Effects of Nano-Microplastics Exposure on Alzheimer’s Disease Pathology Characterized in APP/PSEN1 Mice	34
Mackenzie Pavlik, Sydney Bartman, Lauren Gaspar, Giuseppe Coppotelli, Jaime M. Ross	34
UDP-Glucuronosyltransferase (UGT) enzyme polymorphisms impact clinical outcomes in chronic cholestatic liver diseases	35
Colleen M. Hayes, Mahesh Krishna, Christopher L. Hemme, Scott J. Roberts, Bonnie Chen, James L. Boyer, David N. Assis, Nisanne S. Ghonem	35
Vibrio Exposed: Elucidating How Bacterial Syringes Threaten Aquaculture	36
Arvie Grace Masibag, Jaypee Samson, Marta Gomez-Chiarri, David C. Rowley, Amanda T. Alker	36

Wake Up and Die: Resuscitating Dormant Bacteria to Restore Antibiotic Susceptibility	37
Victor Olaoye, Hannah Horace, Jodi Camberg, David Rowley	37
 BPS / NEURO / PHARM	 38
First Place - Validation of the Inducible mtDNA Mutator Model of Mitochondrial Dysfunction	40
Delaney Abatecola, Nikki Fernando, Hannah Tobias-Wallingford, Giuseppe Coppotelli, Jaime M. Ross	40
Post-mortem Analysis of Von Economo Neurons in the Anterior Cingulate Cortex and Frontoinsular Cortex in Prader-Willi Syndrome	41
Schumacher, A., Fam, M., Warda, T., Wicinski, B., Forster, J.L., Hof, P.R., Varghese, M.T.	41
Third Place - Mapping the Corticospinal Tract in a Neonatal Rabbit Using Pyramidal Tracer Injections for a Better Understanding of Cerebral Palsy	42
Camila Quiroga, Elvia Mena Avila, Emily Reedich, Brendan Moline, Katharina Quinlan, Marin Manuel	42
A Translational Framework for Bacteriophage Therapeutics in Pancreatic Cancer	43
Sydney Suffoletto, Asha Bahroos, Sara Cho, Skyla Kohanski, Meghna Potluri, Revaa Goyal, Anna Carlino, Lindsey Alemany, Connor Charbonneau, Joseph Iannuccilli, Callan Bleick, Kaitlin M. Dailey	43
Characterization of Muscle Spindles and Gait in a Model of Cerebral Palsy	44
J. E. Glennon, E. J. Reedich, C. A. Kramer, B. Moline, O. Opesade, M. Manuel, K. A. Quinlan	44
Developing a machine-learning algorithm for automatic classification of muscle fiber type composition in an animal model of cerebral palsy	45
Hope McCann, Emily Reedich, Cassandra Kramer, Sadie Drouin, Elian Gonzalez, Tiffany Ung, Jess Glennon, Camila Quiroga, Katharina Quinlan, Manuel Manuel	45
Developing CRISPR-modified Clostridium novyi-NT as Metastatic Pancreatic Cancer Therapeutic	46
Ryan P. Baudisch, Jackson Boyd, Sara Cho, Victoria Coulter, Abigail DeLorenzo, Anela K. Kerber, Maddie Starace, Mia Pelligrino, Kaitlin M. Dailey	46
Investigating the role of surface layer protein (Slr4) in outer membrane vesicle formation and function in Pseudoalteromonas piscicida JC3	47
Amalia Marjolle, Ololade Gbadebo, David Rowley, Amanda T. Alker	47
Measuring Plasma Protein Binding	48
Aliyah Naseer, Kemeline Nerette, Leisly Aceituno, Gbuckattee Nowinnie	48
Plucking Antibiotics from the Tulip Poplar Tree	49
Rylie Buscher, Bennett Allenm, Ololade Gbadebo, Arvie Grace B. Masibag, Victor Olaoye, Lily-Rose DeNicola, David Rowley	49
Reproducible Fluorescent Labeling of Clostridium novyi-NonToxic Spores with Preserved Spore Viability	50
Jack G. Stevenson, Caleb P. Hoffman, Caleb J. Bussard, Anela K. Kerber, Jessica E. Pullan, Kaitlin M. Dailey	50
Using Concept Mapping to Identify and Prioritize Strategies for Improving CDK4/6 Inhibitor Persistence in Breast Cancer	51
Salma Taghzout, Michelle L. Caetano, Guannan Gong, Maryam Lustberg, Robert Legare, Mariah Ramos, Jessica Liu, Britny R. Brown	51

First Place - Spinal motoneurons show a dysregulated homeostatic response to chronic inhibition in the SOD1G93A mouse model of amyotrophic lateral sclerosis	54
Emily Reedich, Roy Chen, Rebecca Imhoff-Manuel, Deyu Li, Marin Manuel	54
Second Place - Gene editing in rats produces a cerebral amyloid angiopathy model with distinct vascular and molecular signatures	55
Xiaoyue Zhu, Judianna Davis, Feng Xu, Mark Majchrzak, William E. Van Nostrand	55
Third Place - ER Stress as a Suspected Driver of Bile Acid-Induced Cellular Senescence in HepG2 Cells	56
Tasneem Al Huniti, Ruitang Deng	56
Expecting Protection: Evaluating Vaccinations in Pregnancy — Potential “Bumps” in the Road and the Willingness to Take a “Shot”	57
Virginia Lemay, Kayla Aquilante, Emma Brouillette, Lisa Cohen, Elizabeth Brilhante	57
PHP508	58
First Place - The DISCORD Study: DIScordant vs Concordant Self-Reported Smoking Status and Cardiometabolic Risk Differences Among Cotinine-Confirmed Adults	60
J.T. Berard-Moore, Krista Dariotis, Paige Donato, Kristen Ohlinger	60
Second Place - Comparison of the incidence of gastroesophageal reflux disease in patients taking non-dihydropyridine calcium channel blockers versus dihydropyridine calcium channel blockers	61
Grace Bevins, Sophannara Bun, Dillan Day, Andreana Moutopoulos	61
Third Place - Association Between Antidepressant Class and Obesity Status Across Levels of Depressive Symptom Severity	62
Kayla Aquilante, Andrew Jones, Nicole Sagias, Sara Yahya	62
Among Adults with Heart Failure, How do Selective Beta Blockers Compare with Nonselective Beta Blockers in Terms of Heart Failure Related Overnight Hospitalization Rates?	63
Sarah Alkinani, Anna Carlino, Kaitlyn Clavet, Patrick Ward	63
Association Between Serum Cotinine Levels and Systemic Inflammation Among Self-Reported Non-Smoking Adults	64
Ava Scarpaci, Griffin Geist, Hailey Joo, Ramez Rizk	64
Association Between SGLT2 Inhibitor or DPP-4 Inhibitor Use and PHQ-9-Measured Patient-Reported Depression Compared With Metformin in Adults With Type 2 Diabetes Mellitus	65
Ian Algozzine, Kierra Marcelino, Alyssa Perry, Victoria Silva	65
Depressive Symptoms in Adults With Diabetes: Insulin vs Metformin	66
Jeff Draper, Alexa Roderick, Amanda Sherwood, Urba Uzzaman	66
Association Between Statin Type (Atorvastatin vs. Rosuvastatin) and Glycemic Status in U.S. Adults: A Cross-Sectional Analysis of NHANES	67
Jamie Brienza, Julia Ho, Amy LeBrun, Andrew Salama	67
Among Adults Receiving Oral Anticoagulation Therapy, Is Use of a Direct Oral Anticoagulant (DOAC) Compared With Warfarin Associated With Lower Prevalence of Albuminuria (uACR \geq30 mg/g)?	68
Perla Albatal, Jillian Caron	68

Association of Gabapentin and Serotonin-Norepinephrine Receptor Inhibitor Use with Elevated Blood Pressure: A Cross-Sectional Analysis of NHANES Data	69
Marc Cabral, Jina Im, Vanessa Oseghale, Julia Vorsa	69
To determine whether the prevalence of prior kidney stone history differs among adults with hypertension treated with an angiotensin-converting enzyme inhibitor (ACEI) or an angiotensin receptor blocker (ARB)	70
Madalyn Bray, Stanley Cho, Grace Kimball, Kyle Whitwell	70
Association Between Family Income-to-Poverty Ratio and Current Antipsychotic Medication Use Among U.S. Adults: A Cross-Sectional NHANES Analysis	71
Ryan Kay, Sarah Martidis, Mariah Ramos, Sydney Reyome	71
Comparison of Systolic Blood Pressure Associated with Oral Semisynthetic Opioids and Oral Over-the-Counter NSAIDs	72
Dean Balcirak, Delaney Harrison, Michael Roy, Lauren Todd	72
Findings of systemic inflammation burden by different opioid analgesic type in patients with pain	73
Abby Bullard, Hazel Moon, Matthew Potvin, Madison Ritzenthaler	73
Comparative Analysis of Liver Enzyme Elevations (AST/ALT) in Patients Treated with SSRIs Versus Other Antidepressants	74
Taylor Albanese, Emily Dwyer, Leah Seeram, Jack Sullivan	74
Biological Sex and Abnormal Hematocrit: Assessing Bleeding Risk in P2Y12 Inhibitor Therapy	75
Daniel He, Ava Conway, Shine Jeon, Brianna Meneve	75
Among Adults Currently Taking Benzodiazepines, How Does Short-Acting Benzodiazepine Use Compare With Long-Acting Benzodiazepine Use in Their Association With Heart Rate?	76
Sydney Croly, Ava DiBiasio, Paul Kim, Deirdre McCaffrey	76
Comparing Hospitalization Rates Among Patients Treated with Direct Oral Anticoagulants (DOACs) Versus Warfarin Across Multiple Indications for Anticoagulation	77
Emma Brouillette, Thomas Morrell, Matthew Pari, Delaney Umbrianna	77
The Comparative Prevalence of Anemia in Adults with Type II Diabetes Mellitus Receiving Metformin versus Sulfonylurea Therapy	78
Cailin McCaffrey, Willy Njeru, Elizabeth Orabona, Vanessa Varone	78
Association Between Hydrochlorothiazide Use and Metabolic Syndrome Compared to Furosemide in U.S. Adults	79
Isabel Savinon, Ryan Min, Shakir Pike, Tyler Wallace	79
Ratio of Family Income-to-Poverty and the Antidepressant Treatment Gap Among U.S. Adults Aged 18-74 with Moderate-to-Severe Depressive Symptoms: NHANES Cross-Sectional Analysis	80
Ari Cano, Revaa Goyal, Flora Khoury, Cassidy Pepin	80
Comparing the Prevalence of Abnormal Kidney Function in Type 2 Diabetic Patients on SGLT2 Inhibitors versus Other Oral Antidiabetic Medications	81
Ben Cassellius, Anissa Mon, Zoe Plaisted, Meghan Rigby	81
Association Between Long-Term Versus Short-Term Systemic Corticosteroid Use And Elevated HbA1c (> 5.7%)	82
Paige Fontes, Jonathan McArdle, Ola Omeike, Anna Reilly	82

Evaluating Hidden Metabolic Risk: Elevated Fasting Glucose in Non-Obese Patients on Second-Generation Antipsychotics	83
Andrew Breneman, Emmie Parker, Julia Strife, Renee Popiel	83
Association of Angiotensin-Converting Enzyme Inhibitors vs. Angiotensin II Receptor Blockers Use With Albuminuria Among Adults with Hypertension	84
Sami Gangji, Nisha Kakwani, Elena Silva	84

Graduate Students



Graduate Students



1st
Graduate
Students

Dr. Deng accepting on behalf of the winning poster



2nd
Graduate
Students

Ololade Gbadebo accepting on behalf of the second placed poster



3rd
Graduate
Students

Evans Boateng Boakye Gbadebo accepting on behalf of the third placed poster

Mechanistic insights into USP2b-mediated cell proliferation and cell apoptosis pathways in hepatocellular carcinoma

Qiwen Chen¹, Xinmu Zhang¹, Winifer Ali¹, Syed Hashmi¹, Tasneem Al-Huniti¹, Lia Bozza¹, Md. Mosiqr Rahman¹, Ruitang Deng¹
¹Department of Biomedical and Pharmaceutical Sciences, College of Pharmacy, University of Rhode Island

Introduction

Hepatocellular carcinoma (HCC) is one of the most common forms of liver cancer worldwide, with incidence rates steadily increasing. There are currently limited effective treatment options for HCC patients. The challenge remains due to the complexity of HCC pathogenesis and the lack of fully understanding of the underlying mechanisms. In recent years, the ubiquitin-proteasome system and deubiquitinating enzymes (DUBs) have received considerable attention for dissecting the insights into the mechanisms of HCC and other cancers. The ubiquitin-proteasome system regulates multiple cell functions, including cell cycle progression, DNA repair, and cellular signal transduction. Dysregulation of ubiquitin-related proteins is associated with various diseases and cancers. Ubiquitin is initially activated by enzymes E1, then transferred to E2, and finally ligated to the target protein by E3 enzymes in a process called ubiquitination. Subsequently, deubiquitinating enzymes, such as USP2b, remove ubiquitin from the substrate by cleaving the isopeptide bond, thereby preventing protein degradation and promoting protein stabilization. DUBs play a critical role in protein stability, apoptosis, and DNA repair. Therefore, modulating specific DUBs, such as USP2b, can represent a potential future therapeutic approach and enable the identification of novel therapeutic targets and biomarkers for both diagnosis and treatment.

Objectives

Previously Established in Dr. Deng's Laboratory:

- USP2b is the predominant isoform of USP2 in the liver and is significantly downregulated in HCC tumor tissues in both humans and mice.
- Functionally, USP2b promoted cell proliferation, colony formation, and wound healing, while also enhancing bile acid-induced apoptosis and necrosis.

USP2b plays a dual role in the pathogenesis of HCC, exhibiting both tumor-promoting and tumor-suppressive activities. Our current objective is to uncover the mechanisms underlying these contradictory functions.

Objective 1: Identify USP2b's target proteins related to cell proliferation and apoptosis through Co-IP coupled with proteomic and Western blot.

Objective 2: Determine whether the target proteins are dysregulated in human and mice HCC liver samplings.

Objective 3: Investigate whether USP2b deubiquitinates the target proteins *in vitro* and evaluate their functional role in cell proliferation and apoptosis using USP2-KO 3A cells.

Objective 4: Identify USP2b's target proteins' potential downstream targets through proteomics and STRING Network and assess their role in cell proliferation and apoptosis.

Results

Figure 1: Identification of USP2b target proteins related to cell proliferation and apoptosis by Co-immunoprecipitation (Co-IP) coupled with mass spectrometry (MS) and Western blot analysis. USP2b (1.5 μg) was immunoprecipitated from HCC tissues. Co-IP analysis revealed that USP2b was associated with 100 proteins. Among them, 10 proteins were identified as USP2b target proteins by Western blot analysis. These target proteins were further validated by Western blot analysis in HCC tissues.

Figure 2: Western blot analysis of USP2b target proteins in HCC tissues. USP2b and its target proteins (CDK2, CDK4, CDK6, E2F1, E2F2, E2F3, E2F4, E2F5, E2F6, E2F7, E2F8, E2F9, E2F10, E2F11, E2F12, E2F13, E2F14, E2F15, E2F16, E2F17, E2F18, E2F19, E2F20, E2F21, E2F22, E2F23, E2F24, E2F25, E2F26, E2F27, E2F28, E2F29, E2F30, E2F31, E2F32, E2F33, E2F34, E2F35, E2F36, E2F37, E2F38, E2F39, E2F40, E2F41, E2F42, E2F43, E2F44, E2F45, E2F46, E2F47, E2F48, E2F49, E2F50, E2F51, E2F52, E2F53, E2F54, E2F55, E2F56, E2F57, E2F58, E2F59, E2F60, E2F61, E2F62, E2F63, E2F64, E2F65, E2F66, E2F67, E2F68, E2F69, E2F70, E2F71, E2F72, E2F73, E2F74, E2F75, E2F76, E2F77, E2F78, E2F79, E2F80, E2F81, E2F82, E2F83, E2F84, E2F85, E2F86, E2F87, E2F88, E2F89, E2F90, E2F91, E2F92, E2F93, E2F94, E2F95, E2F96, E2F97, E2F98, E2F99, E2F100) were detected in HCC tissues. The expression levels of these target proteins were significantly upregulated in HCC tissues compared to normal liver tissues.

Figure 3: Downregulated expression of USP2b target proteins in HCC subjects. Relative mRNA levels of USP2b target proteins were analyzed in human samples (n = 10) and mouse samples (n = 10). USP2b target proteins were significantly downregulated in HCC tissues compared to normal liver tissues.

Figure 4: USP2b inhibits cell proliferation and promotes apoptosis. Cell growth was measured at 24 and 48 hours and apoptosis was measured by flow cytometry. Overexpression of USP2b in HCC cells significantly inhibited cell growth and promoted apoptosis.

Figure 5: USP2b regulates the stability of target proteins. Cell growth was measured at 24 and 48 hours and apoptosis was measured by flow cytometry. Overexpression of USP2b in HCC cells significantly inhibited cell growth and promoted apoptosis.

Figure 6: USP2b regulates the stability of target proteins. Cell growth was measured at 24 and 48 hours and apoptosis was measured by flow cytometry. Overexpression of USP2b in HCC cells significantly inhibited cell growth and promoted apoptosis.

Figure 7: Effects of USP2b and its target proteins on cell growth. Cell growth was measured at 24 and 48 hours and apoptosis was measured by flow cytometry. Overexpression of USP2b in HCC cells significantly inhibited cell growth and promoted apoptosis.

Figure 8: Effects of overexpression of target proteins on cell apoptosis. Overexpression of USP2b target proteins (CDK2, CDK4, CDK6, E2F1, E2F2, E2F3, E2F4, E2F5, E2F6, E2F7, E2F8, E2F9, E2F10, E2F11, E2F12, E2F13, E2F14, E2F15, E2F16, E2F17, E2F18, E2F19, E2F20, E2F21, E2F22, E2F23, E2F24, E2F25, E2F26, E2F27, E2F28, E2F29, E2F30, E2F31, E2F32, E2F33, E2F34, E2F35, E2F36, E2F37, E2F38, E2F39, E2F40, E2F41, E2F42, E2F43, E2F44, E2F45, E2F46, E2F47, E2F48, E2F49, E2F50, E2F51, E2F52, E2F53, E2F54, E2F55, E2F56, E2F57, E2F58, E2F59, E2F60, E2F61, E2F62, E2F63, E2F64, E2F65, E2F66, E2F67, E2F68, E2F69, E2F70, E2F71, E2F72, E2F73, E2F74, E2F75, E2F76, E2F77, E2F78, E2F79, E2F80, E2F81, E2F82, E2F83, E2F84, E2F85, E2F86, E2F87, E2F88, E2F89, E2F90, E2F91, E2F92, E2F93, E2F94, E2F95, E2F96, E2F97, E2F98, E2F99, E2F100) in HCC cells significantly promoted cell growth and inhibited apoptosis.

Figure 9: Effects of overexpression of target proteins on cell apoptosis. Overexpression of USP2b target proteins (CDK2, CDK4, CDK6, E2F1, E2F2, E2F3, E2F4, E2F5, E2F6, E2F7, E2F8, E2F9, E2F10, E2F11, E2F12, E2F13, E2F14, E2F15, E2F16, E2F17, E2F18, E2F19, E2F20, E2F21, E2F22, E2F23, E2F24, E2F25, E2F26, E2F27, E2F28, E2F29, E2F30, E2F31, E2F32, E2F33, E2F34, E2F35, E2F36, E2F37, E2F38, E2F39, E2F40, E2F41, E2F42, E2F43, E2F44, E2F45, E2F46, E2F47, E2F48, E2F49, E2F50, E2F51, E2F52, E2F53, E2F54, E2F55, E2F56, E2F57, E2F58, E2F59, E2F60, E2F61, E2F62, E2F63, E2F64, E2F65, E2F66, E2F67, E2F68, E2F69, E2F70, E2F71, E2F72, E2F73, E2F74, E2F75, E2F76, E2F77, E2F78, E2F79, E2F80, E2F81, E2F82, E2F83, E2F84, E2F85, E2F86, E2F87, E2F88, E2F89, E2F90, E2F91, E2F92, E2F93, E2F94, E2F95, E2F96, E2F97, E2F98, E2F99, E2F100) in HCC cells significantly promoted cell growth and inhibited apoptosis.

Figure 10: Effects of overexpression of target proteins on cell apoptosis. Overexpression of USP2b target proteins (CDK2, CDK4, CDK6, E2F1, E2F2, E2F3, E2F4, E2F5, E2F6, E2F7, E2F8, E2F9, E2F10, E2F11, E2F12, E2F13, E2F14, E2F15, E2F16, E2F17, E2F18, E2F19, E2F20, E2F21, E2F22, E2F23, E2F24, E2F25, E2F26, E2F27, E2F28, E2F29, E2F30, E2F31, E2F32, E2F33, E2F34, E2F35, E2F36, E2F37, E2F38, E2F39, E2F40, E2F41, E2F42, E2F43, E2F44, E2F45, E2F46, E2F47, E2F48, E2F49, E2F50, E2F51, E2F52, E2F53, E2F54, E2F55, E2F56, E2F57, E2F58, E2F59, E2F60, E2F61, E2F62, E2F63, E2F64, E2F65, E2F66, E2F67, E2F68, E2F69, E2F70, E2F71, E2F72, E2F73, E2F74, E2F75, E2F76, E2F77, E2F78, E2F79, E2F80, E2F81, E2F82, E2F83, E2F84, E2F85, E2F86, E2F87, E2F88, E2F89, E2F90, E2F91, E2F92, E2F93, E2F94, E2F95, E2F96, E2F97, E2F98, E2F99, E2F100) in HCC cells significantly promoted cell growth and inhibited apoptosis.

Figure 11: Summary diagram of the USP2b signaling pathway. USP2b deubiquitinates target proteins (CDK2, CDK4, CDK6, E2F1, E2F2, E2F3, E2F4, E2F5, E2F6, E2F7, E2F8, E2F9, E2F10, E2F11, E2F12, E2F13, E2F14, E2F15, E2F16, E2F17, E2F18, E2F19, E2F20, E2F21, E2F22, E2F23, E2F24, E2F25, E2F26, E2F27, E2F28, E2F29, E2F30, E2F31, E2F32, E2F33, E2F34, E2F35, E2F36, E2F37, E2F38, E2F39, E2F40, E2F41, E2F42, E2F43, E2F44, E2F45, E2F46, E2F47, E2F48, E2F49, E2F50, E2F51, E2F52, E2F53, E2F54, E2F55, E2F56, E2F57, E2F58, E2F59, E2F60, E2F61, E2F62, E2F63, E2F64, E2F65, E2F66, E2F67, E2F68, E2F69, E2F70, E2F71, E2F72, E2F73, E2F74, E2F75, E2F76, E2F77, E2F78, E2F79, E2F80, E2F81, E2F82, E2F83, E2F84, E2F85, E2F86, E2F87, E2F88, E2F89, E2F90, E2F91, E2F92, E2F93, E2F94, E2F95, E2F96, E2F97, E2F98, E2F99, E2F100) and promotes cell proliferation and inhibits apoptosis.



First Place - Mechanistic Insights into USP2b-Mediated Cell Proliferation and Cell Apoptosis Pathways in Hepatocellular Carcinoma



Qiwen Chen, Xinmu Zhang, Winifer Ali, Syed Hashmi, Tasneem Al-Huniti, Lia Bozza, Md. Mosiqr Rahman, Ruitang Deng

Hepatocellular carcinoma (HCC) is one of the most common forms of liver cancer worldwide and accounts for 90% of liver cancer cases. By 2025, it is estimated to have more than one million cases globally. Hepatitis B virus and hepatitis C virus are the main risk factors for HCC development. Early-stage HCC patients may profit from multiple treatment options, including surgical resection, liver transplantation, arterial embolization, radioembolization, or systemic targeted agents. Currently, there is a limited effective option in treating HCC patients. There is an urge to develop more effective therapies for HCC. However, the challenge remains due to the complexity of HCC pathogenesis and the lack of understanding of the complex mechanism. In recent years, the ubiquitin-proteasome system (UPS) and deubiquitinating enzymes (DUBs) have emerged as an important topic for understanding the mechanism of HCC and other cancers. The ubiquitin-proteasome system is one of the most important posttranslational modification pathways in eukaryotic cells that regulates cell functions, including cell cycle progression, DNA repair, and signal transduction. Ubiquitination can be reversed by deubiquitinating enzymes (DUBs) such as ubiquitin-specific peptidase 2 (USP2) that can cleave ubiquitin or ubiquitinated proteins from targeted proteins. In our previous study, we found that the overexpression of USP2b exhibited tumorigenic activities through promoting cell proliferation, colony formation, and wound healing in HepG2-WT and Huh 7 cells. Interestingly, overexpression of USP2b exhibited tumor suppressor characteristics through enhancing bile acid-induced apoptosis and necrosis in HepG2-WT and Huh7 cells upon bile acid treatment. Through a coimmunoprecipitated (Co-IP) – coupled proteomic analysis and western blot, novel USP2b-regulated downstream target proteins involved in the cell proliferation signaling pathway and the apoptosis signaling pathways have been identified. These newly identified USP2b target proteins were significantly upregulated or downregulated in HCC subjects. This finding reveals that USP2b exhibited both oncogenic and tumor-suppressing activities by regulating different signaling pathways. Therefore, delineating the novel mechanism in which USP2b promotes tumorigenesis while also expressing tumor-suppressing activities will provide the basis for developing more effective therapies by targeting USP2b or its downstream signaling pathways.

Does the marine pathogen *Tenacibaculum discolor* lift iron to outcompete rivals?

Ololade Gbadebo¹, Walter Balansa^{1,2}, Yan-Song Ye¹, Qihao Wu¹, David C. Rowley¹

¹Department of Biomedical and Pharmaceutical Sciences, College of Pharmacy, University of Rhode Island, Kingston, RI, USA
²Department of Fisheries and Maritime Technology, Institut Teknologi Negeri Nias Utara, North Sulawesi, Indonesia
³Department of Pharmaceutical Sciences, University of Pittsburgh, Pittsburgh, PA, USA

INTRODUCTION

Disease is a major bottleneck limiting aquaculture production, particularly during the vulnerable larval stages of bivalves. While *Vibrio* species are well-established pathogens of oyster larvae, the pathogenic potential of *Tenacibaculum* species in bivalve systems remains largely unexplored. Preliminary studies showed that a *Tenacibaculum* strain isolated from larval oysters induced significant larval mortality and exhibited hemolytic activity. Although siderophore production is not universally classified as a virulence factor, iron acquisition is essential for microbial survival and may contribute to pathogenicity. Here, we report the discovery of new siderophores produced by *Tenacibaculum discolor* DEN13. Following 48-hour cultivation, culture supernatants were extracted by solid-phase extraction and analyzed by HPLC, mass spectrometry, and NMR. This analysis identified known siderophores and 15 previously undescribed hydroxamate siderophores. These findings expand the chemical diversity known for the genus *Tenacibaculum* and provide insight into potential mechanisms underlying oyster larval disease.

METHODS




Figure 1. Oyster (Pinctada mazatlanica) shells (a) that soon after death by *Tenacibaculum* (b) (Dobson et al., 2018).

Figure 2. Study workflow. The sequenced genome of *T. discolor* DEN13 was analyzed using antiSMASH. A BLAST search was performed on UniProtKB, and the sequences were analyzed using siderophore databases, and identified 5 factors. Fractions 2-6 were analyzed using mass spectrometry. Purification was performed by reverse-phase HPLC, and the purified compounds were analyzed by mass spectrometry and NMR.

RESULTS




Figure 3. AntiSMASH analysis of the 7-discolor DEN13 genome identified biosynthetic gene clusters, including those for NR-siderophores.

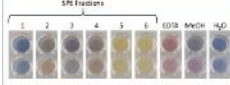


Figure 4. Chrome Azurol S (CAS) assay-based detection of siderophore production by *T. discolor* DEN13.

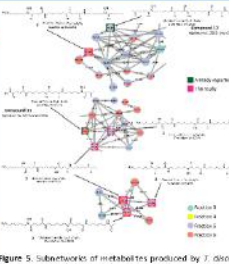


Figure 5. Substructures of metabolites produced by *T. discolor* DEN13, generated by ChemPy. Pie charts in notes represent abundance in the different fractions.

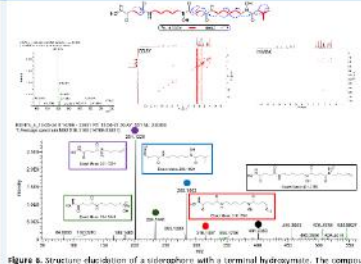


Figure 6. Structure elucidation of a siderophore with a terminal hydroxamate. The compound was isolated by HPLC and analyzed by tandem mass spectrometry and NMR. COSY correlations and MSⁿ confirmed the presence of an unusual terminal hydroxamate group.

Compound	Observed mass (MSE)	Theoretical mass (MSE)	Charge
1	502.2826	502.2832	5:17
2	505.3046	505.3052	0:16
3	505.3053	505.3059	-1:16
4	572.2862	572.2868	1:10
5	587.4135	587.4141	3:12
6	588.2938	588.2944	2:16
7	588.2764	588.2770	0:13
8	425.2918	425.2924	0:16
9	602.2802	602.2808	2:15
10	617.3126	617.3132	0:16
11	642.4060	642.4066	1:12
12	642.4030	642.4036	-0:15
13	632.4237	632.4243	0:19
14	647.4535	647.4541	1:19
15	488.2436	488.2442	1:17
16	648.3631	648.3637	2:16
17	625.4009	625.4015	1:12

Figure 7. Mass-based structure prediction and annotation of two new hydroxamate siderophores: the masses of protonated molecules (MH)⁺ and m/z of detected fragments are shown. Data was acquired on an Orbitrap MS.

Figure 8. Mass-based structure prediction of new hydroxamate siderophores, proterioquinamine and tenacibactin D identified in *T. discolor* DEN13 extracts.

CONCLUSIONS

- Tenacibaculum discolor* DEN13 produces a diverse array of hydroxamate siderophores, including those with an unusual terminal hydroxamate.
- 15 new hydroxamate siderophores were identified from a single cultivation of DEN13.
- A future direction is to determine the importance of *Tenacibaculum* siderophores for creating infections in oyster larviculture.

REFERENCES

1. Gbadebo, O., Balansa, W., Ye, Y., Wu, Q., Rowley, D. C. (2024). Does the marine pathogen *Tenacibaculum discolor* lift iron to outcompete rivals? *Journal of Inorganic Biochemistry*, 250, 111111. <https://doi.org/10.1016/j.jinorgbio.2024.111111>

2. Balansa, W., Gbadebo, O., Ye, Y., Wu, Q., Rowley, D. C. (2024). Discovery of 15 new hydroxamate siderophores from the marine pathogen *Tenacibaculum discolor* DEN13. *Journal of Inorganic Biochemistry*, 250, 111111. <https://doi.org/10.1016/j.jinorgbio.2024.111111>

3. Balansa, W., Gbadebo, O., Ye, Y., Wu, Q., Rowley, D. C. (2024). Discovery of 15 new hydroxamate siderophores from the marine pathogen *Tenacibaculum discolor* DEN13. *Journal of Inorganic Biochemistry*, 250, 111111. <https://doi.org/10.1016/j.jinorgbio.2024.111111>

4. Balansa, W., Gbadebo, O., Ye, Y., Wu, Q., Rowley, D. C. (2024). Discovery of 15 new hydroxamate siderophores from the marine pathogen *Tenacibaculum discolor* DEN13. *Journal of Inorganic Biochemistry*, 250, 111111. <https://doi.org/10.1016/j.jinorgbio.2024.111111>

5. Balansa, W., Gbadebo, O., Ye, Y., Wu, Q., Rowley, D. C. (2024). Discovery of 15 new hydroxamate siderophores from the marine pathogen *Tenacibaculum discolor* DEN13. *Journal of Inorganic Biochemistry*, 250, 111111. <https://doi.org/10.1016/j.jinorgbio.2024.111111>

ACKNOWLEDGEMENTS


This work was supported by the National Science Foundation (NSF) Grant IOB-2010101. We thank the members of the Rowley laboratory for their assistance in the laboratory.



Second Place - Does the marine pathogen *Tenacibaculum discolor* lift iron to outcompete rivals?

Ololade Gbadebo, Walter Balansa, Yan-Song Ye, Qihao Wu, David Rowley

Disease is a major bottleneck limiting aquaculture production, particularly during the vulnerable larval stages of bivalves. While *Vibrio* species are well-established pathogens of oyster larvae, the pathogenic potential of *Tenacibaculum* species in bivalve systems remains largely unexplored. Preliminary studies showed that a *Tenacibaculum* strain isolated from larval oysters induced significant larval mortality and exhibited hemolytic activity. Although siderophore production is not universally classified as a virulence factor, iron acquisition is essential for microbial survival and may contribute to pathogenicity. We hypothesized that siderophore production contributes to the pathogenicity of *T. discolor* in oyster larvae. Here, we report the discovery of new siderophores produced by *Tenacibaculum discolor* DEN13. The bacterial whole genome was sequenced and annotated. The genome was analyzed using antiSMASH to identify biosynthetic gene clusters, including that of NRPS-independent siderophores. Following 48-hour cultivation, culture supernatants were extracted by solid-phase extraction using 20%, 40%, 60%, 80% methanol/water, and 100% methanol. Extracts were fractionated and purified using reverse-phase MPLC followed by reverse-phase HPLC. Extracts and isolates were analyzed by reverse-phase HPLC, mass spectrometry, and NMR spectroscopy, followed by metabolomics analysis. Iron-binding activity was determined using the Chrome Azurol S (CAS) assay. These analyses identified known siderophores and 15 new hydroxamate siderophores. These findings expand the chemical diversity known for the genus *Tenacibaculum* and provide insight into potential mechanisms underlying oyster larval disease.



THE UNIVERSITY OF RHODE ISLAND

AlkB-family Enzymes Catalyzed Oxidation of Exocyclic Dimethyl RNA Nucleobases: Kinetic and Computational Insights

Evans Boateng-Boakye¹, Shubham Chatterjee², Xianhao Zhou¹, Jose P. Madriaga², Jian Ma¹, Yi-Tzai Chen¹, Bongsup Cho¹, G. Andrés Cisneros^{2*}, Deyu Li^{1*}

¹ Department of Biomedical and Pharmaceutical Sciences, College of Pharmacy, University of Rhode Island, RI, USA
² Department of Chemistry and Biochemistry, The University of Texas at Dallas, Richardson, TX, USA.

INTRODUCTION

- RNA contains a wide variety of chemical modifications that influence its structure, stability, and function. Among these, the exocyclic dimethyl modifications are especially notable because they are bulkier and more sterically distinct than canonical monomethyl modifications.
- These marks are associated with important biological processes, including ribosome maturation, mitochondrial translation, tRNA function, and viral RNA biology.
- Although some AlkB-family enzymes have been reported to act on dimethyl modifications, it remains unclear how these bulky substrates are processed and how their reactivity compares with that of the corresponding monomethyl modifications.
- Resolving this question is important for understanding AlkB-family substrate selectivity and the biological fate of RNA dimethyl marks.
- Here, we used *E. coli* AlkB as a model enzyme and integrated comparative kinetics with computational analysis to define the oxidation behavior of exocyclic dimethyl nucleobases.

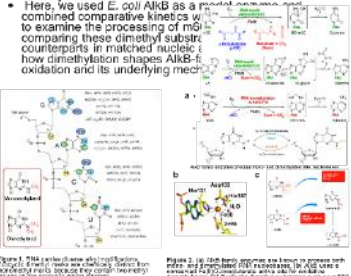


Figure 1. RNA pathways and AlkB family enzymes. (a) RNA pathways including translation, mitochondrial translation, tRNA, and viral RNA. (b) AlkB family enzymes (AlkB, AlkBH1, AlkBH2, AlkBH3) and their substrates (m6A, m6G, m4C). (c) AlkB active site structure.

RESULTS

Dimethyl RNA Nucleobases are processed by AlkB family enzymes

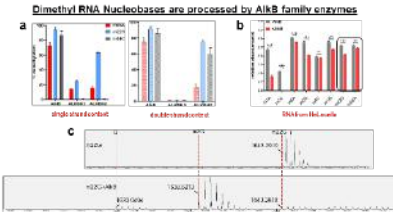


Figure 4. AlkB efficiently oxidized exocyclic dimethyl nucleobases m6A, m6G, and m4C, while AlkBH2 and AlkBH3 showed substrate- and strand-dependent activity on selected dimethyl modifications. (a) Relative activity of AlkB on dimethyl and monomethyl substrates in single-stranded (SS) and double-stranded (DS) RNA contexts. (b) Time-course analysis of AlkB activity on dimethyl and monomethyl substrates. (c) AlkB active site structure.

Dimethyl modification oxidation is sequential and biphasic with a rapid first step rate

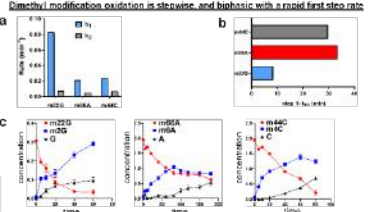


Figure 5. Kinetic analysis of AlkB activity on dimethyl and monomethyl substrates. (a) Relative activity of AlkB on dimethyl and monomethyl substrates. (b) Time-course analysis of AlkB activity on dimethyl and monomethyl substrates. (c) AlkB active site structure.

Dimethyl RNA Nucleobases vs. corresponding monomethyl counterparts

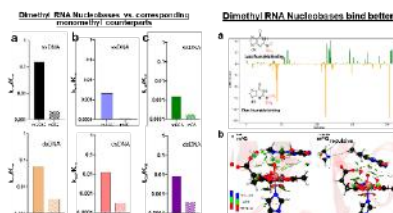


Figure 6. Comparison of AlkB activity on dimethyl and monomethyl substrates. (a) Relative activity of AlkB on dimethyl and monomethyl substrates. (b) Time-course analysis of AlkB activity on dimethyl and monomethyl substrates. (c) AlkB active site structure.

Dimethyl RNA Nucleobases bind better

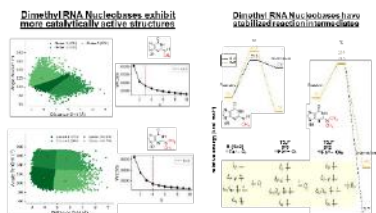


Figure 7. Computational analysis of AlkB binding to dimethyl and monomethyl substrates. (a) Molecular docking models. (b) Interaction energy profiles.

Dimethyl RNA Nucleobases exhibit more catalytically active structures

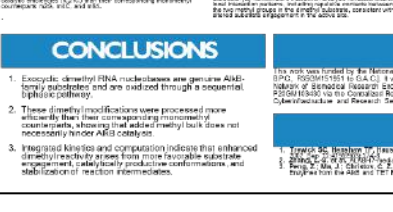


Figure 8. Computational analysis of AlkB binding to dimethyl and monomethyl substrates. (a) Molecular docking models. (b) Interaction energy profiles.

Dimethyl RNA Nucleobases have stabilized reaction intermediates




Figure 9. Reaction energy profiles for AlkB activity on dimethyl and monomethyl substrates. (a) Energy profiles for m6A, m6G, and m4C. (b) Energy profiles for m6A, m6G, and m4C.

METHODS

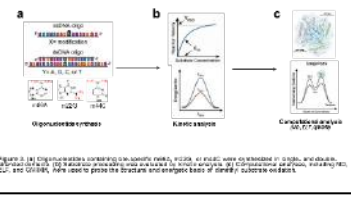


Figure 10. Experimental workflow for AlkB activity assays. (a) Synthesis of oligonucleotides. (b) AlkB activity assays. (c) Computational analysis.

CONCLUSIONS

1. Exocyclic dimethyl RNA nucleobases are genuine AlkB-family substrates and are oxidized through a sequential biphasic pathway.
2. These dimethyl modifications were processed more efficiently than their corresponding monomethyl counterparts, showing that added methyl bulk does not necessarily hinder AlkB catalysis.
3. Kinetic and computational analyses indicate that enhanced dimethyl reactivity arises from more favorable substrate engagement, catalytically productive conformations, and stabilization of reaction intermediates.

ACKNOWLEDGEMENTS

This work was funded by the National Institute of Health (R01NS086603 and R01NS104216) to G.A.C. and by the National Science Foundation (DMS-1908115) to D.L. It was also supported by the National Science Foundation Graduate Research Excellence Fellowship of Bongsup Cho (DMS-1908115) and the National Science Foundation Graduate Research Excellence Fellowship of Xianhao Zhou (DMS-1908115). We thank Dr. Y. Chen for providing the AlkB gene, Dr. J. Ma for providing the AlkBH1, AlkBH2, and AlkBH3 genes, and Dr. S. Cho for providing the AlkB gene. *A.C. and D.L. contributed equally to this work.

REFERENCES

1. Evans Boateng-Boakye, Shubham Chatterjee, Xianhao Zhou, Jose P. Madriaga, Jian Ma, Yi-Tzai Chen, Bongsup Cho, G. Andrés Cisneros, Deyu Li
2. ...
3. ...

Third Place - AlkB-family Enzymes Catalyzed Oxidation of Exocyclic Dimethyl RNA Nucleobases: Kinetic and Computational Insights

Evans Boateng-Boakye, Shubham Chatterjee, Xianhao Zhou, Jose P. Madriaga, Jian Ma, Yi-Tzai Chen, Bongsup Cho, G. Andrés Cisneros, Deyu Li

Exocyclic dimethyl modifications of RNA nucleobases, including N6,N6-dimethyladenosine (m6A), N2,N2-dimethylguanosine (m2G), and N4,N4-dimethylcytidine (m4C), are biologically important marks associated with ribosome maturation, mitochondrial translation, tRNA function, and viral RNA biology. Although some AlkB-family Fe(II)/2-oxoglutarate-dependent dioxygenases have been reported to act on dimethylated nucleobases, how these bulky and sterically distinct substrates are processed, and how their reactivity compares with corresponding monomethyl modifications, remain unclear. Here, we used *Escherichia coli* AlkB as a model enzyme and integrated comparative kinetics with computational analysis to define the oxidation behavior of exocyclic dimethyl nucleobases.

Site-specifically modified oligonucleotides containing m6A, m2G, or m4C were synthesized and examined in matched single-stranded and double-stranded contexts. *In vitro* assays showed that AlkB efficiently oxidizes all three dimethyl substrates, whereas some mammalian homologs showed substrate- and strand-dependent activity on selected dimethyl modifications. Time-course analyses revealed that their oxidation proceeds through a sequential biphasic pathway, with a rapid first demethylation step to the corresponding monomethyl intermediate followed by a slower second demethylation step to the unmodified base. Surprisingly, all three dimethyl substrates were processed more efficiently than their corresponding monomethyl counterparts in both strand contexts.

To explain this unexpected behavior, we performed computational analyses on the mono- and dimethyl substrates. Molecular interaction and conformational analyses showed that the dimethyl RNA nucleobases bind more favorably in the enzyme active site and samples a larger population of catalytically competent structures. Reaction energy profiles also indicated that dimethylation of the RNA nucleobase enhances the stabilization of its reaction intermediate and not necessarily lower its transition state barrier.

Together, this work shows that exocyclic dimethyl RNA-type nucleobases are genuine and efficiently processed AlkB-family substrates. It provides a mechanistic framework for understanding dimethyl substrate selectivity and has implications for RNA modification biology, repair-dependent sequencing strategies, and future engineering of AlkB-family enzymes.

URI College of Pharmacy – 2026 Research Showcase

12

A novel inducible mtDNA mutator mouse model to study mitochondrial dysfunction with temporal and spatial control

Hannah Tobias-Wallingford^{1,2}, Sydney Bartman^{1,2}, Lauren Gaspar^{1,2}, Brian Gallagher¹, Christopher Hemme², Giuseppe Coppotelli^{1,2}, and Jaime M. Ross^{1,2}

¹George & Anne Ryan Institute for Neuroscience, University of Rhode Island, Kingston RI
²Biomedical & Pharmaceutical Sciences, College of Pharmacy, University of Rhode Island, Kingston RI

INTRODUCTION and AIM

- Mitochondrial dysfunction (MD) is implicated in aging and age-related disorders including neurodegenerative diseases, such as Alzheimer's and Parkinson's disease.
- Previous models to study MD include the mtDNA mutator mouse (Trifunovic et al., 2004 & Kujtho et al., 2005).
- This model expresses a proofreading deficient version (D257A) of mtDNA polymerase- γ (PolgA) and accumulates whole-body mtDNA mutations and deletions from gestation.
- Due to the global nature of MD in this model, it is impossible to study the impact of mtDNA mutations on specific processes such as cognition, neural development, motor systems, or more specifically on immune and inflammatory responses.

The aim of this research is to characterize a novel inducible mtDNA mutator mouse model, the i-PolgA mouse. This is a model of MD with temporal and spatial control of mtDNA mutation induced MD.

METHODS

- Novel inducible mtDNA mutator mouse generated and characterized alongside original mtDNA mutator mouse via behavioral assays run at 3, 6, and 9 months of age, phenotype and lifespan analyses. Biochemical analysis of tissues to assess mitochondrial function and mtDNA mutation load were performed.

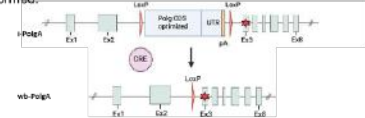


Figure 1. Schematic of the Cre-loxP recombination system utilized to generate the novel inducible mutator mouse. The PolgA CDS contains the entire CDS from exon 3 onwards, following this there is the endogenous untranslated region (UTR) and hG-taa poly-adenylation signal (yellow). The mutation (red star) is within exon 3 and will only be expressed following excision at the LoxP sites by CRE.

RESULTS

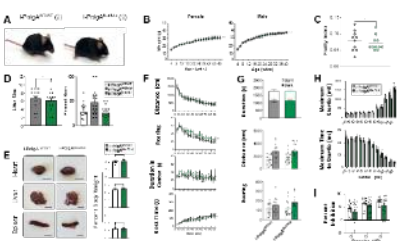


Figure 2. Characterization of the uninduced i-PolgA model. i-PolgA^{M/M}. No change in phenotype (A), body weight (B), lifespan (C), fecundity and organ size (E). Additionally, no change in exploratory behavior, locomotion, anxiety-like behavior, startle response, or pre-pulse inhibition (F, G, H, I) was found.

RESULTS

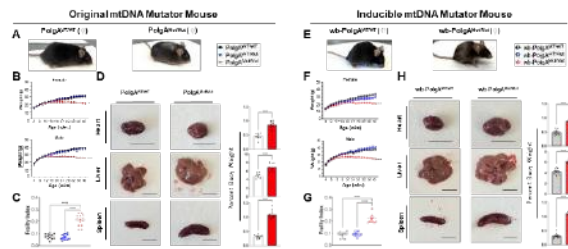


Figure 3. Characterization of the novel inducible mtDNA Mutator Mouse compared to the original mtDNA Mutator Mouse. Representative images of female PolgA and wb-PolgA mice at 35 weeks of age, show similar premature aging phenotypes in mutator mice (A, E). Decreased body weight in mutator mice is similar in both models (B, F). Average frailty index scores across genotypes are consistent between models (C, G). Enlarged heart, liver, and spleen observed in both mutator mice of both models (D, H).

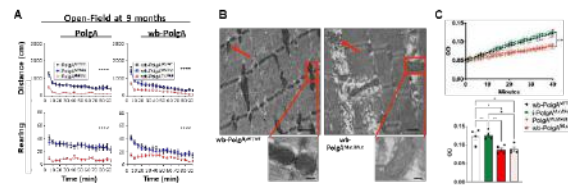


Figure 4. Behavioral characterization of the novel wb-PolgA model and the original PolgA model. Exploratory behavior and spontaneous locomotion assessed using the open field behavioral assay (A), mitochondrial structural and functional changes in both the novel wb-PolgA mutator and the original PolgA models as shown with representative transmission electron microscopy images of the gastrocnemius muscle (B), mitochondrial Complex I activity in liver tissues (C).

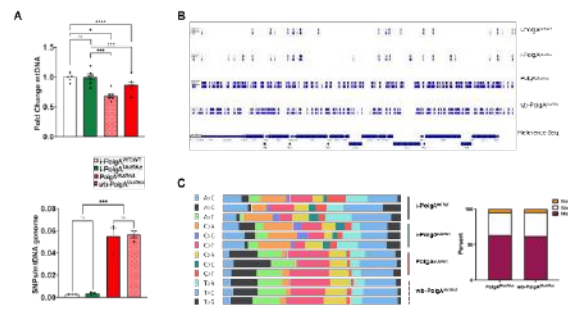


Figure 5. Decreased mtDNA copy number and increased mtDNA mutation load were found in both the novel and original mutator models (A). Visualization of mutation load (B) and mutation type (C).

RESULTS CONT

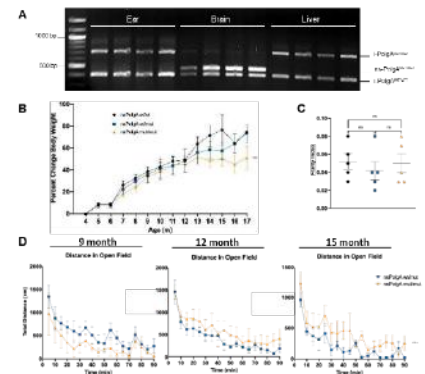


Figure 6. Preliminary characterization of a nervous system-specific mtDNA mutator mouse (nsPolgA^{M/M}). Confirmation of tissue-specificity in the i-PolgA model (A). Decreased percent change in body weight over lifespan in the nsPolgA^{M/M} was observed (B). Similar aging phenotype scores across genotypes at 15 months (C). Exploratory behavior and spontaneous locomotion assessed with open-field, showing nsPolgA^{M/M} exploratory behavior increases relative to controls during repeated trials indicating possible cognitive impairment.

CONCLUSIONS

- Novel inducible mtDNA Mutator mouse model is viable, fertile, and offspring are born in a Mendelian fashion
- Whole-body induced (wb) PolgA^{M/M} mice recapitulate the original mtDNA-PolgA^{M/M} mutator mouse model
 - Behavioral analyses showed similar trends across assays
 - Phenotypic characteristics of the mtDNA-PolgA mutator mouse model are also observed in the novel wb-PolgA mutator mouse
 - Biochemical analysis of mitochondrial dysfunction parameters are similar in both models
- This model provides the ability to study the accumulation of mtDNA mutations and deletions in a tissue-specific manner and will allow the effects and more specifically, the regulation of these mutations and deletions to be better understood
- Preliminary characterization of the nervous system-specific model indicates no change in phenotype, body weight, or lifespan relative to controls. Behavioral assessment demonstrates potential impairment of cognition and working memory.

Acknowledgments

Funding provided by the NIH Office of the Director R21OD037651 (GC, JMR), the National Institute on Aging R01AG092603 (GC, JMR), the URI First-Year Doctoral Fellowship (RTM), the URI College of Pharmacy Seed Funding (GC), the George & Anne Ryan Institute for Neuroscience (GC, JMR), The Reddy Foundation (GC, JMR), and Konung Gustaf V:s och Drottning Victorias Frimurarestiftelse
 *Special thanks to Dr. Jaime Ross, Dr. Giuseppe Coppotelli, Dr. Chris Hemme, Sydney Bartman, Lauren Gaspar, Brian Gallagher, Sajida Jan, Mackenzie Pavlik, Delaney Abatecola, Nikki Fernando, RH-NBRE, NH-NBRE, and Leduc Biomedical Facility.

A novel inducible mtDNA mutator mouse model to study mitochondrial dysfunction with temporal and spatial control

Hannah Tobias-Wallin, Sydney Bartman, Lauren Gaspar, Brian Gallagher, Christopher Hemme, Giuseppe Coppotelli, Jaime M. Ross

Mitochondrial dysfunction is a hallmark of numerous age-related diseases including neurodegenerative diseases, such as Alzheimer's and Parkinson's disease. A wealth of studies supports the accumulation of mitochondrial DNA (mtDNA) mutations as a contributing factor of mitochondrial dysfunction in aging and disease. One of the best models to study the relationship between mtDNA mutations and mitochondrial dysfunction is the mtDNA mutator mouse, which expresses a proofreading-deficient version of mtDNA polymerase-gamma (PolgA), resulting in accelerated accumulation of mtDNA mutations and aging-like mitochondrial dysfunction. Despite its groundbreaking contributions to mitochondrial biology and aging research, this model is limited by the whole-body accumulation of mtDNA mutations, which prevents the investigation of tissue-specific differences in mitochondrial dysfunction. To overcome this limitation, we developed a novel inducible knock-in mtDNA mutator mouse model (iPolgA) that allows spatial and temporal control of mtDNA mutations, enabling the precise study of mitochondrial dysfunction in a tissue- and time-specific manner. Here, we report the generation and validation of this novel model through whole-body induction via Cre recombinase. Our data demonstrate that, upon induction, this model recapitulates the phenotype of the original mtDNA mutator mouse manifesting the same behavioral and biochemical alterations. Additionally, we are working towards demonstrating functionality of the novel iPolgA model and are generating a nervous system-specific mtDNA mutator mouse to evaluate the effects of mitochondrial dysfunction specifically in brain. This work highlights the iPolgA model as a powerful tool for studying the impact of mtDNA mutations on aging and neurodegenerative disorders with enhanced specificity and control

Introduction

Cellular senescence is a state of permanent, stress-induced cell cycle arrest first described by Hayflick and Moorhead (1961). While senescent cells remain metabolically active, they are resistant to apoptosis and secrete pro-inflammatory cytokines. Senescence is beneficial for a short time, but chronic senescence drives inflammation. In hepatocytes, bile acid toxicity is a key senescence trigger, implicating protein homeostasis pathways in its regulation. The ubiquitin-proteasome system (UPS) is a primary way of controlled protein degradation, with deubiquitinating enzymes (DUBs) regulating this process by removing ubiquitin tags and preventing premature protein degradation. Among liver-enriched DUBs, USP2b is the predominant isoform expressed in liver tissue (Nadolny et al., 2021), yet its role in hepatocyte senescence remains unknown.

Research question

We propose that USP2b dysregulation impairs endoplasmic reticulum (ER) protein homeostasis, thereby promoting bile acid-induced hepatocyte senescence. In this project, we will address the question: How does USP2b expression modulate bile acid-induced senescence?

Methods

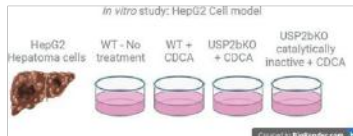
In vivo — chenodeoxycholic acid (CDCA) diet mouse model

Experimental groups: USP2b knockout control, USP2b overexpression, and catalytic inactive mutant (C276A), all on CDCA diet. Endpoint: liver tissue harvest. Readouts: SA- β -galactosidase staining, p21/p16/GRP78 western blot (cell cycle exit and ER stress)



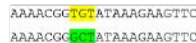
In vitro — HepG2 cell model

Experimental groups: wild-type no treatment, wild-type + CDCA, USP2bKO + CDCA, and catalytic inactive mutant + CDCA. Readouts: SA- β -galactosidase staining, p21/p16/GRP78 western blot



Tool – Catalytic mutant C276A substitution

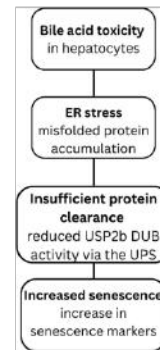
Active site Cys \rightarrow Ala eliminates hydrolysis activity. This controls for protein expression vs. enzymatic function of USP2b.



Ongoing Work

- (1) Does USP2b expression alter cell cycle progression?
- (2) Does the overexpression of USP2b reduce ER stress through activation of ER protein homeostasis machinery in hepatocytes?

Proposed pathway of USP2b activity in bile acid induced senescence



Understanding this pathway may reveal new therapeutic targets in cholestatic liver disease.

References

- Hayflick et al (1961) Exp Cell Res 25:3
Nadolny C et al (2021) Am J Cancer Res 11:10
Images created in <https://BioRender.com> and Canva.com

This work was supported by grants from the National Institutes of Health to RD under grant numbers R01CA213419 and R01DK139489. This work was also supported by the Institutional Development Award (IDeA) Network for Biomedical Research Excellence from the National Institute of General Medical Sciences of the National Institutes of Health under grant number P20GM103430. We thank Dr. Qiwen Chen for breeding USP2b^{+/+} and USP2b^{-/-} animal lines (University of Rhode Island), Dr. Xinmu Zhang for creating USP2bKO-3A in HepG2 cell lines (University of Rhode Island), and Ms. Janet Atoyán (RI INBRE) for use of instrumentation.



Activity of USP2b in Cellular Senescence

Lia Bozza, Tasneem Al-Huniti, Qiwen Chen, Md. Mosiqr Rahman, Xinmu Zhang, Winifer Ali, Syed Hashmi, Ruitang Deng

Cellular senescence is characterized by terminal cell cycle arrest coupled with sustained metabolic function. Under liver injury conditions, elevated bile acid levels can induce cellular senescence, but whether senescence contributes to disease or is a result of it remains an open question. Addressing this requires an understanding of the molecular regulators involved in senescence in the liver: among them is ubiquitin-specific peptidase isoform 2 (USP2b), an enzyme that deubiquitinates proteins tagged for proteasome-mediated degradation. Previous work in the lab of Dr. Deng has shown that USP2b is highly expressed in the liver tissue and it exhibits anti-senescence functions in both mouse and cell models. When USP2b was overexpressed in HepG2 cells and treated with bile acid to induce cellular stress, the number of senescent cells was significantly reduced compared to the control. These findings suggest that USP2b has anti-senescence activity, and this project aims to investigate the mechanisms responsible.

Adverse Event Associated with Elafibranor: Disproportionality Analysis of US FDA Adverse Event Reporting System

Abimbola Sola-Aremu, MS Candidate, B.Pharm, A. R. Caffrey, PhD, MS

Department of Pharmacy Practice and Clinical Research, College of Pharmacy, University of Rhode Island, Kingston, RI



Background	Results	Results/Discussions																								
<ul style="list-style-type: none"> Primary sclerosing cholangitis (PSC) is a rare, chronic liver disease of unknown etiology in which the bile ducts become progressively inflamed, narrowed, and scarred. As the disease advances, impaired bile flow leads to cholestasis, irreversible liver damage, and fibrosis. PSC can progress to end-stage liver failure and carries an elevated risk of cholangiocarcinoma, without effective intervention. There are no FDA-approved disease-modifying treatments for PSC.¹ Globally, PBC has a prevalence of 18.1 cases per 100,000 people. In the United States, PBC prevalence is 40.9 per 100,000 adults. Mostly white women aged 45-65.2 Elafibranor was approved by the FDA on June 10 2024, for the treatment of primary biliary cholangitis (PBC), as a monotherapy for those unable to tolerate ursodeoxycholic acid (UDCA) or for adults with inadequate response to UDCA. As Elafibranor becomes widely used in real-world clinical practice, it is important to monitor its safety. 	<table border="1"> <thead> <tr> <th colspan="4">Table 1: Count of Cases and Non-cases for Gastrointestinal Disorder (GID)</th> </tr> <tr> <th></th> <th>Present</th> <th>Absent</th> <th>Total</th> </tr> </thead> <tbody> <tr> <td>Elafibranor</td> <td>22</td> <td>98</td> <td>120</td> </tr> <tr> <td>Other drugs</td> <td>110189</td> <td>2075048</td> <td>2185237</td> </tr> <tr> <td>Total</td> <td>110211</td> <td>2075146</td> <td>2185357</td> </tr> </tbody> </table>	Table 1: Count of Cases and Non-cases for Gastrointestinal Disorder (GID)					Present	Absent	Total	Elafibranor	22	98	120	Other drugs	110189	2075048	2185237	Total	110211	2075146	2185357	<ul style="list-style-type: none"> With 58,615 reports for nervous system disorders, the reporting rate for Elafibranor was significantly compared to other drugs (ROR 5.58, 95% CI 3.20–9.26; PRR 4.97, 95% CI 3.15–7.85). Our analysis detected statistically significant disproportionality signals for Elafibranor. Gastrointestinal disorders showed significant increase in proportional reporting compared to other drugs. Nervous system disorders showed a stronger signal, suggesting potential underrecognized neurological risks such as headache, dizziness, or peripheral neuropathy, and the strongest signal was observed for musculoskeletal and connective tissue disorders. Across all categories, the order of signal magnitude based on ROR and PRR estimates: musculoskeletal and connective tissue disorders > nervous system disorders > gastrointestinal disorders. 				
	Table 1: Count of Cases and Non-cases for Gastrointestinal Disorder (GID)																									
		Present	Absent	Total																						
	Elafibranor	22	98	120																						
Other drugs	110189	2075048	2185237																							
Total	110211	2075146	2185357																							
<table border="1"> <thead> <tr> <th colspan="4">Table 2: Count of Cases and Non-cases for Musculoskeletal and Connective Tissue Disorder</th> </tr> <tr> <th></th> <th>Present</th> <th>Absent</th> <th>Total</th> </tr> </thead> <tbody> <tr> <td>Elafibranor</td> <td>13</td> <td>107</td> <td>120</td> </tr> <tr> <td>All other drugs</td> <td>38862</td> <td>2146375</td> <td>2185237</td> </tr> <tr> <td>Total</td> <td>38875</td> <td>2146482</td> <td>2185357</td> </tr> </tbody> </table>	Table 2: Count of Cases and Non-cases for Musculoskeletal and Connective Tissue Disorder					Present	Absent	Total	Elafibranor	13	107	120	All other drugs	38862	2146375	2185237	Total	38875	2146482	2185357						
Table 2: Count of Cases and Non-cases for Musculoskeletal and Connective Tissue Disorder																										
	Present	Absent	Total																							
Elafibranor	13	107	120																							
All other drugs	38862	2146375	2185237																							
Total	38875	2146482	2185357																							
<table border="1"> <thead> <tr> <th colspan="4">Table 3: Count of Cases and Non-cases for Nervous System Disorder</th> </tr> <tr> <th></th> <th>Present</th> <th>Absent</th> <th>Total</th> </tr> </thead> <tbody> <tr> <td>Elafibranor</td> <td>16</td> <td>104</td> <td>120</td> </tr> <tr> <td>All other drugs</td> <td>58599</td> <td>2126638</td> <td>2185237</td> </tr> <tr> <td>Total</td> <td>58615</td> <td>2126742</td> <td>2185357</td> </tr> </tbody> </table>	Table 3: Count of Cases and Non-cases for Nervous System Disorder					Present	Absent	Total	Elafibranor	16	104	120	All other drugs	58599	2126638	2185237	Total	58615	2126742	2185357						
Table 3: Count of Cases and Non-cases for Nervous System Disorder																										
	Present	Absent	Total																							
Elafibranor	16	104	120																							
All other drugs	58599	2126638	2185237																							
Total	58615	2126742	2185357																							
<table border="1"> <thead> <tr> <th colspan="5">Table 4: PRR and ROR for Major Adverse Events Associated with Elafibranor</th> </tr> <tr> <th>Elafibranor</th> <th>ROR</th> <th>95% CI</th> <th>PRR</th> <th>95% CI</th> </tr> </thead> <tbody> <tr> <td>Gastrointestinal Disorder</td> <td>4.23</td> <td>2.66-6.71</td> <td>3.64</td> <td>2.49-5.30</td> </tr> <tr> <td>Musculoskeletal and connective tissue disorder</td> <td>6.71</td> <td>3.77-11.93</td> <td>6.02</td> <td>3.65-10.18</td> </tr> <tr> <td>Nervous system Disorder</td> <td>5.58</td> <td>3.20-9.26</td> <td>4.97</td> <td>3.15-7.85</td> </tr> </tbody> </table>	Table 4: PRR and ROR for Major Adverse Events Associated with Elafibranor					Elafibranor	ROR	95% CI	PRR	95% CI	Gastrointestinal Disorder	4.23	2.66-6.71	3.64	2.49-5.30	Musculoskeletal and connective tissue disorder	6.71	3.77-11.93	6.02	3.65-10.18	Nervous system Disorder	5.58	3.20-9.26	4.97	3.15-7.85	<p>Conclusions</p> <ul style="list-style-type: none"> Our disproportionality analysis detected an association between Elafibranor and reported adverse events including gastrointestinal disorder reports, musculoskeletal and connective tissue disorders, and nervous system disorders. Further studies are needed to confirm these findings and to quantify the real-world safety profile of Elafibranor.
Table 4: PRR and ROR for Major Adverse Events Associated with Elafibranor																										
Elafibranor	ROR	95% CI	PRR	95% CI																						
Gastrointestinal Disorder	4.23	2.66-6.71	3.64	2.49-5.30																						
Musculoskeletal and connective tissue disorder	6.71	3.77-11.93	6.02	3.65-10.18																						
Nervous system Disorder	5.58	3.20-9.26	4.97	3.15-7.85																						
<p>Objectives</p> <p>This study aimed to assess adverse events for gastrointestinal disorder, nervous system disorder, and musculoskeletal and connective tissue disorder adverse events associated with Elafibranor through a disproportionality analysis using the Food and Drug Administration Adverse Event Reporting System (FAERS).</p>	<p>Results</p> <ul style="list-style-type: none"> During the overall study period, a total of 2,185,357 adverse events met our inclusion criteria and were included in the analysis. With 110,211 gastrointestinal disorder reports in the FAERS database, the reporting rates for Elafibranor were significantly higher than other medications (ROR 4.23, 95% CI 2.66-6.71; PRR 3.64, 95% CI: 2.49-5.30). With 38,875 adverse musculoskeletal and connective tissue disorders events, reporting rates for Elafibranor were significantly higher than other medications with ROR of 6.71 (95% CI: 3.77–11.93) and PRR of 6.09 (95% CI: 3.65–10.18). 	<p>References</p> <ol style="list-style-type: none"> Kowdley, K. V. <i>et al.</i> Efficacy and Safety of Elafibranor in Primary Biliary Cholangitis. <i>N. Engl. J. Med.</i> 390, 795–805 (2024). Levy, C. <i>et al.</i> Safety and efficacy of elafibranor in primary sclerosing cholangitis: The ELMWOOD phase II randomized-controlled trial. <i>J. Hepatol.</i> 84, 74–85 (2026). Tan, J. J.-R., <i>et al.</i> (2026). Global Epidemiology of Primary Biliary Cholangitis: An Updated Systematic Review and Meta-Analysis. <i>Clinical Gastroenterology and Hepatology</i>, 24(3), 621–632. https://doi.org/10.1016/j.cgh.2025.03.025 																								
<p>Methods</p> <ul style="list-style-type: none"> This case-non-case study analyzed FAERS surveillance data from June 2024 through December 2025. Adverse events reports with missing data for event, date, age, or sex were excluded. Elafibranor was identified using the search terms "Elafibranor" and "Iqirvo." Adverse events were coded using the Medical Dictionary for Regulatory Activities (MedDRA) and grouped by system organ class. Medical Dictionary for regulatory activities (MedDRA) search terms: "gastrointestinal disorders", "musculoskeletal and connective tissue disorders", and "nervous system disorders". Reporting odds ratios (RORs), proportional reporting ratios (PRRs), and corresponding 95% confidence intervals (CIs) were calculated using SAS OnDemand for academics. 	<p>References</p>																									

Adverse Event Associated with Elafibranor: Disproportionality Analysis of US FDA Adverse Event Reporting System

Abimbola Sola-Aremu, A. R. Caffrey

Background: Elafibranor, approved by the U.S. Food and Drug Administration (FDA) in June 2024 for the treatment of primary biliary cholangitis (PBC), represents a novel therapeutic option for patients who are intolerant to or inadequately responsive to ursodeoxycholic acid. As its use expands in real-world clinical practice, comprehensive safety evaluation is essential. This study aimed to assess adverse event (AE) signals associated with Elafibranor using post-marketing surveillance data.

Methods: A retrospective disproportionality analysis was conducted using the FDA Adverse Event Reporting System (FAERS) database from June 2024 through December 2025. Reports with missing key variables were excluded. Elafibranor-related AEs were identified using standardized drug names and coded based on the Medical Dictionary for Regulatory Activities (MedDRA). Adverse events were grouped into system organ classes, including gastrointestinal, musculoskeletal and connective tissue, and nervous system disorders. Reporting odds ratios (RORs), proportional reporting ratios (PRRs), and 95% confidence intervals (CIs) were calculated to detect safety signals.

Results: A total of 2,185,357 AE reports met inclusion criteria. Elafibranor demonstrated statistically significant disproportionality signals across all evaluated categories. Gastrointestinal disorders showed elevated reporting (ROR 4.23, 95% CI 2.66–6.71; PRR 3.64, 95% CI 2.49–5.30). Musculoskeletal and connective tissue disorders exhibited the strongest signal (ROR 6.71, 95% CI 3.77–11.93; PRR 6.02, 95% CI 3.65–10.18). Nervous system disorders also showed a significant association (ROR 5.58, 95% CI 3.20–9.26; PRR 4.97, 95% CI 3.15–7.85), suggesting potential underrecognized neurological risks.

Conclusions: This analysis identified significant safety signals associated with Elafibranor across multiple organ systems. These findings highlight the importance of continued pharmacovigilance and may inform clinicians and regulators regarding potential risks. Further studies are warranted to validate these signals and better characterize the real-world safety profile of Elafibranor

Albumin is a critical factor contributing to plasma per- and polyfluoroalkyl substances (PFAS) concentration and retention *in vivo*



Olga Skende¹, Sangwoo Ryu¹, Simon Vojta², Jitka Becanova², Fabian Fischer¹, Jingmei Zeng¹, Rainer Lohmann², Angela Slitt¹

¹Department of Biomedical and Pharmaceutical Sciences, University of Rhode Island, Kingston, RI (USA)
²Graduate School of Oceanography, University of Rhode Island, Kingston, RI (USA)



ABSTRACT

Per- and polyfluoroalkyl substances (PFAS) are a class of synthetic molecules composed of chain-linked carbon-fluorine bonds. There are 10,000+ PFAS, with perfluorooctane sulfonate (PFOS) and perfluorobutane sulfonate (PFBS) being some most frequently detected PFAS in serum of the United States general population. Newer PFAS, such as perfluorobutane sulfonic acid (PFBS) and 6:2-fluorotelomer sulfonic acid (6:2 FTS), are now also detected in human serum. As a class of chemicals, PFAS undergo limited biotransformation and are slowly excreted. PFOS and PFBS exhibit a strong binding affinity for serum albumin, which is hypothesized to be the predominant mechanism that dictates their slow elimination from the body. It is thought that albumin binding retains PFAS in circulation and prevents PFAS from undergoing renal excretion. However, to date, albumin binding as a critical factor for PFAS elimination has only been studied and modeled using *in vitro* assays. Thus, it was hypothesized that mice deficient in albumin would have reduced plasma PFAS concentrations and increased tissue PFAS concentrations due to decreased PFAS retention in plasma by albumin. C57BL/6J mice expressing (Alb+/+) or lacking (Alb-/-) albumin were administered a single oral dose of a PFAS cocktail consisting of 0.1 mg/kg PFOS, PFHxS, PFBS, and 6:2FTS at equal ratios (10 mg/kg, n=3-6/group). Plasma was collected at 1, 4, 24, and 72 hours, followed by 1, 2, 4, 6, 8, and 10 weeks. Tissues were collected at 4 hours, 24 hours and 1 week. At 12 weeks post PFAS dosing, plasma and tissues were collected. Albumin deficiency decreased PFHxS, PFBS, 6:2FTS, and PFOS AUC to 9.8%, 7.6%, 17.2%, and 38.7%, respectively, of the controls. Albumin deficiency increased PFHxS and PFBS liver concentrations after 4 hours, PFHxS and 6:2FTS concentrations after 24 hours, and PFHxS concentrations 1 week after PFAS dosing. This is the first study to demonstrate that albumin is a critical factor contributing to plasma and liver concentration and retention of a PFAS cocktail *in vivo*. This project highlights variability in albumin levels, influenced by disease and genetic factors, as a potential mechanistic contributor to inter-individual differences in PFAS exposure and toxicity.

INTRODUCTION

- Albumin is the most abundant serum protein, responsible for binding and transporting molecules such as fatty acids and small molecule drugs.
- In vivo* assays demonstrate PFAS binding to human, rat, and mouse albumin.
- Albumin binding may be a driver of PFAS half-life.

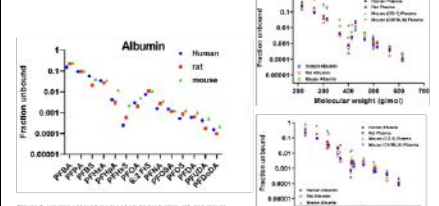
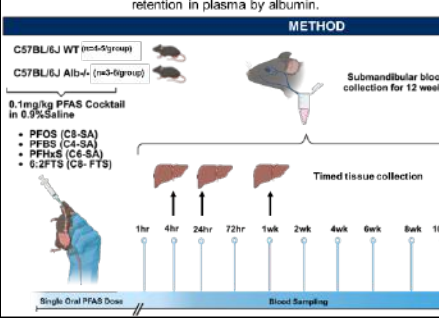


Figure 1. Molecular weight distribution of PFAS in human, rat, and mouse. The graph shows the fraction of unbound PFAS versus molecular weight (log scale). PFAS are categorized into PFOS, PFHxS, PFBS, 6:2FTS, and PFOS. Human, rat, and mouse albumin binding curves are shown for comparison.

HYPOTHESIS

Mice lacking albumin will have reduced plasma PFAS concentrations and increased tissue PFAS concentrations due to decreased PFAS retention in plasma by albumin.



RESULTS

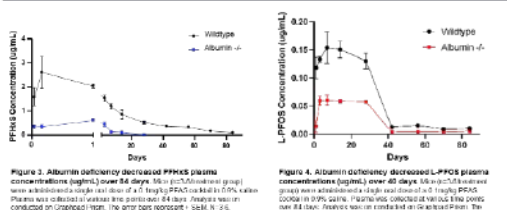


Figure 3. Albumin deficiency decreased PFOS plasma concentrations (ug/mL) over 84 days (n=3-6/group). The graph shows PFAS concentration (ug/mL) over 84 days for PFOS in wildtype and albumin-/- mice. The y-axis ranges from 0 to 3 ug/mL, and the x-axis from 0 to 84 days. Wildtype mice show higher plasma concentrations that decrease over time, while albumin-/- mice show significantly lower concentrations.

Parameter	Unit	WT Value	Alb-/- Value
Half-life	days	22 ± 2	8 ± 1
Cmax	ug/mL	2.6 ± 0.8	0.6 ± 0.1
Tmax	days	0.16	1
Vd	mL/kg	75 ± 25	427 ± 280
Clearance	mL/kg/d	2.0 ± 1.2	80 ± 36
AUC	ug/mL/d	48.7 ± 4.1	4.5 ± 1.3

Table 1. PFOS pharmacokinetic parameters in wildtype and albumin deficient mice. Parameters were calculated as discussed in Methods. Data are presented as mean ± SEM. Significant differences are indicated by asterisks (*p < 0.05, **p < 0.01, ***p < 0.001, ****p < 0.0001). The error bars represent ± SEM. N = 3-6.

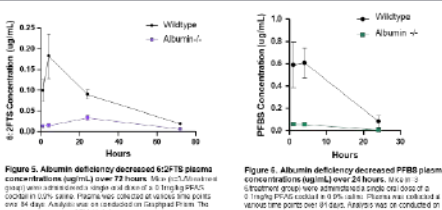


Figure 4. Albumin deficiency decreased PFBS plasma concentrations (ug/mL) over 30 hours (n=3-6/group). The graph shows PFBS concentration (ug/mL) over 30 hours for wildtype and albumin-/- mice. The y-axis ranges from 0 to 1.0 ug/mL, and the x-axis from 0 to 30 hours. Wildtype mice show higher plasma concentrations that decrease over time, while albumin-/- mice show significantly lower concentrations.

Parameter	Unit	WT Value	Alb-/- Value
Half-life	hours	33 ± 24	15 ± 8
Cmax	ug/mL	0.15 ± 0.1	0.13 ± 0.1
Tmax	hours	4	24
Vd	mL/kg	129 ± 726	1191 ± 708
Clearance	mL/kg/h	24.1 ± 1.1	66.7 ± 41.1
AUC	ug/mL/h	7.24 ± 1	1.25 ± 0.21

Table 2. PFBS pharmacokinetic parameters in wildtype and albumin deficient mice. Parameters were calculated as discussed in Methods. Data are presented as mean ± SEM. Significant differences are indicated by asterisks (*p < 0.05, **p < 0.01, ***p < 0.001, ****p < 0.0001). The error bars represent ± SEM. N = 3-6.

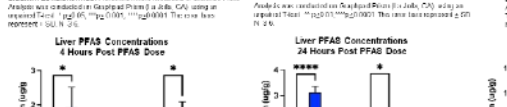


Figure 5. Albumin deficiency increased PFHxS and 6:2FTS liver concentrations 24 hours after administration of a single oral dose of a PFAS cocktail (n=3-6/group). The graph shows liver PFAS concentrations (ug/g) 24 hours post PFAS dose for PFHxS and 6:2FTS in wildtype and albumin-/- mice. The y-axis is concentration (ug/g). For PFHxS, albumin-/- mice show significantly higher liver concentrations compared to wildtype. For 6:2FTS, albumin-/- mice also show significantly higher liver concentrations.

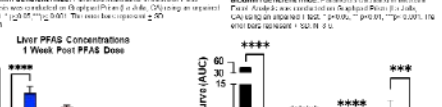


Figure 6. Albumin deficiency increased PFHxS but decreased L-PFOS, 6:2FTS, and PFBS liver concentrations 1 week after PFAS dosing (n=3-6/group). The graph shows liver PFAS concentrations (ug/g) 1 week post PFAS dose for PFHxS, L-PFOS, 6:2FTS, and PFBS in wildtype and albumin-/- mice. The y-axis is concentration (ug/g). For PFHxS, albumin-/- mice show significantly higher liver concentrations. For L-PFOS, 6:2FTS, and PFBS, albumin-/- mice show significantly lower liver concentrations.

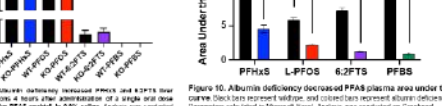
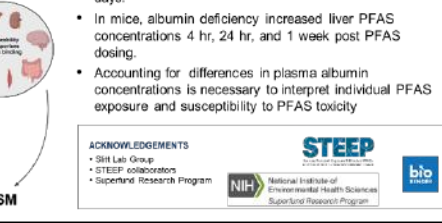


Figure 7. Albumin deficiency decreased PFAS plasma area under the curve (AUC) for PFHxS, L-PFOS, 6:2FTS, and PFBS over 84 days (n=3-6/group). The graph shows AUC (ug/dL) for PFHxS, L-PFOS, 6:2FTS, and PFBS in wildtype and albumin-/- mice. The y-axis is AUC (ug/dL). For PFHxS, albumin-/- mice show significantly higher AUC. For L-PFOS, 6:2FTS, and PFBS, albumin-/- mice show significantly lower AUC.

CONCLUSION

- In mice, albumin deficiency decreased total systemic exposure to PFHxS, L-PFOS, 6:2FTS and PFBS over 84 days.
- In mice, albumin deficiency increased liver PFAS concentrations 4 hr, 24 hr, and 1 week post PFAS dosing.
- Accounting for differences in plasma albumin concentrations is necessary to interpret individual PFAS exposure and susceptibility to PFAS toxicity.



ACKNOWLEDGMENTS: SHI Lab Group, STEEP collaborators, Sponsoring Research Program, NIH, National Institute of Environmental Health Sciences Superfund Research Program, STEEP

Albumin is a critical factor contributing to plasma per- and polyfluoroalkyl substances (PFAS) concentration and retention *in vivo*

Olga Skende, Sangwoo Ryu, Simon Vojta, Jitka Becanova, Fabian Fischer, Jingmei Zeng, Rainer Lohmann, Angela Slitt

Per- and polyfluoroalkyl substances (PFAS) are a class of synthetic molecules composed of chain-linked carbon-fluorine bonds. There are 10,000+ PFAS, with perfluorooctane sulfonate (PFOS) and perfluorobutane sulfonate (PFBS) being some most frequently detected PFAS in serum of the United States general population. Newer PFAS, such as perfluorobutane sulfonic acid (PFBS) and 6:2-fluorotelomer sulfonic acid (6:2 FTS), are now also detected in human serum. As a class of chemicals, PFAS undergo limited biotransformation and are slowly excreted. PFOS and PFHxS exhibit a strong binding affinity for serum albumin, which is hypothesized to be the predominant mechanism that dictates their slow elimination from the body. It is thought that albumin binding retains PFAS in circulation and prevents PFAS from undergoing renal excretion. However, to date, albumin binding as a critical factor for PFAS elimination has only been studied and modeled using *in vitro* assays. Thus, it was hypothesized that mice deficient in albumin would have reduced plasma PFAS concentrations and increased tissue PFAS concentrations due to decreased PFAS retention in plasma by albumin. C57BL/6J mice expressing (Alb+/+) or lacking (Alb-/-) albumin were administered a single oral dose of a PFAS cocktail consisting of 0.1 mg/kg PFOS, PFHxS, PFBS, and 6:2FTS at equal ratios (10 mg/kg, n=3-6/group). Plasma was collected at 1, 4, 24, and 72 hours, followed by 1, 2, 4, 6, 8, and 10 weeks. Tissues were collected at 4 hours, 24 hours and 1 week. At 12 weeks post PFAS dosing, plasma and tissues were collected. Albumin deficiency decreased PFHxS, PFBS, 6:2FTS, and PFOS AUC to 9.8%, 7.6%, 17.2%, and 38.7%, respectively, of the controls. Albumin deficiency increased PFHxS and PFBS liver concentrations after 4 hours, PFHxS and 6:2FTS concentrations after 24 hours, and PFHxS concentrations 1 week after PFAS dosing. This is the first study to demonstrate that albumin is a critical factor contributing to plasma and liver concentration and retention of a PFAS cocktail *in vivo*. This project highlights variability in albumin levels, influenced by disease and genetic factors, as a potential mechanistic contributor to inter-individual differences in PFAS exposure and toxicity.

Cluster of differentiation 36 (CD36) has a modest effect on Perfluorooctanesulfonic acid (PFOS)-induced liver alterations and disposition

Jingmei Zeng¹, Juliana Agudelo Areiza¹, Olga Skende¹, Chang Liu¹, Simon Vojta², Jitka Becanova², Fabian C. Fischer¹, Angela L. Slitt¹

¹Department of Biomedical and Pharmaceutical Sciences, University of Rhode Island, Kingston, RI (USA)
²Graduate School of Oceanography, University of Rhode Island, Kingston, RI (USA)



ABSTRACT

Perfluorooctanesulfonic acid (PFOS) is a synthetic perfluoroalkyl substance widely present in the environment that is persistent and associated with adverse human health effects. PFOS exposure in humans is associated with elevation of serum liver injury markers and liver disease. In preclinical models, such as mice, PFOS administration markedly increases liver weight. Cluster of differentiation 36 (CD36) is a membrane glycoprotein that facilitates the import of long-chain fatty acids into cells and contributes to lipid accumulation within the liver. Because the chemical structure of PFOS closely resembles a long-chain fatty acid, it has been hypothesized that CD36 may facilitate PFOS uptake into the liver, and that CD36 is a critical mediator for PFOS uptake and adverse liver effects. In vitro and in vivo studies have shown that CD36 is a critical mediator for PFOS uptake and adverse liver effects. In vitro and in vivo studies have shown that CD36 is a critical mediator for PFOS uptake and adverse liver effects. In vitro and in vivo studies have shown that CD36 is a critical mediator for PFOS uptake and adverse liver effects.

INTRODUCTION

- CD36 is a membrane-associated protein, responsible for mediating the uptake of long chain fatty acids (LCFA)
- Due to the similar structures between per- and polyfluoroalkyl substances (PFAS) and LCFA, CD36 may facilitate the PFAS uptake into the liver
- Proteomic pathway analysis demonstrated that PFOS has the strongest binding affinity for CD36

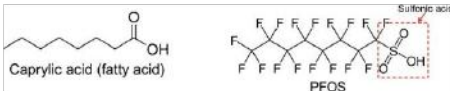
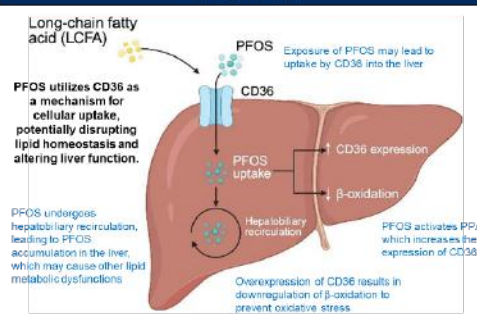


Figure 1. Chemical structure of a fatty acid chain and PFOS.

Ligand	ID	Chemical Structure	Binding
Palmitic acid	PLMS12	C ₁₆ H ₃₂ O ₂	-7.29
Perfluorononanoic acid	PFNA	C ₉ HF ₁₇ O ₂	-11.42
Perfluorooctanesulfonic acid	PFOS	C ₈ HF ₁₇ O ₂ S	-12.56
Perfluorooctanoic acid	PFOA	C ₈ HF ₁₅ O ₂	-10.64
Perfluorohexanesulfonic acid	PFHxS	C ₆ HF ₁₃ O ₂ S	-10.56
GenX	GenX	C ₈ H ₁₁ NO ₃	-9.27
Perfluorobutanesulfonic acid	PFBS	C ₄ HF ₉ O ₂ S	-8.77
Perfluorobutanoic acid	PFBA	C ₄ HF ₇ O ₂	-6.96

Figure 2. Molecular docking analysis shows that PFAS exhibit a strong binding affinity to CD36, suggesting potential competitive uptake with LCFA and lipid metabolism disruption. The binding values are in kcal/mol.

HYPOTHESIS



METHODS



Treatment Method: C57BL/6J mice expressing CD36 (CD36^{fl/fl}) or lacking CD36 (CD36^{-/-}) received daily oral doses of vehicle (0.5% Tween20 in 1X PBS) or 10 mg/kg PFOS (10 mg/kg PFOS in 0.5% Tween20 in 1X PBS) for 7 days. After the final dose, perfusion was performed for lipid extraction, and liver and plasma samples were analyzed for cholesterol and triglycerides.

LIVER ENDPOINT RESULTS

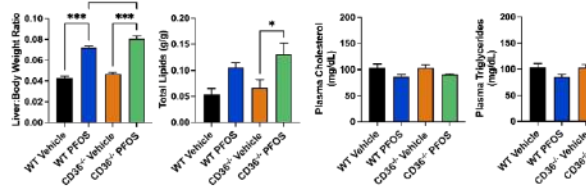


Figure 4. PFOS exposure increased liver-to-body weight ratio and total lipids of WT and CD36^{-/-} mice. Mice (n=6) were administered daily oral doses with either vehicle (0.5% Tween20 in 1X PBS) or 10 mg/kg PFOS formulated in vehicle for seven consecutive days. Analysis was conducted on GraphPad Prism (San Jose, CA) using unpaired ANOVA followed by a comparison test using Sidak's test. * p < 0.05, ** p < 0.01, *** p < 0.001.

RESULTS

CD36 PFOS Concentrations in Liver

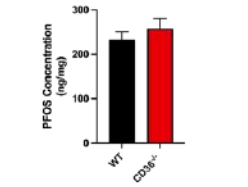


Figure 3. Deletion of CD36 did not alter PFOS concentrations in the liver. Wild-type and CD36^{-/-} mice (n=6/treatment group) were administered daily oral doses of 10 mg/kg PFOS (10 mg/kg PFOS in 0.5% Tween20 in 1X PBS) for seven consecutive days. PFOS concentrations were measured using Sciex X5000 GC/MS-MSM system (Framingham, MA). Data were analyzed in GraphPad Prism (La Jolla, CA) using a two-tailed unpaired t-test and results are presented as mean ± SEM.

Figure 5. PFOS exposure had no effect on plasma cholesterol and plasma triglycerides of WT and CD36^{-/-} mice. Mice (n=6) were administered daily oral doses of either vehicle (0.5% Tween20 in 1X PBS) or 10 mg/kg PFOS formulated in vehicle for seven consecutive days. Analysis was conducted on GraphPad Prism (San Jose, CA) using unpaired ANOVA followed by a comparison test using Sidak's test. * p < 0.05, ** p < 0.01, *** p < 0.001.

Figure 6. PFOS exposure increased liver triglycerides of WT mice. Mice (n=6) were administered daily oral doses of either vehicle (0.5% Tween20 in 1X PBS) or 10 mg/kg PFOS formulated in vehicle for seven consecutive days. Analysis was conducted on GraphPad Prism (San Jose, CA) using unpaired ANOVA followed by a comparison test using Sidak's test. * p < 0.05, ** p < 0.01, *** p < 0.001.

CONCLUSION

- Oral PFOS administration increased the liver-to-body weight ratio by approximately 65-70% and total hepatic lipids by ~97% in both wild-type and CD36^{-/-} mice, while liver triglycerides increased by ~60% in wild-type only.
- Deletion of CD36 did not significantly alter PFOS concentrations in the liver.
- Hepatic proteomics showed overlapping PFOS-associated alterations in lipid metabolism and oxidative stress pathways in both WT and CD36^{-/-} mice, suggesting that PFOS-induced hepatocellular metabolic stress occurs independently of CD36.

FUTURE DIRECTIONS

- Measure PFOS concentrations in the plasma and other relevant tissues.
- Histopathological analysis of liver tissues to evaluate PFOS-associated steatosis between WT and CD36^{-/-} mice.

ACKNOWLEDGEMENTS

- SR Lab Grant
- STEEP Collaborator
- Biomedical Research Program

The work was supported by grant P43ES027278



Cluster of differentiation 36 (CD36) has a modest effect on Perfluorooctanesulfonic acid (PFOS)-induced liver alterations and deposition

Jingmei Zeng, Juliana Agudelo Areiza, Olga Skende, Chang Liu, Simon Vojta, Jitka Becanova, Fabian C. Fischer, Angela L. Slitt

Perfluorooctanesulfonic acid (PFOS) is a synthetic per- and polyfluoroalkyl substance that is environmentally persistent and associated with adverse health effects. In humans, PFOS exposure has been linked to elevated serum liver injury markers and liver disease, while in mice, PFOS administration markedly increases liver weight. Cluster of differentiation 36 (CD36) is a membrane glycoprotein that facilitates long-chain fatty acid uptake into cells and contributes to hepatic lipid accumulation. Because PFOS structurally resembles a long-chain fatty acid, CD36 has been proposed as a potential mediator of PFOS uptake into the liver and a contributor to PFOS-induced hepatotoxicity. To investigate the in vivo relevance of CD36, wild-type (WT, C57BL/6J) and global CD36 knockout (CD36^{-/-}, B6.129S1-Cd36tm1Mfe/J) mice aged 7–9 weeks were administered vehicle (0.5% Tween 20 in PBS) or PFOS (10 mg/kg in 0.5% Tween 20 in PBS) by oral gavage for seven days. PFOS increased liver-to-body weight ratio by 66% in WT mice and 72% in CD36^{-/-} mice. Total liver lipid concentration increased by approximately 97% in both genotypes. Liver triglycerides increased by 62.3% in WT mice and 19% in CD36^{-/-} mice. However, PFOS concentrations in liver were similar between WT and CD36^{-/-} mice, suggesting that CD36 deletion does not significantly alter PFOS hepatic deposition. Proteomic pathway analysis demonstrated upregulation of PPARα/RXR activation and fatty acid β-oxidation, while also confirming hepatic mitochondrial dysfunction. These pathway-level changes were consistent with a PFOS-induced hepatic response rather than an effect driven by CD36. Overall, these findings suggest that CD36 has a modest effect on PFOS-induced liver alterations.

Contributions of Neutrophil Extracellular Traps to Vascular Pathologies in CAA Model rTg-DI



Dakota Hunter^{1,2}, Riley Sullivan^{1,2}, Feng Xu^{1,2}, Judianne Davis^{1,2}, William Van Nostrand^{1,2}, Joseph Schrader^{1,3}
¹George and Ryan Institute for Neuroscience, University of Rhode Island
²Department of Biomedical and Pharmaceutical Sciences, College of Pharmacy, University of Rhode Island
³Department of Pharmacy Practice and Clinical Research, College of Pharmacy, University of Rhode Island



Abstract

- CAA is characterized by A β deposition in cerebral blood vessels walls, clinically manifesting with microbleeds, intracranial hemorrhage, and cognitive decline
- Utilized the rTg-DI transgenic rat model, which carries Dutch/flowa mutations in humanized-APP, producing age-dependent vascular A β deposition.
- First evidence of NET formation in CAA, confirmed by presence of CitH3, MPO, NE markers in regions of pathology.
- Robust microglial recruitment and activation observed in affected areas, indicating a broader neuroinflammatory response.
- Structurally distinct A β fibril species differentially drive neutrophil recruitment and NETosis.

Introduction

- CAA is a common age-related cerebral small-vessel disease, and co-morbidity of Alzheimer's disease.
- Over 25% above 50, and 50% above 80 years old have moderate to severe CAA.
- Neutrophils are innate immune cells, that comprise many WBCs.
- NETs or neutrophil extracellular trap are used to kill pathogens, matrix of DNA and proteins.
- NETs act as a molecular scaffold for thrombus and involved in platelet activation and coagulation.
- Currently, the pathological link between vascular A β deposition, micro thrombosis, and neuroinflammation in CAA is unknown.

Methodology

- Heterozygote rTg-DI rodents were raised until 12 months, and tissues were taken and perfused. Brains were sectioned sagittally and in the sagittal plane, starting from the corpus callosum to the cerebral cortex.
- Immunohistochemistry was done using a SuperBlock™ Blocking Buffer from ThermoFisher, and 0.3% Triton-X-100, and then stain using primary antibodies (1:200 standard dilution), and then followed up the next day with secondary antibodies (1:1000 standard dilution).
- rTg-DI microglia were isolated from rTg-DI rodents and cultured using standard cellular media. Upon setting up experimental conditions, cells were fixed in 4% paraformaldehyde, and then blocked using SuperBlock™ Blocking Buffer from ThermoFisher, and 0.3% Triton-X-100, and then stain using primary antibodies (1:200 standard dilution), and then followed up the next day with secondary antibodies (1:1000 standard dilution).
- Regional proteomic comparison of early and late disease stage rTg-DI CAA rats. Microdissection was done to isolate cortex, hippocampus, thalamus and corpus callosum (CC), and lysate was run through the Sequential Window Acquisition of Theoretical Mass Spectra (SWATH-MS) and analyzed through the Ingenuity Pathway Analysis.

Results

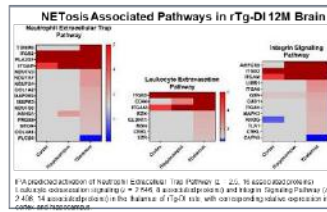


Figure 1: Heatmap showing NETosis Associated Pathways in rTg-DI 12M Brain. The heatmap compares pathways like Neutrophil Extracellular Trap Pathway, Leukocyte Extracellular Matrix Pathway, and Inflammation Signaling Pathway across different brain regions (Cortex, Hippocampus, Thalamus) in wild-type and rTg-DI mice.

Neutrophils in rTg-DI Occluded Cerebral Vessels

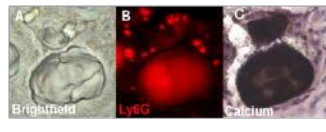


Figure 2: Micrographs showing neutrophils in occluded cerebral vessels. Panel A shows a brightfield image, B shows Ly6G staining, and C shows calcium staining. Scale bars are provided.

NETs in rTg-DI Occluded Cerebral Vessels

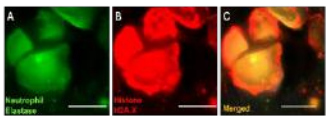


Figure 3: Fluorescence microscopy images showing NETs in occluded cerebral vessels. Panels A, B, and C show individual channels for neutrophil elastase, citrullinated histone 3, and merged images. Scale bars are provided.

Presence of Activated Microglia Around NET Markers

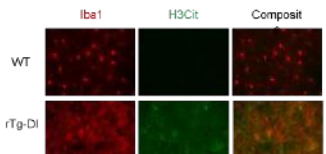


Figure 4: Immunofluorescence images showing activated microglia around NET markers. Panels show Iba1, H3Cit, and Composit staining in WT and rTg-DI mice. Scale bars are provided.

Presence of Additional NET Marker in rTg-DI Thalamus

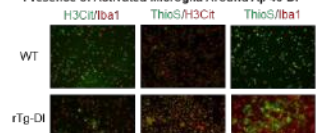


Figure 5: Immunofluorescence images showing additional NET markers in rTg-DI thalamus. Panels show MPO, citrullinated histone 3, and MPO/citrullinated histone 3 staining in WT and rTg-DI mice. Scale bars are provided.

Presence of Activated Microglia Around A β -40

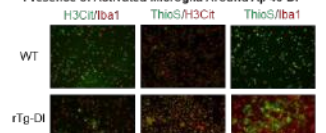


Figure 6: Immunofluorescence images showing activated microglia around A β -40. Panels show H3Cit/Iba1, ThioS/H3Cit, and ThioS/Iba1 staining in WT and rTg-DI mice. Scale bars are provided.

Conclusions

- The population is getting older, which is leading to an increase in age-related disorders.
- CAA is a cerebrovascular disorder where A β deposition in vasculature leads to brain bleeds
- The rTg-DI rat model displays a punctual and localized CAA pathology
- Neutrophils release extracellular traps in response to both pathogens and damage and may act as the link between vascular deposition and CAA symptoms.
- Within the rTg-DI model, neutrophil markers are not only present, but also abundant and confirmed with multiple markers.
 - Additionally, they are present in occluded vessels and respond to A β -40-DI

Future Directions

- The population is getting older, which is leading to an increase in age-related disorders.
- CAA is a cerebrovascular disorder where A β deposition in vasculature leads to brain bleeds
- The rTg-DI rat model displays a punctual and localized CAA pathology
- Neutrophils release extracellular traps in response to both pathogens and damage and may act as the link between vascular deposition and CAA symptoms.
- Within the rTg-DI model, neutrophil markers are not only present, but also abundant and confirmed with multiple markers.
 - Additionally, they are present in occluded vessels and respond to A β -40-DI

References

- Schrader et al. (2024). Cerebral Proteomic Changes in the rTg-D Rat Model of Cerebral Amyloid Angiopathy Type-2 With Cortical Microhemorrhages and Cognitive Impairments
- Schrader et al. (2025). Parenchymal and Dyschoric Fibrillar Amyloid Pathology in the rTg-D Rat Model of Cerebral Amyloid Angiopathy Type-2
- Davis et al. (2022). rTg-D: A novel transgenic rat model of cerebral amyloid angiopathy Type-2

Acknowledgements

I would like to thank Dr. Joseph Schrader for his guidance, and mentorship during this project. Thank you to Riley Sullivan, Erica Kilbourne, Britany Monle, Feng Xu, and Judianne Davis for their support during this project. This work was supported in part by NIH grant NS104147, R03AG085082, and the Advance RI-CTR Pilot Award (IDEA-CTR U54GM115877)


Contributions of Neutrophil Extracellular Traps to Vascular Pathologies in CAA Model rTg-DI

Dakota Hunter, Riley Sullivan, Feng Xu, Judianne Davis, William Van Nostrand, Joseph Schrader

Cerebral amyloid angiopathy (CAA) is a cerebrovascular disorder characterized by progressive deposition of amyloid- β (A β) peptides within cerebral blood vessel walls, affecting an estimated 60% of individuals over 85. CAA is strongly associated with microbleeds, intracranial hemorrhage, and cognitive decline, yet its neuroimmune mechanisms remain poorly understood.

Using the preclinical rTg-DI transgenic rat model, we investigated the role of neutrophils and neutrophil extracellular traps (NETs) in CAA pathology. NETs are web-like structures released during innate immune responses that promote thrombus formation and sterile inflammation. Immunohistochemical analyses revealed NET markers, such as citrullinated histone H3 (H3Cit), myeloperoxidase (MPO), and neutrophil elastase (NE), within regions of active vascular A β deposition, alongside robust microglial activation. This represents the first evidence of NET formation in CAA.


We hypothesize that distinct A β fibril species differentially modulate NETosis, driving vascular deterioration. Future work will characterize fibril-neutrophil interactions in vitro and evaluate pharmacological NETosis inhibition as a therapeutic strategy.



Determine the Role of Mitochondrial Dysfunction in Age-Associated Sarcopenia

Bibi SJ^{1,2}, Tobias-Wallingford H^{1,2}, Jaime M. Ross^{1,2}, Giuseppe Coppotelli^{1,2}

¹Department of Biomedical and Pharmaceutical Sciences, College of Pharmacy, University of Rhode Island, Kingston, RI
²George and Anne Ryan Institute for Neuroscience, University of Rhode Island, Kingston, RI



INTRODUCTION

Mitochondrial Dysfunction in the Aging Process

- Mitochondrial dysfunction is a hallmark of aging and leads to impaired oxidative phosphorylation, increased ROS, and disrupted energy homeostasis.
- Aging tissues including neurons, astrocytes, cardiac muscle, and skeletal muscle show abnormal glycogen accumulation, suggesting impaired glycogen metabolism.
- Although glycogen buildup is associated with aging and metabolic stress, the link between mitochondrial dysfunction and glycogen accumulation in muscle is not well understood.
- The potential role of this glycogen dysregulation in sarcopenia (age-related muscle loss) remains unclear.




Figure 1. The 12 Hallmarks of Aging. (Lopez et al., 2023).

Hypothesis: Mitochondrial dysfunction promotes free glycogen accumulation in metabolically active tissues, and this abnormal glycogen buildup contributes to impaired muscle metabolic and contractile function, linking mitochondrial dysfunction to sarcopenia.

Mitochondrial DNA (mtDNA) Mutator Mouse Model

- The mtDNA mutator mouse was the first model to experimentally test the contribution of mitochondrial dysfunction driven by mtDNA mutations in the aging process.
- mtDNA Mutator mice express a proof-reading deficient version (D257A) of the nuclear-encoded mtDNA polymerase-gamma (PolgA), causing increased mtDNA mutations and deletions.
- These mice show premature signs of aging, such as hair loss (alopecia), graying fur, kyphosis, reduced subcutaneous fat, reduced body size, decrease in lifespan, etc.

Animals Used in the Study:

- PolgA^{D257A/D257A} mtDNA mutator mice and age-matched wild-type controls. Tissues were collected at age 9 months of age.

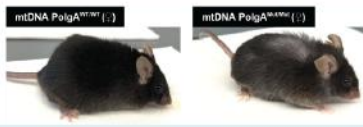


Figure 2. Representative images of 9-month-old mtDNA PolgA^{WT} (♀) and mtDNA PolgA^{mutator} (♀) mutator mice. Mutator mice carry a proofreading-deficient PolgA allele (D257A), leading to increased mtDNA mutations.

RESULTS

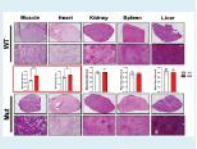


Figure 3. PAS staining and glycogen quantification in tissues from 9-month-old mtDNA mutator and WT mice. Representative 5X tiled images (top row) and 20X high-magnification images (bottom row) showed PAS-positive glycogen deposits across tissues. Heart and skeletal muscle from mtDNA mutator mice exhibited a marked increase in PAS staining, indicating greater glycogen accumulation ($p < 0.05-0.001$). Kidney, spleen, and liver showed no notable differences between genotypes.

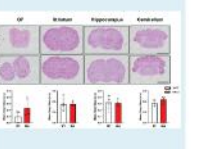


Figure 4. PAS staining and glycogen quantification in brain tissues of 9-month-old mtDNA mutator and WT mice. Representative images at 5X (top row) and 20X (high-magnification, bottom) showed PAS-positive glycogen deposits across multiple brain regions. Quantification revealed no significant differences between genotypes in any of the four regions. Although mtDNA mutator mice showed slightly higher PAS intensity in the olfactory bulb and cerebellum, these differences were not statistically significant.

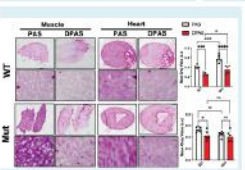


Figure 5. PAS and DPAS staining revealed free glycogen accumulation in muscle and heart tissues. Frozen/OCT-embedded muscle and heart sections (14 μ m) were stained with PAS and diastase-PAS (DPAS) to distinguish total glycogen (PAS) from DPAS signal. Representative tiled low-magnification (5X) and high-magnification (20X) images demonstrated robust PAS staining in mtDNA mutator tissues compared to WT mice, with DPAS digestion reducing staining intensity where glycogen was diastase-sensitive. **Muscle:** mtDNA mutator samples showed visibly stronger PAS staining that was largely eliminated after DPAS treatment, indicating elevated free glycogen. **Heart:** PAS and DPAS staining appeared to be similar, suggesting minimal free glycogen accumulation. Quantification of mean gray values showed a significant PAS-to-DPAS decrease in muscle, particularly in mutator mice ($*p < 0.05$ to $**p < 0.001$), confirming high levels of free glycogen. No significant PAS-DPAS difference was detected in heart tissue.

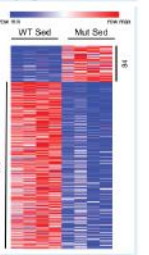


Figure 6. Proteomic analysis of deregulated proteins in skeletal muscle of 9-month-old mtDNA PolgA mutator mice. Heatmap of differentially expressed proteins reveals coordinated downregulation (blue) of proteins involved in glycogen breakdown and glucose utilization, alongside upregulation (red) of stress-response and mitochondrial compensatory proteins in mutator mice.

RESULTS CONT.

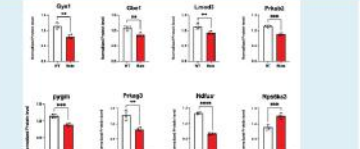
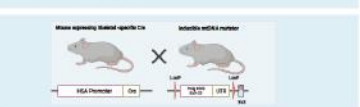


Figure 7. Differential protein expression in mtDNA mutator and WT mice. Quantitative analysis of normalized protein levels showed that the majority of proteins (Gys1, Gbe1, Lmo3, Pfkfb2, Pymg, Pfkfb3, and Ndufs3) were significantly downregulated in mtDNA mutator mice compared to WT controls ($p < 0.05-0.001$). In contrast, Rps33 was significantly upregulated in mtDNA mutator mice.

IN-VIVO VALIDATION IN MUSCLE

- Cre-loxP method is being used to generate a skeletal muscle-specific, inducible mtDNA mutator mouse model.
- Enables targeted induction of mitochondrial dysfunction in muscle, allowing for the study of aging-like phenotypes without systemic effects.



CONCLUSIONS & FUTURE DIRECTIONS

- Systemic mitochondrial dysfunction leads to abnormal glycogen accumulation in skeletal muscle and heart from mtDNA mutator mice.
- TMT proteomic profiling revealed dysregulation of several proteins involved in glycogen synthesis and breakdown in mtDNA mutator mice.
- Validation of mass-spectrometry (MS) hits by Western blot.

ACKNOWLEDGEMENTS

I would like to thank my supervisors Dr. Jaime Ross and Dr. Giuseppe Coppotelli, as well as the members of the Ross Lab: Hannah Tobias-Wallingford, Sydney Bartman, Lauren Gasper, and Mackenzie Pawlik. We thank the NIH Office of the Director (R21OD037651), R21OD037651, NIA/NIH R01AG092603, the Roddy Foundation, the College of Pharmacy at URI, the George & Anne Ryan Institute of Neuroscience at URI, and RH-INSRE.

Determining the Role of Mitochondrial Dysfunction in Age-Associated Sarcopenia

Bibi SJ, Tobias-Wallingford H, Jaime M. Ross, Giuseppe Coppotelli

As global life expectancy increases, the prevalence of age-related diseases such as sarcopenia continues to rise. Although the cellular mechanism of aging is not fully understood, gerontologists have identified several major hallmarks of aging including epigenetic alteration, chronic inflammation and mitochondrial dysfunction. Among these, mitochondrial dysfunction is a key hallmark of aging, characterized by cellular and tissue damage, increased reactive oxygen species, and impaired glucose metabolism. Age-associated glycogen accumulation has been observed in various aging cell types, including neurons, astrocytes, and muscle cells. In this study, we investigated glycogen accumulation in association with mitochondrial impairment using the mtDNA mutator (PolgAD257A/D257A) mouse, a model of accelerated aging caused by systemic mitochondrial dysfunction due to increased mitochondrial DNA (mtDNA) mutations and deletions. Histological analyses with Periodic Acid-Schiff (PAS), diastase-PAS (dPAS) staining and colorimetric glycogen quantification analyses revealed that mitochondrial dysfunction promotes free glycogen deposition in skeletal muscle and to some extent cardiac tissue. These findings suggest that mitochondrial dysfunction disrupts glycogen metabolism, leading to abnormal glycogen processing and free glycogen accumulation in metabolically active tissues. We propose that this glycogen buildup may impair contractile and metabolic functions, thereby contributing to sarcopenia, the age-related loss of muscle mass and strength. Future studies will further investigate the relationship between glycogen accumulation and age-associated sarcopenia using a muscle-specific mitochondrial dysfunction mouse model, as well as determine whether interventions such as exercise can mitigate these effects by enhancing oxidative metabolism and promoting efficient glycogen utilization. Together, these findings identify disrupted glycogen metabolism as a potential biochemical hallmark linking mitochondrial dysfunction to systemic aging and muscle decline.

Keywords: Mitochondrial dysfunction, Glycogen metabolism, Sarcopenia, PAS staining, Aging



THE UNIVERSITY OF RHODE ISLAND COLLEGE OF PHARMACY

Development and optimization of liquid chromatography-tandem mass spectrometry (LC-MS/MS) methods to measure bile acids in human plasma

Daniella R. Cross¹, Mariam O. Oladepo¹, David Assis², and Nisanne S. Ghonem¹

¹URI College of Pharmacy, Biomedical and Pharmaceutical Sciences, Kingston, RI

²Yale School of Medicine, Section of Digestive Diseases, Liver Center, New Haven, CT



YALE

INTRODUCTION

- Bile acids facilitate compound absorption, digestion, and elimination
- There are three main types of bile acids: primary-CA, CDCA, secondary-DCA, LCA, HCA, HDCA conjugated; bile acids conjugated to taurine, glycine, glucuronic acid, or sulfate
- Primary biliary cholangitis (PBC) and primary sclerosing cholangitis (PSC) are chronic cholestatic liver diseases characterized by the accumulation of toxic bile acids in the liver.
- The peroxisome proliferator-activated receptor (PPAR) has three isoforms (α, β, γ), some of which regulate bile acid metabolism
- We previously demonstrated that combination treatment with ursodeoxycholic acid (UDCA) + fenofibrate (PFARA agonist, FDA-approved to treat dyslipidemia) reduces serum bile acid toxicity in PBC and PSC¹, presented in Figure 1.
- Previously, bile acid data were obtained with a Shimadzu Nexera UPLC system coupled to a Sciex Q-TrappESI system² which has been replaced with an Agilent 6470 Triple Quadrupole Liquid Chromatography-Tandem Mass Spectrometry (LC-MS/MS) System.



Figure 1. Effects of PPAR α activation on bile acid metabolism¹.

OBJECTIVE

Develop LC-MS/MS methods (Agilent) to quantify primary, secondary, glycine- and taurine-conjugated bile acids in persons with PBC and PSC.

METHODS

- Bile acids are extracted from human plasma by protein precipitation. Plasma samples are diluted in acetonitrile, vortexed, and centrifuged (10,000 g x 15 min, 4°C). Supernatants are dried (45°C).
- Samples are reconstituted in 5/50/50 methanol/water either 1:1 or 4:1 (sample:volume) for detection and quantification.
- Bile acids are separated with a reverse-phase column and quantified by LC-MS/MS (Agilent 6470 QQQ, RI-MS/MS).
- Two chromatographic methods were developed to capture variations in compound polarity (internal standard), detailed in Table 1 & 2.
- 1. 70-minute:** CA, CA64⁴, CDCA, DCA, DCA64⁴, GCA, GCDCa, GCA64⁴, HDCA, TCDCa, TDCA, TLCA, TUDCA, and UDCA
- 2. 10-minute:** C4, LCA, LCA64⁴, and LCA-S

ABBREVIATIONS

C4: 1- α -hydroxy-4-cholestene-3-one; CA: cholic acid; CDCA: chenodeoxycholic acid; DCA: deoxycholic acid; GCA: glycocholic acid; GCDCa: glycochenodeoxycholic acid; GDCA: glycodeoxycholic acid; HCA: hyocholic acid; HDCA: hypodeoxycholic acid; LCA: lithocholic acid; LCA-S: lithocholic acid-sulfate; TCA: taurocholic acid; TCDCa: taurochenodeoxycholic acid; TDCA: taurodeoxycholic acid; TLCA: taurolicholic acid; TUDCA: tauroursodeoxycholic acid; UDCA: ursodeoxycholic acid

RESULTS

A. Mobile phase gradient for chromatographic separation.

B. Dynamic multi-reaction monitoring (dMRM) parameter for quantifier ions.

Time (min)	%A (water + 0.2% NH ₄ OH)	%B (acetonitrile)	Flow rate (mL/min)
0	99	1	1.2
10	99	1	1.2
15	99	1	1.2
20	99	1	1.2
25	99	1	1.2
30	99	1	1.2
35	99	1	1.2
40	99	1	1.2
45	99	1	1.2
50	99	1	1.2
55	99	1	1.2
60	99	1	1.2
65	99	1	1.2
70	99	1	1.2
75	99	1	1.2
80	99	1	1.2
85	99	1	1.2
90	99	1	1.2
95	99	1	1.2
100	99	1	1.2

Table 1. LC-MS/MS conditions for the 70-minute method.

Time (min)	%A (water + 0.2% NH ₄ OH)	%B (acetonitrile)	Flow rate (mL/min)
0	99	1	1.2
10	99	1	1.2
15	99	1	1.2
20	99	1	1.2
25	99	1	1.2
30	99	1	1.2
35	99	1	1.2
40	99	1	1.2
45	99	1	1.2
50	99	1	1.2
55	99	1	1.2
60	99	1	1.2
65	99	1	1.2
70	99	1	1.2
75	99	1	1.2
80	99	1	1.2
85	99	1	1.2
90	99	1	1.2
95	99	1	1.2
100	99	1	1.2

Table 2. LC-MS/MS conditions for the 10-minute method.

Concn. (ng/mL)	20,000	15,000	10,000	7,500	5,000	2,500	1,000	750	500	250	150	75	50	25	15	7.5	5	2.5	1
Dilution																			
Extraction	1:1	1:1	1:1	1:1	1:1	1:1	1:1	1:1	1:1	1:1	1:1	1:1	1:1	1:1	1:1	1:1	1:1	1:1	1:1
Extraction	4:1	4:1	4:1	4:1	4:1	4:1	4:1	4:1	4:1	4:1	4:1	4:1	4:1	4:1	4:1	4:1	4:1	4:1	4:1

Table 3. Bile acid standards for current (Agilent) LC-MS/MS methods. The full standard curve for the 70 minute method (1-20,000 ng/mL) and the 10-minute method (1-5,000 ng/mL).

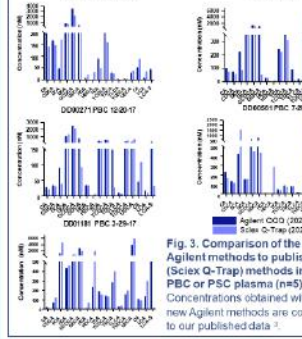


Figure 3. Comparison of the new Agilent methods to published (Sciex Q-Trapp) methods in human PBC or PSC plasma (n=5). Concentrations obtained with the new Agilent methods are comparable to our published data².

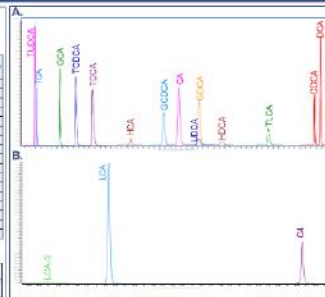


Figure 2. Representative MRM chromatograms of bile acid standards. Instrument signal plotted against method acquisition time. Peaks are from the quantifier ions of each bile acid. A. Chromatogram of a 20,000 ng/mL standard (1:1 extraction) run with the 70-min method. B. Chromatogram of a 5,000 ng/mL standard (4:1 extraction) run with the 10-min method.

RESULTS (CONT.)

QC AFTER OPTIMIZATION

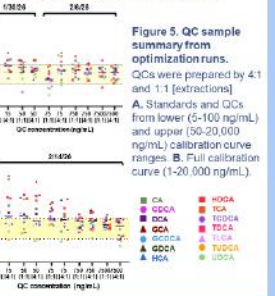


Figure 5. QC sample summary from optimization runs. QC samples were prepared by 4:1 and 1:1 [extractions]. A. Standards and QCs from lower (5-100 ng/mL) and upper (50-20,000 ng/mL) calibration curve ranges. B. Full calibration curve (1-20,000 ng/mL).

CONCLUSIONS

- Two LC-MS/MS methods (Agilent) have been developed to quantify bile acids in human plasma obtained from patients with PBC and PSC (Yale Liver Center, New Haven, CT).
 - Elimination of some (4:1) standards has improved method efficiency.
 - Further method optimization is required to improve QC accuracy for confidence in quantifying patient samples with unknown bile acid concentrations.
 - Additional optimization is ongoing to improve QC accuracy and the methods accordingly.
 - Compound carryover may contribute to inaccurate low QC sample concentrations, investigations underway
- Next steps:**
- Determine the source of compound carryover
 - Column extend column wash time within Agilent method
 - System e.g. injection needle, stronger needle washes
- Run a complete standard curve and set of QC samples once carryover has been eliminated to evaluate accuracy
 - Quantify bile acids in patients with PBC and PSC (n: 100)
 - Develop additional LC-MS/MS methods to expand our bile acid analyses, e.g., urinary, and bile acid glucuronides.

ACKNOWLEDGMENTS

Research presented in this publication was supported in part and made possible by equipment and services provided by the Institutional Development Award (IDeA) Network for Biomedical Research Excellence from the NIGMS of the NIH P20: 084133425 (URI) and the Shih O. Conte Digestive Diseases Research Core Center, P30DK093588 (Yale Liver Center). REFERENCES: 1. Galucci, GM et al (2021). Hepatol Cholangiol. 2. Galucci, GM et al (2024). Cells. 3. Ghonem, NS et al (2020). Clin Pharmacol Ther.

Development and optimization of liquid chromatography-tandem mass spectrometry (LC-MS/MS) methods to measure bile acids in human plasma

Daniella R. Cross, Mariam O. Oladepo, David Assis, Nisanne S. Ghonem

The liver is a major excretory organ in the body, and bile acids, which are produced by the liver, are important endogenous regulators of compound absorption and excretion. However, bile acids are also hydrophobic molecules that become toxic at elevated concentrations. Primary biliary cholangitis (PBC) and primary sclerosing cholangitis (PSC) are chronic cholestatic liver diseases, characterized by an accumulation of bile acids, i.e.,

bile acid-induced liver injury. Left untreated, PBC and PSC often progress to cirrhosis and liver failure. Until recently, ursodeoxycholic acid (UDCA) was the only FDA-approved treatment for cholestasis. Recently, two peroxisome proliferator-activated receptor (PPAR) agonists received accelerated FDA approval for second-line treatment of PBC. Notably, PPAR regulates bile acid synthesis, metabolism, and detoxification pathways. Our lab has previously demonstrated that adjunct fenofibrate, a PPAR α agonist, in combination with UDCA, reduces bile acid-induced liver injury in patients with PBC and PSC. New analytical methods are needed to determine the effects of adjunct fenofibrate therapy on bile acid levels and composition for patients with PBC and PSC. We recently developed two liquid chromatography-tandem mass spectrometry (LC-MS/MS) methods to quantify 17 primary, secondary, and glycine- and taurine-conjugated bile acids. While individual bile acids may vary, the full range of quantification is from 1 – 20,000 ng/mL. Despite preliminary results that demonstrate our LC-MS/MS methods quantify bile acids in human plasma, further optimization is underway to improve efficiency and accuracy, e.g., quality control, of the methods, including elimination of analyte carryover following the injection of highly concentrated standards. Additional LC-MS/MS methods are in development to expand our research and quantify the effect of PPAR agonist therapy on bile acid metabolism and excretion in PBC and PSC.

Dual roles of in situ generated HSP70 in antigen delivery and immunoregulation

Xinliang Kang†, Zhuofan Li†, Jayachandra Reddy Nakkala, Yibo Li, Labone Akter, Yiwen Zhao and Xinyuan Chen*
College of Pharmacy, University of Rhode Island



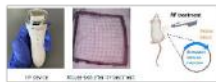
INTRODUCTION

Heat shock protein 70 (HSP70) is a stress-induced chaperone that can be released extracellularly and influence immune responses. While exogenous HSP70 has been studied as an adjuvant and tumor vaccine carrier, the role of *in situ* generated HSP70 under physiological conditions remains poorly understood.

Using a radiofrequency adjuvant (RFA) to induce endogenous HSP70, we investigate its role in antigen delivery and immunoregulation.

METHODS

WT and HSP70 KO mice were treated with RFA followed by intradermal OVA administration. HSP70 release and antigen association were assessed by ELISA, IP/IB, and PLA. Antigen uptake by dendritic cells in skin and lymph nodes was analyzed using AF647-OVA and flow cytometry. DC activation (CD80, CD86, CD40), NF- κ B signaling (p-p65), and cytokine production (IL-6) were evaluated by immunoprecipitation, western blot, and ELISA. Statistical significance was determined using t-tests or ANOVA.



RESULTS

RFA vigorously induces HSP70 expression in DCs

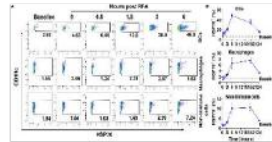


Fig. 1. RFA or sham treated skin was analyzed by flow cytometry to assess cell type-specific HSP70 induction.

HSP70 is released into extracellular space

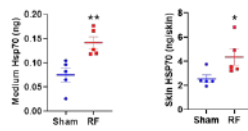


Fig. 2. HSP70 level in skin and culture medium was measured by ELISA.

RFA-induced HSP70 Directly Binds Antigen In Situ

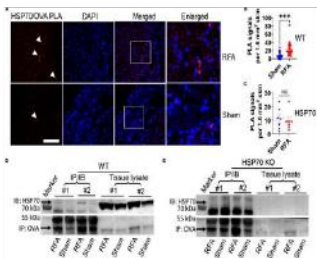


Fig. 3. RFA or sham treated WT and HSP70 KO skin was analyzed for HSP70-OVA interaction by PLA and immunoprecipitation.

RFA induces TIRAP/MyD88 but not TRAM/ TRIF association

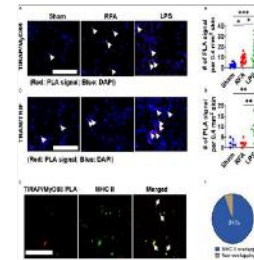


Fig. 5. Skin from RFA, sham, or LPS treated mice was analyzed for MyD88 relevant pathway by PLA.

HSP70 contributes to RFA-enhanced antigen uptake

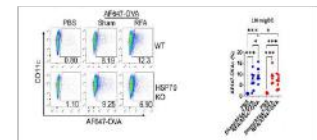


Fig. 4. WT and HSP70 KO mice treated with RFA or sham with intradermal AF647-OVA, and skin and draining LNs were analyzed by flow cytometry.

HSP70 suppresses RFA-induced TLR4/IRAK/ NFκB signaling

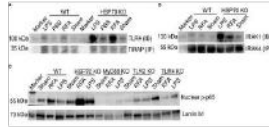


Fig. 6. IP and immunoblotting were used to assess TLR4-IRAP and IRAK1-IRAK1 interactions.

CONCLUSIONS

- RFA-induced HSP70 enhances antigen delivery to dendritic cells while suppressing NF- κ B and IL-6.
- HSP70 mediates RFA effects and limits transient local inflammation.
- Reveals the *in vivo* role of HSP70 in coordinating antigen delivery and immune regulation.



REFERENCES

- Srivastava P. Roles of heat-shock proteins in innate and adaptive immunity. *Nat Rev Immunol.* 2002;2:185-194.
- Cao Y et al. Augmentation of vaccine-induced humoral and cellular immunity by a physical radiofrequency adjuvant. *Nat Commun.* 2018;9:3695.

ACKNOWLEDGEMENTS

Microplate reader and BD FACVerse were supported by NIH NIGMS IDeA grant P20GM103430. Leica Cryostat was supported by NIH equipment grant S100D032209.

Created with DiaperPoster Poster Bullidit

Dual roles of in situ generated HSP70 in antigen delivery and immunoregulation

Xinliang Kang, Zhuofan Li, Jayachandra Reddy Nakkala, Yibo Li, Labone Akter, Yiwen Zhao, Xinyuan Chen

Introduction: Extracellular release of inducible HSP70 spurred interests to explore its potential interactions with innate immune systems. Both pro- and anti-inflammatory roles have been reported though the immunostimulatory roles were largely disputed due to the likely use of contaminated HSP70. The anti-inflammatory roles inspired the exploration of HSP70 to treat autoimmune diseases by suppressing pathological inflammatory responses. Besides immunomodulation, HSP70 has been explored as tumor vaccine carriers to elicit cytotoxic T lymphocyte responses due to its ability to deliver bound peptides to MHC I presentation pathway. With increasing understanding of the potential use of ex vivo prepared HSP70 in vaccination and therapy, the functions and potential applications of *in situ* induced HSP70 in antigen delivery and immunomodulation remain largely unexplored.

Methods: This study utilizes physical radiofrequency adjuvant (RFA) to induce HSP70 synthesis accompanied with mild inflammation followed by intradermal injection of vaccine antigens into RFA-treated skin in murine models to explore its potential roles in antigen delivery and immunomodulation.

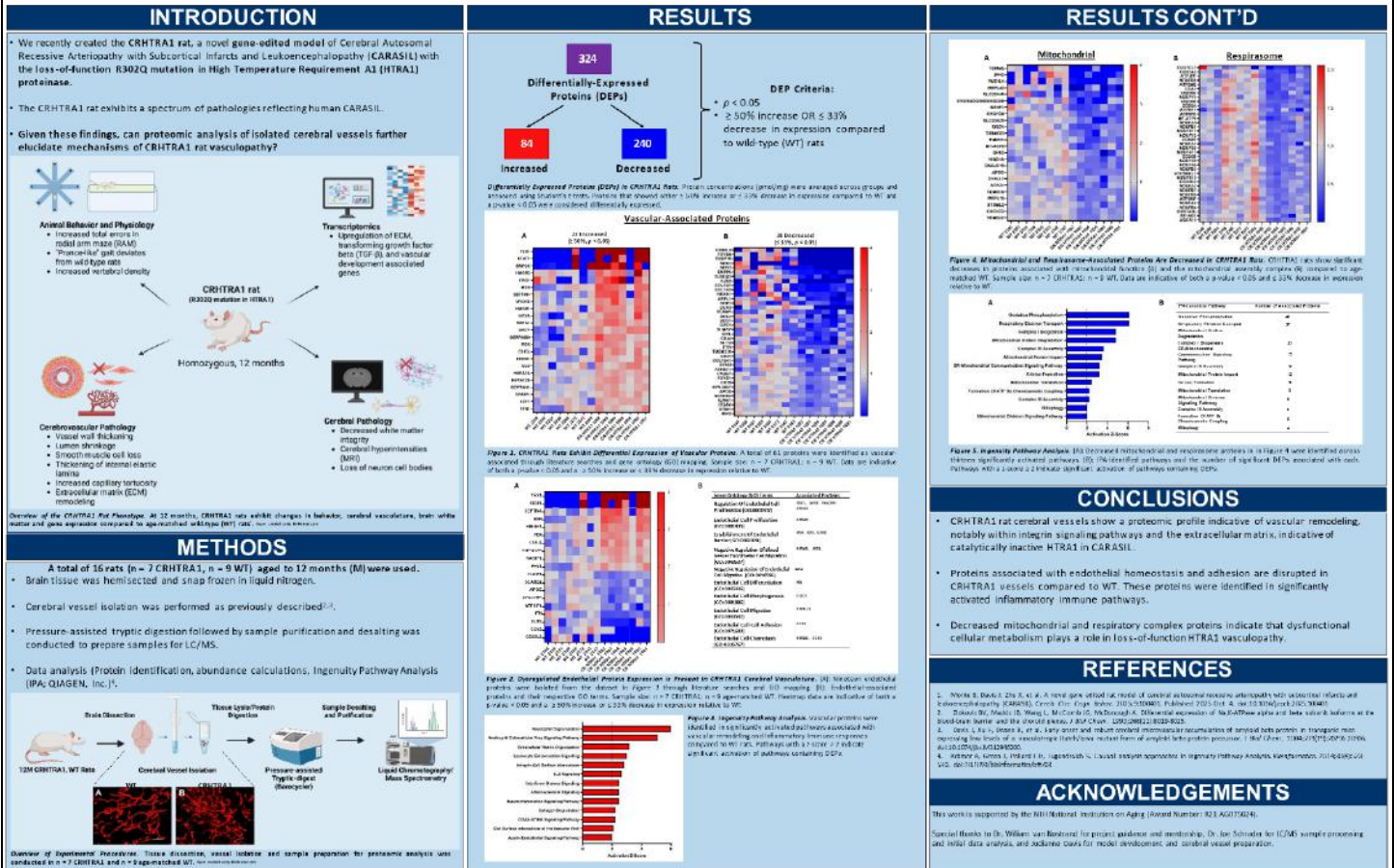
Results: We found *in situ* induced HSP70 could bind intradermally injected model antigen ovalbumin and contribute to enhanced antigen uptake in skin and draining lymph nodes. HSP70 failed to induce dendritic cell maturation and rather suppressed RFA-induced TLR4/IRAK/NF κ B activation and IL-6 expression.

Discussion: These results indicate dual roles of *in situ* induced HSP70 in antigen delivery and immunoregulation at physiological conditions. These dual functions highlight opportunities to exploit endogenous HSP70 for both vaccine adjuvantation and immunomodulation.

Identification of Differentially Expressed Vascular Proteins in a Novel Gene-Edited Rat Model of CARASIL




Brittany Monte¹, Joseph Schrader^{1,2}, Judianne Davis^{1,2}, and William E. Van Nostrand^{1,2}
 1. University of Rhode Island Department of Biomedical and Pharmaceutical Sciences, Kingston, RI, USA
 2. George and Anne Ryan Institute for Neuroscience, University of Rhode Island, Kingston, RI, USA



Identification of Differentially Expressed Vascular Proteins in a Novel Gene-Edited Rat Model of CARASIL

Brittany Monte, Joseph Schrader, Judianne Davis, William E. Van Nostrand



Recently, we created the CRHTRA1 rat, a novel gene-edited model of Cerebral Autosomal Recessive Arteriopathy with Subcortical Infarcts and Leukoencephalopathy (CARASIL) harboring the homozygous R302Q mutation in the High Temperature Requirement A1 (HTRA1) serine proteinase. In 12 months (M) old CRHTRA1 animals, we identified several behavioral, cerebrovascular, brain white matter and cerebral transcriptomic alterations that reflect human CARASIL pathology. To further examine underlying mechanisms of cerebral vasculopathy observed in CRHTRA1 rats, proteomic analysis was performed on isolated cerebral vessels. Analysis of vessel-enriched samples was conducted in 12M CRHTRA1 rats (n = 7) and age-matched wild-type (WT) rats (n = 9). We identified a total of 324 differentially expressed proteins (DEPs), 84 of which were significantly increased and 240 significantly decreased in CRHTRA1 rats. Further investigation of these DEPs resulted in the identification of multiple functional categories, including vascular associated, mitochondrial function, and respirasome-associated proteins. Using Ingenuity Pathway Analysis (IPA), we identified activated pathways associated with extracellular matrix (ECM) remodeling, atherosclerosis signaling, collagen degradation and integrin cell surface interactions. Proteins associated with the maintenance of the vascular endothelium and adherens junctions were identified in pathways of neuroinflammation and immune system activation. Respirasome and mitochondrial proteins were identified in pathways of respiratory complex formation, oxidative phosphorylation, and mitochondrial dysfunction. These findings provide new insight into how the R302Q HTRA1 mutation affects cerebral vessels contributing to the pathology of CARASIL.



Impact of Albuminuria on PFAS Kinetics using Physiologically Based Toxicokinetic (PBTK) Modeling

Jake Bunis¹, Hannah Sharkey², Angela Slitt¹, Jesse A Goodrich², Jonathan W Nelson³, Fabian Christoph Fischer¹

¹ Department of Biomedical and Pharmaceutical Sciences, College of Pharmacy, University of Rhode Island, Kingston, RI 02881
² Division of Environmental Health, Department of Population and Population Health Sciences, Keck School of Medicine, University of Southern California
³ Division of Nephrology, Department of Medicine, Keck School of Medicine, University of Southern California

Abstract# 4504
jacob.bunis@uri.edu

Abstract

Per- and polyfluoroalkyl substances (PFAS) are persistent environmental contaminants that bioaccumulate and have been linked to diverse adverse health effects. Previous studies demonstrate that serum albumin binding governs the accumulation of PFAS with six or more perfluorinated carbons by retaining them in circulation. In advanced kidney disease such as Diabetic Kidney Disease (DKD), and Chronic Kidney Disease (CKD), glomerular damage and impaired proximal tubular reabsorption contribute to progressive albuminuria, or elevated excretion of albumin through the urine. These conditions are extremely common, especially in those with diabetes. We hypothesized that albumin-bound PFAS would be co-excreted during albuminuria, accelerating their elimination. Using a mechanistic physiologically based toxicokinetic (PBTK) model, we investigated how albuminuria influences renal clearance of albumin-bound PFAS species. We modeled how albuminuria alters PFAS clearance pathways while accounting for parallel competing distribution and elimination processes.

We extended an established PBTK framework to simulate perfluorohexanoic acid (PFHxA), Perfluoroheptanoic acid (PFHpA), perfluorooctanoic acid (PFOA), perfluorononanoic acid (PFNA), perfluorodecanoic acid (PFDA), perfluoroundecanoic acid (PFUDA), perfluorobutanesulfonic acid (PFBS), perfluorohexanesulfonic acid (PFHxS), perfluorooctanesulfonic acid (PFOS) (npfc = 4-10). The novel model incorporates tissue blood flows, membrane permeability, albumin and phospholipid binding, and renal/hepatic transport processes. Wild-type parameters were derived from in vitro transporter/binding data and in vivo mouse studies. We modeled albuminuria by reducing serum albumin concentrations by 40% and increasing urinary albumin excretion from under 0.02 mg/day to 3 mg/day, to reflect impaired proximal tubular reabsorption. Model performance was evaluated by comparing half-lives, areas under the plasma concentration-time profile (AUC), and urine concentrations between wild-type and DKD phenotypes following single oral doses of 5mg/kg.

Results: Simulations support the hypothesis that albuminuria accelerates PFAS elimination in a manner proportional to albumin-binding affinity. Following oral administration, the t_{1/2} of PFOA decreased by 25% and AUC by 61%. PFOS showed a 20% reduction in t_{1/2} and 39% decrease in AUC. The strongest effects were observed for PFUDA, with a 31% reduction in t_{1/2}. PFBS, which exhibits weak binding to albumin, showed only a 6.6% reduction in t_{1/2} but a 52% decrease in AUC, consistent with primary renal handling of this PFAS species.

These findings suggest albumin-mediated renal elimination as a newly appreciated and key mechanism contributing to PFAS clearance under albuminuric conditions, underscoring the need to incorporate disease-related changes in protein binding and renal function into PBTK models. Future directions include the integration of clinical data from individuals with albuminuria to evaluate model performance and quantify the impact of progressive albuminuria on PFAS exposure in clinical cohorts of patients with DKD.

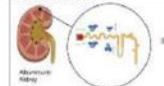
Introduction

PFAS are persistent environmental contaminants that bioaccumulate and have been linked to diverse adverse health effects such as immunotoxicity, increased cancer risk, and metabolic disruption.

Studies show serum albumin binding governs accumulation of PFAS with ≥6 perfluorinated carbons. As serum albumin is excreted in the proximal tubule, we see PFAS increasing t_{1/2} and AUC.

Approximately half of patients with Type 2 Diabetes and one third of patients with Type 1 Diabetes will develop Chronic Kidney Disease (CKD) which is defined by elevated urinary albumin excretion or Albuminuria.

We hypothesize that Albumin-bound PFAS would be co-excreted during albuminuria, accelerating their elimination. Using a mechanistic physiologically based toxicokinetic model (PBTK) we investigated PFAS toxicokinetics in mice to see the effect kidney disease has on PFAS toxicokinetics.



Methods

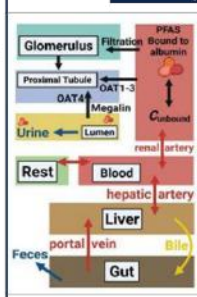


Table 1: MICEE Data of Albumin Excretion Rates in Mice:

CL-Albumin (mg/day)	Mean	SD
Median	3.11	
25% Q1	1.50	
75% Q3	12.63	
MIN	0.32	
MAX	8116.12	

Equation for PFAS Clearance:

$$Cl_{PFAS} = \frac{1}{1 + (K_{a1}/K_{a2}) + (K_{a3}/K_{a4})} \cdot (V_{d,plasma} \cdot V_{d,urine} + K_{a1} \cdot V_{d,plasma} + K_{a2} \cdot V_{d,urine} + K_{a3} \cdot V_{d,plasma} + K_{a4} \cdot V_{d,urine})$$

PFAS Albumin Clearance:

$$Cl_{PFAS, albumin} = f_{albumin} \cdot Cl_{PFAS} \cdot \left(\frac{V_{d,plasma}}{V_{d,urine}} + \frac{V_{d,urine}}{V_{d,plasma}} \right)$$

Urinary Albumin Excretion Rate:

$$UAE = \frac{U_{albumin}}{P_{albumin}} \cdot V_{urine}$$

Results

Figure 1: % Change in AUC Amount

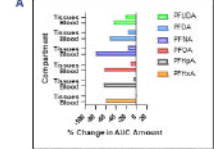


Figure 2: % Change in t1/2

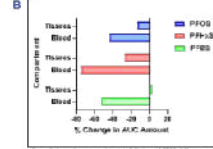


Figure 3: Mean Data Analysis of PFOA plasma concentration-time profile

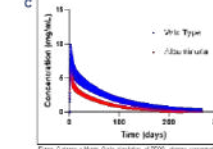


Figure 4: Mean Data Analysis of PFOS plasma concentration-time profile

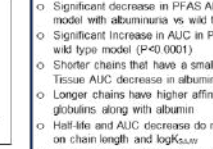


Table 2: Mean Data Analysis of PFOA plasma concentration-time profile

PKC1	PKC2	PKC3	PKC4	PKC5	PKC6
N	6	4	3	4	3
t _{1/2} (h)	3.59	4.68	4.17	4.26	4.57
AUC (ng·h/mL)	12.4	12.95	12.41	12.95	12.71
U _{PFAS} (ng/day)	-2.4%	-21.9%	-24.4%	-23.2%	-22.7%

Table 3: Mean Data Analysis of PFOS plasma concentration-time profile

PKC1	PKC2	PKC3	PKC4	PKC5	PKC6
N	4	4	0	3	3
t _{1/2} (h)	3.61	4.68	4.55		
AUC (ng·h/mL)	6.6	18.2%	19.2%		
U _{PFAS} (ng/day)	-52.0%	-73.6%	-43.0		

Discussion & Next Steps

- Significant decrease in PFAS AUCs, Tissue AUCs, and Half-lives in model with albuminuria vs wild type model
- Significant increase in AUC in PFAS in albuminuria model vs wild type model (P<0.0001)
- Shorter chains that have a smaller logK_{ow} tend to have a smaller Tissue AUC decrease in albuminuria models vs wild type models
- Longer chains have higher affinities to structural proteins and globulins along with albumin
- Half-life and AUC decrease do not seem to have a direct correlation on chain length and logK_{ow}
- Next steps include binding assays with different PFAS chains to calculate binding coefficients
- Using calculated binding coefficients, more PFAS models can be created and tested.

References

Fischer, Fabian C et al. Understanding Mechanisms of PFAS Absorption, Distribution and Elimination Using a Physiologically Based Toxicokinetic Model. *Environmental Science & Technology* 54(10):1020-1029, 2020. doi:10.1021/acs.est.9b07979

Goodrich, Jesse A et al. The proximal tubule and albuminuria: *npj* Journal of the American Society of Nephrology. *ACS* vol. 11.5 (2014): 445-451. doi:10.1038/nrn.2013.205

Thomas MC, Brummett W, Guzman H, Jandori-Cohen VA, Zouaga G, Rostand D, Gentry DL, Cooper HC, Cullberg H, Hines Deane, Halperin L, Liu-Fleming J, et al. (2017) *npj* 10:1232-1239. doi:10.1038/s41551-017-0026-2

Acknowledgements

This work was supported by the STEEP Superfund Research Grant

Impact of Albuminuria on PFAS Kinetics using Physiologically Based Toxicokinetic (PBTK) Modeling

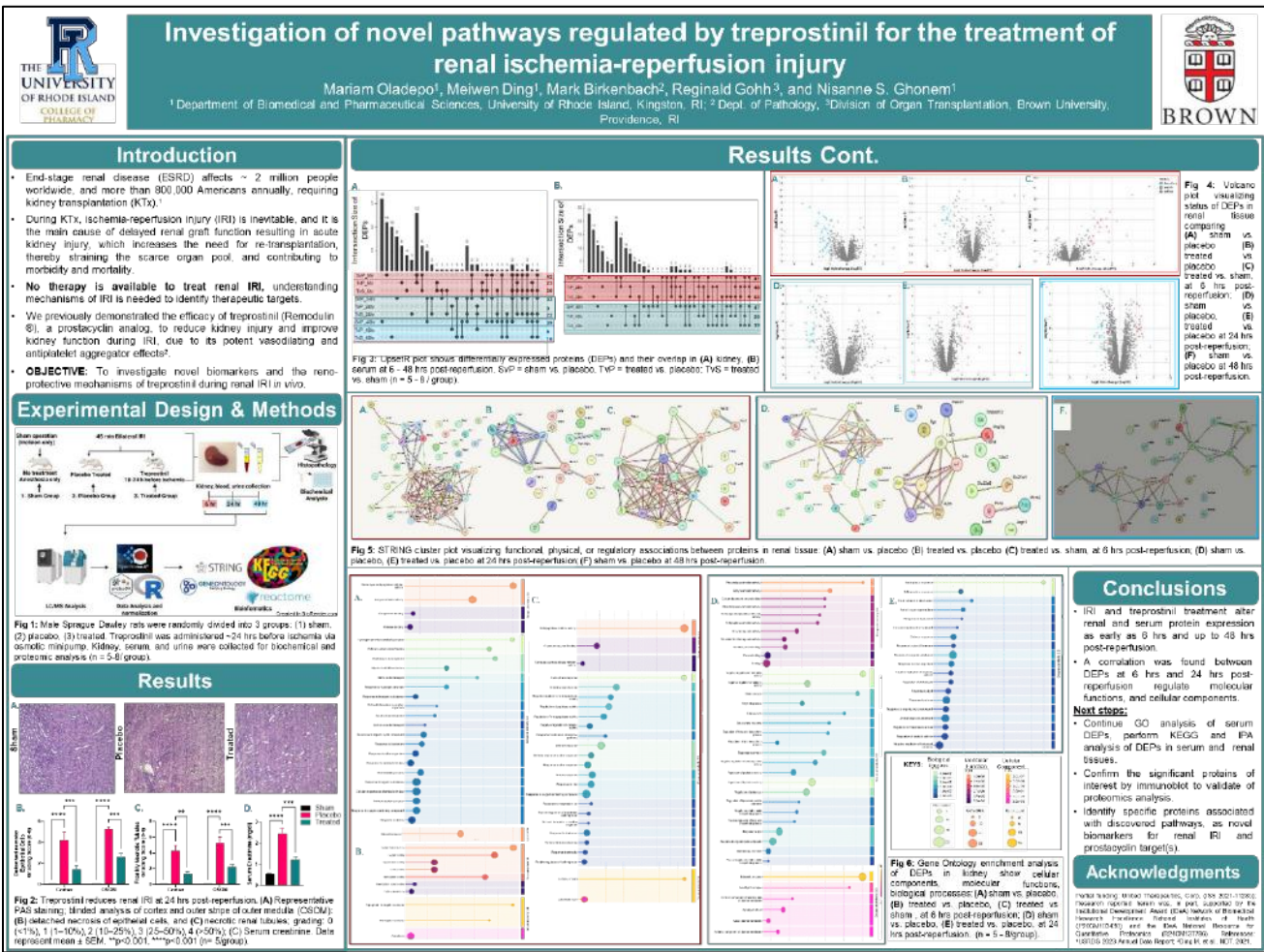
Jake Bunis, Hannah Sharkey, Angela Slitt, Jesse A. Goodrich, Jonathan W Nelson, Fabian C. Fischer

Per- and polyfluoroalkyl substances (PFAS) are persistent environmental contaminants that bioaccumulate and have been linked to diverse adverse health effects. Previous studies demonstrate that serum albumin binding governs the accumulation of PFAS with six or more perfluorinated carbons by retaining them in circulation. In advanced kidney disease such as Diabetic Kidney Disease (DKD), and Chronic Kidney Disease (CKD), glomerular damage and impaired proximal tubular reabsorption contribute to progressive albuminuria, or elevated excretion of albumin through the urine. These conditions are extremely common, especially in those with diabetes. We hypothesized that albumin-bound PFAS would be co-excreted during albuminuria, accelerating their elimination. Using a mechanistic physiologically based toxicokinetic (PBTK) model, we investigated how albuminuria influences renal clearance of albumin-bound PFAS species. We modeled how albuminuria alters PFAS clearance pathways while accounting for parallel competing distribution and elimination processes.

We extended an established PBTK framework to simulate perfluorohexanoic acid (PFHxA), Perfluoroheptanoic acid (PFHpA), perfluorooctanoic acid (PFOA), perfluorononanoic acid (PFNA), perfluorodecanoic acid (PFDA), perfluoroundecanoic acid (PFUDA), perfluorobutanesulfonic acid (PFBS), perfluorohexanesulfonic acid (PFHxS), perfluorooctanesulfonic acid (PFOS) (npfc = 4-10). The novel model incorporates tissue blood flows, membrane permeability, albumin and phospholipid binding, and renal/hepatic transport processes. Wild-type parameters were derived from in vitro transporter/binding data and in vivo mouse studies. We modeled albuminuria by reducing serum albumin concentrations by 40% and increasing urinary albumin excretion from under 0.02 mg/day to 3 mg/day, to reflect impaired proximal tubular reabsorption. Model performance was evaluated by comparing half-lives, areas under the plasma concentration-time profile (AUC), and urine concentrations between wild-type and DKD phenotypes following single oral doses of 5mg/kg.

Results: Simulations support the hypothesis that albuminuria accelerates PFAS elimination in a manner proportional to albumin-binding affinity. Following oral administration, the t_{1/2} of PFOA decreased by 25% and AUC by 61%. PFOS showed a 20% reduction in t_{1/2} and 39% decrease in AUC. The strongest effects were observed for PFUDA, with a 31% reduction in t_{1/2}. PFBS, which exhibits weak binding to albumin, showed only a 6.6% reduction in t_{1/2} but a 52% decrease in AUC, consistent with primary renal handling of this PFAS species.

These findings suggest albumin-mediated renal elimination as a newly appreciated and key mechanism contributing to PFAS clearance under albuminuric conditions, underscoring the need to incorporate disease-related changes in protein binding and renal function into PBTK models. Future directions include the integration of clinical data from individuals with albuminuria to evaluate model performance and quantify the impact of progressive albuminuria on PFAS exposure in clinical cohorts of patients with DKD.



Investigation of novel pathways regulated by treprostinil for the treatment of renal ischemia-reperfusion injury

Mariam Oladepo, Meiwen Ding, Mark Birkenbach, Reginald Gohh, Nisanne Ghonem

Renal ischemia-reperfusion injury (IRI) is a significant renal contributor to acute kidney injury and delayed graft function post-kidney transplantation, with no treatment available. We previously demonstrated the efficacy of treprostinil (Remodulin®), an FDA-approved prostacyclin (PGI2) analog, in reducing renal IRI in vivo. This study investigates novel biomarkers and reno-protective mechanisms of treprostinil during renal IRI in vivo.

Male Sprague Dawley rats were randomly divided into sham, placebo, treated groups, and subjected to bilateral renal IRI (45 mins) followed by reperfusion (1-48 hrs). Treprostinil was administered subcutaneously and serum and kidney tissue were collected for biochemical and proteomic analyses.

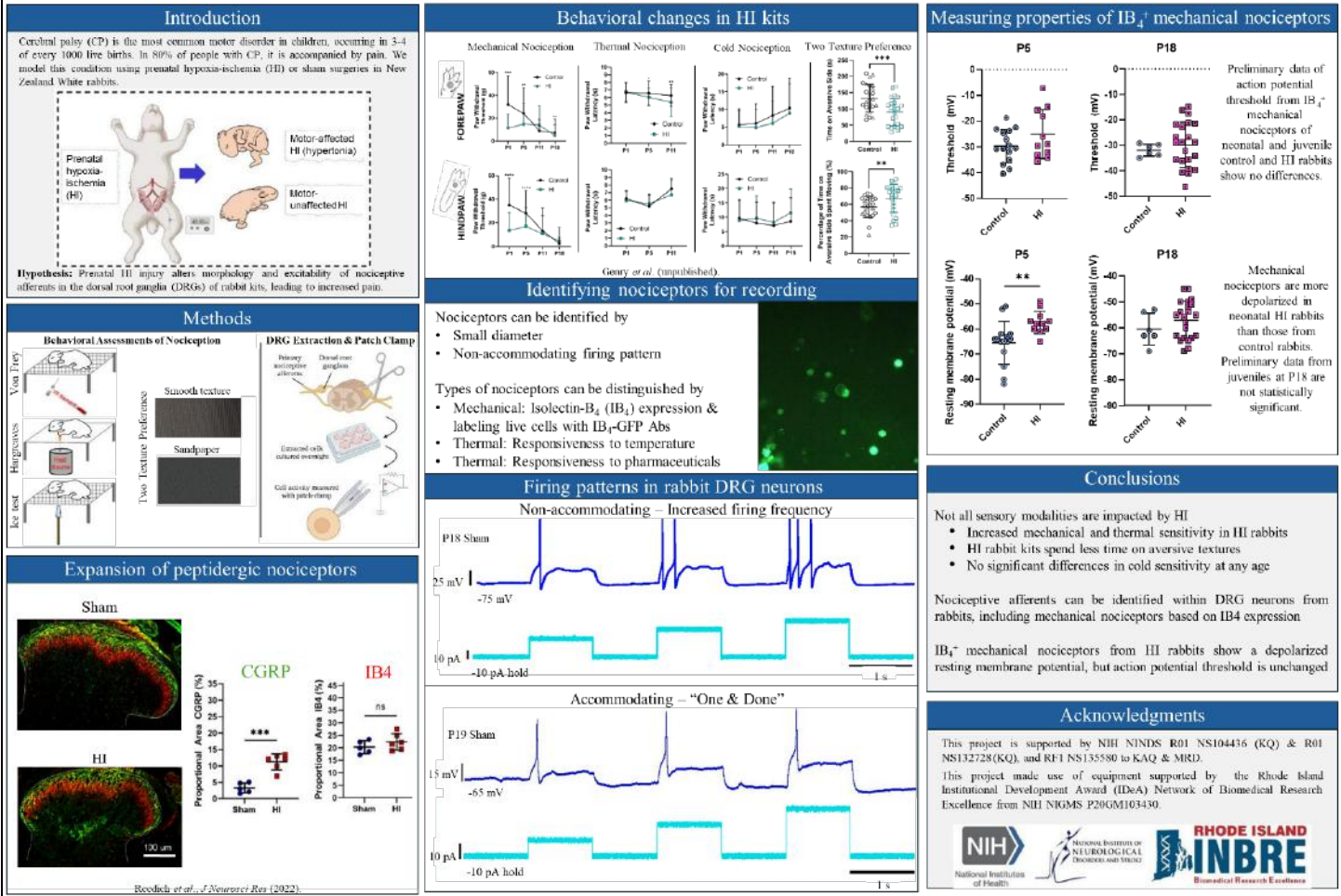
Treprostinil reduced peak serum creatinine levels by 52% (P<0.05), and histology data showed necrotic tubules of kidney tissues by ~50% vs. placebo (P<0.01) at 24 hrs post-reperfusion.

Proteomic profiling in renal tissues detected 2931 proteins, with a total of 91, 58 and 60 differentially expressed proteins (DEPs) at 6, 24, and 48 hrs post-reperfusion, respectively. Similarly, 806 proteins were detected in serum, with a total of 197 and 106 DEPs at 24 and 48 hrs, respectively (>1-fold at p<0.05) at 24 hrs post-reperfusion. A correlation was found using STRING and GO analysis between DEPs at 6 hrs and 24 hrs post-reperfusion, including proteins that regulate molecular functions, e.g., oxygen, heme, hemoglobin, protease and complement binding; biological processes, e.g., acute phase response, response to external stimulus and stress, as well as proteins involving cellular components of the extracellular space, cytoplasm and some apical parts of the cell.

In conclusion, IRI and treprostinil therapy alter renal and serum protein expression as early as 6 hr and up to 48 hr post-reperfusion. These findings identify specific proteins regulated during renal IRI which provide mechanistic insight to identify novel biomarkers involved in IRI and therapeutic targets of treprostinil.

Moline BC^{1,2}, Mena Avila E^{1,2}, Genry LT^{1,2,3}, Reedich EJ^{1,2}, Kramer CA^{1,2,3}, Santos T^{1,2,3}, Matson SG^{1,2,3}, Dowaliby L^{1,2}, Detloff MR⁴, Quinlan KA^{1,2,3}

¹Department of Biomedical and Pharmaceutical Sciences, College of Pharmacy, University of Rhode Island, Kingston, RI, USA; ²George and Anne Ryan Institute for Neuroscience, University of Rhode Island, Kingston, RI, USA; ³Interdisciplinary Neuroscience Program, University of Rhode Island, Kingston, RI, USA; ⁴Department of Neurobiology and Anatomy, Marion Murray Spinal Cord Research Center, College of Medicine, Drexel University, Philadelphia, PA, USA



Mechanical Nociceptor Properties in an Experimental Model of Cerebral Palsy Pain

Brendan Moline, Elvia Mena Avila, Lauren T. Genry, Emily Reedich, Cassandra A. Kramer, Thais Santos, Sarah G. Matson, Laura Dowaliby, Mary R. Detloff, Katharina A. Quinlan

Cerebral palsy (CP) is a movement disorder typified by abnormalities in muscle tone, spasticity, and pain. Studies estimate that ~75% of people with CP experience pain, but the causes are understudied. Thus, we use an animal model of CP-related pain to evaluate changes in nociceptor excitability. In utero hypoxia-ischemia (HI) injury at 70-90% gestation in New Zealand White rabbits produces cell death in the brain and spinal cord, muscle stiffness like humans with CP, and behavior consistent with mechanical allodynia. To test if nociceptors (sensory neurons which detect and respond to noxious stimuli) in general, and more specifically the nociceptors responding to noxious mechanical stimuli are impacted by perinatal injuries, we measure neuron excitability in cells from dorsal root ganglia (DRGs) from rabbits exposed to prenatal HI, sham surgical procedure, or naive controls. At postnatal day (P)1, rabbits undergo assessments of mechanical or thermal pain. At P5 & 18, DRGs are isolated, cultured, stained with fluorescent isolectin-B4 (IB4-GFP) a marker of mechanical nociceptors, and cellular electrical activity is recorded using whole-cell patch clamp. Preliminary findings indicate that rabbit DRG neurons exhibit firing patterns consistent with nociceptors and light touch sensory afferents, the former displaying repeated firing (non-accommodating) and the latter displaying singular firing (rapidly accommodating) when stimulated. Restricting our analysis to only mechanical nociceptors that expressed IB4, we found that mechanoreceptors from HI rabbits had a depolarized resting membrane potential at P5, but not P18 based on unpaired t-tests. This shift in membrane potential would allow these nociceptors to fire more readily than the equivalent neurons from control animals with the same stimuli. With a greater understanding of DRG neuron firing properties and excitability in HI rabbits, we can elucidate how perinatal injuries could impact pain in CP, allowing for development of safer and more efficacious treatments than currently available.

Mechanisms Driving Per- and Polyfluoroalkyl Substances (PFAS) Disposition in Human Breast Milk: Roles of Efflux

Transporters, Permeability, and Binding

Liam Geyer¹, Grayson Norman¹, Miguel Rodriguez¹, Jitka Becanova², Simon Vojta², Roberta King¹, Angela L. Slitt¹, Sangwoo Ryu¹, Kaitlin M. Dailey¹, Fabian C. Fischer¹

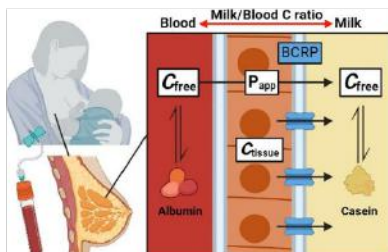
¹ Department of Biomedical and Pharmaceutical Sciences, College of Pharmacy, University of Rhode Island, Kingston, RI 02881

² Graduate School of Oceanography, University of Rhode Island, Narragansett, RI 02882



INTRODUCTION

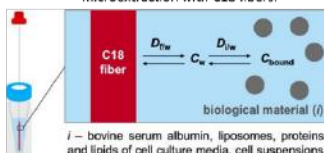
- Per- and polyfluoroalkyl substances (PFAS) are widespread environmental pollutants linked to neurodevelopmental disorders in children.
- Maternal transfer of PFAS through breastfeeding represents a critical exposure pathway during early life.
- This study investigated:
 - Breast cancer resistance protein (BCRP) efflux
 - Passive membrane permeability
 - PFAS binding in human serum and breast milk.



MATERIALS & METHODS

1.) C-18 Fiber Binding Assays:

PFAS binding in human serum and breast milk was quantified using solid phase microextraction with C18 fibers.

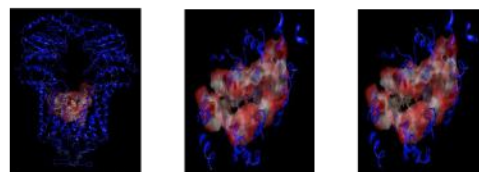
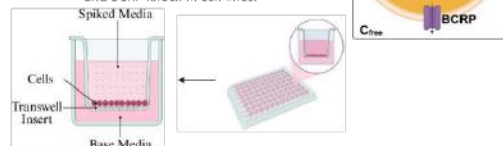


3.) MOE Docking Modeling:

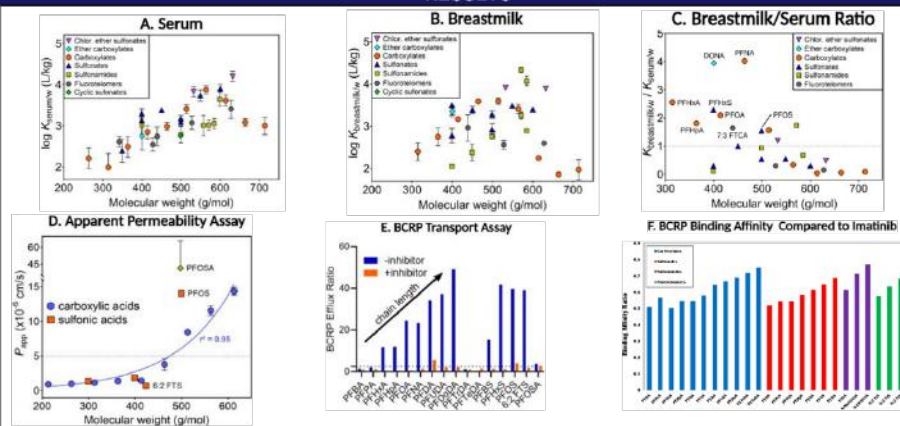
A computational model of BCRP was used to simulate binding affinity with the PFAS examined in this study, and this data was compared to the results of the BCRP transport assays.

2.) Trans-Well Cell Culture Assays:

Passive permeability and BCRP-mediated transport were assessed in trans-well *in vitro* assays using transporter knock-out and BCRP knock-in cell lines.



RESULTS



DISCUSSION & NEXT STEPS

- Molecular weight strongly influences PFAS transfer into breast milk, with higher molecular weight compounds exhibiting:
 - Increased binding
 - Greater passive permeability
 - Enhanced BCRP-mediated transport
- PFAS functional group may be correlated to the binding of specific biomolecules, but further investigation is required.
- Our MOE model of BCRP shows comparative scores to previous BCRP transport studies, but further refinement of the model is required.
- The mechanistic data will be integrated into a physiologically based toxicokinetic model to simulate PFAS transfer into breast milk under human physiological conditions, accounting for inter-individual variability such as BCRP polymorphisms and hypoalbuminemia as potential risk factors for disproportionate transfer of PFAS to the breastfeeding infant during lactation.
- Investigation of other transporters, such as:
 - P-gp
 - MRP1
- Investigation of separate, transfected cell lines, including:
 - Caco-2
 - HepARG
- Further development of *in Silico* transporter models

Acknowledgements

This work was supported by the Advanced CTR Pilot Program (NIH Grant 5U54GM115677 - 09) and the STEEP Superfund Research Grant (NIH Grant P42ES027706)

References

Ryu, Sangwoo, et al. "Evaluation of 14 PFAS for permeability and organic anion transporter interactions: implications for renal clearance in humans." *Chemosphere*, vol. 361, Aug. 2024, p. 142390. <https://doi.org/10.1016/j.chemosphere.2024.142390>.

Mechanisms Driving Per- and Polyfluoroalkyl Substances (PFAS) Disposition in Human Breast Milk: Roles of Efflux Transporters, Permeability, and Binding

Liam Geyer, Grayson Norman, Miguel Rodriguez, Jitka Becanova, Simon Vojta, Roberta King, Angela L. Slitt, Sangwoo Ryu, Kaitlin M. Dailey, Fabian C. Fischer

Per- and polyfluoroalkyl substances (PFAS) are widespread environmental pollutants linked to several disorders in children. Maternal transfer of PFAS through breastfeeding represents a critical exposure pathway during early life. This study investigated the toxicokinetic mechanisms driving PFAS transfer into breast milk by evaluating interactions with the efflux transporter Breast Cancer Resistance Protein (BCRP), passive membrane permeability, and PFAS binding in human serum and breast milk. PFAS binding in human serum and breast milk was quantified using solid-phase microextraction with C18 fibers. Passive permeability and BCRP-mediated transport were assessed in trans-well *in vitro* assays using transporter knock-out and BCRP knock-in cell lines and the results were compared to molecular docking simulations using the Molecular Operating Environment (MOE) software. PFAS binding in breast milk increased linearly with molecular weight for sulfonic acid and sulfonamide groups. In contrast, carboxyl and fluorotelomer PFAS followed this trend only up to 500 g/mol, after which binding declined. BCRP-mediated transport increased with molecular weight, with efflux ratios ranging from 10- to 50-fold higher in BCRP-expressing cells compared to inhibited controls, agreeing with molecular docking simulations. Similarly, passive permeability increased with molecular weight, with the highest permeability observed for PFAS above 500 g/mol. Our preliminary results show that molecular weight strongly influences PFAS transfer into breast milk, with higher molecular weight compounds exhibiting increased binding, greater passive permeability, and enhanced BCRP-mediated transport. The mechanistic data will be integrated into a physiologically based toxicokinetic model to simulate PFAS transfer into breast milk under human physiological conditions, accounting for inter-individual variability such as BCRP polymorphisms and hypoalbuminemia as potential risk factors for disproportionate transfer of PFAS to the breastfeeding infant during lactation.

Molecular Mechanisms and Therapeutic Targets of Bile Acid Dysregulation in Pregnancy Complications Associated with Liver Disorders



Md Mosiqr Rahman¹, Tasneem Al-Huniti¹, Qiwen Chen¹, Lia Bozza¹, Ruitang Deng¹

¹Department of Biomedical and Pharmaceutical Sciences, College of Pharmacy, University of Rhode Island



Introduction

- Intrahepatic cholestasis of pregnancy (ICP) is a pregnancy-specific liver disorder characterized by elevated bile acids and is associated with increased risk of preterm birth (PTB) and stillbirth.
- Clinical evidence shows that higher maternal bile acid levels strongly correlate with adverse fetal outcomes.
- Bile acids act as signaling molecules via receptors such as TGR5 receptor and Farnesoid X receptor, regulating metabolism and inflammation.
- Emerging evidence suggests that TGR5-mediated inflammatory signaling at the maternal-fetal interface may contribute to the onset of labor and pregnancy complications.
- Nonalcoholic fatty liver disease is increasingly linked to ICP and adverse pregnancy outcomes, potentially due to impaired bile acid transport.
- Downregulation of the bile salt export pump disrupts bile acid homeostasis, leading to accumulation and toxicity.
- Targeting bile acid pathways represents a promising therapeutic strategy to reduce PTB and stillbirth in high-risk pregnancies. [1-5]

Aims

- Aim 1: To investigate the roles of TGR5 signaling pathway in the indication of pregnancy complications by elevated bile acids.
- Aim 2: To investigate increased risk and underlying mechanisms for NAFLD subjects to develop ICP and its associated pregnancy complications of PTB and stillbirth.
- Aim 3: To assess the potential therapeutic effects of FDA-approved drugs on reducing or preventing pregnancy complications in subjects with liver disorders.

Methods

Animal Models & Disease Induction

- Studies utilized timely pregnant TGR5-knockout (TGR5-KO) and wild-type (wt) mice to evaluate signaling pathways.
- Non-alcoholic fatty liver (NAFL) was induced in female mice by providing a high-fat diet (HFD) for 12 weeks prior to mating.
- The cholic acid (CA)-induced complication model was established by administering 1.5% CA in the maternal diet starting at GD 14.5 until labor.

Data Collection & Analytical Techniques

- Primary observational endpoints included the recording of gestational days, live birth rates, and stillbirth rates.
- Newborn wellbeing was clinically monitored for the first two weeks following birth.



Figure 1: Flowchart of Methodology

Results

Figure 2: Average gestational day (GD) of TGR5 KO mice and the control mice (with 1.5% CA treatment). *P<0.05, **P<0.01, ***P<0.001 with Student's t test pair wise comparison.

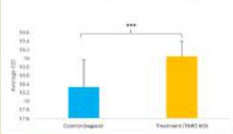


Figure 3: Percentage of stillbirth of TGR5 KO mice and the control mice (with 1.5% CA treatment). *P<0.05, **P<0.01, ***P<0.001 with Student's t test pair wise comparison.

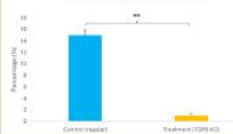


Figure 4: Aspartate aminotransferase (AST) and Serum total bile acids (sTBA) level of high fat diet (HFD) mice and the control mice. *P<0.05, **P<0.01, ***P<0.001 with Student's t test pair wise comparison.

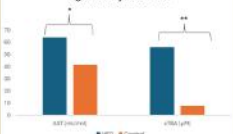


Figure 5: Percentage of stillbirth of High Fat Diet (HFD) mice and the control mice. *P<0.05, **P<0.01, ***P<0.001 with Student's t test pair wise comparison.

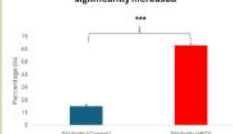


Figure 6: Average Gestational day (GD) of control regular mice and the 4-PBA treatment group mice. *P<0.05, **P<0.01, ***P<0.001 with Student's t test pair wise comparison.

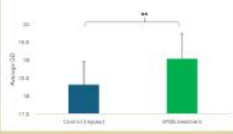
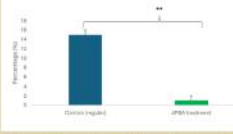


Figure 7: Percentage of stillbirth of control regular mice and the 4-PBA treatment group mice. *P<0.05, **P<0.01, ***P<0.001 with Student's t test pair wise comparison.



Conclusion

- Early-stage nonalcoholic fatty liver (NAFL) strongly predisposes pregnant individuals to ICP. This is driven by the downregulation of the bile salt export pump (BSEP), causing toxic bile acid accumulation.
- Elevated bile acids act as signaling molecules that disrupt metabolic homeostasis. Specifically, TGR5-mediated inflammatory signaling at the maternal-fetal interface is a critical driver of labor onset, PTB, and stillbirth.
- High-fat diet mice models successfully replicated clinical observations, showing that underlying metabolic liver disorders elevate AST and serum bile acids, directly translating to increased rates of stillbirth.
- Targeting these specific hepatocellular signaling and bile acid transport pathways with FDA-approved therapies (such as 4-PBA) represents a highly promising strategy to prevent severe pregnancy complications in high-risk patients

Future Studies

- To establish a correlation between TGR5 agonistic potencies and pregnancy complications among different bile acid species.
- To define the effects of TGR5 agonism and antagonism on bile acids-induced pregnancy complications of PTB and stillbirth.
- To investigate the increased susceptibility of NAFL mice to estrogen-induced pregnancy complications of PTB and stillbirth.
- To investigate the protective effects of restoring BSEP expression on CA-induced pregnancy complications of PTB and stillbirth in NAFL mice.

References

- Geenes, V., Chappell, L. C., Seed, P. T., Steer, P. J., Knight, M., & Williamson, C. (2014). Association of severe intrahepatic cholestasis of pregnancy with adverse pregnancy outcomes: A prospective population-based case-control study. *The Lancet*, 384(9959), 1919-1927.
- Williamson, C., Hems, L. M., Gouls, D. G., Walker, I., Chambers, J., Donaldson, O., Swiet, M. D., & Johnston, D. G. (2004). Clinical outcome in a series of cases of obstetric cholestasis identified via a patient support group. *BJOG: An International Journal of Obstetrics & Gynaecology*, 111(7), 676-681.
- Li, T., & Chiang, J. Y. L. (2014). Bile acid signaling in metabolic disease and drug therapy. *Pharmacological Reviews*, 66(4), 948-983.
- Brouwers, L., Koster, M. P. H., Page-Christiaens, G. C. M. L., Kemperman, H., Boon, J., Evers, I. M., & Lely, A. T. (2015). Intrahepatic cholestasis of pregnancy: Maternal and fetal outcomes associated with elevated bile acid levels. *American Journal of Obstetrics and Gynecology*, 212(1), 100.e1-100.e7.
- Stieger, B. (2011). The role of the bile salt export pump (BSEP/ABC11) in normal and pathological bile formation. *Handbook of Experimental Pharmacology*, 201, 205-259.

Acknowledgement

The work was supported by grants from National Institutes of Health (NIH)

Molecular Mechanisms and Therapeutic Targets of Bile Acid Dysregulation in Pregnancy Complications Associated with Liver Disorders

Md. Mosiqr Rahman, Tasneem Al-Huniti, Qiwen Chen, Lia Bozza, Ruitang Deng

Nonalcoholic fatty liver disease (NAFLD) is an increasingly prevalent metabolic disorder that has recently been implicated in adverse pregnancy outcomes. Intrahepatic cholestasis of pregnancy (ICP) is a pregnancy-specific liver disorder characterized by impaired bile acid homeostasis and is strongly associated with preterm birth (PTB) and stillbirth. In our preliminary analysis of a cohort of 36,755 pregnant women, individuals with NAFLD demonstrated a markedly higher prevalence of ICP, with 14.1% of NAFLD patients developing ICP compared to the general population incidence of 1.37%. Moreover, women diagnosed with both NAFLD and ICP exhibited significantly elevated risks of PTB and stillbirth. Both NAFLD and ICP were associated with dysregulated bile acid metabolism, as indicated by increased serum total bile acid (sTBA) levels and reduced expression of the bile salt export pump (BSEP), a critical transporter responsible for bile acid excretion. Based on these observations, we hypothesize that early-stage NAFLD, specifically nonalcoholic fatty liver (NAFL), predisposes pregnant women to ICP and its associated complications through impaired BSEP-mediated bile acid clearance and subsequent bile acid accumulation. This study aims to elucidate the molecular mechanisms linking NAFL to ICP, with a particular focus on bile acid transport dysregulation and hepatocellular signaling pathways. Understanding these mechanisms may reveal novel therapeutic targets and inform preventive strategies for managing pregnancy complications in women with underlying liver disorders.

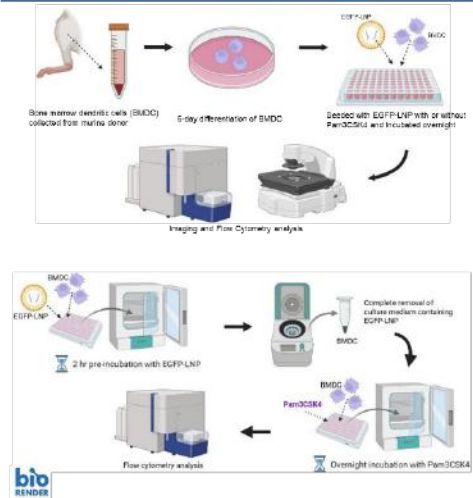
ABSTRACT

Messenger ribonucleic acid (mRNA) vaccines require translation in host cells to elicit antigen-specific immune responses. Dendritic cells (DCs) are known to be professional antigen-presenting cells (APCs), responsible for bridging adaptive immunity. Thus, enhancing mRNA translation in DCs has important implications to enhance mRNA vaccine efficacy. This study found toll-like receptor 2 (TLR2) agonist Pam3CSK4 was highly potent to enhance lipid nanoparticle (LNP) encapsulated enhanced green fluorescent protein (EGFP) mRNA translation in murine bone marrow-derived DCs (BMDCs) at concentrations as low as 1 ng/mL. We further found Pam3CSK4 could enhance DiD-encapsulated LNP uptake with high dependence on TLR2. Pre-incubation of BMDCs with EGFP mRNA for 2 hours followed by washing away EGFP mRNA in the medium and overnight incubation with Pam3CSK4 found Pam3CSK4 could still enhance EGFP expression. Thus, our data support that Pam3CSK4 could simultaneously enhance LNP uptake and EGFP mRNA translation in BMDCs.

RESEARCH OBJECTIVES

- Explore toll-like receptor 2 (TLR2) agonist Pam3CSK4 mediated enhancement of EGFP mRNA translation in BMDC and compare with other TLR agonists
- Explore the role of Pam3CSK4 in nanoparticle uptake and mRNA translation within BMDC

MATERIALS AND METHODS



RESULTS

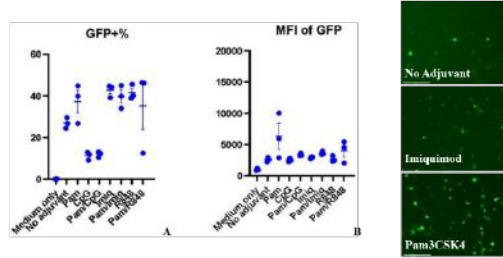


Figure 1. Pam3CSK4 enhances both uptake and expression of the EGFP mRNA in BMDC. Murine-derived BMDC were differentiated for 6 days before seeded in a 96-well plate in 10⁵/mL density. 0.4 μg/mL EGFP-LNP and 1 μg/mL TLR 2/7/8/9 agonist are then added to each corresponding wells before overnight incubation. (A) Fraction of EGFP expressing cells. (B) Mean fluorescence intensity of the cells. (Images: Difference in MFI between groups shown with fluorescence imaging.)

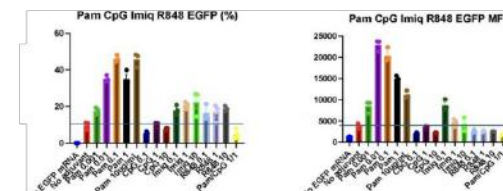


Figure 2. Pam3CSK4 shows dose-dependent enhancement of both uptake and expression of EGFP mRNA and superior potency in BMDC. 6-day differentiated BMDC were seeded in a 96-well plate in 10⁵/mL density. 0.4 μg/mL EGFP-LNP and TLR 2/7/8/9 agonist in various concentration ranging from 1 ng/mL to 10 μg/mL are then added to each corresponding wells before overnight incubation. (Left) Fraction of EGFP expressing cells. (Right) Mean fluorescence intensity of the cells)

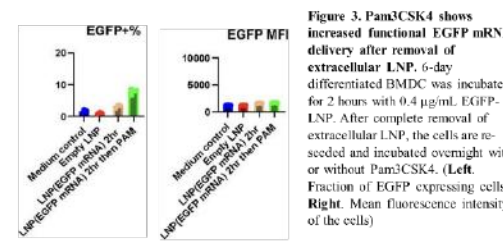


Figure 3. Pam3CSK4 shows increased functional EGFP mRNA delivery after removal of extracellular LNP. 6-day differentiated BMDC was incubated for 2 hours with 0.4 μg/mL EGFP-LNP. After complete removal of extracellular LNP, the cells are re-seeded and incubated overnight with or without Pam3CSK4. (Left) Fraction of EGFP expressing cells. (Right) Mean fluorescence intensity of the cells)

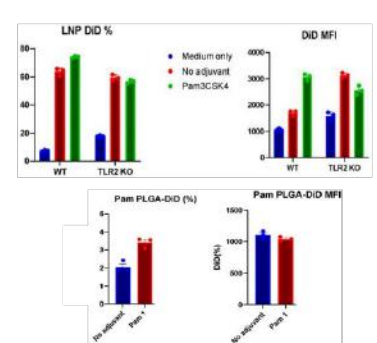


Figure 4. Pam3CSK4 shows TLR2 pathway dependent enhancement of nanoparticle uptake in BMDC, with LNP formulation contributing to the result. After 6-day differentiation and seeding, fluorescence dye (DiD)-incorporated LNP or PLGA-NP were added in the corresponding wells with or without the addition of 1 μg/mL concentration Pam3CSK4 before overnight incubation. (A) LNP formulation. (B) PLGA-NP formulation. (C) LNP formulation. (D) PLGA-NP formulation. (A,B Left) Fraction of DiD-incorporated nanoparticle taken up by the cells. (A,B Right) Mean fluorescence intensity.)

CONCLUSIONS

- TLR2 agonist Pam3CSK4 significantly enhances EGFP mRNA translation in BMDC and uptake of LNP at concentrations as low as 1 ng/mL.
- Pam3CSK4 is able to increase functional EGFP mRNA delivery after removal of extracellular LNP
- Lipid nanoparticle formulation contributes to Pam3CSK4 enhanced uptake of nanoparticles and shows superiority over PLGA-based nanoparticle.

ACKNOWLEDGEMENTS & REFERENCES

This work is supported by the University of Rhode Island. We thank Yibo Li, Ph.D., and INBRE facility for their help in this project.



Potent Enhancement of Lipid Nanoparticle Uptake and EGFP mRNA Translation in Dendritic Cells - Pam3CSK4, a Toll-Like Receptor 2 Agonist

Yuna Song, Xinliang Kang, Labone Akter, Minkyung Cho, Youbin Kim, Xinyuan Chen

Messenger ribonucleic acid (mRNA) vaccines require translation in host cells to elicit antigen-specific immune responses. Dendritic cells (DCs) are known to be professional antigen-presenting cells (APCs), responsible for bridging adaptive immunity. Thus, enhancing mRNA translation in DCs has important implications to enhance mRNA vaccine efficacy. This study found toll-like receptor 2 (TLR2) agonist Pam3CSK4 was highly potent to enhance lipid nanoparticle (LNP) encapsulated enhanced green fluorescent protein (EGFP) mRNA translation in murine bone marrow-derived DCs (BMDCs) at concentrations as low as 1 ng/mL. We further found Pam3CSK4 could enhance DiD-encapsulated LNP uptake with high dependence on TLR2. Pre-incubation of BMDCs with EGFP mRNA for 2 hours followed by washing away EGFP mRNA in the medium and overnight incubation with Pam3CSK4 found Pam3CSK4 could still enhance EGFP expression. Thus, our data support that Pam3CSK4 could simultaneously enhance LNP uptake and EGFP mRNA translation in BMDCs.

PROTEOMICS ANALYSIS REVEALS ETC ASSEMBLY AND MITOCHONDRIAL PROTEOSTASIS PATHWAYS ARE MORE DERANGED IN THE RV THAN LV AND ASSOCIATE WITH DEGREE OF DYSFUNCTION IN EXPLANTED FAILING HUMAN HEARTS

Joseph Owusu-Sarfo¹, Wenzhuo Ma¹, Lauren Bazinet¹, Benison Aguocha¹, Kenneth S. Campbell², Gaurav Choudhary³, Peng Zhang³, Richard T. Clements¹.
¹Univ of Rhode Island, Kingston, RI, USA, ²Univ of Kentucky, Dept of Physiology, Lexington, KY, USA, ³Providence VAMC and Brown Medical School, Providence, RI, USA.

INTRODUCTION

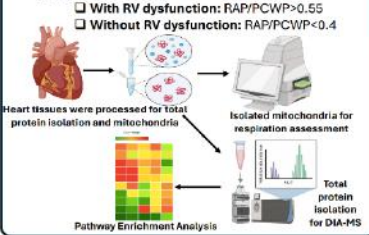
Right ventricular (RV) dysfunction is a major determinant of morbidity and mortality in patients with left heart failure, particularly in the presence of group II pulmonary hypertension, where elevated left-sided filling pressures chronically increase RV afterload. Although therapies targeting left ventricular (LV) dysfunction have improved outcomes, progression to RV failure remains associated with poor prognosis and limited therapeutic options. The molecular mechanisms underlying RV vulnerability and the transition from compensated dysfunction to overt RV failure remain incompletely defined.

Mitochondrial dysfunction has emerged as a central feature of heart failure, as impaired oxidative phosphorylation, disrupted electron transport chain (ETC) assembly, and altered mitochondrial protein quality control contribute to energetic failure and contractile dysfunction in animal models. However, whether mitochondrial remodeling is similar in human tissue with and without RV dysfunction is unclear, and if this changes are similar to failing LV.

To address this, we performed data-independent acquisition (DIA) proteomic profiling of RV and LV tissue from explanted hearts of patients with end-stage left heart failure and compared molecular signatures between patients with mild and severe RV dysfunction and unused donor hearts. Our analysis aimed to identify proteomic pathways associated with RV deterioration, with particular focus on mitochondrial and proteostasis pathways that may underlie RV-specific vulnerability in advanced heart failure.

METHODS

- Hearts were acquired from Gill Cardiovascular Repository, University of Kentucky Medical Center
- Controls were unused donors (n=14, 7M/7F)
- Heart transplant patients were divided into two groups:
 - With RV dysfunction: RAP/PCWP>0.55
 - Without RV dysfunction: RAP/PCWP<0.4



RESULTS

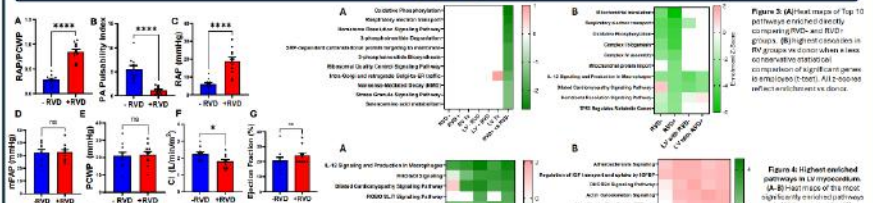


Figure 1. Mitochondrial energetics of transplant recipients with and without right ventricular (RV) dysfunction. (A) Heatmap of the top 10 pathways enriched in RV. (B) Heatmap of the top 10 pathways enriched in LV. (C) Bar chart of RBP/PCWP. (D) Bar chart of PA Pulmonary Index. (E) Bar chart of PAP (mmHg). (F) Bar chart of CI (ml/min/m2). (G) Bar chart of Ejection Fraction (%). Data are presented as mean ± SEM (n = 11 per group; 7 male/4 female).



Figure 2. Highest enriched pathways in RV mitochondria. (A) Heatmap of the top 10 pathways enriched in RV mitochondria. (B) Heatmap of the top 10 pathways enriched in LV mitochondria. (C) Bar chart of RBP/PCWP. (D) Bar chart of PA Pulmonary Index. (E) Bar chart of PAP (mmHg). (F) Bar chart of CI (ml/min/m2). (G) Bar chart of Ejection Fraction (%). Data are presented as mean ± SEM (n = 11 per group; 7 male/4 female).

Pathway	Upregulated Proteins	Downregulated Proteins
ETC Assembly	221	213
Mitochondrial Proteostasis	319	254

CONCLUSION
 Our findings show pronounced downregulation of mitochondrial proteostasis pathways and ETC assembly in the RV compared to LV of left heart failure patients and these changes associated with impairment in respiration and disease severity. This highlights a heightened bioenergetic vulnerability in the RV vs LV in HF.

Pathway	Upregulated Proteins	Downregulated Proteins
Mitochondrial Proteostasis	319	254
ETC Assembly	221	213

REFERENCES
 • Huang DW, Sherman BT, Lempicki RA. Systematic and integrative analysis of large gene lists using DAVID bioinformatics resources. *Nature Protoc.* 2009;4(1):44-57. [PubMed]
 • Huang DW, Sherman BT, Lempicki RA. Bioinformatics enrichment tools: paths toward the comprehensive functional analysis of large gene lists. *Nucleic Acids Res.* 2009;37(1):1-13.

ACKNOWLEDGEMENTS
 • Gill Cardiovascular Repository, University of Kentucky Medical Center
 • The Rhode Island IDEA Network of Biomedical Research Excellence (RI-INBRE)

Proteomics analysis reveals etc assembly and mitochondrial proteostasis pathways are more deranged in the RV than LV and associate with degree of dysfunction in explanted failing human hearts

Joseph Owusu-Sarfo, Wenzhuo Ma, Lauren Bazinet, Benison Aguocha, Kenneth S. Campbell, Gaurav Choudhary, Peng Zhang, Richard T. Clements

RV dysfunction associated with group II pulmonary hypertension significantly increases mortality in left heart failure. However, signaling changes associated with progression of RV dysfunction remains poorly understood. We performed a DIA proteomic analysis of explanted left-heart failure patient RV and LV tissue and compared patients with mild and severe RV dysfunction to unused donor hearts.

Explanted hearts (n=22) were obtained at transplant and unused donor hearts (controls) (n=16, 7M/7F) were provided by the Gill Cardiovascular Biorepository, University of Kentucky. All transplant patients exhibited left heart failure and pulmonary hypertension. Right atrial pressure to pulmonary wedge pressure ratio (RAP/PCWP) from right heart catheterization defined RV mild (RAP/PCWP<0.4, n=11, 7M/4F) and severe dysfunction (RAP/PCWP>0.55, n=11, 7M/4F). Total protein was isolated for DIA-MS analysis and mitochondria for isolated frozen mitochondrial respiration assessment.

DIA-MS analysis reliably measured ~4000 proteins/group. Mild RV dysfunction showed 221 up- and 213 downregulated proteins versus donors; severe dysfunction had 319 up- and 254 downregulated proteins (B-H adj P < 0.05). LV changes were less pronounced. Enriched pathways downregulated in RV included mitochondrial translation, respiratory electron transport, oxidative phosphorylation, complex I biogenesis, and complex IV assembly, with greater enrichment in severe dysfunction. LV tissue showed minimal changes in these cascades but increased inflammatory signaling. 302 RV proteins correlated with CI-dependent and 532 with CII-dependent respiration, enriched for oxidative phosphorylation, RV cardiomyopathy, and mitochondrial disease signatures.

Our findings show significant downregulation of mitochondrial proteostasis pathways and ETC assembly in the RV compared to LV of left heart failure patients and these changes associated with impairment in respiration and disease severity. This highlights a heightened bioenergetic vulnerability in the RV vs LV in HF.

Psychiatric Outcomes Associated with GLP-1 RA Use among Patients with Type 2 Diabetes Mellitus: A Target Trial Emulation

Hafizan Yusuf¹, Joseph Nardolillo¹, Lisa Cohen¹, Todd Brothers¹, Kristina E. Ward¹, Xuerong Wen, PhD¹

¹Department of Pharmacy Practice and Clinical Research, The University of Rhode Island, College of Pharmacy, Kingston, RI



Background

- Glucagon-like Peptide 1 receptor agonists (GLP-1 RAs) were introduced in 2005. Steadily increasing utilization.
- The risk of psychiatric outcomes remains controversial.
- Pharmacovigilance and cohort studies have reported higher rates of psychiatric events among patients using GLP-1 RAs.
- Target trial emulations have been conducted; however, their generalizability and the range of assessed outcomes remain limited.

Objectives

To assess the association between GLP-1 RA use with psychiatric outcomes compared with DPP-4i and SGLT2i among patients with type 2 diabetes mellitus

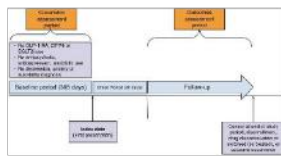
Methods

- Data Source: Commercial insurance claims data from Northeastern of the U.S. spanning from January 2012 - July 2024.
- Target Trial Emulation:

Eligibility Criteria	Diagnosed with type 2 diabetes mellitus; ≥ 18 years old; continuously enrolled along the observation period; no history use of GLP-1 RA, DPP-4i, SGLT2i; no history of major depressive disorder, anxiety, suicidal ideation/attempt; no history use of antipsychotics/antidepressants/antidepressants.
Treatment Assignment	GLP-1 RA users as treatment group DPP-4i or SGLT2i users as comparator group
Outcome Assessment	Validated ICD-9 and ICD-10 with at least 1 claim for major depressive disorder, anxiety, or suicidal ideation/attempt
Covariate Adjustment	Propensity score fine stratification with 50 strata
Causal Contrast	Observational analog of intention-to-treat
Statistical Analysis	Cox proportional hazard model; time-to-event analysis

- A series of subgroup and sensitivity analysis was conducted

Figure 1. Study Design



Results

Figure 2. Cohort Selection Flow Chart

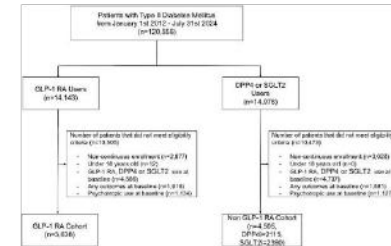


Figure 3. Adjusted Hazard Ratio of Psychiatric Outcomes among GLP-1 RA Initiators vs DPP-4i/SGLT2i Initiators

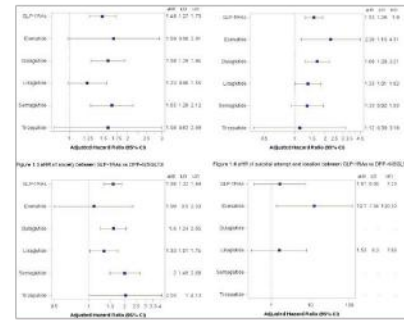


Figure 4. Subgroup Analysis of Psychiatric Outcomes among GLP-1 RA Initiators vs DPP-4i/SGLT2i Initiators



Acknowledgement

The author gratefully acknowledges the support of the Fulbright Foreign Student Program.

Subgroup Analysis

- Male are at higher risk rather than female.
- Higher magnitude of risk among patient with obesity compared who not.
- There is no different between younger and older patients

Sensitivity Analysis:

Consistent results were observed:

- Applying IPTW to adjust for confounding
- Observational Per-Protocol Analogues (Censoring for discontinuation/switching)
- Ignoring grace period

Discussion

- GLP-1 RAs use among patients with T2DM is associated with an increased risk of major depressive disorders and anxiety, compared to SGLT-2i and DPP-4i use.
- The risks differ by gender, obesity status, and individual GLP-1 RAs.
- Consistent with previously published observational studies, which reported an increased risk of psychiatric outcomes associated with GLP-1 RA use.
- This study implemented a TTE framework and included almost all specific agent of GLP-1 RAs.
- Limitations: Residual confounding; SES, severity of T2DM, family history, uncaptured medical history, potential misclassification bias; Some subgroup analyses comprised small sample sizes; Generalizability: commercial insurance data, limited race variability

Conclusion

- GLP-1 RA initiation was associated with higher hazards of psychiatric outcomes compared with alternative antidiabetic therapies, interpreted in light of potential residual confounding.
- Highlight the importance of monitoring psychiatric outcomes following treatment initiation.
- Further research is warranted to clarify causality.

References

1. Yusuf H, Nardolillo J, Cohen L, et al. (2024) Psychiatric Outcomes Associated with GLP-1 RA Use among Patients with Type 2 Diabetes Mellitus: A Target Trial Emulation. *Journal of Clinical Pharmacy and Therapeutics*, 49(1), 1-10. <https://doi.org/10.1111/jcpt.12800>

2. American Diabetes Association. (2023) Standards of Medical Care in Diabetes—2023. *Diabetes Care*, 46(Suppl 1), S19-S207. <https://doi.org/10.2337/dc23-s1>

3. American Psychiatric Association. (2013) *Diagnostic and Statistical Manual of Mental Disorders*, 5th Edition. Washington, DC: Author.

4. American Psychiatric Association. (2013) *Diagnostic and Statistical Manual of Mental Disorders*, 5th Edition. Washington, DC: Author.

5. American Psychiatric Association. (2013) *Diagnostic and Statistical Manual of Mental Disorders*, 5th Edition. Washington, DC: Author.

Psychiatric Outcomes Associated with GLP-1 RA Use among Patients with Type 2 Diabetes Mellitus: A Target Trial Emulation

Hafizan Yusuf, Joseph Nardolillo, Lisa Cohen, Todd Brothers, Kristina E. Ward, Xuerong Wen

Background: The utilization of Glucagon-like peptide-1 receptor agonists (GLP-1 RAs) has dramatically increased in the United States (U.S.) recently. However, the association between GLP-1 RAs use and psychiatric disorders, such as depression, anxiety, and suicidality, remains inconsistent.

Objective: To evaluate the association between GLP-1 RA and psychiatric outcomes compared with dipeptidyl peptidase-4 inhibitors (DPP-4i) or sodium–glucose cotransporter-2 inhibitors (SGLT2i) among patients with type 2 diabetes mellitus (T2DM) by implementing a target trial emulation framework.

Methods: Target trial emulations were conducted using a U.S. administrative claims database. The primary outcome was a composite of major depressive disorder, anxiety disorder, and suicide attempt or ideation. Propensity score fine stratification was applied to balance baseline covariates. Cox proportional hazards models with robust sandwich variance estimators were used to estimate adjusted hazard ratios (HRs) and 95% confidence intervals (CIs). Sensitivity and subgroup analyses were conducted to evaluate the robustness of the results.

Results: A total of 8,143 patients were included, of whom 3,638 were treated with GLP-1 RAs, 2,115 with DPP-4i, and 2,390 with SGLT2i. GLP-1 RAs initiation compared with DPP-4i or SGLT2i was associated with a higher risk of any psychiatric event (HR: 1.48; 95% CI 1.27-1.73), as well as major depressive disorder (HR:1.55; 95% CI 1.26-1.90) and anxiety (HR:1.58; 95% CI 1.32-1.89). In agent-specific analyses, dulaglutide and liraglutide were associated with elevated hazards of major depressive disorder and anxiety; exenatide with major depressive disorder and suicide attempt or ideation; and semaglutide with anxiety.

Conclusion: GLP-1 RA initiation was associated with higher hazards of psychiatric disorders compared with alternative antidiabetic therapies. These findings highlight the importance of monitoring psychiatric outcomes following treatment initiation, although the results should be interpreted in light of potential residual confounding. Further research is warranted to clarify causality and identify patients at greatest risk.

Phytochemical Profiling and Biological Evaluation of Peppermint (*Mentha x piperita*) Leaf Extracts for Cosmeceutical Applications

Chalissa Dibya Iranisha, Huifang Li, Hang Ma

Bioactive Botanical Research Laboratory, Department of Biomedical and Pharmaceutical Sciences, College of Pharmacy, University of Rhode Island, Kingston, RI, USA

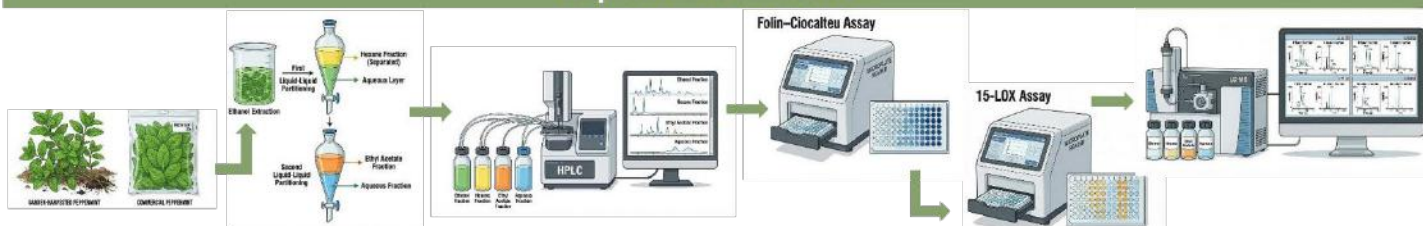
Background

- Peppermint essential oil is widely used in cosmetics, but leaf-derived nonvolatile bioactives are less explored for skin applications.
- Peppermint leaves contain phenolic and flavonoid compounds with reported antioxidant and anti-inflammatory relevance.^{1,2}
- Fraction-specific chemistry and its relation to skin-relevant activity are still not well defined.

Study Aim

To determine the fraction-specific chemical composition of peppermint leaves and evaluate its relationship to skin-relevant bioactivity.

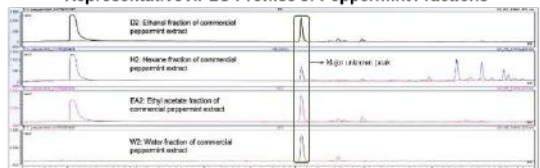
Experimental Workflow



Key Findings

Conclusions & Future Work

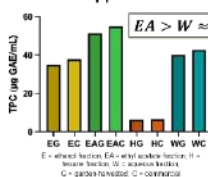
Representative HPLC Profiles of Peppermint Fractions



Distinct fraction-specific chromatographic patterns were observed, with a recurring major unknown peak across all fractions.

An optimized 15-LOX assay with NDGA as positive control and quercetin as reference inhibitor³ was established for screening prioritized peppermint fractions.

Total Phenolic Content of Peppermint Fractions



- HPLC revealed a recurring major unknown peak across all fractions.
- Folin-Ciocalteu assay indicated the highest phenolic content in ethyl acetate fractions, especially EAC and EAG.
- An optimized 15-LOX assay provides a platform for skin-related anti-inflammatory screening of prioritized fractions.
- Future work:** identify major unknown peaks by LC-MS and test prioritized fractions in 15-LOX and additional skin-relevant assays.

References

- Dorman HJD, et al. *Nat Prod Commun.* 2009;4(4):535–542.
- Cirlini M, et al. *Plants.* 2021;10:550.
- Suzuki Y, et al. *Bioorg Med Chem.* 1998;6(8):1317–1322.

Acknowledgments

URI Medicinal Garden (Heber W. Youngken Jr. Medicinal Garden)

THE UNIVERSITY OF RHODE ISLAND

RHODE ISLAND INBRE

FULBRIGHT

CONTACT DETAIL:

chalissa.iranisha@uri.edu

Phytochemical Profiling and Biological Evaluation of Peppermint (*Mentha x piperita*) Leaf Extracts for Cosmeceutical Applications

Chalissa Dibya Iranisha, Huifang Li, Hang Ma

Peppermint (*Mentha x piperita*) is widely used in cosmetic formulations, primarily in the form of essential oils, while the bioactive potential of peppermint leaves remains comparatively underexplored. Leaf-derived extracts are rich in phenolic and flavonoid compounds with reported antioxidant and anti-inflammatory properties; however, their fraction-specific chemical composition and relationship to skin-relevant bioactivity are not well defined. In this study, peppermint leaves from garden-harvested and commercial sources were extracted and partitioned into ethanol, hexane, ethyl acetate, and aqueous fractions to obtain chemically distinct components. Phytochemical profiles of each fraction were analyzed by HPLC and compared against selected reference standards, including rosmarinic acid, pebrellin, gardenin B, wedelolactone, and eriodictyol-7-O-glucoside. Distinct chromatographic patterns were observed across fractions, with several peaks corresponding to putative phenolic markers such as rosmarinic acid and eriodictyol-7-O-glucoside. A major unknown constituent is being further characterized by LC-MS analysis. Preliminary Folin-Ciocalteu assay results showed that ethyl acetate fractions contained the highest phenolic content, followed by aqueous and ethanol fractions, compared to non-polar hexane fractions. The anti-inflammatory potential of each fraction and selected standards is being evaluated using an optimized lipoxygenase (15-LOX) inhibition assay with NDGA as positive control and quercetin as reference inhibitor. These findings highlight peppermint leaves as a promising and underutilized source of bioactive compounds and provide a phytochemical and functional basis for their development in cosmeceutical applications.

Introduction

Problem: With high incidence rates of cancer in the U.S., how can treatment be personalized to increase its effectiveness?

Proposed strategy: self-amplifying RNA vaccine encoding tumor neoantigen¹

Advantage of saRNA over traditional mRNA: intrinsic self-replication²

Role of adjuvants⁴

- Molecules that provide danger signals to stimulate immune response → important if neoantigen is not very immunogenic
- Many serve as agonists for immune recognition mechanisms such as toll-like receptor (TLR) pathways
- Commonly used in FDA-approved vaccines

In vitro dose escalation studies

Luciferase expression in C2C12 cells (24 hours post-transfection)

Luciferase expression in DC2.4 cells (24 hours post-transfection)

mCherry expression in C2C12 cells (24 hours post-transfection)

mCherry expression in DC2.4 cells (24 hours post-transfection)

In vitro adjuvant studies

Constant dose of saRNA: 100 ng per well

Luciferase expression in C2C12 cells (24 hours post-transfection)

Luciferase expression in C2C12 cells (24 hours post-transfection)

Increase in dose of poly(I:C) (TLR3 agonist) → saRNA suppression at all doses explored

Increase in dose of CpG 1018 (TLR9 agonist) → Significant saRNA suppression only at very high doses

Conclusions

- saRNA significantly increases protein expression compared to mRNA in both C2C12 and DC2.4 cells
- saRNA induces increasing protein expression over 3 days
- poly(I:C) suppresses saRNA translation in C2C12 cells, while CpG 1018 suppresses translation only at very high doses

Hypothesis

saRNA vaccines co-delivered with adjuvants that are not TLR 3, 7 or 8 agonists will generate stronger and more durable anti-tumor immunity.

Methods

Cell lines:

- C2C12 mouse myoblast cells → RNA vaccines are given intramuscularly
- DC2.4 mouse dendritic cells → important for priming T and B cells

Workflow for cell transfection studies with saRNA-loaded LNPs:

In vitro expression duration studies

mCherry expression in C2C12 cells (24, 48, 72 hours post-transfection)

mCherry expression in DC2.4 cells (24, 48, 72 hours post-transfection)

Future work

- Optimize LNP design for transfection of DC2.4 cells by conducting a lipid screen
- Investigate immune response to saRNA *in vitro* and *in vivo*
- Determine how protein expression is affected by adjuvant timing (co-delivery with saRNA vs. delayed delivery)

Acknowledgments

We would like to thank the RI INBRE Core Facility, Dr. Xinyuan Chen, and the following funding sources.

References

- Image adapted from: <https://www.ncbi.nlm.nih.gov/pmc/articles/PMC6048481/> - Lipid-based therapy: Understanding Cancer Immunotherapy Research.
- Image adapted from: <https://www.ncbi.nlm.nih.gov/pmc/articles/PMC6048481/> - Lipid-based therapy: Understanding Cancer Immunotherapy Research.
- Publication et al. (2022), Emerging concepts in the science of vaccine adjuvants. *Front. Oncol.*, 12(9), 104-115.

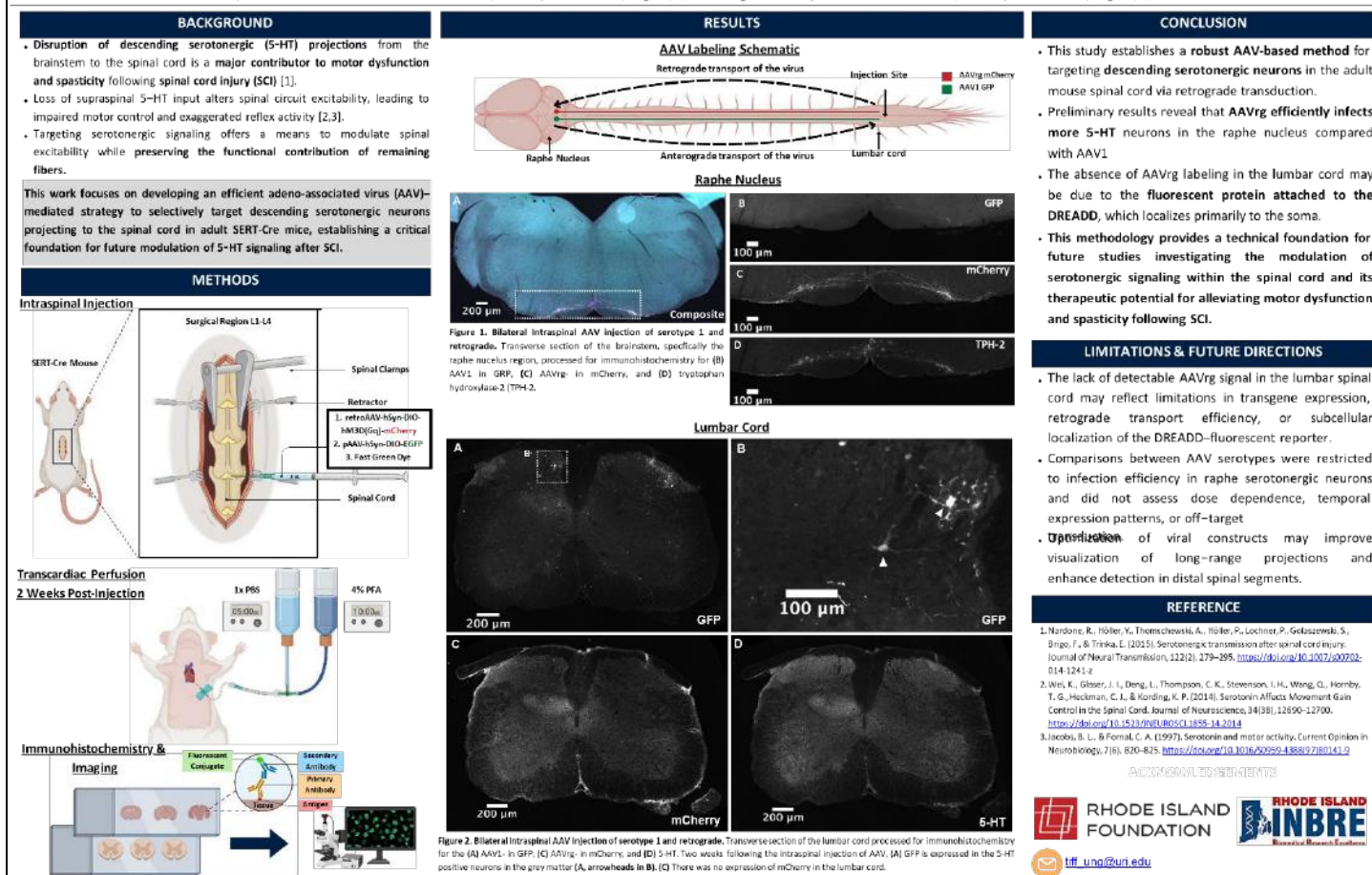
Contact email: ischellenberg@uri.edu, charles_jouaneh@uri.edu, tsih@uri.edu

Shih Lab | Avidislan.460

Self-amplifying RNA (saRNA) Vaccines as a Platform for Cancer Treatment

Iris Schellenberg, Charles Jouaneh, Ting-Yu Shih

Cancer is the second leading cause of death worldwide, demonstrating the need for more effective therapies. While existing cancer treatments can be successful, they are often limited by toxicity, tumor recurrence, and variable clinical efficacy. Cancer vaccines offer a promising alternative by harnessing the immune system to recognize and eliminate tumor cells. Recent advances in mRNA technology provide a versatile avenue for expressing tumor antigens and eliciting an anti-tumor immune response; however, they typically produce relatively transient antigen expression, limiting the effectiveness of this approach. To address this limitation, we propose using self-amplifying RNA (saRNA) augmented by immune adjuvants. The saRNA encodes viral replication machinery that enables self-replication of the RNA transcript, leading to stronger and more sustained protein production. Adjuvants are molecules commonly incorporated in vaccines, boosting immune activation through specific recognition mechanisms such as Toll-like receptor (TLR) pathways. However, several of these pathways, such as TLRs 3, 7, and 8, induce a type I interferon response that suppresses RNA translation. We hypothesized that saRNA vaccines co-delivered with adjuvants that are not TLR 3, 7, or 8 agonists will generate stronger and more durable anti-tumor immunity. Using firefly luciferase and mCherry reporter systems as the payload for the RNA, we compared protein expression from saRNA and mRNA with or without adjuvants. Our results demonstrated that saRNA drives significantly higher and longer-lasting protein expression in both reporter systems. Co-delivery with poly(I:C), a TLR3 agonist, suppresses saRNA translation compared to an saRNA control with no adjuvant. In contrast, CpG 1018, a TLR9 agonist, shows saRNA suppression only at very high doses. Taken together, our novel saRNA technology provides a promising platform for cancer vaccination.



Serotonin After Spinal Cord Injury: Establishing AAV-Mediated Targeting of Descending Serotonergic Fibers

Tiffany Ung, Rebecca Manuel, Marin Manuel

Objective: Disruption of descending serotonergic (5-HT) projections from the brainstem to the spinal cord is a major contributor to motor dysfunction and spasticity following spinal cord injury (SCI). Loss of supraspinal 5-HT input alters spinal circuit excitability, leading to impaired motor control and exaggerated reflex activity. Targeting serotonergic signaling offers a means to modulate spinal excitability while preserving the functional contribution of remaining fibers. This work focuses on developing an efficient adeno-associated virus (AAV)-mediated strategy to selectively target descending serotonergic neurons projecting to the spinal cord in adult SERT-Cre mice, establishing a critical foundation for future modulation of 5-HT signaling after SCI.

Method: Cre-dependent adeno-associated viruses (AAV) were injected into SERT-Cre adult mice via intraspinal injection into the lumbar spinal cord. Two different AAV serotypes were compared for their ability to infect 5-HT neurons and be retrogradely transported to the raphe nucleus. Two weeks after injection, the brainstem and spinal cord tissues were collected and processed for immunohistochemistry. Tryptophan hydroxylase-2 (TPH-2) and 5-HT antibodies were used to confirm positive 5-HT neurons. Fluorescence imaging and manual cell counts were performed to quantify viral specificity and infection efficiency.

Results: Both viral strategies successfully labeled serotonergic neurons and their descending projections. Quantitative analysis revealed differences in the proportion of TPH-2-positive neurons infected by each AAV, indicating distinct efficiencies between approaches for targeting descending 5-HT.

Conclusion: This study establishes a robust AAV-based method for targeting descending serotonergic neurons in the adult spinal cord. The methodology provides a critical technical foundation for future studies investigating modulation of serotonergic signaling within the spinal cord and its therapeutic potential in alleviating motor dysfunction and spasticity following SCI.

Introduction

Nano- and microplastics (NMPs), plastic particles < 1µm and < 5 mm in size respectively, are an emerging concern for the environment and human health, yet, little is known about their effects. Thus far, NMPs have been found in human liver, lungs, blood, colon, brain, and placenta, as well as breast milk, feces, and blood clots. Previously, the Ross Lab investigated the general and age-dependent effects of polystyrene (PS) NMPs exposure on mice. PS-NMPs were identified in every tissue examined, most notably, in the brain. This resulted in altered behavior during open-field and light/dark assays, as well as alterations to immune markers in liver and brain, in particular glial fibrillary acidic protein (GFAP). This decrease in GFAP expression may be indicative of early neurological decline, such as in Alzheimer's disease (AD). While the exact cause of AD is unknown, certain lifestyle factors such as exposure to pollutants have been linked to increased risk. Furthermore, accumulation of amyloid-beta plaques is a key biomarker of AD pathology. We thus investigated if exposure to PS-NMPs influences plaque onset and progression as well as cognition using a mouse model of AD pathology (APP/PSEN1).

Methods

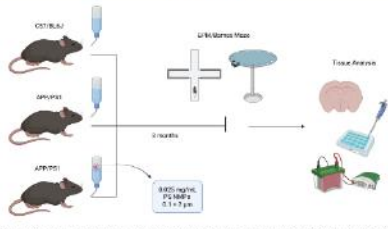


Figure 1. Study Design. 3 month exposure to PS-NMPs in female APP/PSEN1 mice and appropriate controls (n=10 per group), followed by behavioral testing and tissue analyses.

Mice were exposed to regular water or 0.025mg/mL pristine fluorescently-labeled PS-NMPs for three months followed by EPM and Barnes Maze testing. Mice spent 5 minutes in the EPM while time spent and distance traveled in the open arms versus closed arms were recorded. For Barnes maze, mice completed 4 training days, with four 180 second trials each day. On Day 5, mice completed a 90 second probe test with the target box removed to assess spatial memory. Brains were then collected and analyzed using IHC for plaque load (Aβ-42), astrocytes (GFAP), and microglia localization (IBA1).

Results

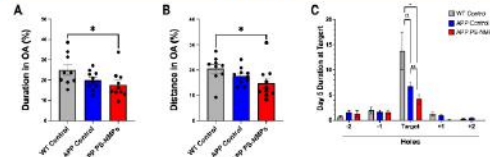


Figure 2. Effects of PS-NMPs Exposure on Anxiety-Like Behavior and Spatial Memory. APP mice exposed to PS-NMPs spent significantly less time (A) and traveled less (B) in the open arms (OA) in comparison to wild-type controls. Significances were determined by unpaired t-test with * $p < 0.05$. (C) Effects of PS-NMPs exposure on spatial memory and learning using Barnes maze. Time spent at target hole decreased with exposure to PS-NMPs, indicating NMPs exposure increases cognitive deficits in APP mice. Significances determined by unpaired t-test;

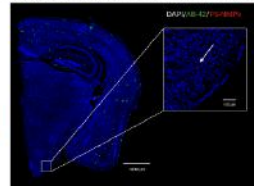


Figure 3. Confirmation of PS-NMPs Localization in Brain Tissue Following Three Months of Exposure. Presence of fluorescent PS-NMPs (red, indicated by arrow) in the brain of an exposed APP/PSEN1 mouse. Amyloid plaques (green) were visualized by IHC and sections were co-stained with DAPI (blue). Scale bar = 1000 µm, 100 µm, respectively.

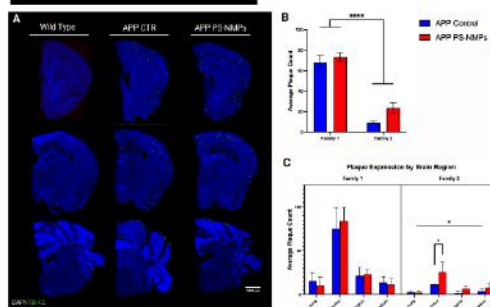


Figure 4. Amyloid-Beta Plaque Analysis. (A) Accumulation of amyloid-beta plaques (Aβ-42, green, indicated by arrows) in prefrontal cortex, hippocampus, and cerebellum sections. Sections were co-stained with DAPI (blue). Scale bar = 1000 µm. (B) Average plaque count per brain section. Mice were separated into two groups based on family line (F1 and F2). (C) Average plaque count by brain region in F1 and F2 lines. Significances determined by 2-way ANOVA with multiple comparisons; * $p < 0.05$, **** $p < 0.0001$, and a $p < 0.10$ as trending.

Results Cont.

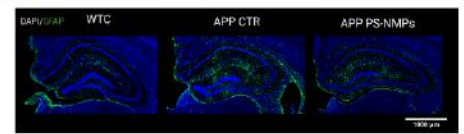


Figure 5. Neuroinflammation Following PS-NMPs Exposure Representative images of GFAP (green) expression in hippocampus region of DAPI-stained brain sections (Blue). Scale Bar = 1000 µm.

Discussion/Conclusions

Following a three month exposure to 0.025mg/mL PS-NMPs, APP/PSEN1 mice displayed increased anxiety-like behavior in the EPM and worsening spatial memory in the Barnes Maze. When analyzing the Aβ plaques, we found that mice from one family (F2) had significantly lower plaque counts. APP/PSEN1 mice have been found to have variability in the timeline of plaque accumulation based upon the genetic background (Couch et al., *J Comparative Neurology* 2013). Furthermore, Aβ plaques have been shown to have rapid progression initially followed by a saturation phase (Burgold et al., *Acta Neuropathol. Commun.*, 2014). As such, small changes in the timeline can result in significant differences early on. Considering this, we decided to separate the APP/PSEN1 mice into two groups (F1 and F2) for plaque analysis. Mice from the F2 family were found to have a significantly lower overall plaque load as compared to mice from the F1 family. Mice from the F1 family did not show a difference in plaque load based on exposure to PS-NMPs; however, there was a significant increase in plaque load of the F2 mice by brain region with PS-NMPs exposure. This is consistent with previous findings that PS-NMPs can speed up the initial deposition of Aβ in vitro, but have a less pronounced effect at high concentrations of Aβ (Gou et al., *J Hazard Mater*, 2024). Results show no differences in terms of plaque size. Preliminary analysis of GFAP and IBA1 via IHC is consistent with previous studies from the Ross Lab, indicating a decrease in both GFAP and IBA1. Future work will include Western blot to quantify the decrease in GFAP and IBA1.

Acknowledgments

Thank you to Dr. Jaime Ross, Dr. Giuseppe Coppotelli, Dr. Lauren Gaspar, Tommy Kelly, Miah Wainio, Dr. Sydney Bartman, Hannah Tobias-Wallingford, and Sajida Jan for their contributions to this work. Thank you to our funding sources: Rhode Island Foundation, URI Plastics Initiative, RI-INBRE, Fred M. Roddy Foundation, URI Preclinical Development Grant, URI George & Anne Ryan Institute for Neuroscience, URI College of Pharmacy.

The Effects of Nano-Microplastics Exposure on Alzheimer's Disease Pathology Characterized in APP/PSEN1 Mice

Mackenzie Pavlik, Sydney Bartman, Lauren Gaspar, Giuseppe Coppotelli, Jaime M. Ross

Alzheimer's disease and related dementias (AD/ADRD) are one of the most prevalent cognitive disorders, affecting more than 6 million Americans over the age of 65. While the exact cause of AD and ADRD is still unknown, several risk factors have been identified, including exposure to environmental toxins. In recent years, nano- and microplastics (NMPs), defined as particles ≤ 1 µm and ≤ 5 mm in size, respectively, have emerged as pervasive environmental pollutants. Previous studies have shown NMPs are able to accumulate in peripheral tissues throughout the body of both humans and mice, raising concerns regarding their potential health impacts. Furthermore, NMPs have been demonstrated to cross the blood-brain barrier to accumulate through the brain, resulting in alterations in cognitive behavior and immune markers consistent with neurological disease. We recently demonstrated that polystyrene (PS)-NMPs exposure in transgenic mice carrying the APOE4 variant, the largest known risk-factor for developing AD, resulted in marked sex-dependent alterations in locomotion and recognition memory, as well as changes to astrocytic and microglial markers in the brain. Building on these results, we are now examining the effects of NMPs exposure in a mouse model of Alzheimer's disease pathology (APP/PSEN1). Specifically, this study aims to determine whether chronic exposure to 0.1 µm and 2 µm polystyrene NMPs influences the onset and/or progression of amyloid-beta plaque deposition, alters neuroimmune markers, and affects cognitive function. Preliminary results indicate that chronic exposure to PS-NMPs in APP/PSEN1 mice worsens cognitive impairments, while plaque accumulation was observed to increase taking into account the plaque variability of the family line. Ongoing analyses are also investigating the histological, biochemical, and immunological changes resulting from PS-NMPs exposure.



THE UNIVERSITY OF RHODE ISLAND COLLEGE OF PHARMACY

UDP-Glucuronosyltransferase (UGT) enzyme polymorphisms impact clinical outcomes in chronic cholestatic liver diseases

Colleen M. Hayes¹, Mahesh Krishna², Christopher L. Hemme¹, Scott J. Roberts², Bonnie Chen², James L. Boyer², David N. Assis², Nisanne S. Ghonem¹

¹URI College of Pharmacy, Biomedical and Pharmaceutical Sciences, Kingston, RI; ²Yale School of Medicine, Liver Center, New Haven, CT



INTRODUCTION

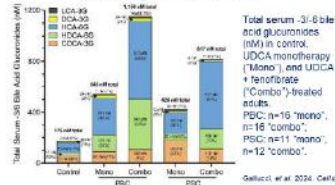
- Primary biliary cholangitis (PBC) and primary sclerosing cholangitis (PSC) are chronic cholestatic liver diseases characterized by the accumulation of toxic bile acids.
- Bile acid glucuronidation is a major pathway of bile acid detoxification in the liver, catalyzed by UDP-Glucuronosyltransferase (UGT) enzymes.
- Fenofibrate, a peroxisome proliferator-activated receptor (PPAR α) agonist, is used as adjunct therapy in combination with ursodeoxycholic acid (UDCA) for refractory PBC and PSC. Fenofibrate reduces bile acid toxicity by altering the composition and concentration of bile acid glucuronides in PBC and PSC, Fig. 1.
- Many UGTs are regulated by the nuclear receptor PPAR α , however, UGT1A and UGT2B gene families are polymorphic.
- UGT polymorphisms impact bile acid glucuronidation in healthy adults¹ and clinical outcomes in PSC².

AIM

Investigate the frequency and effects of UGT polymorphisms on clinical outcomes and treatment response in PBC and PSC.

BACKGROUND

Figure 1. Adjunct fenofibrate (+ UDCA) reduces bile acid toxicity in PBC and PSC.



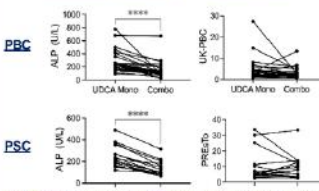
Total serum 3-O-bile acid glucuronides (nM) in control, UDCA monotherapy ("Mono"), and UDCA + fenofibrate ("Combo")-treated adults. PBC: n=16 "mono", n=16 "combo", PSC: n=11 "mono", n=12 "combo".

METHODS

- Genomic DNA was extracted from de-identified human plasma samples from healthy controls (BioIVT), and PBC and PSC patients with refractory cholestasis despite UDCA treatment (13-15 mg/kg/day) who received adjunct fenofibrate therapy (145-160 mg/day) at the Yale Liver Clinic (New Haven, CT).
- Genotyping was performed using rhAmpTM single nucleotide polymorphism assays (A) for: UGT1A3 -66T>C, -1A3 31T>C, -1A4 Trp11, -2B4 1374A>T, and -2B7 802T>C.
- Correlation of UGT genotypes, serum levels of the liver injury marker alkaline phosphatase (ALP) and clinical risk scores for PBC (UK-PBC 10-yr) and PSC (PRESto) were analyzed.

RESULTS

Figure 2. Combined fenofibrate + UDCA treatment decreases serum ALP in PBC and PSC.



Paired sample analysis from patients with PBC (n=28-31 pairs) or PSC (n=16-17 pairs) pre- (UDCA monotherapy, "Mono"), and post-fenofibrate treatment (UDCA + fenofibrate, "Combo"). ****p<0.0001 analyzed by paired t-test.

Figure 3. Genotype frequencies of UGT polymorphisms in healthy controls and patients with PBC and PSC.

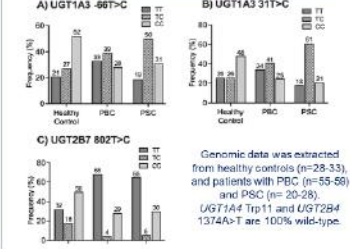
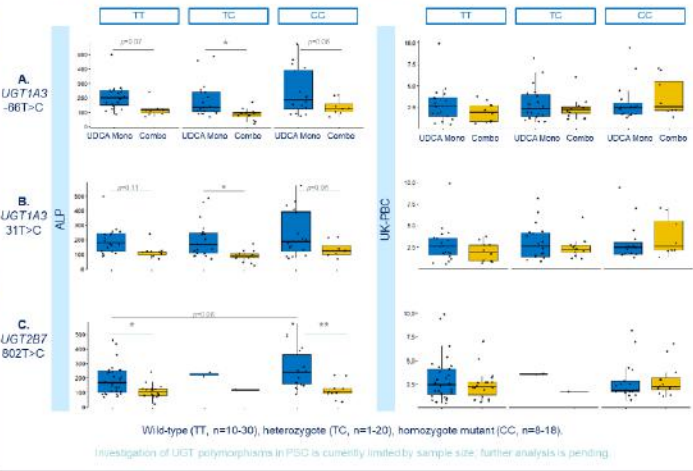
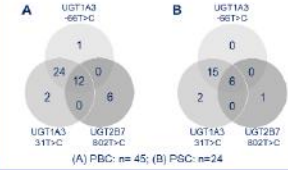


Figure 4. Effect of UGT polymorphisms on serum ALP levels and UK-PBC risk scores in PBC.



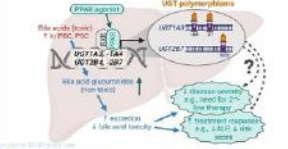
RESULTS (CONT.)

Figure 5. Number of PBC (A) and PSC (B) patients with ≥ 1 UGT polymorphism.



SUMMARY

Figure 6. Schematic representation of hypothesized effects of UGT polymorphisms.



CONCLUSIONS

- Paired analysis shows combination therapy (fenofibrate + UDCA) significantly reduces serum ALP levels vs. UDCA alone in PBC & PSC (Fig. 2)
- UGT polymorphisms are detected in PBC and PSC (Fig. 3A, 3B, 3C).
- In PBC (Fig. 4A, 4B, 4C), UGT1A3 and UGT2B7 variant genotypes are associated with:
 - elevated ALP levels in patients on UDCA monotherapy, i.e., "non-responders".
 - higher UK-PBC scores in patients on adjunct therapy with fenofibrate.
- Most patients carry >1 UGT polymorphism (Fig. 5), requiring further investigation.

These data suggest that UGT polymorphisms may impact clinical outcomes in PBC.

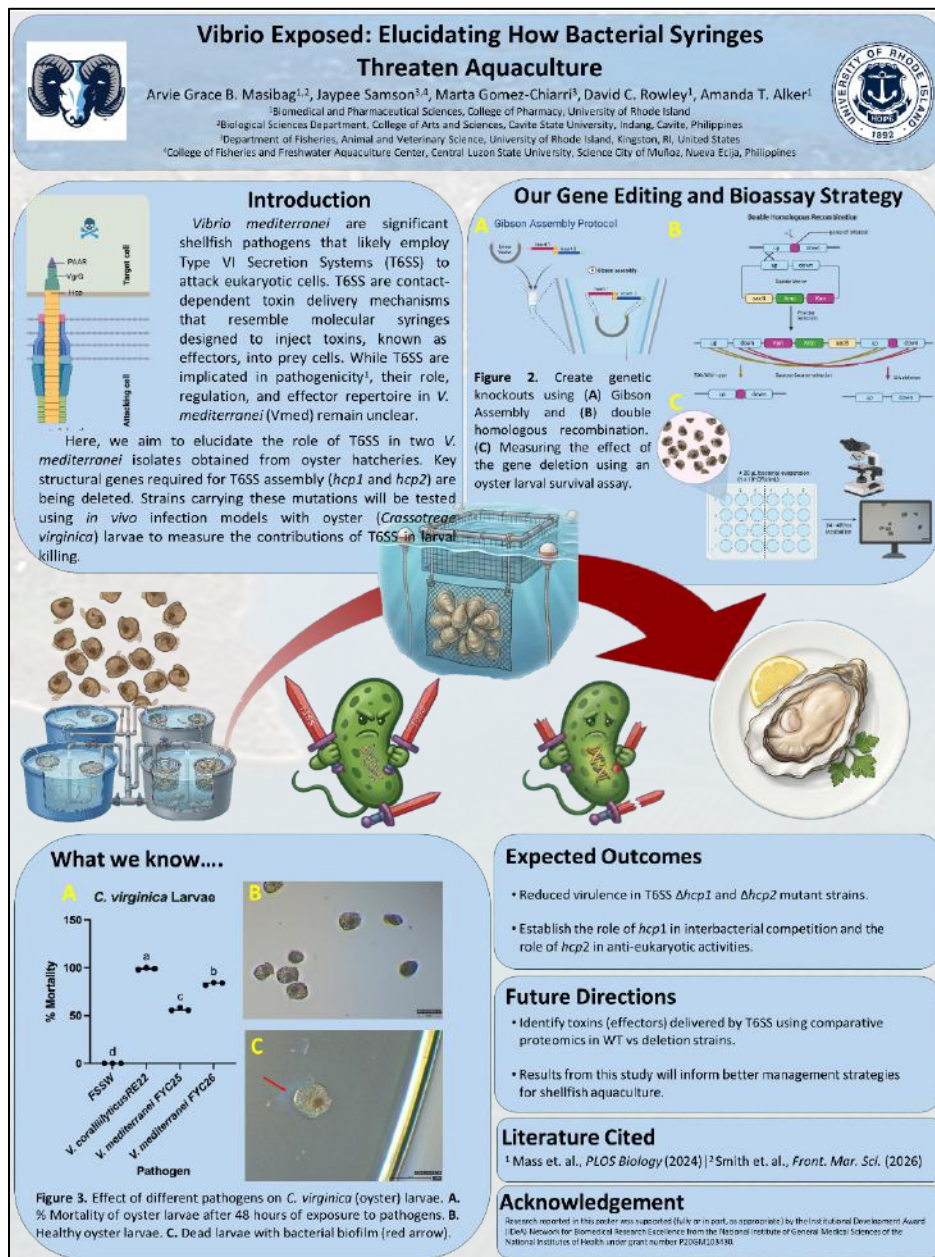
ACKNOWLEDGMENTS

Research was supported in part by: American Liver Foundation Pilot Research Award, RI-Dea Network of Biomedical Research Excellence (NIAMS, P20GM103430), Silvio O. Conte Digestive Diseases Research Core Center, P30DK034869 (Yale Liver Center). REFERENCES: 1. Trotter, et al. 2013. 2. Weismuller, et al. 2020

UDP-Glucuronosyltransferase (UGT) enzyme polymorphisms impact clinical outcomes in chronic cholestatic liver diseases

Colleen M. Hayes, Mahesh Krishna, Christopher L. Hemme, Scott J. Roberts, Bonnie Chen, James L. Boyer, David N. Assis, Nisanne S. Ghonem

Primary biliary cholangitis (PBC) and primary sclerosing cholangitis (PSC) are chronic cholestatic liver diseases characterized by the accumulation of toxic bile acids in the liver. Glucuronidation is a major pathway of bile acid detoxification in which UDP-glucuronosyltransferase (UGT) enzymes conjugate glucuronic acid to bile acids, enhancing their elimination. In humans, bile acid glucuronidation is catalyzed by UGT1A1, -1A3, -1A4, -2B4, and -2B7 enzymes, which are regulated by the peroxisome proliferator-activated receptor alpha (PPAR α). Importantly, two PPAR agonists received FDA-approval as second-line therapy for PBC, however, UGT enzymes are encoded by the polymorphic UGT1A and -2B genes, which can alter glucuronidation and, consequently, affect bile acid levels and subsequent liver injury. This study evaluates the frequency and clinical impact of UGT polymorphisms in people with PBC and PSC with refractory cholestasis requiring adjunct treatment of fenofibrate (a PPAR α agonist) in combination with ursodeoxycholic acid. Genomic DNA was extracted from de-identified PBC and PSC plasma samples (Yale Liver Center Biorepository, New Haven, CT), and genotyping was performed for UGT1A3 -66T>C, -1A3 31T>C, -2B4 1374A>T, and -2B7 802T>C polymorphisms. The impact of UGT genotypes on clinical markers of liver injury, e.g., serum alkaline phosphatase (ALP), and clinical risk scores of end-stage liver disease (UK-PBC, PRESto) was assessed. UGT polymorphisms were found in PBC and PSC patients, and all three genotypes (wild-type, heterozygous, homozygous mutant) were detected for UGT1A3 -66, -1A3 31, and -2B7 802. Notably, the UGT2B7 802T>C homozygous variant was associated with higher ALP levels in PBC patients receiving ursodeoxycholic acid therapy (p=0.06), suggesting a potential role of UGT polymorphisms in the treatment response to anti-cholestatic therapy. The data also show that many patients carry multiple UGT polymorphisms. These findings support further investigation into UGT polymorphisms as potential factors underlying clinical outcomes, and the response to anti-cholestatic therapy in PBC and PSC.

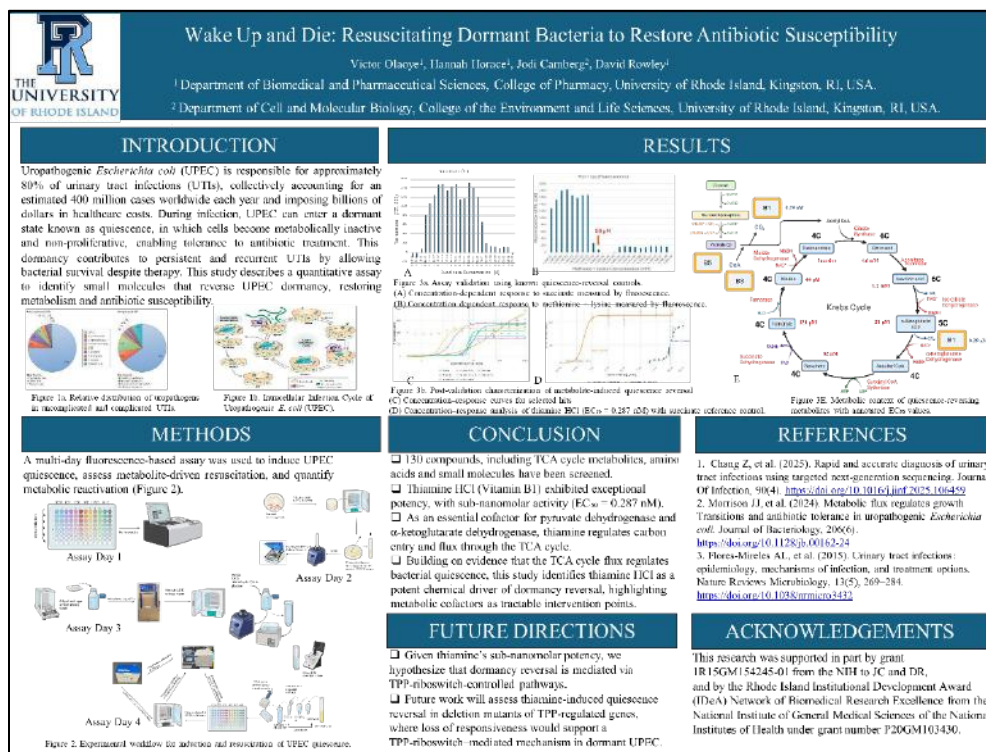


Vibrio Exposed: Elucidating How Bacterial Syringes Threaten Aquaculture

Arvie Grace Masibag, Jaypee Samson, Marta Gomez-Chiarri, David C. Rowley, Amanda T. Alker

Vibrio mediterranei are significant shellfish pathogens that likely employ Type VI Secretion Systems (T6SS) to attack eukaryotic cells. T6SS are contact-dependent toxin delivery mechanisms that resemble molecular syringes designed to inject toxins, known as effectors, into prey cells. While T6SS are implicated in pathogenicity, their role, regulation, and effector repertoire in *V. mediterranei* (Vmed) remain unclear.

Here, we aim to elucidate the role of T6SS in two *V. mediterranei* isolates obtained from oyster hatcheries. Key structural genes required for T6SS assembly (*hcp1* and *hcp2*) are being deleted. Strains carrying these mutations will be tested using *in vivo* infection models with oyster (*Crassostrea virginica*) larvae to measure the contributions of T6SS in larval killing.



Wake Up and Die: Resuscitating Dormant Bacteria to Restore Antibiotic Susceptibility

Victor Olaoye, Hannah Horace, Jodi Camberg, David Rowley

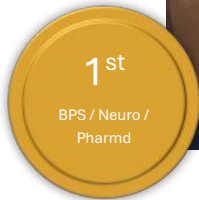
Recurrent urinary tract infections (UTIs) are frequently caused by uropathogenic *Escherichia coli* (UPEC) that persist in a dormant, quiescent state. Quiescent bacteria exhibit reduced metabolic activity and antibiotic tolerance, contributing to treatment failure and infection recurrence. While prior studies have characterized mechanisms governing entry into and exit from bacterial quiescence, experimental approaches to identify dormancy-reversing molecules have relied largely on agar-plate assays. These platforms are inherently low throughput, limited in sensitivity, poorly suited for systematic small-molecule screening, and unable to efficiently generate quantitative dose-response relationships. To address this gap, we developed a novel, high-throughput, fluorescence-based quiescence reversal assay compatible with 96-well plate formats. This platform enables sensitive, quantitative measurement of metabolic reactivation, supports rapid determination of concentration-response relationships and EC_{50} values, and provides improved statistical power for compound screening. Using this assay, 130 compounds, including TCA cycle metabolites, amino acids, and small molecules, were screened for their ability to restore metabolic activity under quiescent conditions, with known quiescence-reversing metabolites validating assay performance. Thiamine (vitamin B1) exhibited exceptional potency, with sub-nanomolar activity ($EC_{50} = 0.3 \text{ nM}$). Thiamine is an essential cofactor for pyruvate dehydrogenase and α -ketoglutarate dehydrogenase, enzymes that regulate carbon entry and flux through the TCA cycle. Consistent with prior evidence linking TCA cycle flux to bacterial exit from quiescence, these findings identify thiamine as a potent chemical driver of dormancy reversal and highlight metabolic cofactors as tractable intervention points for targeting dormancy-driven recurrent UTIs caused by UPEC.

To address this gap, we developed a novel, high-throughput, fluorescence-based quiescence reversal assay compatible with 96- and 384-well plate formats. This platform enables sensitive, quantitative measurement of metabolic reactivation, supports rapid determination of concentration-response relationships and EC_{50} values, and provides improved statistical power for compound screening. Using this assay, 130 compounds, including TCA cycle metabolites, amino acids, and small molecules, were screened for their ability to restore metabolic activity under quiescent conditions, with known quiescence-reversing metabolites validating assay performance.

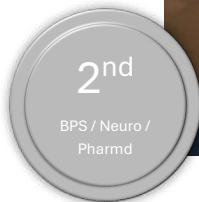
A limited subset of screened metabolites induced reversal of quiescence, with activity observed predominantly at millimolar to micromolar concentrations. However, thiamine HCl (vitamin B1) exhibited exceptional potency, with sub-nanomolar activity ($EC_{50} = 0.287 \text{ nM}$). Thiamine is an essential cofactor for pyruvate dehydrogenase and α -ketoglutarate dehydrogenase, enzymes that regulate carbon entry and flux through the TCA cycle. Consistent with prior evidence linking TCA cycle flux to bacterial exit from quiescence, these findings identify thiamine HCl as a highly potent chemical driver of dormancy reversal and highlight metabolic cofactors as tractable intervention points for targeting persistent UPEC. Ongoing work will investigate the contribution of TPP-riboswitch-regulated pathways to thiamine-induced resuscitation in dormant UPEC.

BPS / Neuro / PharmD

BPS / Neuro / PharmD



Delaney Abatecola accepting on behalf of the winning poster



Anna Schumacher accepting on behalf of the second placed poster



Camila Quiroga accepting on behalf of the third placed poster

Validation of the Inducible mtDNA Mutator Model of Mitochondrial Dysfunction

Delaney Abatecola^{1,2,1}, Nikki Fernando^{1,2,1}, Hannah Tobias-Wallingford^{1,2}, Giuseppe Coppotelli^{1,2}, and Jaime M. Ross^{1,2}

¹George & Anne Ryan Institute for Neuroscience, University of Rhode Island, Kingston RI
²Biomedical & Pharmaceutical Sciences, College of Pharmacy, University of Rhode Island, Kingston RI
 *These authors contributed equally to this work.

INTRODUCTION and AIM

- Mitochondrial dysfunction (MD) is a hallmark of aging and has been involved in many neurodegenerative diseases, such as Alzheimer's and Parkinson's disease, and in furthering neurocognitive deficits.
- Many previous models that study MD include the mtDNA mutator mouse (Trifunovic et al., 2004 & Kujoth et al., 2005). The model expresses a proofreading deficient version (D257A) of mtDNA polymerase- γ (PolgA) and gathering whole-body mtDNA mutations and deletions from gestation.
- As a result of the global nature of MD in this model, it has been challenging to study the impact of mtDNA mutations on specific processes such as cognition, neural development, motor systems, or particularly on inflammatory and immune responses. Additionally, it is impossible to study the impact of mutations occurring at different time points during development.
- A novel inducible knock-in mtDNA mutator mouse model, i-PolgA, has been developed to study MD with greater tissue and temporal specificity.

The aim of this research is to characterize a novel inducible mtDNA mutator mouse model, the i-PolgA mouse. This is a model of MD with temporal and spatial control of mtDNA. This work aims to validate the temporal control of the model via induction of the mutation and assessment of recombination across tissues.

METHODS

- Novel inducible mtDNA mutator mouse generated and induced via five consecutive days of intraperitoneal Tamoxifen injections (75 mg/kg) at one month of age. Following induction and tamoxifen washout period, tissues were obtained.
- Western blot, immunohistochemistry, and cell analyses were performed to assess recombination efficiency and specificity.
- Fibroblasts from untreated mice were cultured followed by 4-OHT treatment for 48 hours prior to imaging.

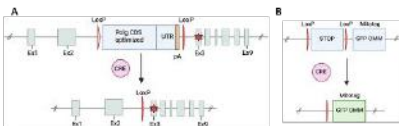


Figure 1. (A) Schematic of the Cre-LoxP recombination system utilized to generate the novel inducible mutator mouse. The PolgA CDS contains the entire CDS from exon 3 onwards, following this there is the endogenous untranslated region (UTR) and hNha poly-adenylation signal (yellow). The mutation (red star) is within exon 3 and will only be expressed following excision at the LoxP sites by CRE. (B) Schematic of Mitotag reporter mouse being used in conjunction to assess CRE recombination. Following tamoxifen treatment, CRE will recombine, removing the STOP cassette and allowing for expression of GFP localized to the outer mitochondrial membrane.

RESULTS

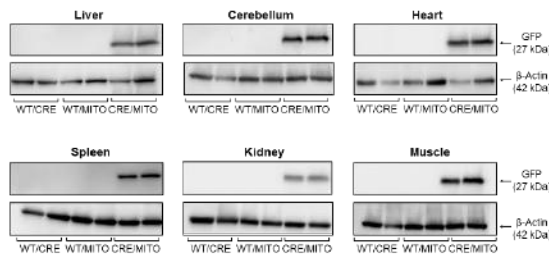


Figure 2. Validation of CRE recombination in the i-PolgA model via Western blot analyses. Detection of GFP expression across various tissues following tamoxifen treatment in i-PolgA mice expressing both CRE and Mitotag, confirming GFP in the Mitotag reporter mouse is appropriately expressed and tamoxifen treatments are sufficient to induce recombination.

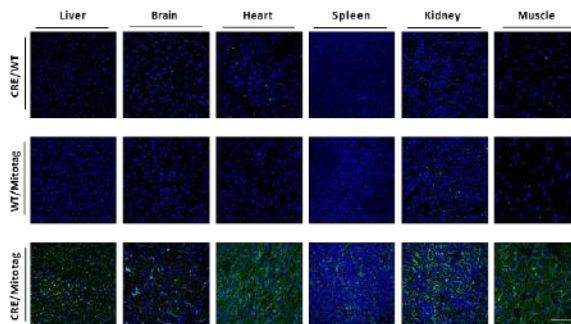


Figure 3. Validation of CRE recombination following Tamoxifen treatment in i-PolgA mice assessed via immunohistochemistry analyses of GFP. Representative images of GFP expression (green) in various Hoechst-stained (blue) tissue samples. Expression of GFP is limited to CRE/Mitotag in i-PolgA animals, confirming that GFP expression in the Mitotag reporter mouse is appropriately expressed and tamoxifen treatments are sufficient to induce CRE recombination. Scale bar 100 um.

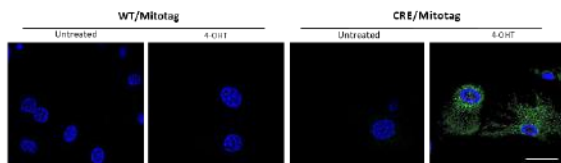


Figure 4. i-PolgA fibroblasts treated with control or 4-OHT (tamoxifen) validate Cre recombination, with Mitotag GFP expression (green) observed in 4-OHT-treated cells. Nuclei are stained with Hoechst (blue). Scale bar 200 um.

CONCLUSIONS

- Tamoxifen induction of the i-PolgA model produces consistent CRE recombination across tissues, confirmed by GFP expression from the Mitotag reporter as assessed by both Western blot and immunohistochemistry analyses.
- These findings demonstrate consistent and reliable recombination efficiency across multiple tissue types.
- This work provides the first validation of temporal control in the novel i-PolgA model, establishing its utility for inducible, time-specific genetic manipulation *in vivo*.
- Validation and systematic assessment of CRE recombination following tamoxifen treatment establish a strong experimental foundation for future studies aimed at understanding the impacts of development of mitochondrial mutations at different stages of development.

NEXT STEPS

- Quantify recombination efficiency by measuring residual CDS abundance via qPCR following tamoxifen induction to further validate recombination completeness.
- Characterize the temporal progression and severity of mitochondrial dysfunction following induction using a cell-based model.
- Utilize this model to address long-standing questions regarding the impact of mitochondrial mutations that arise post-embryogenesis and at distinct developmental or aging time points, with a focus on tissue-specific outcomes.

Acknowledgments

*Special thanks to Dr. Jaime Ross, Dr. Giuseppe Coppotelli, Sajida Jan-Bibi, and Mackenzie Pavlik.

Funding:

OD/NIH R21OD037651 (GC, JMR), NIA/NIH R01AG092603 (GC, JMR), URI College of Pharmacy Seed Funding (GC), George & Anne Ryan Institute for Neuroscience (GC, JMR), The Roddy Foundation (GC, JMR), and Konung Gustaf V:s och Drottning Victorias Frimurarestiftelse (JMR).



First Place - Validation of the Inducible mtDNA Mutator Model of Mitochondrial Dysfunction

Delaney Abatecola, Nikki Fernando, Hannah Tobias-Wallingford, Giuseppe Coppotelli, Jaime M. Ross

Mitochondrial dysfunction is a central feature of aging and many age-related diseases, and although the exact molecular mechanisms leading to the decline of mitochondrial function with aging remains to be elucidated, the accumulation of mitochondrial DNA (mtDNA) mutations is thought to play a major role in this decline. In this regard, various studies have demonstrated a dramatic increase in mtDNA mutations with aging not only in human tissues but also in experimental animal models. To better understand the link between mtDNA mutations and mitochondrial dysfunction in aging and diseases, Nils-Göran Larsson's group generated the original mtDNA mutator mouse. This model expresses a proofreading-deficient version of mtDNA polymerase-gamma (PolgA), resulting in an accelerated accumulation of mtDNA mutations and aging-like mitochondrial dysfunction. Although this model has significantly advanced research in mitochondrial biology and aging, it is limited by the whole-body accumulation of mtDNA mutations occurring from gestation. Given this, it is impossible to understand tissue-specific and temporal differences in mtDNA mutations and to investigate the impact of mutations occurring at different times during development. To overcome this limitation, we developed a novel inducible knock-in mtDNA model (iPolgA). Here, we validate this system by inducing expression of the deficient polymerase and assessing recombination across multiple tissues using Western blotting, immunohistochemistry, and cell-based assays. Our results confirm induction and temporal control, establishing the functionality of the model and providing a framework for investigating future questions about mitochondrial biology and aging.



Post-mortem Analysis of Von Economo Neurons in the Anterior Cingulate Cortex and Frontoinsular Cortex in Prader-Willi Syndrome

Schumacher, A.¹, Fam, M.², Warda, T.², Wicinski, B.², Forster, J.L.³, Hof, P.R.², Varghese, M.T.⁴

¹ Interdisciplinary Neuroscience Program, University of Rhode Island, Kingston, RI 02881, USA

² Nash Family Department of Neuroscience, Friedman Brain Institute, and Ronald M. Loeb Center for Alzheimer's Disease, Icahn School of Medicine at Mount Sinai, New York, NY 10019, USA.

³ Pittsburgh Partnership, Pittsburgh, PA 15228

⁴ George and Anne Ryan Institute for Neuroscience, and Department of Biomedical and Pharmaceutical Sciences, University of Rhode Island, Kingston, RI 02881, USA



Introduction

- Prader-Willi Syndrome (PWS) is a rare neurodevelopmental genomic imprinting disorder caused by a lack of gene expression from the paternal (60%) or maternal (35%) chromosome 15.¹⁹
- fMRI shows increased activation of the Insula and ACC showing impairment in the ability to percept inner physiological states.^{22,19,7,8}
- The anterior cingulate cortex (ACC) plays a role in emotional regulation, motivation, and autonomic stability.^{28,12}
- The frontoinsular cortex (FI) plays a role in interoception, emotional and social processing, and decision-making.²⁹
- Pyramidal neurons support cortico-cortical connectivity.²⁹
- VENs (Von Economo neurons) are morphologically distinct spindle cells that rapidly transmit social and physiological signals critical for homeostasis.²⁰
- Increased VENs quantity may correlate with greater capacity for negative self-appraisal.²
- Abnormality in the number and hemispheric distribution of VENs has been found in autism, schizophrenia, alexithymia, and frontotemporal dementia.^{5,12}

Figure 1. Key interrelated behavioral features of PWS.

Materials / Methods

Our study is conducted using post-mortem PWS ACC and FI tissue provided by NIH NeuroBank. Samples were stained with cresyl violet and quantified under high-resolution microscopy using Stereo Investigator software. VENs and pyramidal neurons were quantified using the optical fractionator, and regional volume was estimated using the Cavalieri principle. Pyramidal cell volume was estimated using the nucleator.

Sample Demographics:

- 19 total samples, 11 samples included; 100% caucasian; 4 females, 7 males
- Median IQ fell in the mild range of intellectual deficiency
- BMI range: 32.4-90; average 50.8, mean 43
- Age at death: 17-59 years (mean 37)
- 7 raised in group homes; 4 lived with family
- Mortality causes: hypoventilation 5, GI complications 2, hypothermia 1, syndrome complications 3

Figure 3. Contoured PWS ACC tissue section.

Discussion

- Uncovering the neuronal density and morphology of the ACC and FI of PWS allows for insight into the syndrome's neuropathology
- Sampling error resulted in predominantly posterior insula tissue rather than anterior insula, leading to the unexpected finding of VENs in the posterior insula
- A major limitation is the small sample size, with only 11 of the 19 samples usable. Exclusions were due to tissue integrity and staining quality on preliminary testing
- Stereology is constrained by time-intensive tissue analysis
- Included cases lack genetic subtype and cause of death data

Figure 6. Image of PWS ACC section with 20x magnification.

Results

ACC Findings

- Increased density of layer V VENs
- Higher ratio of VENs to pyramidal neurons in PWS compared to controls
- Pyramidal neuron cell body volumes similar to controls

FI Findings

- VENs present in the posterior insula in PWS
- Abnormal VEN and pyramidal spatial orientation noted in some cases
- Increased number of VENs in PWS brains compared to ASD

Figure 4. Visualization of pyramidal neurons showing typical morphology. Scatter plots compare pyramidal cell density (top) and volume (bottom).

Figure 5. Visualization of normal spindle-shaped VENs with increased density in a 17 year old with PWS. Scatter Plots show VEN quantity (top) and ratio of VENs to pyramidal neurons (bottom).

Future Work

- Continue data collection for tissue samples from the FI
- Expand tissue analysis to the orbitofrontal cortex¹¹, dorsolateral prefrontal cortex¹⁴ and, fusiform gyrus¹⁰
- Correlate data to PWS genetic subtypes⁴
- Increase sample size

References

- Altman, J. M., Tetreault, N. A., Hameem, A. Y., Manayo, K. F., Semendafeni, K., Erwin, J. W., Park, S., Coubert, V., & Hof, P. R. (2019). The von Economo neurons in frontoinsular and anterior cingulate cortex in great apes and humans. *Brain Structure and Function*, 24(5-6), 495-517. <https://doi.org/10.1093/bst/029-010-0294-0>
- Brins, M., Schödel, A., Karau, R., Faustmann, P. M., Dermietzel, R., Juckel, G., & Reusch-Jarvez, E. (2011). Neuroanatomical Correlates of Suicide in Psychosis: The Possible Role of von Economo Neurons. *PLoS ONE*, 6(6), e20936. <https://doi.org/10.1371/journal.pone.0020936>
- Butler, M. G., Miller, J. L., & Forster, J. L. (2019). Prader-Willi Syndrome - Clinical Genetics, Diagnosis and Treatment Approaches: An Update. *Current Pediatric Reviews*, 15(4), 207-244. <https://doi.org/10.2174/1573396315068190716120925>
- Honea, R. A., Hosen, L. M., Lepping, R. J., Peres, R., Butler, M. G., Brooks, W. M., & Savage, C. R. (2012). The neuroanatomy of genetic subtype differences in Prader-Willi syndrome. *American Journal of Medical Genetics. Part B: Neuropsychiatric Genetics: The Official Publication of the International Society of Psychiatric Genetics*, 159B(2), 243-253. <https://doi.org/10.1002/ajmb.b.32022>
- Klabunde, M., Sagger, M., Husyl, K. M., Hammond, J. L., Reiss, A. L., & Hall, S. S. (2015). Neural correlates of self-injurious behavior in Prader-Willi syndrome. *Human Brain Mapping*, 36(10), 4135-4143. <https://doi.org/10.1002/hbm.22503>

See citation handout for full reference list.

Acknowledgments

Funding provided from the Prader-Willi Research Foundation (PRH, MTV).


2nd

BPS / Neuro / Pharmd

Post-mortem Analysis of Von Economo Neurons in the Anterior Cingulate Cortex and Frontoinsular Cortex in Prader-Willi Syndrome

Schumacher, A., Fam, M., Warda, T., Wicinski, B., Forster, J.L., Hof, P.R., Varghese, M.T.

Prader-Willi syndrome (PWS) is a neurodevelopmental genomic imprinting disorder causing a lack of gene expression from the paternal (60%) or, less commonly, the maternal (35%) chromosome 15. PWS is characterized by hypotonia, poor suck, and failure to thrive in infancy, followed by hypogonadism, hyperphagia, obesity, and behavioral problems, including skin picking and tantrums. The anterior cingulate cortex (ACC) plays a role in emotional regulation, motivation, and error detection. The frontoinsular cortex (FI) plays a role in interoception, emotional and social processing, and decision-making. In these regions, pyramidal neurons support the computational output functions of these regions. Von Economo neurons (VENs) in these regions are morphologically distinct neurons associated with controlling homeostasis, behavior, and social behavior. Those with PWS exhibit neurobehavioral phenotypes, such as cognitive deficit and emotional instability, suggesting potential connectivity and molecular differences in these neurons. We aim to identify the number and distribution of VENs and pyramidal neurons in layer V of the anterior cingulate cortex (ACC) and the frontoinsular cortex (FI). We hypothesize that VENs will be abnormal in distribution and/or number in those with PWS compared to controls. Post-mortem PWS ACC and FI specimens provided by NIH NeuroBank were stained with cresyl violet and quantified under high-resolution microscopy using Stereo Investigator software. VENs and pyramidal neurons were quantified using the optical fractionator, and regional volume was estimated using the Cavalieri principle. Preliminary results confirm the presence of increased density of VENs in layer V of the ACC. The ratio of VENs to pyramidal neurons in the ACC was higher in PWS compared to controls. The pyramidal cell bodies of the ACC had volumes similar to those of controls. Preliminary results in the ACC show abnormal proliferation and migration of VENs in PWS development. The data collection of the FI is ongoing. Uncovering the neuronal density and morphology of the ACC and FI of those with PWS allows for a view into the neuropathology of the syndrome.





UNIVERSITY OF RHODE ISLAND
1892

SPECIAL FIELD
PHARMACY

Mapping the Corticospinal Tract in Neonatal Rabbit Model Using Pyramidal Tracer Injections to Better Understand Cerebral Palsy

Camila Quiroga^{1,2}, Elvia Mena Avila^{1,2}, Emily Reedich^{1,2}, Brendan Moline^{1,2}, Katharina Quinlan^{1,3,4}, Marin Manuel^{1,2}

¹Department of Pharmaceutical Sciences, College of Pharmacy, University of Rhode Island, 1152 Vesey Street, Narragansett, Rhode Island 02882; ²Department of Pharmaceutical Sciences, University of Rhode Island, 1152 Vesey Street, Narragansett, Rhode Island 02882; ³Department of Pharmaceutical Sciences, College of Pharmacy, University of Rhode Island, 1152 Vesey Street, Narragansett, Rhode Island 02882; ⁴Department of Pharmaceutical Sciences, College of Pharmacy, University of Rhode Island, 1152 Vesey Street, Narragansett, Rhode Island 02882

Introduction

- Cerebral palsy (CP) is lifelong motor disorder that is caused by perinatal injuries, with incidence of ~1/345 children.
- Hypoxic-ischemic (HI) injury is a risk factor for CP.
- The corticospinal tract (CST) is a motor pathway that originates in the primary motor cortex and projects through the brainstem to the spinal cord.
- The CST is critical for voluntary motor control and is commonly disrupted due to cortical damage or periventricular leukomalacia in CP (~80% cases).
- Despite its involvement in CP, the precise alterations between the CST and spinal interneurons following HI injury are poorly understood.


Goals

The trajectory of the CST not well documented in neonatal rabbits thus knowledge gap limits our ability to investigate CST-specific contributions to motor deficits in CP.

Because the anatomy of the CST in the neonatal rabbit model is poorly understood, anatomical mapping will help in identifying specific disruptions relevant to motor deficits for future studies.

Methods

Injection



Brains were ventrally injected at the level of the medullary pyramids using fluorescent lipophilic dyes (DiO and DiI).

Tissue Processing

Tissue was cryoprotected, using OCT, frozen at -80 °C, and cryosectioned.

Layer	Thickness	Thickness
Cerebrum	50µm	50µm
Cerebellum	50µm	50µm
Spinal cord	10µm	10µm

Analysis

Fluorescent labeling was visualized using epifluorescence microscopy.

- DiO: Excitation at 647 nm, emission at 668 nm
- DiI: Excitation at 487 nm, emission at 504 nm

Conclusion

- Retrogradal diffusion of DiO to cervical spinal cord and motor cortex would require a longer incubation period.
- Although extending incubation from two to four weeks enhanced dye diffusion, the overall limited spread and prolonged timeline indicate that post-mortem lipophilic dye tracing is not an efficient method for CST visualization in neonatal rabbit tissue.
- Despite two rounds of tracer injections, no DiO-labeled CST fibers was visualized in either control or CP model tissue.
- Absence of signal suggests a potential technical issue with the DiO dye or injection protocol.
- Lipophilic dye DiO remains good candidate for CST axonal mapping.

Limitations

- Tissue temperature shock:
 - Initial PFA changes were done with cold PFA (4°C) as opposed to PFA that matched incubation temperature.
- Injection approach:
 - Tissue analysis shows injection depth to be much greater than intended (1mm).
 - Dyes did not directly target medullary pyramids.
 - Neural pruning through meninges could explain extra depth in injection.
- Protocol limitations:
 - Protocol used may have off the control model.
 - No standardized protocol for the rabbit model exists.

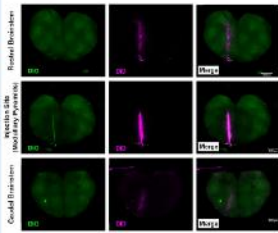
Future Directions

- Future injections will use a shallower injection depth to better target the pyramids.
- PFA changes will use PFA with a temperature matched to that of the incubation temperature (37°C).
- Future injections will be done after the removal of the meninges.
- Next steps include transitioning to in-vivo tracer injections using a ventral entry point to enhance labeling efficiency.
- Maintaining animal viability for the estimated 7-day diffusion period presents a key technical challenge.

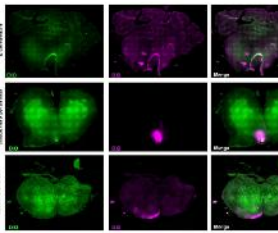
Results

Visualization of Lipophilic Dye Diffusion in Brainstem

Trial 1. Two Week Incubation



Trial 2. Four Week Incubation



Fluorescence imaging of transverse sections (30 µm) of brainstem with DiO axonal tracing in the right pyramid. Intense fluorescence was observed at the DiO injection site and traced in both the caudal and rostral directions.

Acknowledgments

This project was supported by URI Research and Innovation (R&I) through funding and support and by NIH (NS105260).

Results reported here are not supported by the Rhode Island Health and Development Fund (RHDF) through a grant of Research and Innovation Support for the National Institute of Health (NIH) grant NS105260. We also received support from the Rhode Island Health and Development Fund (RHDF) through a grant of Research and Innovation Support for the National Institute of Health (NIH) grant NS105260.

The research reported in this paper was supported by the URI Research and Innovation (R&I) grant NS105260 and the Rhode Island Health and Development Fund (RHDF) through a grant of Research and Innovation Support for the National Institute of Health (NIH) grant NS105260.

Methods

HI Procedure

- Balloon catheter was used to occlude blood flow to uterine horns (40 minutes at 70-80% gestation).
- Sham procedure was also performed (no catheter insertion/inflation), serving as a surgical control condition.



DiI Unlabeled (fluorophoreless)



HI-Affected (hypertonic)



Tissue Processing

- Postnatal day (P)1: Transcardial perfusion with paraformaldehyde to preserve brain and spinal cord tissue for downstream processing.
- Post-fixation, brain and spinal cord were extracted intact for CST mapping.



Third Place - Mapping the Corticospinal Tract in a Neonatal Rabbit Using Pyramidal Tracer Injections for a Better Understanding of Cerebral Palsy

Camila Quiroga, Elvia Mena Avila, Emily Reedich, Brendan Moline, Katharina Quinlan, Marin Manuel

Cerebral palsy (CP) is a common motor disorder in children, with approximately 1 in 345 children diagnosed in the United States. Hypoxic ischemic injury (HI) during the perinatal period is a major risk factor and can disrupt the development of descending motor pathways, particularly the corticospinal tract (CST).

The CST originates in the primary motor cortex and projects through the brainstem to the spinal cord, playing a critical role in voluntary motor control. Despite its involvement in CP, the precise relationship between the CST and spinal interneurons following HI injury remains poorly understood. We use a neonatal HI rabbit model, which recapitulates key features of human CP, to investigate these changes. However, the trajectory and cortical origins of the CST are not well defined in neonatal rabbits, limiting our ability to study CST-specific contributions to motor deficits.

The goal of this study is to identify the location and trajectory of the CST in neonatal rabbits. Pregnant rabbits undergo surgery to induce HI injury in developing kits. At postnatal day 1, kits are perfused, and the brain and spinal cord are dissected intact. Lipophilic dyes (DiO, DiI) are injected into the medullary pyramids, where CST axons converge before decussation. These dyes integrate into axonal membranes and travel bidirectionally over time, allowing CST projections to be traced to both the primary motor cortex and the spinal cord.

Mapping the CST is essential for identifying the primary motor cortex in neonatal rabbits. This enables future studies to manipulate CST activity and examine its role in spinal reflex circuits. Our findings show that extended incubation improves tracer diffusion, highlighting both the feasibility and limitations of postmortem CST mapping in this model. Overall, this study establishes a foundation for investigating CST organization and dysfunction in CP.

Bacteriophage Therapeutics in Pancreatic Cancer: Microbiome-Linked Rationale, Barriers, and Opportunities

Sydney Suffoletto¹, Asha Bahroos¹, Sara Cho¹, Skyla Kohanski¹, Meghna Potluri¹, Revaa Goyal¹, Anna Carlino¹, Lindsey Alemany¹, Connor Charbonneau¹, Joseph Iannucci¹, Callan Bleick¹, and Kaitlin M. Dailey^{1,2,3*}
 1) College of Pharmacy, University of Rhode Island, Kingston RI; 2) Rhode Island INBRE, University of Rhode Island, Kingston RI; 3) Legorreta Cancer Center, Brown University, Providence, RI * indicates corresponding author: Kaitlin.dailey@uri.edu

Summary

Pancreatic ductal adenocarcinoma (PDAC) is an aggressive cancer with poor prognosis and limited treatment options. Emerging evidence shows that tumor-associated and gut bacteria influence PDAC progression through immune modulation, metabolic interactions, and drug inactivation, including gemcitabine resistance via bacterial cytidine deaminase.^{1,2} Bacteriophages offer a precision approach to selectively target tumor-associated bacteria while preserving the broader microbiome.^{3,4} Engineered phages may also enable targeted delivery and biomarker-guided patient selection.^{3,4} This work presents a translational framework spanning microbial detection, biomarker identification, phage selection, and delivery optimization to develop clinically actionable bacteriophage-based therapeutics.^{3,4}

Background

CLINICAL BACKGROUND

PDAC is one of the deadliest solid malignancies and is frequently diagnosed at advanced stages. Its dense desmoplastic stroma, poor vascularization, and immunosuppressive microenvironment limit therapeutic penetration and contribute to treatment resistance. Alarming, the 5-year survival rate for PDAC remains below 12% - and it is projected to become the second leading cause of cancer-related deaths in the U.S. by 2030, claiming over 50,000 lives annually. There remains an urgent need for more targeted and biologically engineered therapeutic strategies.

TUMOR MICROBIOME IN PDAC

- Emerging evidence suggests that microbial communities associated with PDAC may influence tumor progression, immune tone, and treatment response.
- Proposed mechanisms include inflammatory signaling, metabolic interactions, and drug biotransformation.
- Intratumoral Gammaproteobacteria have been implicated in gemcitabine inactivation, supporting microbiome-targeted therapeutic strategies.

Methodology

- Narrative translational literature synthesis and conceptual framework development
- Reviewed PDAC tumor biology, tumor microbiome-associated resistance, bacteriophage therapeutic strategies, phage display technologies, and translational barriers
- Findings organized into rationale, barriers, and opportunity domains

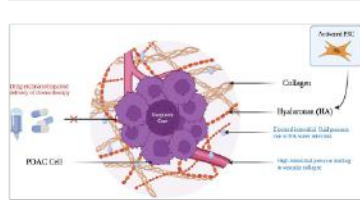
Figure 1. Why Phages in PDAC?



Phages offer a precision strategy in PDAC by targeting tumor-associated bacteria linked to inflammation, stroma or metabolism, and the resistance and/or limiting broader microbiome disruption.

Results

Figure 2. Stromal Barriers in PDAC



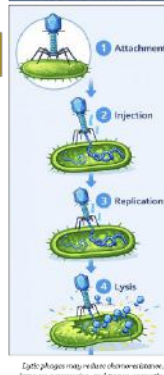
The dense PDAC stroma restricts vascular perfusion, drug penetration, and immune access, creating a major barrier to effective therapeutic delivery.

Figure 3. Candidate Microbial Targets in PDAC



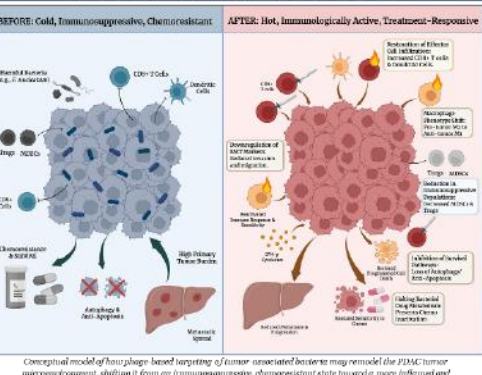
Selected tumor-associated bacteria can promote PDAC progression / treatment resistance representing potential targets for intervention.

Figure 4. Lytic Phage Cycle



Lytic phages may reduce chemoresistance, immune suppression, and tumor-promoting signaling in PDAC via selective bacterial lysis.

Figure 5. Cold-to-Hot Tumor Microenvironment Shift in PDAC

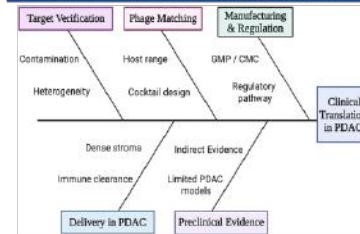


Conceptual model of how phage-based targeting of tumor-associated bacteria may remodel the PDAC tumor microenvironment, shifting it from an immunosuppressive, chemoresistant state toward a more inflamed and treatment-responsive phenotype.

Conclusions

- MAJOR TRANSLATIONAL BARRIERS**
- Dense stroma, immune clearance, and poor vascularization may limit intratumoral delivery.
 - Additional bottlenecks include target verification, phage matching, resistance, and manufacturing/regulatory complexity.

Figure 5. Translational Barriers to Phage Therapy in PDAC



Clinical translation to PDAC is limited by challenges in target verification, phage matching, delivery through dense stroma, and manufacturing/regulatory readiness.

- KEY FINDINGS**
- PDAC-associated microbes may contribute to progression and chemoresistance.
 - Phages may selectively target implicated bacteria while preserving broader microbiome integrity.
 - Direct PDAC-specific phage evidence remains limited, but related microbiome and phage-platform work supports further study.

Future Directions

Phages offer a selective, microbiome-linked therapeutic opportunity in PDAC, particularly where tumor-associated bacteria may contribute to chemoresistance. However, meaningful translation will require PDAC-specific validation, improved delivery, and resolution of major regulatory and manufacturing barriers.

References & Acknowledgements

1. Esguerra, et al. *Cell* **2019**. PMID: 31398227
2. Geller ET, et al. *Science* **2019**. PMID: 31012244
3. Zhang J, et al. *J Cancer Res Clin Oncol* **2023**. PMID: 41384994
4. Wang Y, et al. *Mol Cancer* **2019**. PMID: 31782510

Funded by URI College of Pharmacy, Biomedical and Pharmaceutical Sciences Department, and RI-INBRE State-1p funds to KMD and CB. The authors would like to thank the support of their institutions and colleagues. The authors acknowledge the use of BioRender.com to create the figures contained within this paper. Beyond presenting authors, authors are in alphabetical order and all have contributed equally.

A Translational Framework for Bacteriophage Therapeutics in Pancreatic Cancer

Sydney Suffoletto, Asha Bahroos, Sara Cho, Skyla Kohanski, Meghna Potluri, Revaa Goyal, Anna Carlino, Lindsey Alemany, Connor Charbonneau, Joseph Iannucci, Callan Bleick, Kaitlin M. Dailey

Pancreatic cancer has one of the poorest prognoses of any solid malignancy. This disease is driven by a desmoplastic, hypoxic tumor microenvironment that promotes metabolic reprogramming, inhibits therapeutic activity, and ultimately leads to treatment resistance. Emerging evidence suggests that tumor-adjacent and gut microbial communities shape pancreatic tumor biology through metabolism-linked mechanisms including immune modulation, nutrient competition, and drug biotransformation. Gammaproteobacteria recently demonstrated the clinical relevance of the tumor microbiome with enzymatic inactivation of gemcitabine by intratumoral via cytidine deaminase, converting active drug to an inactive metabolite and contributing to chemoresistance.

Bacteriophages have the potential to be leveraged as a metabolically informed precision therapeutic with selective depleting bacteria implicated in tumor-promoting inflammation and/or drug-modifying enzymatic activity while minimizing broader microbiome disruption. Beyond bacterial lysis, engineered phage platforms would support targeted delivery and biomarker development to stratify patients whose tumor-microbiome profiles suggest metabolically mediated resistance. Translation of pancreatic cancer therapeutics faces distinct barriers such as contamination-prone tumor samples, narrow phage host range and delivery constraints imposed by dense stroma. Manufacturing and regulatory requirements for biologics-grade phage products further limit rapid iteration and must be accounted for even at early stages of experimentation.

Here, we synthesize the potential and constraints of bacteriophage-based therapeutics as a translational roadmap. The framework begins with detection strategies and orthogonal validation, moves through biomarker identification with rapid phage matching and cocktail design, addresses delivery optimization under pancreatic tumor stromal constraints, and culminates in plausible clinical applications ultimately eliciting positive patient response. This approach aims to convert mechanistic plausibility into clinical trial-ready strategies for bacteriophage-mediated therapeutics in pancreatic cancers.



Characterization of muscle spindles and gait in a model of cerebral palsy

J. E. Glennon^{1,2}, E. J. Reedich^{1,2}, C. A. Kramer^{1,2,3}, B. Moline^{1,2}, O. Opesade^{1,2,3}, M. Manuel^{1,2}, K. A. Quinlan^{1,2}

¹ George and Anne Ryan Institute for Neuroscience, University of Rhode Island, Kingston, RI, USA; ² Department of Biomedical and Pharmaceutical Sciences, College of Pharmacy, University of Rhode Island, Kingston, RI, USA; ³ Interdisciplinary Neuroscience Program, University of Rhode Island, Kingston, RI, USA



INTRODUCTION

Cerebral palsy (CP) is a common cause of lifelong motor disability

- Caused by injuries to the developing nervous system
- Stretch reflexes are overactive, resulting in hyperreflexia (spasticity)
- Can manifest through gait impairments, decrease quality of life

Muscle spindles are responsible for stretch reflexes

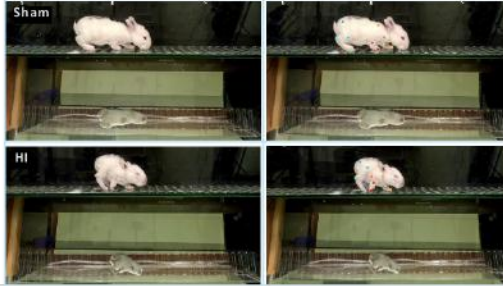
Stretch reflexes are used to stabilize limb trajectory and may impact walking ability in CP

Hypothesis: CP-affected rabbits will demonstrate delayed muscle spindle development, and delayed spindle development or abnormalities contribute to hyperreflexia and gait impairments in CP.

METHODS

Analyzing gait with DeepLabCut

- HI and sham rabbits are video recorded at P14
- Quantify stride length, joint angles, and pattern of limb activity



CONCLUSIONS

- Neonatal muscle spindles may be larger in HI rabbits, which could contribute to spasticity and hyperreflexia
- It is easier to identify muscle spindles via optically cleared tenuissimus muscles than teased soleus fibers
- Motor end plates can be labeled with αBTX using IDISCO and solvent-based optical clearing techniques
- Newfound optical clearing methods may be useful for investigating the NMJ in skeletal muscle

FUTURE DIRECTIONS

- Collect, stain, and analyze tenuissimus muscle spindles over postnatal development (P1, P5, P8, P11, P14, and P31)
- Evaluate intrafusal fiber morphology in sham versus HI muscle spindles

- Investigate muscle spindles of kits used in gait analysis
- Continue video processing and analysis of gait in P14 kits via DeepLabCut™



METHODS

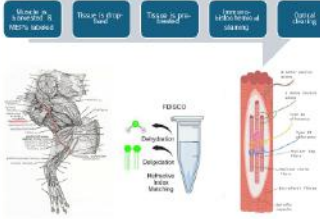
Prenatal hypoxia-ischemia

Hypoxia-ischemia (HI) surgery is performed on New Zealand White Rabbits



- Occlude blood flow to uterine horns
- 40 minutes at ~70% gestation
- Sham group present

Visualizing muscle spindles



PRELIMINARY RESULTS

Teased HI soleus fibers demonstrate a trend towards larger spindle sizes

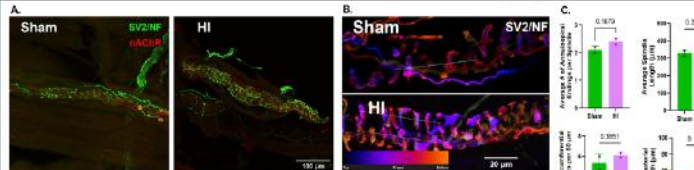


Figure 1. Maximum intensity z-projections of soleus muscle spindles at P8 visualized at (A) 20x magnification and (B) 100x magnification using immunofluorescence against neurofilament (NF) and synaptic vesicle 2 (SV2) in sham and HI rabbits. (C) Morphological properties of muscle spindles from sham and HI rabbits (n=3-5 spindles per rabbit, N=2 rabbits per group) at P8.

Optical clearing techniques allow for improved muscle spindle visualization

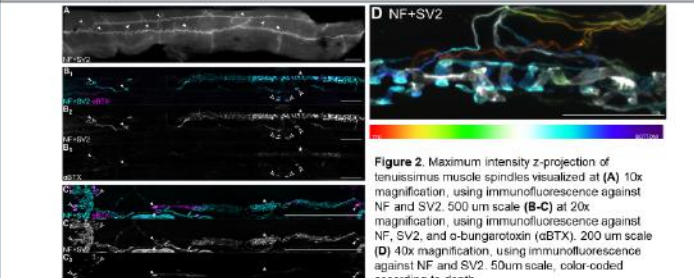


Figure 2. Maximum intensity z-projection of tenuissimus muscle spindles visualized at (A) 10x magnification, using immunofluorescence against NF and SV2. 500 μm scale. (B-C) at 20x magnification, using immunofluorescence against NF, SV2, and α-bungarotoxin (αBTX). 200 μm scale. (D) 40x magnification, using immunofluorescence against NF and SV2. 50 μm scale, color-coded according to depth.

ACKNOWLEDGEMENTS

This project is supported by NIH NINDS R01 NS104436 (KQ), R01 NS132728 (KQ and MM), and RF1 NS135580 (KQ).

We made use of Biorender and equipment supported by the Rhode Island Institutional Development Award (IDeA) Network of Biomedical Research Excellence from NIH NIGMS P20GM103430.




REFERENCES

1. Khan MM, Chenkeri P, Hegro P, Rajati A, Fakhrovi P, Barsoi V, et al. (2022) EPR2 and EPR3 promote the development of gamma motor neuron functional properties required for proprioceptive movement control. *PLoS Biol* 20(12): e3001923. <https://doi.org/10.1371/journal.pbio.3001923>
2. Barrett P, Quirk T, J., Madira V, & Payer, D. J. (2020). Generating intrafusal skeletal muscle fibres in vitro: Current state of the art and future challenges. *Journal of tissue engineering*, 11, 204173420985205. <https://doi.org/10.1177/204173420985205>
3. Crouch J.E. (1989) Test-Artas Cf Cat Anatomy. Lea & Febiger
4. Fibre typing of striated fibres - Scientific Figure on ResearchGate. Available from: <https://www.researchgate.net/publication/319414649-Image-of-the-central-region-of-the-muscle-spindle-in-rat-triceps-muscle> [accessed 25 Jul 2025].

Characterization of Muscle Spindles and Gait in a Model of Cerebral Palsy

J. E. Glennon, E. J. Reedich, C. A. Kramer, B. Moline, O. Opesade, M. Manuel, K. A. Quinlan

Cerebral palsy (CP) is a collection of motor disorders that is the most common cause of lifelong motor disability worldwide, affecting approximately 1 in 500 live births. It is caused by injuries to the developing nervous system during late gestation or early childhood, and typically involves spasticity (marked by hyperreflexia) and difficulties with gait (e.g. crouch gait). Stretch reflexes are attributed to sensory organs called muscle spindles, which detect stretch in skeletal muscles and activate Ia sensory afferents. Hyperreflexia in CP could involve irregularities in muscle spindle physiology, but this remains unexplored. In turn, hyperreflexia and irregular muscle spindle morphology may be correlated with gait abnormalities seen in CP. To explore this, we are investigating muscle spindle structure in developing rabbits that have experienced prenatal hypoxia-ischemia (HI) injury (via surgical procedure at 70-80% gestation) and in sham-operated control rabbits that have been prenatally exposed to anesthetics but not HI. We have developed a tissue clearing and immunofluorescence pipeline for three dimensional visualization of muscle spindles in the tenuissimus, which has high spindle density and plays an important role in proprioceptive sensory feedback in the hindlimb. We hypothesize that muscle spindles from HI rabbits will demonstrate delayed development when compared to that of sham kits; it is possible that delayed development or structural abnormalities within muscle spindles could contribute to hyperreflexia and gait abnormalities in CP. Gait will be assessed in rabbit kits at two weeks of age using video recording and then analyzed in DeepLabCut™ to assess stride length, joint angle, and other limb activity seen within sham and HI rabbits. Findings from this project will contribute to further understanding of neuromuscular impairment in CP and development of potential therapeutic strategies to normalize muscle spindle physiology in this disorder.




THE UNIVERSITY OF RHODE ISLAND
GEORGE & ANNE RYAN INSTITUTE FOR NEUROSCIENCE

Developing a machine-learning algorithm for automatic classification of muscle fiber type composition in an animal model of cerebral palsy

Hope McCann^{1,2}, Emily Reedich^{1,2}, Cassandra Kramer^{1,2}, Sadie Drouin^{1,2}, Elian Gonzalez^{1,2}, Tiffany Ung^{1,2}, Jess Glennon^{1,2}, Camila Quiroga^{1,2}, Katharina Quinlan^{1,2}, Manuel Manuel^{1,2}

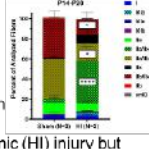
¹ George and Anne Ryan Institute for Neuroscience, University of Rhode Island, Kingston, RI; ² Department of Biomedical and Pharmaceutical Sciences, College of Pharmacy, University of Rhode Island, Kingston, RI



INTRODUCTION

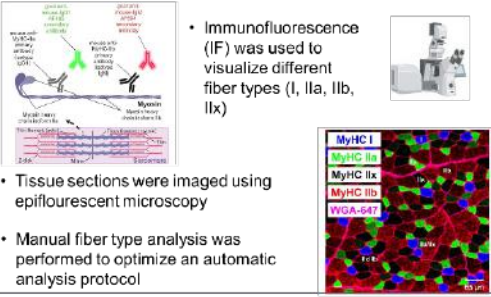
- Cerebral palsy (CP) is a non-progressive condition affecting the neurological and musculoskeletal systems
- CP results from injury to the developing brain and spinal cord
- Changes in sarcomere length and muscle fiber cross-sectional area are present in CP
- Previous research suggests significant difference in muscle fiber type composition for rabbits affected with a hypoxic-ischemic (HI) injury but results were limited by: sample size, muscle group examined, and accuracy of the classification algorithm.

Hypothesis: Muscle fiber composition will be altered between sham and HI rabbits across developmental stages.



METHODS

- Immunofluorescence (IF) was used to visualize different fiber types (I, IIa, IIb, IIx)
- Tissue sections were imaged using epifluorescent microscopy
- Manual fiber type analysis was performed to optimize an automatic analysis protocol

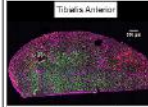


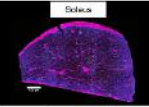
CONCLUSIONS

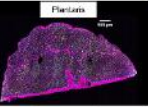
- Muscle fiber type composition matures between the second postnatal week and weaning age (P31)
- We are currently analyzing differences in muscle fiber type composition between sham and HI rabbits
- Alterations in fiber type composition between sham and HI rabbits likely imply functional changes in muscle contractile properties like force and fatigability

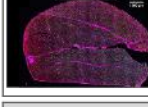
PRELIMINARY RESULTS

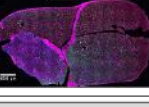
Composite Muscle Images

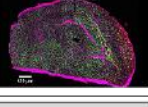






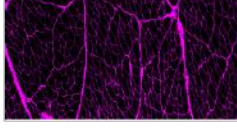






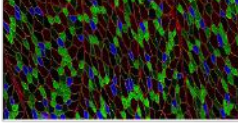
Cellpose Analysis

Step 1: Cell Segmentation



- Wheat germ agglutinin (WGA) stain used to train model to outline muscle fibers

Step 2: Measure Fluorescence



- Our algorithm will classify muscle fiber physiological type based on fluorescence intensities

FUTURE DIRECTIONS

ACKNOWLEDGEMENTS

- R01 NS132728
- Rhode Island IDeA Network of Biomedical Research Excellence (NIH NIGMS P20GM103430)



Developing a machine-learning algorithm for automatic classification of muscle fiber type composition in an animal model of cerebral palsy

Hope McCann, Emily Reedich, Cassandra Kramer, Sadie Drouin, Elian Gonzalez, Tiffany Ung, Jess Glennon, Camila Quiroga, Katharina Quinlan, Manuel Manuel

Cerebral palsy (CP) is a nonprogressive condition that affects the neurological and musculoskeletal systems due to injury to the developing brain and spinal cord, resulting in symptoms of hypertonia, spasticity, and increased neuromuscular activity. In addition to neural deficits, skeletal muscle pathologies are present in CP, including changes to sarcomere length and muscle fiber cross-sectional area. Skeletal muscle is composed of heterogeneous fiber physiological types defined by myosin heavy chain (MHC) isoform expression, and it remains unclear whether CP is associated with systematic shifts in fiber type composition.

MHC type I fibers are slow-twitch fibers that are fatigue resistant and produce small forces. Type IIa fibers are fast-twitch, oxidative-glycolytic fibers which are less fatigue resistant than type I fibers and produce intermediate forces. Type IIx and IIb fibers are fast-twitch glycolytic fibers that are highly fatigable but have the greatest force-generative capacity. Whether the relative proportions of these fiber types are altered in CP has not been clearly established.

To address this question, we are using a rabbit model of CP, in which a prenatal hypoxic-ischemic (HI) injury is performed in the pregnant dam, enabling analysis of neuromuscular alterations in newborn kits. We performed immunofluorescent staining to label muscle fiber types across various muscles from hypertonic HI, non-hypertonic HI, and sham rabbits at two developmental stages. We are developing an automatic analysis pipeline to classify the fiber type of large numbers of muscle fibers, and measure the percentage of each fiber type.

This work will provide a quantitative assessment of how prenatal HI injury influences muscle fiber composition, establishing a foundation for future studies aimed at understanding disease mechanisms and evaluating therapeutic strategies.

Developing CRISPR-modified *Clostridium novyi*-NT as Metastatic Pancreatic Cancer Therapeutic

Ryan P. Baudisch¹, Jackson Boyd¹, Sara Cho¹, Victoria Coulter¹, Abigail DeLorenzo¹, Anela K. Kerber¹, Maddie Starace¹, Mia Pelligrino¹, Kaitlin M. Dailey^{1,2,3}*

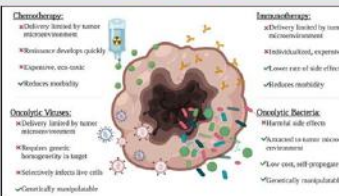
¹ College of Pharmacy, University of Rhode Island, Kingston, RI
² Rhode Island INBRE, University of Rhode Island, Kingston, RI
³ Legorreta Cancer Center, Brown University, Providence, RI
 *Corresponding author: kaitlin.dailey@unri.edu



SUMMARY

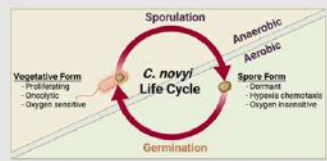
An attenuated bacterium, *Clostridium novyi*-NT¹, has demonstrated selective solid tumor penetration, lysis from hypoxic tumor core, and potent immune restimulation at normally oxygenated margins without sepsis or off target effects¹⁻³. *C. novyi*-NT-based IV oncotherapeutics present unique opportunities to: target physicochemical and molecular attributes nearly ubiquitous to all solid tumors; potentially activate the immune system at tumor margins; ultimately enact tumor lysis directly, or in the future, deliver agents to hypoxic areas of tumors. Our application of CRISPR/Cas9 generated a viable mechanism for customization to overcome the remaining challenges and move this novel therapeutic toward clinical translation.

INTRODUCTION



Although a variety of chemotherapeutic strategies exist, their efficacy in pancreatic cancer is limited by (1) late-stage diagnosis, (2) poor vascularity, and (3) rapid resurgence of tumor cells due to chemotherapeutic resistance. As a result of their ability to move rapidly through subtle cytokine, pH, and/or oxygen gradients, oncolytic bacteria have re-emerged as promising cancer therapeutics¹⁻⁴. *Clostridium novyi*-NT - a sporulating, attenuated, obligate anaerobic oncolytic bacteria - has demonstrated the ability to penetrate, precisely colonize, and eradicate both solid tumors and small malignant tumor islands^{1,2}. The ability of these motile bacteria to elicit a sensitive chemotactic response has shown an ability to "home" to and rapidly penetrate into the solid tumor core¹⁻³, effectively lysing the tumor from the inside out in stark contrast to traditional approaches. Several promising pre-clinical and early phase clinical trials have been successfully completed with intratumoral injections! However, the development of an intravenous *C. novyi*-NT-based therapeutic has been hampered by the rapid clearance of the mononuclear phagocyte system (MPS).

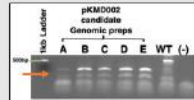
BACKGROUND



Schematic representation of the *C. novyi* life cycle within environmental context.

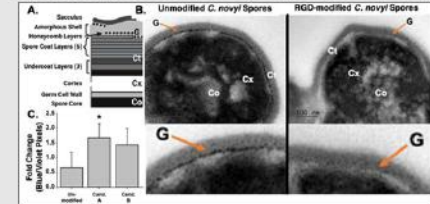
RESULTS

CRISPR-mediated Genomic Incorporation of RGD Motif¹



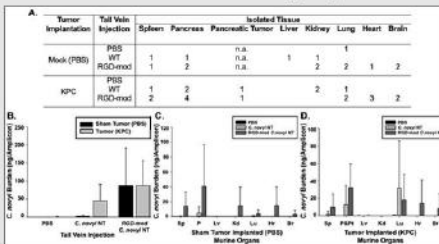
Calcium competent *C. novyi* were transformed with pKMO002, a CRISPR/Cas9 cassette, generating candidates A-E. (WT-wild type) Genomic DNA isolation and restriction digestion confirmed modification status: singlet is negative for genomic insertion, doublet is positive due to the presence of a *EcoRV* site designed within the insert.

Physical and Functional Incorporation of RGD Peptide



(A) Schematic representation of the published *C. novyi* spore coat architecture¹ and figure legend. Our method of isolation removes the sacculus. (B) Transmission electron microscopy (TEM) representative images of Wild Type and RGD-modified candidate A *C. novyi* spores. (C) An adhesion assay conducted using $\alpha_5\beta_1$ integrin coated surfaces to probe functional capacity of the expressed RGD motif. Fold change in adhesion as measured directly by counting retained crystal violet-stained spores on surface. * $p < 0.05$.

Syngeneic, Immunocompetent Orthotopic Pancreatic Cancer Mouse Model (Pilot)

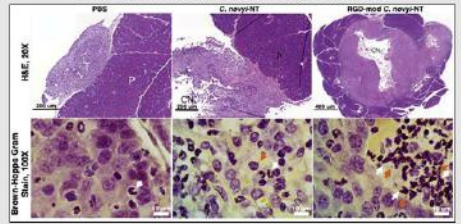


Quantifying *C. novyi* spores after intravenous (IV) injection. (A) Biodistribution of *C. novyi* spores after IV injection. PCR primers designed with spore specificity for *C. novyi* 16S rRNA determined spore biodistribution 24hrs after IV injection. Numbers indicate the quantity of animals from each cohort (n=4) in which *C. novyi* DNA was positively identified. (B) Further differential PCR was conducted with template concentrations normalized. The combined bioburden of all major organs within each cohort and each major organ within a cohort when (C) sham tumor implantation surgery occurred versus when (D) tumor implantation with KPC cells was conducted.

Legend: NT - wild type *C. novyi*; spore tail vein injection; RGD-mod - RGD-modified *C. novyi* tail vein injection; Sp - spleen; P - pancreas; P&T - pancreas and pancreatic tumor; Lv - liver; Kd - kidney; Lu - lung; Ht - heart; Br - brain.

RESULTS

Syngeneic, Immunocompetent Orthotopic Pancreatic Cancer Murine Model (Pilot), continued



Histopathological analysis of pancreatic tumors for bacterial inflammation. Histological evidence from representative slides selected by a clinical pathologist (JMS) blinded to sample treatment show evidence of spore-like particles and neutrophil invasion around a larger necrotic core in RGD-modified *C. novyi*-NT treated mice. Importantly, our clinical pathologist analyzed slides from all major organs treated with multiple stains without finding inflammation indicative of bacterial infection (i.e., off target localization). Legend: Orange arrows - spore like particles; white arrows - granulocytes; CN - central necrosis; T - tumor; P - pancreas.



Laser capture microdissection (LCM) of pathologist selected representative slides. LCM and subsequent species-specific differential PCR of DNA (above) indicate presence of *C. novyi*-NT spores in cohort treated with RGD-modified spores. A sample of DNA previously identified as *C. novyi*-NT was used as a positive control (*C. novyi*-NT gDNA).

FUTURE DIRECTIONS

- Determine RGD-modified *C. novyi*-NT spore biodistribution, tumor lysis, and impact on immune stimulation after intravenous injection in a cohort capable of statistical significance.
- Use these methods to further spore modification towards developing *C. novyi*-NT-based IV oncotherapeutics capable of accomplishing multistep (e.g., primary tumor and metastases) localization in a single dose.

ACKNOWLEDGMENTS

Research Program's most recent publication: Dailey KM, et al. (2023) PLOS ONE 18:1-12. [10.1371/journal.pone.0281053](https://doi.org/10.1371/journal.pone.0281053)
 Authors are in alphabetical order after presenting author. Project partially supported by ShellCo funds to KMD from URI College of Pharmacy, Biomedical and Pharmaceutical Sciences Department. URI INBRE as well as a Tripp Grant, Foundation Medical Research Seed Grant to KMD. Project partially supported by Anela Kerber's NIH CORSE grant 1P30NS106236 to AKB, the Center for Diagnostic and Therapeutic Innovation in Pancreatic Cancer (DITC), and the National Cancer Institute's National Cancer Research Training Program (NCRT) 5T32CA020508 to KMD, M&H, and KWB. Disclosures: funds to speakers: M&H and KWB.

REFERENCES

1. Cho S, et al. Clostridium novyi-NT: A Novel Oncotherapeutic for Pancreatic Cancer. *Cancers* 2021; 13(12):3000. <https://doi.org/10.3390/cancers13123000>
2. Cho S, et al. Clostridium novyi-NT: A Novel Oncotherapeutic for Pancreatic Cancer. *Cancers* 2021; 13(12):3000. <https://doi.org/10.3390/cancers13123000>
3. Cho S, et al. Clostridium novyi-NT: A Novel Oncotherapeutic for Pancreatic Cancer. *Cancers* 2021; 13(12):3000. <https://doi.org/10.3390/cancers13123000>
4. Cho S, et al. Clostridium novyi-NT: A Novel Oncotherapeutic for Pancreatic Cancer. *Cancers* 2021; 13(12):3000. <https://doi.org/10.3390/cancers13123000>

Developing CRISPR-modified *Clostridium novyi*-NT as Metastatic Pancreatic Cancer Therapeutic

Ryan P. Baudisch, Jackson Boyd, Sara Cho, Victoria Coulter, Abigail DeLorenzo, Anela K. Kerber, Maddie Starace, Mia Pelligrino, Kaitlin M. Dailey

Clostridium novyi has demonstrated selective efficacy against solid tumors largely due to the microenvironment contained within dense tumor cores. The core of a solid tumor is typically hypoxic, acidic, and necrotic—impeding the penetration of current therapeutics. *C. novyi* is attracted to the tumor microenvironment and once there, can both lyse and proliferate while simultaneously re-activating the suppressed immune system. *C. novyi* systemic toxicity is easily mitigated by knocking out the phage DNA plasmid encoded alpha toxin resulting in *C. novyi*-NT; but, after intravenous injection spores are quickly cleared by phagocytosis before accomplishing significant tumor localization. *C. novyi*-NT could be designed to accomplish intravenous delivery with the potential to target all solid tumors and their metastases in a single dose. This study characterizes CRISPR/Cas9 modified *C. novyi*-NT to insert the gene for RGD, a tumor targeting peptide, expressed within the promoter region of a spore coat protein. Expression of the RGD peptide on the outer spore coat of *C. novyi*-NT indicates an increased capacity for tumor localization of *C. novyi* upon intravenous introduction based on the natural binding of RGD with the $\alpha v\beta 3$ integrin commonly overexpressed on the epithelial tissue surrounding a tumor, and lead to immune stimulation.

Investigating the role of surface layer protein (Slr4) in outer membrane vesicle formation and function in *Pseudoalteromonas piscicida* JC3

Amalia Marjollet, Ololade Gbadebo, David Rowley, Amanda T. Alker
Biomedical and Pharmaceutical Sciences, University of Rhode Island



Abstract

- *Pseudoalteromonas piscicida* strain JC3 produces outer membrane vesicles (OMVs) that may be potentially useful as a drug delivery system.
- OMVs package sensitive molecules, such as antimicrobial compounds and proteins, for extracellular transport.
- Proteomics of JC3 OMVs show that a surface layer protein called Slr4 is the most abundant across all growth conditions.
- The Slr4 proteins contribute to the extracellular matrix, but their role in the formation of OMVs and their function in packaging and delivering antimicrobials is not well understood.
- The goal of this project is to determine the role of Slr4 in OMV formation by generating an in-frame deletion mutation of the slr4 gene using double homologous recombination with a sucrose counterselection.

Knocking out surface layer protein Slr4 in *Pseudoalteromonas piscicida* JC3

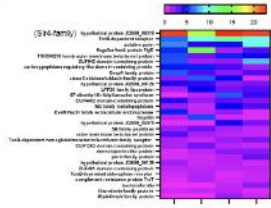


Figure 1. Heatmap showing proteomic data for Slr4 family proteins. Slr4 is the most abundant protein across all growth conditions.

Proteomics on *P. piscicida* reveals that Slr4 family proteins are the most abundant.

Troubleshooting PCR amplification of each homology arm resulted in a gel electrophoresis band that corresponded with the size of the target homology insert.

Gibson assembly was used after successful amplification of plasmid backbone and both homology arms.

Conjugating the knockout vector into *P. piscicida* JC3

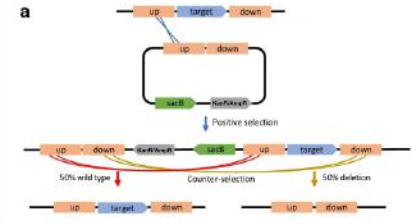


Figure 2. Schematic diagram of the conjugation process. The process involves positive selection and counter-selection to create a 50% wild type and 50% deletion.

Pseudoalteromonas sp. JC3 produces OMVs

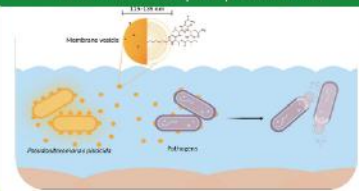


Figure 3. Pseudoalteromonas sp. JC3 produces outer membrane vesicles (OMVs) through a process of blebbing and explosive cell lysis.

In silico plasmid design

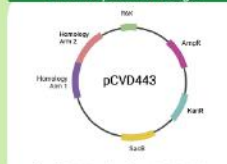


Figure 4. In silico plasmid design showing the location of the Slr4 gene and the homology arms used for deletion.

Plasmid digest and PCR amplification

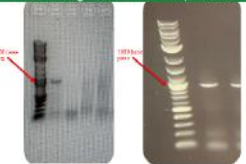


Figure 5. Gel electrophoresis image showing the results of plasmid digestion and PCR amplification.

Successful JC3 transformation with green fluorescent protein



Figure 6. Image showing the successful transformation of JC3 cells with green fluorescent protein (GFP).

Conclusions & Future Experiments

Molecular cloning of the plasmid is nearly complete with conjugation into JC3 on the horizon. Future experiments, such as nanoparticle tracking and antimicrobial testing, are necessary to assess formation and structure of wild-type JC3 vesicles compared to those with the deletion mutation and their efficiency in packaging antimicrobials.

References and Acknowledgements

- 1. Marjollet, A., Gbadebo, O., Rowley, D., Alker, A. T. (2023). Investigating the role of surface layer protein (Slr4) in outer membrane vesicle formation and function in *Pseudoalteromonas piscicida* JC3. *Journal of Cellular Biochemistry*, 124(1), 1-10.
- 2. Alker, A. T., Marjollet, A., Gbadebo, O., Rowley, D., (2023). Investigating the role of surface layer protein (Slr4) in outer membrane vesicle formation and function in *Pseudoalteromonas piscicida* JC3. *Journal of Cellular Biochemistry*, 124(1), 1-10.

Investigating the role of surface layer protein (Slr4) in outer membrane vesicle formation and function in *Pseudoalteromonas piscicida* JC3

Amalia Marjollet, Ololade Gbadebo, David Rowley, Amanda T. Alker

Pseudoalteromonas piscicida strain JC3, a marine bacterium isolated from whiteleg shrimp, is known to produce outer membrane vesicles (OMVs) that may be potentially useful as a drug delivery system. Prokaryotic cells use OMVs to package sensitive molecules such as nucleic acids, enzymes, lipophilic compounds, and other specialized metabolites. In particular, JC3 has been found to produce a class of compounds called bromoalterochromides, which possess antibacterial properties against human pathogens. OMVs produced by JC3 serve as packaging and delivery systems of toxic cargo, like bromoalterochromides, against bacterial pathogens and competitors.¹ Proteomics of JC3 OMVs found that an s-layer protein named Slr4 was by far the most abundant. These Slr4 proteins form lattices that compose the outermost layer of prokaryotic cells and contribute to the extracellular matrix of *Pseudoalteromonas* biofilms. However, the role of Slr4 in the formation of OMVs and their function in packaging antimicrobials such as bromoalterochromides remains largely unclear.²

This project will determine the role of Slr4 in antimicrobial vesicles formation of JC3 by generating an in-frame deletion mutation of the Slr4 gene using double homologous recombination with a sucrose counterselection. Molecular cloning of the plasmid is nearly complete with conjugation on the horizon. Future experiments, such as nanoparticle tracking and antimicrobial testing, are necessary to assess formation and structure of wild-type JC3 vesicles compared to those with the deletion mutation and their efficiency in packaging bromoalterochromides.

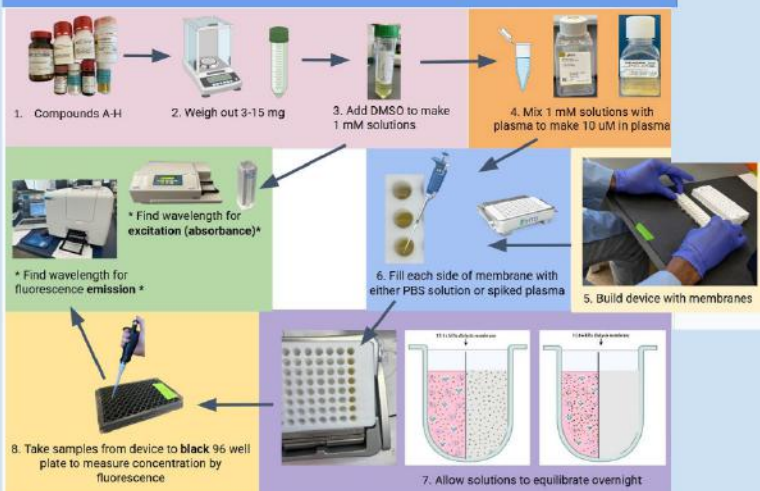
Introduction and Conclusion

- Plasma protein binding is a key determinant of drug distribution, as it influences the proportion of free (pharmacologically active) drug available in circulation.
- Equilibrium dialysis is a standard method used to evaluate this interaction by separating bound and unbound drug across a semipermeable membrane.
- In this study, a Pfizer-adapted protocol utilizing a high-throughput dialysis (HTD) device was implemented.
- Combining this approach with equilibrium dialysis enabled assessment of drug-protein binding behavior and comparison with literature values.
- In conclusion, our study provides a robust method for assessing drug-protein binding and comparing it with existing data. This information can help in the development of new drugs and optimize existing therapies.

Data and Results

Molecule Name	A: 2,4-dichloro-6-nitro-phenol	B Ketoprofen	C Niflumic Acid	D Quercetin	E Quinidine	F Probenecid	G Sulindac	H Tolbutamide
Literature % unbound	Not available	0.8 ± 0.2 %	10 %	2 %	10 - 26 %	5 - 15 %	< 10%	1 - 5 %
Our result, March 25	12 ± 4 %	39 ± 2 %	7 ± 4 %	12 ± 3 %	5 ± 2 %	28 ± 12 %	14 ± 4 %	22 ± 7 %
Our result, March 12th	10 ± 4 %	8 ± 1 %	6 ± 1 %	10 ± 2 %	6 ± 1 %	12 ± 3 %	34 ± 12 %	28 ± 10 %

Methods



Molecule Name	Mix 1 mM solution	Structure	UV-Vis Scan	Fluorescence Scan	Wavelength used
A 2,4-dichloro-6-nitrophenol, FW 206 g/mol	2.1 mg/10.0 mL 2.6 mg/12.5 mL	<chem>Oc1cc(Cl)c(Cl)cc1[N+](=O)[O-]</chem>			EX. 420 EM. 490
B Ketoprofen, FW 254.3 g/mol	2.5 mg/10.0 mL 4.0 mg/12.3 mL	<chem>CC(O)C1=CC=C(C=C1)C(=O)C2=CC=CC=C2</chem>			EX. 300 EM. 400
C Niflumic Acid, FW 282.2 g/mol	2.8 mg/10.0 mL 3.5 mg/12.4 mL	<chem>OC(=O)c1ccc(cc1)C(F)(F)F</chem>			EX. 360 EM. 450
D Quercetin Dihydrate, FW 338.3 g/mol	3.4 mg/10.0 mL 3.9 mg/11.5 mL	<chem>Oc1cc(O)c2c(c1)oc(O)c2O</chem>			EX. 400 EM. 500
E Quinidine Anhydrous, FW 324.4 g/mol	3.2 mg/10.0 mL 3.7 mg/11.4 mL	<chem>CN1C=NC2=C1C=CC2</chem>			EX. 300 EM. 370
F Probenecid, FW 285.4 g/mol	2.9 mg/10.0 mL 2.8 mg/9.8 mL	<chem>CCOC(=O)c1ccc(cc1)C(=O)O</chem>			EX. 270 EM. 310
G Sulindac, FW 356.4 g/mol	3.6 mg/10.0 mL 3.7 mg/10.4 mL	<chem>CC1=CC=C(C=C1)C(=O)C2=CC=CC=C2</chem>			EX. 330 EM. 380
H Tolbutamide, FW 270.3 g/mol	2.7 mg/10.0 mL 4.0 mg/14.8 mL	<chem>CCOC(=O)Nc1ccc(cc1)C(=O)N</chem>			EX. 250 EM. 300

Poster presented at the 2026 College of Pharmacy Research Showcase

Measuring Plasma Protein Binding

Aliyah Naseer, Kemeline Nerette, Leisly Aceituno, Gbuckattee Nowinnie

- Plasma protein binding is a key determinant of drug distribution, as it influences the proportion of free (pharmacologically active) drug available in circulation.
- Equilibrium dialysis is a standard method used to evaluate this interaction by separating bound and unbound drug across a semipermeable membrane.
- In this study, a Pfizer-adapted protocol utilizing a high-throughput dialysis (HTD) device was implemented.
- Combining this approach with equilibrium dialysis enabled assessment of drug-protein binding behavior and comparison with literature values.
- In conclusion, our study provides a robust method for assessing drug-protein binding and comparing it with existing data. This information can help in the development of new drugs and optimize existing therapies.

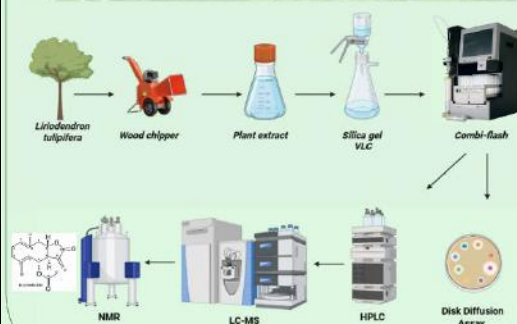
Plucking Antibiotics from the Tulip Poplar Tree

Rylie Buscher, Bennett Allen, Ololade Gbadebo, Arvie Grace B. Masibag, Victor Olaoye, Lily-Rose DeNicola, Dr. David Rowley
Department of Biomedical and Pharmaceutical Sciences, College of Pharmacy, University of Rhode Island

Background

- The Cherokee Tribe used the Tulip Poplar tree, *Liriodendron tulipifera*, to treat numerous ailments.¹
- Extracts were later used during the Civil War for anti-malarial activity.
- Recent studies at URI identified laurenobiolide and tulipinolide as antibacterial specialized metabolites produced by *L. tulipifera*.²
- Based on the rich specialized metabolite profile of our *L. tulipifera* extracts, we hypothesize that there are additional antibacterial compounds awaiting discovery

Experimental Workflow

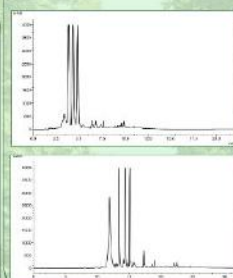
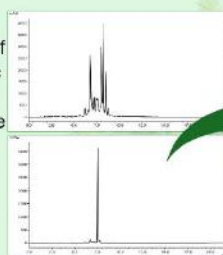


References

- <https://www.nps.gov/articles/000/inside-the-collections-how-5252.htm>
- <https://pubs.acs.org/doi/10.1021/acsomega.2c03539>

Chromatography

Multiple rounds of chromatographic separation were required to isolate single peaks for structure identification.



Chromatography methods required optimization. On the left, mobile-phase gradients were modified to enhance the separation of peaks in reversed-phase HPLC for isolation efforts.

Structure Determination



¹H NMR spectrum and mass spectrometry measurement of an unknown compound isolated during this study.



Sample Number	Representative Zone of Inhibition (mm)
H4/8E 14	14
H4/8E 15	24
H4/8E 16	13
H4/8E 17	12
(+) Control	18
(-) Control	0
17	16
18	13

Non-laurenobiolide-containing fractions that demonstrated substantial antibiotic activity against *Staphylococcus aureus*. These fractions are now prioritized for bioactive compound discovery.

Summary & Future Directions

- Provided rarefied fractions of laurenobiolide and tulipinolide to collaborators for mechanism of action studies.
- Determined that *L. tulipifera* is a prolific producer of specialized metabolites with antibacterial activity.
- We are moving into the final stages of compound isolation, structure determination, and bioassay testing.

Plucking Antibiotics from the Tulip Poplar Tree

Rylie Buscher, Bennett Allen, Ololade Gbadebo, Arvie Grace B. Masibag, Victor Olaoye, Lily-Rose DeNicola, David Rowley

The tulip poplar tree (*Liriodendron tulipifera*) has a long history of medicinal use, including traditional applications by the Cherokee and later reports of antimalarial use during the U.S. Civil War. Recent studies at the University of Rhode Island identified laurenobiolide and tulipinolide as antibacterial specialized metabolites produced by *L. tulipifera*. Based on the rich specialized metabolite profile of *L. tulipifera* extracts, we hypothesized that additional antibacterial compounds remain to be discovered beyond these known constituents.

To investigate this, we fractionated *L. tulipifera* extracts and performed iterative chromatographic separations, optimizing reversed phase HPLC gradients to improve peak resolution for isolation. Bioactivity screening revealed non laurenobiolide-containing fractions with substantial antibiotic activity against *Staphylococcus aureus*, prioritizing these fractions for bioactive compound discovery. Rarefied fractions of laurenobiolide and tulipinolide were also provided to collaborators to support mechanism of action studies. Overall, these findings support *L. tulipifera* as a prolific source of antibacterial specialized metabolites, and ongoing work is focused on completing compound isolation, structure determination, and confirmatory bioassay testing of newly prioritized active fractions.

Reproducible Fluorescent Labeling of *Clostridium novyi*-NonToxic Spores with Preserved Spore Viability



Jack G. Stevenson¹, Caleb P. Hoffman¹, Caleb J. Bussard², Anela K. Kerber³, Jessica E. Pullan¹, and Kaitlin M. Dailey^{3,4*}

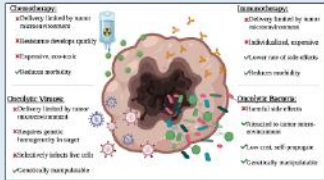
¹) Department of Chemistry and Physics, Southern Utah University, Cedar City, UT
²) Department of Osteopathic Medicine, Rocky Vista University, Irvin, UT
³) College of Pharmacy, University of Rhode Island, Kingston, RI
⁴) Legorreta Cancer Center, Brown University, Providence, RI
*Corresponding author: kaitlin.dailey@uri.edu



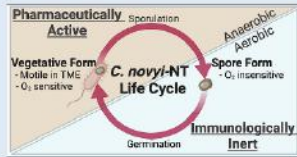
ABSTRACT

Clostridium novyi-NT is a spore-forming bacteria with strong potential for development as a cancer therapeutic modality through the application of engineering biology principles. However, the structure of its spore coat and how the spore interacts with different environmental conditions remains poorly understood. This knowledge gap limits the development of effective fluorescent imaging techniques – particularly for *in vivo* applications. Reliable staining of *Clostridium novyi*-NT spores is critical for pre-clinical characterization and further therapeutic advancements. However, most commercially available fluorescent staining protocols are intended for eukaryotic cells and are poorly suited for bacterial spores due to their complex, multilayered structure, which can limit dye penetration. Here, previously published methods were optimized to stain *C. novyi*-NT spores with carboxyfluorescein succinimidyl ester (CFSE) with adjustments to dye concentration, incubation conditions, and methodological parameters to ensure consistent fluorescence while preserving spore integrity and germination capacity.

INTRODUCTION



Although a variety of chemotherapeutic strategies exist, their efficacy in pancreatic cancer is limited by (1) late-stage diagnosis, (2) poor vascularity, and (3) recurrence due to chemotherapeutic resistance. Oncolytic bacteria have re-emerged as promising therapies due to their ability to move rapidly through subtle cytokine, pH, and/or oxygen gradients¹⁻⁴.



Clostridium novyi-NT (CnNT) is a sporulating, attenuated, obligate anaerobic bacteria with oncolytic properties. It has demonstrated the ability to penetrate, selectively colonize, and eradicate both solid tumors and small malignant tumor islands^{1,2}. These motile bacteria exhibit a sensitive chemotactic response and demonstrate an ability to localize and rapidly penetrate the solid tumor core^{1,3}, effectively lysing the tumor from the inside out. Several promising pre-clinical and early phase clinical trials have supported its therapeutic potential¹. However, the development of a CnNT-based therapeutic has been hampered by knowledge gaps regarding spore surface composition. To support ongoing CnNT research, improved methods to detect and monitor spores are needed.

BACKGROUND

Previous studies have characterized spore coat architecture⁴ and gene expression⁵ in physiological contexts. This research uses carboxyfluorescein succinimidyl ester (CFSE), a common microbial dye, to begin chemically characterizing the spore surface. The strength of dye-spore binding interactions is largely determined by the molecular structure of the dye. By evaluating binding interactions across different molecules, the functional groups present on the *C. novyi*-NT spore surface can be inferred.

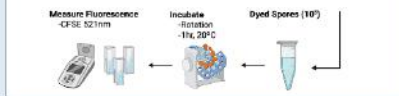
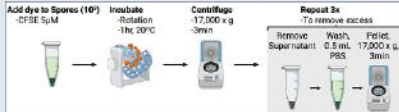
Carboxyfluorescein succinimidyl ester (CFSE)



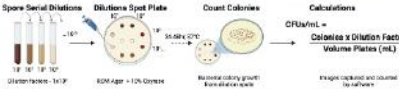
CFSE binds to proteins through covalent modifications in two different steps. Fluorescence occurs when acetyl groups are removed via intracellular esterases, forming hydroxyl functional groups. The binding process is dependent upon the presence of an amino group, most frequently lysine.

METHODS

Staining *Clostridium novyi*-NT Spores



Calculation of Colony Forming Units



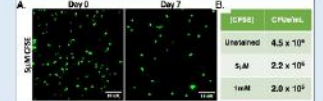
Through exploration of dye concentration, incubation conditions, and post stain washing, this staining protocol was developed to provide persistent labeling of *C. novyi*-NT spores without compromising germination or viability, both crucial for therapeutic efficacy.

REFERENCES

1) Wang, L. et al. *Clostridium difficile*: From a gut pathogen to a model for cancer therapy. *Front. Microbiol.* 10:1664 (2019).
2) Wang, L. et al. *Reproductive and metabolic characteristics of Clostridium novyi-NT spores*. *Appl. Environ. Microbiol.* 86:3006-3014 (2020).
3) Wang, L. et al. *Spore Coat Architecture of Clostridium novyi-NT Spores*. *Appl. Environ. Microbiol.* 86:3006-3014 (2020).
4) Wang, L. et al. *Spore Coat Architecture of Clostridium novyi-NT Spores*. *Appl. Environ. Microbiol.* 86:3006-3014 (2020).
5) Wang, L. et al. *Spore Coat Architecture of Clostridium novyi-NT Spores*. *Appl. Environ. Microbiol.* 86:3006-3014 (2020).

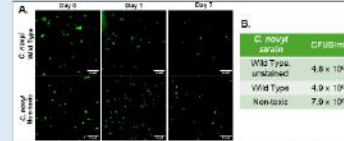
RESULTS

CFSE staining at reduced concentrations did not compromise the germination characteristics of *C. novyi*-NT spores.



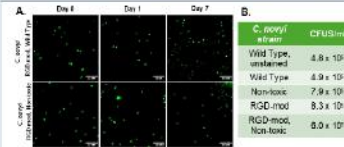
A) Confocal microscopy images of CFSE-stained *Clostridium novyi* Wild Type (unattenuated) spores. Scale bar is 1 μm. B) Colony forming unit counts indicating germination capacity of spores after CFSE staining. CFUs/ml are presented as the mean of three technical replicates.

Attenuation does not impact CFSE signal when stained by this optimized protocol - thereby supporting *in vivo* studies as a detection modality.



A) Confocal microscopy images of CFSE-stained *Clostridium novyi* Wild Type (unattenuated) spores compared to *Clostridium novyi*-NonToxic (attenuated) spores. Scale bar is 1 μm. B) Colony forming unit counts indicating germination capacity of spores after CFSE staining at 5 μM. CFUs/ml are presented as the mean of three technical replicates.

A persistent staining methodology for fluorescence labeling of *C. novyi* spores has been optimized regardless of attenuation or modification.



A) Confocal microscopy images of CFSE-stained RGD-modified *Clostridium novyi* Wild Type spores compared to RGD-modified *Clostridium novyi*-NonToxic spores. Scale bar is 1 μm. B) Colony forming unit counts indicating germination capacity of spores after CFSE staining at 5 μM. CFUs/ml are presented as the mean of three technical replicates.

FUTURE DIRECTIONS

Examination of fluorescence signal longevity and decay, as well as performance under physiologically relevant conditions including serum exposure, pH, and temperature, will improve interpretation of *in vivo* studies. Further investigation of stability following freeze-thaw cycles and long-term storage will support these efforts. In addition, exploration of alternative or complementary dyes will expand *C. novyi*-NT staining strategies.

ACKNOWLEDGEMENTS

Funded by Fred & Pamela Bush Cancer Center Startup funds to RND (URI, UNMC) and Gibson Stegge to JEP (UNMC). Special thanks to Michael A. Haskingsworth and Kenneth W. Dailey (UNMC) for their support of this project. The authors would like to thank the support of their colleagues and institutions, SUU, RVU, UNMC, URI, and Brown University. The authors acknowledge the use of Biocompare.com to create the figures contained within this poster.

Reproducible Fluorescent Labeling of *Clostridium novyi*-NonToxic Spores with Preserved Spore Viability

Jack G. Stevenson, Caleb P. Hoffman, Caleb J. Bussard, Anela K. Kerber, Jessica E. Pullan, Kaitlin M. Dailey

Clostridium novyi-NT is a spore-forming bacteria with strong potential for development as a cancer therapeutic modality through the application of engineering biology principles. However, the structure of its spore coat and how the spore interacts with different environmental conditions remains poorly understood. This knowledge gap limits the development of effective fluorescent imaging techniques – particularly for *in vivo* applications. Reliable staining of *Clostridium novyi*-NT spores is critical for pre-clinical characterization and further therapeutic advancements. However, most commercially available fluorescent staining protocols are intended for eukaryotic cells and are poorly suited for bacterial spores due to their complex, multilayered structure, which can limit dye penetration. Here, previously published methods were optimized to stain *C. novyi*-NT spores with carboxyfluorescein succinimidyl ester (CFSE) with adjustments to dye concentration, incubation conditions, and methodological parameters to ensure consistent fluorescence while preserving spore integrity and germination capacity. Preservation of these capacities directly impacts therapeutic efficacy and are therefore anti-cancer activities. Through development of a low cost, accessible, and reproducible methodology, this approach enables consistent detection and visualization of *C. novyi*-NT spores and provides a framework adaptable to alternative fluorophores and related spore-forming systems. Ultimately, this undergraduate research project developing alternative *C. novyi*-NT detection modalities will expand downstream experimental applications and facilitate clinical translation, including therapeutic strategies for metastatic pancreatic cancer and other solid tumors.

Using Concept Mapping to Identify and Prioritize Strategies for Improving CDK4/6 Inhibitor Persistence in Breast Cancer

Salma Taghzout¹, Michelle L. Caetano, PharmD¹, Guannan Gong, PhD^{2,3}, Maryam Lustberg, MD^{2,3}, Robert Legare, MD³, Mariah Ramos¹, Jessica Liu, BS¹, Britny R. Brown, PharmD, BCOP¹

1. Yale University School of Medicine, 2. University of Rhode Island College of Pharmacy/Ogden, 3. Yale University, New Haven, CT, 4. Yale Cancer Center, New Haven, CT

Introduction

Cyclin-dependent kinase 4/6 inhibitors (CDK4/6i) have significantly improved outcomes in hormone receptor-positive (HR+), HER2-negative breast cancer, yet real-world adherence and persistence remain suboptimal.¹⁻⁴ Stakeholder-informed interventions are needed to address modifiable barriers and support long-term therapy.

Objectives

The primary objective is to identify and prioritize patient- and provider-informed strategies to improve persistence with CDK4/6i in HR+/HER2- breast cancer. Strategies are prioritized by feasibility and expected impact.

Methods

- Phase 1: Qualtrics survey sent to 88 CDK4/6i patients and 94 multidisciplinary clinicians
- Assessed treatment experiences and collected open-ended recommendations to improve persistence
- Responses thematically coded in NVivo by a single analyst and synthesized into candidate strategies
- Three main themes identified:
 - Provider communication and support
 - Symptom and adverse-effect management
 - Social support needs
- Phase 2: Participants rated strategies on feasibility and expected impact

Results

- Response rates for the initial survey were 29/63 patients and 17/94 clinicians, yielding an overall response rate of 29.3%.
- Patients emphasized timely communication, clear expectations, and proactive management of toxicities, particularly fatigue, neutropenia, and diarrhea, as factors that would support longer treatment persistence.
- Clinicians most frequently identified adverse effects as the primary modifiable cause of non-persistence, along with financial and access barriers; discontinuation due to disease progression was also noted.
- Insights from the initial survey were used to organize proposed solutions into six domains for the second survey:
 - Education and informational support
 - Patient monitoring and follow-up
 - Adherence tools and resources
 - Multidisciplinary care and collaboration
 - Financial and access support
 - Treatment optimization
- Response rates for the second survey were 18/63 patients and 17/94 clinicians, yielding an overall response rate of 23.5%.
- Strategies identified in the initial survey were sorted and rated on feasibility and impact by both patients and clinicians.

Figure 1. Priority payoff matrix

Table 1. Strategies in each domain

Strategy	Mean P	Mean I
Education & Informational Support		
1. Provide clear, concise medication and side-effect education	4.11	4.81
2. Offer more educational resources (videos, handouts) to help patients understand their treatment	4.13	4.28
3. Dedicate more time before treatment to discuss what to expect	3.18	4.53
Patient Monitoring & Follow-up		
4. Check in patients regularly (e.g., weekly or after each treatment) through brief surveys to ask about symptoms, side effects, and overall well-being	3.10	3.84
5. Have more nurses or advanced practice providers available between appointments and during visits to answer questions by phone, patient portal, or in person	3.1	4.31
6. Create a follow-up program where healthcare providers contact patients regularly (e.g., weekly or biweekly) to discuss how they're feeling and manage any side effects	3.0	3.2
Tools & Resources for Adherence		
7. Send text or phone reminders to help patients remember to take their medications	3.82	2.72
8. Provide printed tools such as calendars or checklists for tracking medication use	3.87	3.69
9. Offer optional mobile apps to help patients manage their medication schedule	3.17	3.06
10. Offer easy-to-use reminder tools or devices to help patients track their doses	3.18	3.03
Multidisciplinary Care & Collaboration		
11. Have a care team that includes different specialists (e.g., oncologist, nurse, pharmacist) to help manage side effects	3.0	2.72
12. Allow pharmacists to actively collaborate with doctors and nurses by reviewing medications together, discussing treatment plans, and ensuring consistent care for patients	3.67	4.18
13. Offer education or support meetings for patients, either online or in person, in group or one-on-one for results, led by healthcare providers to help patients share experiences and receive guidance	3.47	3.72
Financial Access & Support		
14. Assist patients with individualized financial counseling, such as financial counselors, social workers, or financial navigators, to help them understand coverage options, co-pay assistance programs, and other financial resources for treatment	3.51	4.11
15. Add staff to help patients with insurance questions and appointment scheduling	3.19	4.47
Treatment Optimization		
16. Start some patients on a lower dose and adjust upward as their body tolerates the medicine	3.92	3.27

Discussion

- Figure 1 displays items in a priority payoff matrix based on their impact and feasibility ratings, with the upper right quadrant representing strategies scoring highest in both domains. Items in this quadrant are underlined in Table 1.
- Particularly impactful and feasible strategies include:
 - Providing clear medication and side-effect education
 - Expanding patient resources (e.g., videos, handouts)
 - Dedicating more time for pre-treatment counseling
 - Implementing regular follow-up check-ins
 - Using printed adherence tools (e.g., calendars, checklists)
 - Strengthening pharmacist collaboration with the care team
 - Using dose titration when appropriate
- Table 1 illustrates multidimensional strategies that demonstrate varying levels of feasibility (F) and impact (I).
- Limitations:
 - The sample is drawn from a single institution; although 15 clinics span both academic and community settings within one cancer center, findings may not be broadly generalizable.
 - Opt-in electronic recruitment may preferentially capture more engaged participants, potentially under-representing individuals with lower engagement or limited internet access.
 - Eligibility was limited to English-speaking adults, restricting insight into populations with other language needs or lower health literacy.

Conclusion and Future Directions

- Concept mapping methodology was used to generate stakeholder-driven insights on CDK4/6i adherence, fostering shared ownership of proposed solutions and supporting equitable, patient-centered care.
- By integrating both clinical and lived experiences into strategy development, the project ensured interventions were responsive to the complex and individualized nature of cancer care. These findings informed the development of a patient-reported outcomes module within the electronic medical record.

Disclosures and Acknowledgments

- Funding: This initiative is supported by an independent grant from Lilly. The authors declare no conflicts of interest with respect to the research, authorship, and/or publication of this poster.
- Acknowledgement: The authors would like to acknowledge Edward Tupper for his contributions to the consenting process.

References

1. American Society of Clinical Oncology. (2020). Adjuvant endocrine therapy for breast cancer. *Journal of Clinical Oncology*, 38(26), 3521-3538.
2. American Society of Clinical Oncology. (2020). Adjuvant endocrine therapy for breast cancer. *Journal of Clinical Oncology*, 38(26), 3521-3538.
3. American Society of Clinical Oncology. (2020). Adjuvant endocrine therapy for breast cancer. *Journal of Clinical Oncology*, 38(26), 3521-3538.
4. American Society of Clinical Oncology. (2020). Adjuvant endocrine therapy for breast cancer. *Journal of Clinical Oncology*, 38(26), 3521-3538.

Using Concept Mapping to Identify and Prioritize Strategies for Improving CDK4/6 Inhibitor Persistence in Breast Cancer

Salma Taghzout, Michelle L. Caetano, Guannan Gong, Maryam Lustberg, Robert Legare, Mariah Ramos, Jessica Liu, Britny R. Brown

Cyclin-dependent kinase 4/6 inhibitors (CDK4/6i) have significantly improved outcomes in hormone receptor-positive (HR+), HER2-negative breast cancer; however, real-world adherence and persistence remain suboptimal. Stakeholder-informed interventions are needed to address modifiable barriers and support long-term therapy. This study aimed to identify and prioritize patient- and provider-informed strategies to improve CDK4/6i persistence based on feasibility and expected impact.

A two-phase concept mapping approach was employed. In Phase 1, a Qualtrics survey was distributed to CDK4/6i-treated patients (n=63) and multidisciplinary clinicians (n=94) to assess treatment experiences and collect open-ended recommendations. Responses (29 patients, 17 clinicians; 29.3% response rate) were thematically coded and synthesized into candidate strategies. Three primary themes emerged: provider communication and support, symptom and adverse-effect management, and social support needs. Patients emphasized timely communication, clear expectations, and proactive management of toxicities (e.g., fatigue, neutropenia, diarrhea), while clinicians identified adverse effects, financial and access barriers, and disease progression as key contributors to non-persistence.

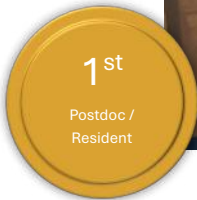
In Phase 2, participants rated proposed strategies on feasibility and expected impact (18 patients, 17 clinicians; 23.5% response rate). Strategies were organized into six domains: education and informational support, patient monitoring and follow-up, adherence tools and resources, multidisciplinary care and collaboration, financial and access support, and treatment optimization. High-priority strategies included enhanced medication and side-effect education, expanded patient resources, dedicated pre-treatment counseling, routine follow-up check-ins, use of adherence tools, increased pharmacist integration, and dose titration when appropriate.

Limitations include single-institution sampling, potential selection bias from opt-in electronic recruitment, and restriction to English-speaking participants. This concept mapping approach generated stakeholder-driven insights, promoting patient-centered, equitable care. Findings informed the development of a patient-reported outcomes module within the electronic medical record.

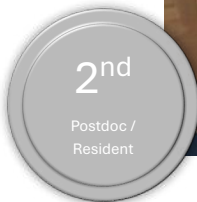
Postdoc / Resident



Graduate Students



Emily Reedich accepting on behalf of the winning poster



Xiaoyue Zhu accepting on behalf of the second placed poster



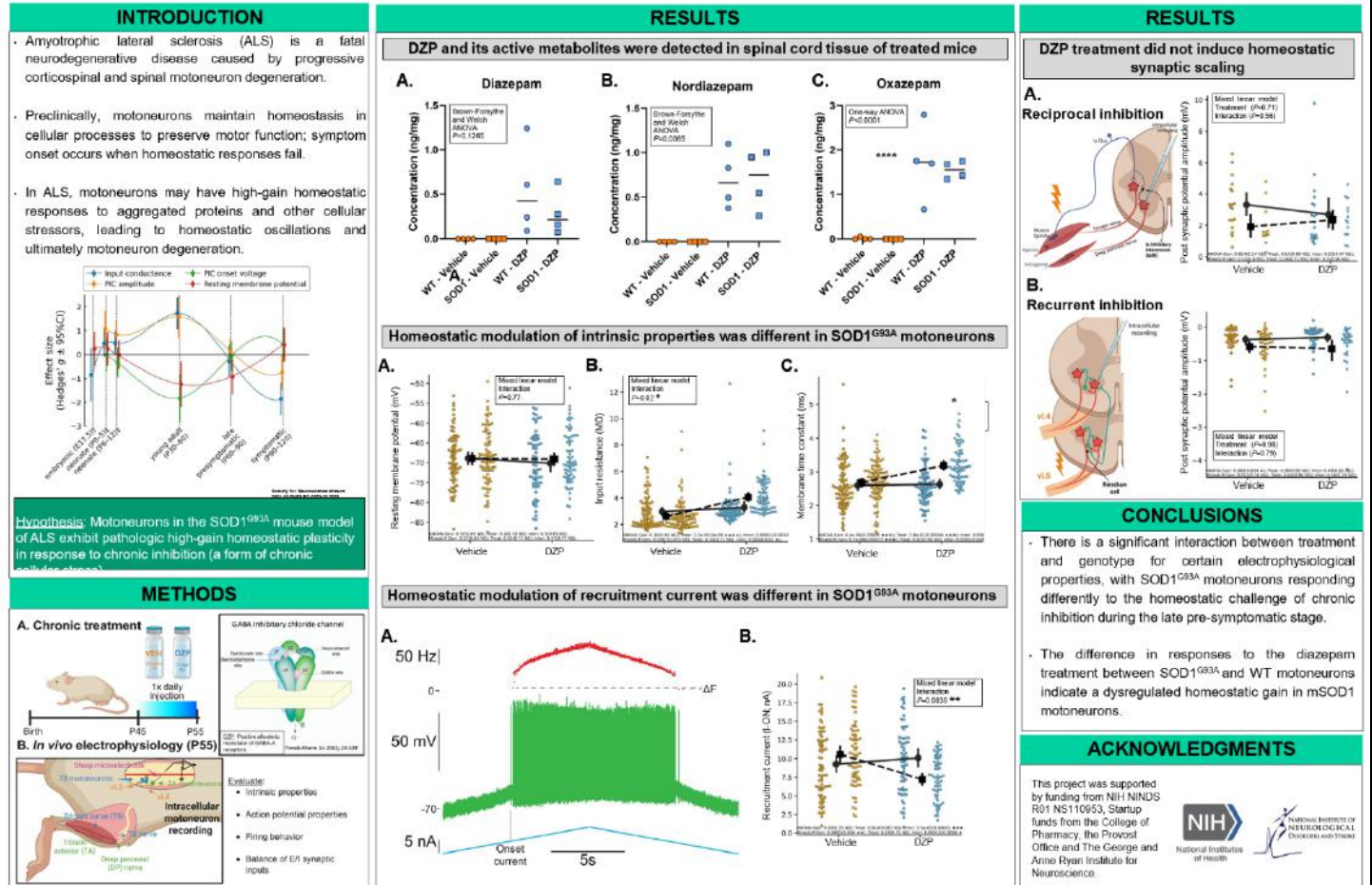
Tasneem Al Huniti accepting on behalf of the third placed poster



Spinal motoneurons show a dysregulated homeostatic response to chronic inhibition in the SOD1^{G93A} mouse model of amyotrophic lateral sclerosis

Emily Reedich^{1,2}, Roy Chen³, Rebecca Imhoff-Manuel^{1,2}, Deyu Li³, Marin Manuel^{1,2}

¹ George and Anne Ryan Institute for Neuroscience, University of Rhode Island; ² Department of Biomedical and Pharmaceutical Sciences, College of Pharmacy, University of Rhode Island; ³ Department of Medical Organic Chemistry, College of Pharmacy, University of Rhode Island



First Place - Spinal motoneurons show a dysregulated homeostatic response to chronic inhibition in the SOD1G93A mouse model of amyotrophic lateral sclerosis

Emily Reedich, Roy Chen, Rebecca Imhoff-Manuel, Deyu Li, Marin Manuel

Amyotrophic lateral sclerosis (ALS) is a fatal neurodegenerative disease that involves rapid paralysis due to progressive corticospinal and spinal motoneuron degeneration. During the preclinical stage, motoneurons maintain homeostasis in cellular processes to effectively preserve motor function; symptom onset occurs when homeostatic responses fail. In ALS, motoneurons may have dysregulated, high-gain homeostatic responses to aggregated proteins and other cellular stressors, leading to homeostatic oscillations and ultimately motoneuron degeneration. Here, we tested the hypothesis that motoneurons in the SOD1G93A mouse model of ALS exhibit pathologic high-gain homeostatic plasticity in response to chronic inhibition (a form of chronic cellular stress). We treated wild type and SOD1G93A mice in the late pre-symptomatic phase with vehicle (sesame oil) or diazepam (15 mg/kg/day; for 10 days), a benzodiazepine that exerts its effects through enhancing inhibitory neurotransmission mediated by gamma-aminobutyric acid (GABA) receptors. On the last day of treatment, we made in vivo intracellular motoneuron recordings in anesthetized mice and measured motoneuron passive properties, active properties, and assessed synaptic scaling. We found that chronic diazepam treatment induced homeostatic plasticity in wild type and mutant SOD1 motoneurons. For the intrinsic properties of input resistance and membrane time constant, as well as recruitment current on a triangular current ramp (the firing property I-ON), there was a significant interaction between treatment and genotype, with mutant SOD1 motoneurons responding differently to the homeostatic challenge of chronic diazepam treatment. The difference in homeostatic responses to chronic inhibition by diazepam suggests a dysregulated homeostatic gain in mutant SOD1 motoneurons.

Gene editing in rats produces a cerebral amyloid angiopathy model with distinct vascular and molecular signatures



Xiaoyue Zhu, Judianne Davis, Feng Xu, Mark Majchrzak, and William E. Van Nostrand*

INTRODUCTION

Cerebral amyloid angiopathy (CAA) is a common cerebral small vessel disease associated with Alzheimer's disease. Existing transgenic mouse models overexpressing human AβPP fail to fully recapitulate human pathology.

We generated a CRISPR/Cas9 gene-edited rat model (CRAβDI) expressing human Dutch/lowa mutant Aβ from the endogenous rat AβPP locus.

CRAβDI rats develop progressive capillary (type-1) and arteriolar (type-2) CAA across multiple brain regions, accompanied by a mild pro-inflammatory and vascular activation signature distinct from transgenic models.

METHODS

- **Gene-edited Rat Model:** Endogenous rat AβPP locus humanized to express the human Aβ sequence with Swedish and Dutch/lowa mutations
- **Histopathology (IHC):** Identify CAA loading and CAA relating cells
- **ELISA Quantification:** Levels of total Aβ40 and Aβ42 were determined in the brain across ages
- **Transcriptomics (Bulk RNA-seq):** Gene expression profiling, signal analysis and biomarker prediction

RESULTS

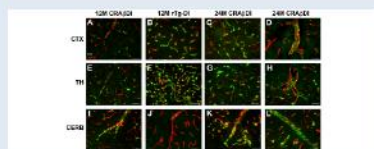


Figure 1. Regional accumulation of cerebral vascular amyloid in CRAβDI rats. CRAβDI rats show progressive capillary CAA in CTX, TH, and CD55. 12M, 18M, 24M, 30M CRAβDI rats were analyzed. Quantification of capillary and arteriolar fibrillar Aβ amyloid burden in CTX (A), TH (B), and CD55 (C) across CRAβDI and rTg-DI models at different ages.

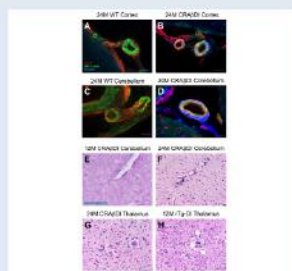


Figure 3. Arteriolar deposition of fibrillar amyloid leads to loss of smooth muscle and microhemorrhages in CRAβDI rats.

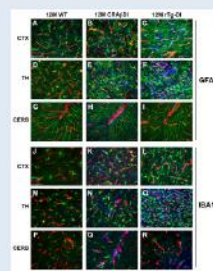


Figure 4. Increased postvascular astrocytes and microglia in CRAβDI rats.

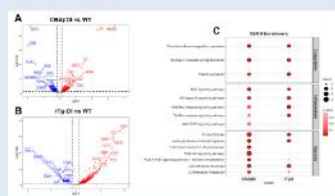


Figure 5. Differential gene expression in brain tissue at 12 months. Volcano plots compare CRAβDI vs WT (A) and rTg-DI vs WT (B), with KEGG pathway enrichment shown in (C).

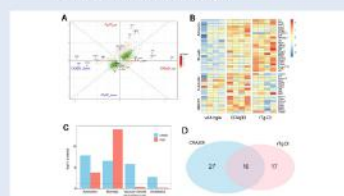


Figure 6. Transcriptomic analysis reveals cell-type enrichment in CRAβDI and rTg-DI rats. (A) Overlap of DEGs between CRAβDI and rTg-DI rats. (B) Heatmaps of cell marker gene expression. (C) GSEA enrichment scores. (D) Shared and unique AD-related DEGs.

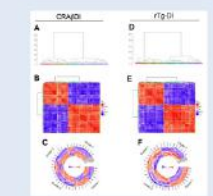
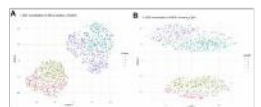


Figure 7. Biomarker candidate prediction in CRAβDI and rTg-DI rats. (A, B) Gene clustering identifies four clusters. (C, E) Pairwise correlation heatmaps of DEGs, with clusters indicated. (D, F) Heatmaps of hub gene candidates selected by lowest standard across samples.

CONCLUSION

- A gene-edited rat model for cerebral amyloid angiopathy (CAA), CRAβDI, was generated.
- CRAβDI rats develop both capillary and arteriolar CAA across multiple brain regions.
- Transcriptomic analyses reveal a vascular-driven phenotype with preserved ion channel-related signalling pathways.
- CRAβDI rats exhibit distinct molecular features compared to transgenic CAA models.
- CRAβDI represents a chronic, moderate disease state, in contrast to the rapid, gliosis-dominated pathology observed in transgenic models.
- This model more closely recapitulates aspects of human disease progression and provides a potential therapeutic window.



Distinct clustering of CRAβDI and rTg-DI transcriptomes

ACKNOWLEDGEMENTS

This work was supported by NIH grant R21NS130390, Foundation Leducq 23CV003, and support from the Roddy Foundation.

Created with BioRender Poster Builder



Second Place - Gene editing in rats produces a cerebral amyloid angiopathy model with distinct vascular and molecular signatures

Xiaoyue Zhu, Judianne Davis, Feng Xu, Mark Majchrzak, William E. Van Nostrand

INTRODUCTION: Cerebral amyloid angiopathy (CAA) is a prevalent cerebral small vessel disease linked to Alzheimer's disease and related disorders, with existing transgenic mouse models overexpressing human amyloid β-protein precursor (AβPP) showing limitations in recapitulating human pathology.

METHODS: A gene-edited rat model was generated (CRAβDI) expressing human Dutch/lowa CAA mutant Aβ via endogenous rat AβPP using CRISPR/Cas9-mediated genome engineering. Pathological and transcriptomic analyses were conducted to assess the resulting CAA phenotype.

RESULTS: CRAβDI rats develop progressive capillary CAA type-1 and significant arteriolar CAA type-2 across multiple brain regions. Transcriptomic analyses reveal a mild pro-inflammatory phenotype with prominent vascular activation, distinguishing it from transgenic models.

DISCUSSION: Gene-edited CRAβDI rats provide a new preclinical model of CAA that exhibits distinct pathological and molecular features compared to transgenic CAA models facilitating improved understanding of disease mechanisms and evaluation of therapeutic strategies.

ER Stress as a Suspected Driver of Bile Acid-Induced Cellular Senescence in HepG2 Cells

Tasneem Al Huniti¹, Ruitang Deng¹

¹Department of Biomedical and Pharmaceutical Sciences, College of Pharmacy, University of Rhode Island



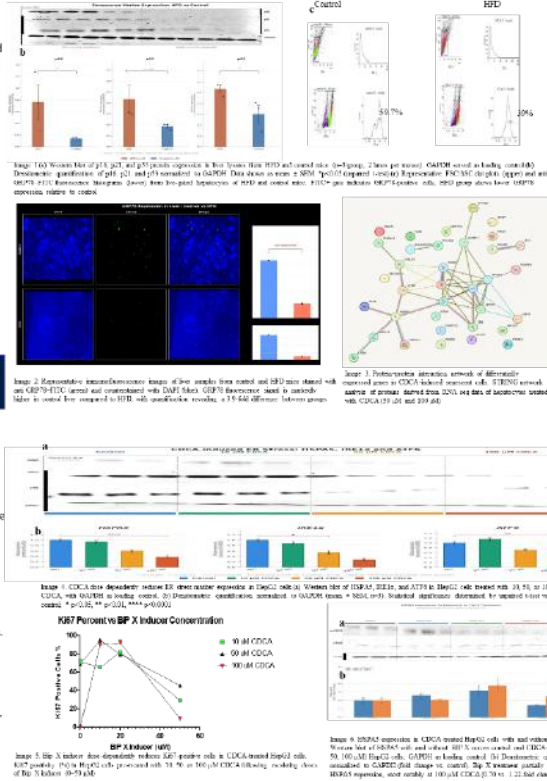
Introduction

- Cellular senescence is a state of stable cell cycle arrest characterized by SASP, p21/p16 upregulation, and β -galactosidase activity. Chronic senescence drives tissue dysfunction, inflammation, and age-related disease. Pathologically elevated bile acids — as seen in cholestatic liver disease and NAFLD — are hepatotoxic and induce senescence in hepatocytes and cholangiocytes. High-fat diet (HFD) mice recapitulate NAFLD with elevated intrahepatic bile acids, hepatic inflammation, and confirmed senescence markers (\uparrow p21, \uparrow p16, \uparrow β -galactosidase), validating this model for studying bile acid-driven senescence.
- The endoplasmic reticulum (ER) is the primary site of protein folding and secretory pathway homeostasis. When misfolded proteins accumulate, the Unfolded Protein Response (UPR) is activated through IRE1 α , PERK, and ATF6. HSPA5 (also known as GRP78 or Bip) is the master ER chaperone of the UPR, binding to UPR sensors under basal conditions. Loss of HSPA5 function is associated with ER stress, UPR dysregulation, and cell fate decisions including apoptosis and senescence.
- This study investigates the mechanistic link between bile acid-induced cellular senescence and ER stress, with a focus on HSPA5 as a potential mediator and a target.

Methods

- For *in vivo* validation, HFD mouse liver samples were analyzed by immunofluorescence, western blot, and flow cytometry to characterize HSPA5 expression and ER stress marker levels across hepatic cell populations.
- Human hepatocyte (HEPG2) cell lines were treated with pathophysiological concentrations of bile acids (chenodeoxycholic acid, CDCA) to induce senescence.
- Senescence was confirmed by: β -galactosidase (SA-Gal) staining, p21/p16 immunofluorescence imaging.
- Total RNA was extracted from bile acid-treated vs. control cells at different concentrations.
- Gene Set Enrichment Analysis (GSEA) and pathway mapping (KEGG, Reactome) identified ER stress and UPR pathways as significantly enriched in senescent cells.
- Western blotting and immunofluorescence were used to quantify HSPA5 (Bip), IRE1 α , PERK, and ATF6 across senescent and control conditions.
- HSPA5 protein levels were correlated with senescence marker expression.
- BIX, a selective inducer of HSPA5, was applied at concentrations ranging from 10-50 μ M to bile acid-treated cells.

Results



Conclusion

This study demonstrates that bile acid-induced cellular senescence is mechanistically linked to ER stress and disruption of the Unfolded Protein Response, specifically through downregulation of the master ER chaperone HSPA5 (Bip/GRP78). High-fat diet (HFD) mice, which develop NAFLD with elevated intrahepatic bile acids and confirmed senescence markers (\uparrow p21, \uparrow p16, \uparrow β -galactosidase), were employed as an *in vivo* model of bile acid-driven hepatic senescence, providing translational validation of the *in vitro* findings.

RNA sequencing of CDCA-treated HepG2 hepatocytes revealed UPR pathway suppression as a key transcriptomic signature of bile acid-induced senescence, and protein-level data confirmed progressive loss of HSPA5 across increasing bile acid concentrations. Consistent with the *in vitro* data, HFD liver samples demonstrated dysregulation of HSPA5 and downstream UPR effectors, supporting the relevance of this axis in a physiologically relevant disease model. These findings position the HSPA5/UPR axis as a novel mechanistic node in bile acid hepatotoxicity and cellular ageing.

Together, these data suggest that strategies to maintain or restore ER proteostasis may represent a viable therapeutic approach to limiting pathological senescence in cholestatic and metabolic liver disease, with the HFD mouse model offering a tractable platform for future preclinical intervention studies.

Future Studies

Alternative strategies to restore HSPA5 Beyond BIX, multiple complementary approaches should be explored to restore HSPA5 function and ER proteostasis. 4-Phenylbutyric acid (4-PBA), a chemical chaperone and ER stress reducer, could be tested alongside BIX to determine whether reducing the overall misfolded protein burden is sufficient to rescue HSPA5 expression. Tauroursodeoxycholic acid (TUDCA), another well-established chemical chaperone, represents a further candidate given its known hepatoprotective and anti-ER stress properties.

Human tissue validation Correlation of HSPA5 expression with senescence markers in human liver biopsy samples from patients with NAFLD, primary biliary cholangitis, and primary sclerosing cholangitis would provide the clinical translational evidence needed to position HSPA5 as a genuine therapeutic target.

References:

1-Zhang Y, et al. "Hepatic cellular senescence pathway genes are induced through histone modifications in a diet-induced obese rat model." *Am J Physiol Gastrointest Liver Physiol.* 2012;302:G558-64.



Third Place - ER Stress as a Suspected Driver of Bile Acid-Induced Cellular Senescence in HepG2 Cells

Tasneem Al Huniti, Ruitang Deng

Cellular senescence is increasingly recognized as a key driver of metabolic liver disease, yet the mechanisms linking bile acid accumulation to hepatocyte senescence remain poorly understood. Using high-fat diet (HFD)-fed mice as an *in vivo* model — which exhibit elevated circulating bile acid levels — we investigated whether bile acid accumulation drives hepatocyte senescence and explored the underlying pathways. *In vitro*, HepG2 cells treated with chenodeoxycholic acid (CDCA; 10, 50, and 100 μ M) demonstrated dose-dependent induction of cellular senescence, confirmed by established senescence markers. RNA sequencing and western blot analysis revealed significant downregulation of HSPA5 (GRP78/Bip), a master regulator of ER stress, alongside reduced expression of the ER stress sensors IRE1 α and ATF6, suggesting impaired unfolded protein response (UPR) signalling in bile acid-induced senescent cells. To investigate whether restoring HSPA5 function could reverse the senescent phenotype, cells were treated with BIP X inducer across multiple CDCA concentrations. BIP X treatment partially rescued HSPA5 protein levels and reduced Ki67-positive cell loss in a dose-dependent manner, indicating attenuation of the senescence programme. Collectively, these findings suggest that bile acid-driven suppression of the UPR, particularly through HSPA5 downregulation, contributes to hepatocyte senescence and that pharmacological restoration of Bip activity may represent a novel therapeutic strategy in metabolic liver disease.

Expecting Protection: Evaluating Vaccinations in Pregnancy — Potential “Bumps” in the Road and the Willingness to Take a “Shot”

Virginia Lemay, PharmD, Kayla Aquilante, PharmD '27, Emma Brouillette, PharmD '27, Lisa Cohen, PharmD, and Elizabeth Brilhante, PharmD
The University of Rhode Island College of Pharmacy, Kingston, RI



Background

- Vaccine hesitancy in pregnancy has increased since the COVID-19 pandemic and remains a significant maternal health concern.
- In the U.S., 60% report hesitancy toward the influenza vaccine and 43% toward Tdap, contributing to reduced vaccination coverage.
- The American College of Obstetrics and Gynecologists (ACOG) recommends influenza, COVID-19, Tdap, and RSV vaccines in pregnancy.
- Hesitancy is driven by misinformation, fetal safety concerns, and limited awareness of current recommendations.
- Knowledge gaps underscore the need for improved maternal vaccine education.

Objectives

- To evaluate the current state of knowledge regarding vaccines recommended during pregnancy among women who could become pregnant, are pregnant, or have been pregnant
- To assess participants' level of vaccine hesitancy and its potential causes

Methods

- An IRB-approved, cross-sectional 31-item survey (Qualtrics®) was distributed to students, pharmacists, healthcare workers (HCWs), and community members from October 22 to December 29, 2025.
- The survey was piloted with representatives from each group.
- The revised survey was disseminated through a public license email database, internal email listservs, social media, campus flyers, one OB-GYN office, and in-person recruitment at the university student union.
- Eligible participants were individuals assigned female at birth aged 18 years or older.
- Participation was voluntary and no personally identifiable information was collected.
- Data were analyzed using SPSS, including descriptive statistics and inferential analyses.

Results

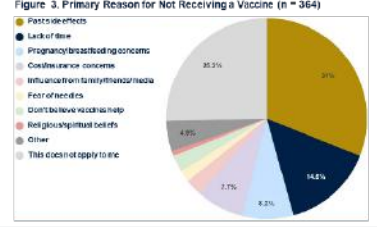
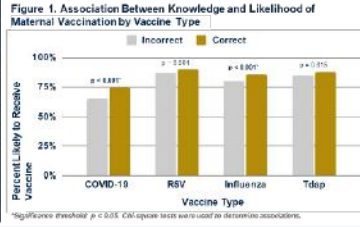
Characteristic	n (%)
Age (years)	n = 365
18-24	96 (26%)
25-29	39 (11%)
30-39	95 (26%)
40-49	90 (14%)
50-59	69 (19%)
60+	16 (4%)
Ethnicity	n = 372
Hispanic, Latino/a, or Spanish origin	16 (4%)
Not Hispanic, Latino/a, or Spanish origin	340 (91%)
Race	n = 377
White/Caucasian	330 (88%)
Black/African American	4 (1%)
Asian or Pacific Islander	17 (5%)
American Indian or Alaskan Native	2 (0.9%)
Pregnancy Status	n = 443
Could become pregnant some day	168 (38%)
Currently pregnant	13 (3%)
Pregnant <5 years ago	46 (10%)
Pregnant 6-10 years ago	10 (2%)
Pregnant >10 years ago	62 (14%)
Postmenopausal	27 (6%)
None of the above	7 (2%)

True or False Question	n (%) Correct
The respiratory syncytial virus (RSV) vaccine is recommended for pregnant patients	319 (85%)
The influenza (flu) vaccine is recommended for pregnant patients	356 (96%)
The tetanus, diphtheria, and pertussis (Tdap) vaccine is recommended for pregnant patients	323 (89%)
The COVID-19 vaccine is recommended for pregnant patients	332 (90%)
The varicella (chickenpox) vaccine is recommended for pregnant patients	136 (37%)
Vaccines may cause miscarriage or other pregnancy complications	60 (16%)
Certain vaccines are considered safe to give during pregnancy	365 (98%)
Percent Correct (mean ± SD)	86% (8.99 ± 1.069)

Vaccine Type	COVID-19 (n = 334)	RSV (n = 339)	Influenza (n = 338)	Tdap (n = 326)
Z score	-4.416	-2.257	-4.878	-3.213
p-value	<0.001*	0.024*	<0.001*	0.001*

*Significance threshold: p < 0.05. Two-tailed comparisons were analyzed using Z-scores and p-values after adjusting for RSV and influenza were adjusted using Bonferroni correction. Z-scores and p-values after adjusting for RSV and influenza were adjusted using Bonferroni correction. Z-scores and p-values after adjusting for RSV and influenza were adjusted using Bonferroni correction.

Reason	Percentage
Pregnancy/breastfeeding concerns	36.3%
Lack of time	14.8%
Cost/expense concerns	9.2%
Influenced by family/friends/media	8.2%
Fear of needles	4.9%
Don't believe needles help	4.9%
Religious/spiritual beliefs	2.7%
Other	2.7%
This does not apply to me	2.7%



Discussion & Conclusion

- A total of 442 participants initiated the survey; 393 (88.9%) completed it, 48 (10.9%) partially completed it, and 1 (0.2%) withdrew.
- Most respondents were aged 18-24 and 30-39 years old, identified as white, and reported the potential to become pregnant in the future.
- The mean percentage of correct responses to knowledge questions was 86%. Participants with correct knowledge about vaccines recommended during pregnancy (Figure 1) were more likely to report intent to receive COVID-19 and influenza vaccines. No significant association was seen for RSV or Tdap.
- Despite high knowledge levels, likelihood of receiving vaccinations during pregnancy was significantly lower compared to general vaccination likelihood and likelihood for newborn or school-aged child vaccination. Perceived vaccine safety during pregnancy was also significantly lower than general vaccine safety perceptions. Reported barriers included prior side effects, time constraints, and pregnancy/breastfeeding concerns.
- Maternal vaccine hesitancy seems driven more by pregnancy-specific safety concerns than by lack of knowledge, highlighting a key opportunity for pharmacists to provide tailored counseling that addresses misconceptions and improves maternal vaccine uptake.

Expecting Protection: Evaluating Vaccinations in Pregnancy — Potential “Bumps” in the Road and the Willingness to Take a “Shot”

Virginia Lemay, Kayla Aquilante, Emma Brouillette, Lisa Cohen, Elizabeth Brilhante

NOTE: Not included in judging, presented only

Background: Vaccine hesitancy in pregnancy has increased since the COVID-19 pandemic, driven by misinformation, fetal safety concerns, and limited awareness of current recommendations, highlighting the need for improved maternal vaccine education.

Objectives: This study evaluated the current state of knowledge regarding vaccines recommended during pregnancy among women who could become pregnant, are pregnant, or have been pregnant, and assessed vaccine hesitancy and factors contributing to it.

Methods: An IRB-approved, cross-sectional 31-item survey was administered via Qualtrics® to students, pharmacists, other healthcare workers (HCWs), and community members between October 22 and December 29, 2025. The piloted survey was distributed through a public license email database, internal listservs, social media platforms, campus flyers, a single OB-GYN office, and in-person recruitment at the university's student union. Eligible participants were assigned female at birth and aged ≥18 years. Participation was voluntary and anonymous. Data were analyzed using SPSS, including descriptive statistics and inferential analyses.

Results: Among 442 participants who initiated the survey, the mean correct response rate on knowledge questions was 86%. Accurate knowledge about pregnancy-recommended vaccines was associated with higher intent to receive COVID-19 and influenza vaccines. However, there was no significant association seen for RSV or Tdap vaccines. Despite high knowledge levels, participants reported lower likelihood of vaccination during pregnancy compared with general vaccination or vaccination of newborns/school-aged children. Perceived vaccine safety during pregnancy was also significantly lower than general vaccine safety perceptions. Common barriers included prior side effects, time constraints, and pregnancy/breastfeeding concerns.

Conclusion: Maternal vaccine hesitancy seems driven more by pregnancy-specific safety concerns than by knowledge gaps, underscoring an opportunity for pharmacists to provide targeted counseling to address misconceptions and improve maternal vaccine uptake. Future research should be performed to explore effective strategies to enhance maternal vaccination during pregnancy.

PHP 508

Note summaries are AI generated for these posters

PHP 508



1st
PHP508

J.T. Berard-Moore, Krista Dariotis, Paige Donato, Kristen Ohlinger



2nd
PHP508

Grace Bevins, Andreana Moutopoulos, Sophannara Bun, Dillan Day



3rd
PHP508

Kayla Aquilante, Sara Yahya, Nicole Sagias, Andrew Jones

The DISCORD Study: DIScordant vs CONcordant Self-Reported Smoking Status and Cardiometabolic Risk Differences Among Cotinine-Confirmed Adults

J.T. Berard-Moore, Krista Dariotis, Paige Donato, Kristen Ohlinger
University of Rhode Island, College of Pharmacy

Background

- Cigarette smoking is a well-established risk factor for cardiometabolic disease, yet smoking status is commonly assessed using self-report, which is vulnerable to misclassification including social desirability bias.¹ Serum cotinine provides an objective measure of nicotine exposure using validated thresholds.²
- Prior studies have demonstrated associations between cotinine-confirmed nicotine exposure and metabolic syndrome, even among individuals who self-identify as non-smokers.³ Additionally, discordance between self-reported smoking status and biochemical markers has been linked to increased risk of metabolic disease, suggesting that under-reporting may reflect a high-risk phenotype rather than random error.⁴
- However, U.S. population-level data examining the cardiometabolic implications of discordant smoking status remain limited.

Objective

- To compare the prevalence and adjusted odds of metabolic syndrome between concordant smokers (self-reported smokers with cotinine-positive status) and discordant smokers (self-reported non-smokers with cotinine-positive status) among U.S. adults.

Methods

Study Design & Data Source

- Cross-sectional analysis of U.S. adults aged ≥18 years from NHANES 2017–March 2020.

Study Cohort

- Adults with complete self-reported smoking data (SMQ040) and serum cotinine ≥10 ng/mL were included. Exclusions included cotinine <10 ng/mL (secondhand exposure only) and missing covariates.²
- Two analytic groups were defined: **concordant smokers** (self-reported smokers, SR+/COT+) and **discordant smokers** (self-reported non-smokers, SR-/COT+).

Exposure Assessment

- Smoking status was determined by self-report (SMQ040) and serum cotinine, with ≥10 ng/mL indicating active nicotine exposure.

Outcome Assessment

- Metabolic syndrome was defined using Adult Treatment Panel III criteria as ≥3 of the following: elevated waist circumference (≥40" men, ≥35" women), triglycerides ≥150 mg/dL, HDL cholesterol <40 mg/dL, men/<50 mg/dL, women, blood pressure ≥130/85 mmHg or antihypertensive use, and fasting glucose ≥100 mg/dL, or diabetes treatment.

Covariates

- Models adjusted for age, sex, race/ethnicity, income-to-poverty ratio, education, alcohol use frequency, and marital status. Metabolic syndrome components were excluded to avoid overadjustment.

Statistical Analysis

- Group differences were assessed using Chi-square, Fisher-exact and t-tests.
- Logistic regression estimated adjusted odds of metabolic syndrome comparing discordant to concordant smokers. Statistical significance was set at p<0.05.
- Analyses were conducted in SPSS 29.0.

Results

Table 1. Comparing Demographic and Clinical Characteristics Between Groups

Characteristic	SR-/COT+	SR+/COT+	p-value
n	159	361	
Female, n (%)	74 (46.5%)	151 (41.8%)	<0.001
Age, mean (SD)	53.8(8.7)	54.4(9.1)	0.889
Married, n (%)	76 (49.4%)	187 (51.8%)	0.497
Metabolic Syndrome			
Overall prevalence, n (%)	107 (67.3%)	117 (32.4%)	<0.001
High triglycerides, n (%)	107 (67.3%)	117 (32.4%)	<0.001
High blood pressure, n (%)	107 (67.3%)	117 (32.4%)	<0.001
High waist circumference, n (%)	107 (67.3%)	117 (32.4%)	<0.001
High fasting glucose, n (%)	107 (67.3%)	117 (32.4%)	<0.001
Low HDL cholesterol, n (%)	107 (67.3%)	117 (32.4%)	<0.001
Demographic Characteristics			
Female, n (%)	74 (46.5%)	151 (41.8%)	<0.001
Age, mean (SD)	53.8(8.7)	54.4(9.1)	0.889
Married, n (%)	76 (49.4%)	187 (51.8%)	0.497
Income-to-poverty ratio, n (%)	107 (67.3%)	117 (32.4%)	<0.001
Education, n (%)	107 (67.3%)	117 (32.4%)	<0.001
Alcohol use frequency, n (%)	107 (67.3%)	117 (32.4%)	<0.001
Marital status, n (%)	107 (67.3%)	117 (32.4%)	<0.001
Health insurance, n (%)	107 (67.3%)	117 (32.4%)	<0.001
Diabetes treatment, n (%)	107 (67.3%)	117 (32.4%)	<0.001
Antihypertensive use, n (%)	107 (67.3%)	117 (32.4%)	<0.001
Triglyceride treatment, n (%)	107 (67.3%)	117 (32.4%)	<0.001
Waist circumference treatment, n (%)	107 (67.3%)	117 (32.4%)	<0.001
Fasting glucose treatment, n (%)	107 (67.3%)	117 (32.4%)	<0.001
HDL cholesterol treatment, n (%)	107 (67.3%)	117 (32.4%)	<0.001

Table 2. Comparing Frequencies of the Outcome Variables Between Comparison Groups (Unadjusted Model)

Outcome	SR-/COT+	SR+/COT+	p-value
Metabolic syndrome, n (%)	107 (67.3%)	117 (32.4%)	<0.001
Elevated blood pressure, n (%)	107 (67.3%)	117 (32.4%)	<0.001
Elevated waist circumference, n (%)	107 (67.3%)	117 (32.4%)	<0.001
High triglycerides, n (%)	107 (67.3%)	117 (32.4%)	<0.001
Elevated fasting glucose, n (%)	107 (67.3%)	117 (32.4%)	<0.001
Low HDL cholesterol, n (%)	107 (67.3%)	117 (32.4%)	<0.001

Table 3. Results of Multivariable Logistic Regression Analysis

Variable	Adjusted OR	95% CI	p-value
Discordant smoker (vs concordant smoker)	1.41	1.11-1.76	<0.001
Demographic Characteristics			
Age (per 10-year increase)	1.22	1.18-1.26	<0.001
Female (vs male)	1.36	0.94-1.96	0.114
Income-to-poverty ratio (vs <1.5)	1.44	0.99-2.08	<0.001
Education (vs high school grad)	1.26	1.12-1.42	<0.001
Alcohol use frequency (vs never)	0.68	0.57-0.82	<0.001
Marital status (vs married)	1.17	0.92-1.49	0.223
Health Status			
Diabetes treatment (vs none)	2.07	1.14-3.74	<0.001
Antihypertensive use (vs none)	1.73	1.49-2.01	<0.001
Triglyceride treatment (vs none)	0.89	0.59-1.34	0.574
Waist circumference treatment (vs none)	1.11	0.88-1.41	0.313
Other Characteristics			
Discordant smoker (vs concordant smoker)	1.33	0.80-2.20	0.334
Discordant smoker (vs concordant smoker) (adjusted)	0.92	0.64-1.34	<0.001

Key Findings: Among 1,950 cotinine-confirmed adults, 1,589 were concordant smokers and 361 were discordant smokers. There was a higher prevalence of metabolic syndrome in discordant smokers. Discordant smoking was associated with greater adjusted odds of metabolic syndrome.

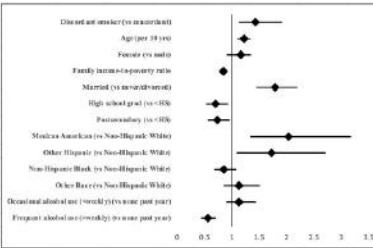


Figure 1. Forest Plot Demonstrating Adjusted Odds Ratios for Metabolic Syndrome

Discussion

Strengths

- Large sample size (1,950 cotinine-confirmed adults); use of serum cotinine, an objective biomarker of nicotine exposure; analysis of a large, nationally collected dataset, standardized and sex-specific definition of metabolic syndrome using established criteria.

Limitations

- Cross-sectional design limits causal inference; analyses were unweighted, which may limit national representativeness; potential residual confounding, including unmeasured sources of nicotine exposure and lifestyle factors.

Conclusions

- Adults who deny smoking despite cotinine-confirmed exposure exhibit elevated cardiometabolic risk comparable to or greater than that of self-reported smokers.
- Reliance on self-reported smoking status alone may under-recognize individuals with elevated cardiometabolic risk.
- Incorporating biochemical verification of smoking exposure may improve cardiometabolic risk stratification in both research and public health settings.

References

1. Flegal DM, et al. (2013). Smoking, 2010-2014. *Journal of the American Medical Association*, 309(12), 1311-1318.
2. U.S. Department of Health and Human Services. (2014). *2014 National Health and Medical Examination Survey: Full Report on Selected Results*. <https://www.cdc.gov/nchs/data/series/wr/2014001.pdf>
3. Lee D, et al. (2018). Cotinine-Confirmed Active Smoking and Cardiometabolic Syndrome Among Self-Reported Nonsmokers. *Diabetes Care*, 41(12), 2311-2317.
4. Ohlinger K, et al. (2020). Self-Reported Smoking Status, Cotinine, and Risk of Metabolic Syndrome: A Cross-Sectional Study. *Diabetes Care*, 43(12), 2311-2317.
5. Ohlinger K, et al. (2020). Self-Reported Smoking Status, Cotinine, and Risk of Metabolic Syndrome: A Cross-Sectional Study. *Diabetes Care*, 43(12), 2311-2317.



First Place - The DISCORD Study: DIScordant vs CONcordant Self-Reported Smoking Status and Cardiometabolic Risk Differences Among Cotinine-Confirmed Adults

J.T. Berard-Moore, Krista Dariotis, Paige Donato, Kristen Ohlinger

Group 18

Summarizes adults whose smoking status is measured two ways: what they report and what their blood test (serum cotinine) shows. The background explains that self-reported smoking can be inaccurate, and cotinine is an objective marker of nicotine exposure. The objective is to compare metabolic syndrome risk between two cotinine-confirmed groups: people who report smoking (concordant smokers) and people who report not smoking even though cotinine indicates active exposure (discordant smokers). In the discussion and conclusions, the authors report that discordant smokers had a higher prevalence of metabolic syndrome and higher adjusted odds of metabolic syndrome compared with concordant smokers. They conclude that relying on self-report alone can miss people with elevated cardiometabolic risk, and that adding biochemical verification may improve risk identification in research and public health settings.

Comparison of the incidence of gastroesophageal reflux disease in patients taking non-dihydropyridine calcium channel blockers versus dihydropyridine calcium channel blockers.

Grace Bevins, Sophannara Bun, Dillan Day, Andreana Moutopoulos
University of Rhode Island, College of Pharmacy

Background

Gastroesophageal reflux disease (GERD) affects approximately 1 billion people worldwide.¹ Calcium channel blockers (CCBs) are prescribed for cardiovascular diseases, and are known to decrease lower esophageal sphincter tone, contributing to GERD. Dihydropyridine (DHP) and non-dihydropyridine (non-DHP) CCBs differ in their smooth muscle effects, which could differ their effect on GERD. There is currently no data that directly compares the association between GERD with DHP CCBs and non-DHP CCBs.

Objectives

The main objective of this study was to compare the incidence of GERD in patients taking non-DHP CCBs versus those taking DHP CCBs.

Methods

- **Data Source:** National Health and Nutrition Examination Survey (NHANES) from January 2017 to March 2020.
- **Study Design:** Cross-sectional survey design of participants receiving any CCB.
- **Cohort Selection:** Participants taking a DHP or a non-DHP CCB were included. Participants taking both DHP and non-DHP CCBs were excluded.
- **Exposure Definition:** The exposure of interest was DHP or non-DHP CCB use.
- **Outcome Assessment:** The outcome of interest was GERD, defined using the ICD-10 code for GERD.
- **Covariates:** Age, gender, smoking history, alcohol use, and BMI
- **Statistical Analysis:** For continuous data, P-values were obtained using a Student T-test. For categorical data, P-values were obtained using a Pearson Chi-Square test. A multivariable logistic regression was performed to compare the exposures of interest after adjusting for covariates. All analyses were conducted using SPSS version 29.0 and a significance level of $p < 0.05$ was used.

Results

Table 1. Comparing Demographic and Clinical Characteristics Between DHP and Non-DHP CCB Groups

Characteristics	DHP CCB N=904	Non-DHP CCB N=117	P value
Age, Years, Mean \pm SD	65.3 \pm 11.9	68.3 \pm 11.2	0.010 ¹
Gender			0.461 ²
Female, N (%)	454 (50.2)	63 (53.8)	
Male, N (%)	450 (49.8)	81 (46.2)	
Smoked \geq 100 Cigarettes in Life			0.495 ²
Yes, N (%)	441 (48.8)	61 (52.1)	
No, N (%)	463 (51.2)	56 (47.9)	
Alcohol Use			0.807 ²
\geq Weekly, N (%)	418 (46.3)	53 (45.3)	
< Weekly, N (%)	276 (30.5)	37 (31.6)	
Missing, N (%)	210 (23.2)	27 (23.1)	
BMI*, BMI \geq 30 (Obese), N (%)	415 (45.9)	59 (50.4)	0.116 ²
BMI < 30, N (%)	395 (43.7)	40 (34.2)	
Missing, N (%)	94 (10.4)	18 (15.4)	

Note:
¹ Student T test; ² Chi-square test
*BMI: Body mass index

Table 2. Comparison of GERD Between DHP CCB and Non-DHP CCB Users

Outcome	DHP CCB N=904	Non-DHP CCB N=117	P value
GERD Yes, N (%)	133 (14.7%)	27 (23.1%)	0.019 ¹
GERD No, N (%)	771 (85.3%)	90 (76.9%)	

Note:
¹ Chi-square test

References

1. Xie F, Yang B, Yan Z, et al. Global temporal trends and projections of gastroesophageal reflux disease prevalence: Age-period-cohort analysis 2021. *PLoS One*. 2025;20:e0334396.
2. Hughes J, Lockhart J, Joyce A. Do calcium antagonists contribute to gastro-oesophageal reflux disease and concomitant noncardiac chest pain? *Br J Clin Pharmacol*. 2007;54:83-9. doi: 10.1111/j.1365-2125.2007.02851.x. Epub
3. Wu JH, Chang CS, Chen GH, Poon SK, Ko CW. Felodipine does not increase the reflux episodes in patients with gastroesophageal reflux disease. *Hepatogastroenterology*. 2003;47:1258-61.

Table 3. Results of Multivariable Logistic Regression Analysis

Characteristics	Adjusted Odds Ratio	95%CI	P Value
non-DHP CCB vs DHP CCB	1.8	(1.1-3.1)	0.02
Age, every 10 years older	1.2	(1.0-1.4)	0.04
Male vs Female	0.8	(0.5-1.1)	0.18
Smoked \geq 100 cigarettes in lifetime vs. Smoked < 100 cigarettes	0.9	(0.6-1.4)	0.73
Alcohol use \geq weekly vs alcohol use < weekly	1.2	(0.8-1.8)	0.39
BMI* \geq 30 (Obese) vs. BMI < 30	1.2	(0.8-1.8)	0.28

Note:
*BMI: Body mass index

Discussion/Conclusion

- The results of this study suggest that patients taking non-DHP CCBs are approximately 80% more likely to have GERD compared to patients taking DHP CCBs (aOR = 1.8, 95% CI 1.1-3.1)
- **Strengths:** Use of NHANES data provided a large, nationally representative sample in a cost-effective manner.
- **Limitations:** The cross-sectional design limits causal inference. Self reported covariates, smoking history and alcohol use, may not accurately reflect behaviors. Unmeasured or unadjusted confounders, such as dose, length of therapy, other medication use, comorbidities, family history, and diet may influence GERD risk.
- Prior studies reported mixed results on the association between DHP and non-DHP CCBs, and GERD,^{2,3} but there were no direct comparisons.
- Further studies are needed to determine the true association and guide future drug selection and monitoring parameters.



Second Place - Comparison of the incidence of gastroesophageal reflux disease in patients taking non-dihydropyridine calcium channel blockers versus dihydropyridine calcium channel blockers

Grace Bevins, Sophannara Bun, Dillan Day, Andreana Moutopoulos

Group 10

Profiles whether the type of calcium channel blocker (CCB) a person takes is linked to gastroesophageal reflux disease (GERD). The background explains that GERD is very common, and that CCBs can lower the tone of the lower esophageal sphincter, which may contribute to reflux. It also notes that dihydropyridine (DHP) and non-dihydropyridine (non-DHP) CCBs affect smooth muscle differently, and that there has not been direct comparison data on GERD between these two CCB types. The objective is to compare how often GERD occurs in people taking non-DHP CCBs versus DHP CCBs. In the discussion and conclusion, the authors report that non-DHP CCB use was associated with higher likelihood of GERD compared with DHP CCB use after adjustment for several patient factors. They note strengths such as using a large, nationally representative dataset, and limitations such as the cross-sectional design and possible missing factors like dose, duration, diet, and other medications. They conclude that more research is needed to confirm the relationship and help guide medication selection and monitoring.

Association Between Antidepressant Class and Obesity Status Across Levels of Depressive Symptom Severity

Kayla Aquilante, PharmD Candidate, Andrew Jones, PharmD Candidate, Nicole Sagias, PharmD Candidate, and Sara Yahya, PharmD Candidate
The University of Rhode Island College of Pharmacy, Kingston, RI



Covariate Medications List

Background

- Typical pharmacologic treatments for depression include selective serotonin reuptake inhibitors (SSRIs), serotonin-norepinephrine reuptake inhibitors (SNRIs), tricyclic antidepressants (TCAs), and other classes. These classes differ in mechanisms and adverse effects, including effects on appetite, metabolism, and weight.^{1,2} Prior studies have demonstrated associations between antidepressant use and weight gain.³⁻⁵
- Obesity frequently co-occurs with depression,⁶⁻⁸ and depressive symptom severity may further influence weight-related behaviors and metabolic risk. Prior studies have demonstrated associations between depressive symptom severity and obesity.⁹ However, few studies have examined obesity differences across antidepressant classes while accounting for depressive symptom severity.

Objectives

- To evaluate the association between antidepressant medication class and obesity status across levels of depressive symptom severity.

Methods

- Data source:** 2012-2020 National Health and Nutrition Examination Survey (NHANES) dataset.
- Study design:** Cross-sectional study.
- Inclusion criteria:** Patients with depression, defined by a prescription for an antidepressant and a corresponding ICD-10 diagnosis code (F32.0-F32.9), with complete data on antidepressant use, obesity status, and depression severity, dichotomized SSRI or non-SSRI monotherapy with a PHQ-9 score ≥10 (n = 3,111; SSRI 1,657, non-SSRI 1,454).
- Exclusion criteria:** Patients receiving combination antidepressant therapy (SSRI and non-SSRI).
- Exposed:** antidepressant class (SSRI vs. non-SSRI), whereas the latter included TCAs (amitriptyline, nortriptyline, clomipramine, doxepin), SNRIs (desvenlafaxine, venlafaxine), duloxetine, and other agents (bupropion, mirtazapine, bupropion + naltrexone) identified among patients receiving non-SSRI monotherapy.
- Outcome:** Obesity status, defined as body mass index (BMI) ≥30 kg/m².
- Effect modifier:** Depressive symptom severity is measured by the Patient Health Questionnaire-9 (PHQ-9) score range 0-27,¹⁰ Moderate-to-moderately severe defined as PHQ-9 score 15-19, Severe defined as PHQ-9 score ≥20.
- Covariates:** Age, gender, race/ethnicity, vigorous work activity, current smoking status, self-reported hypertension, hyperlipidemia, or diabetes; use of antipsychotic, hypothyroidism, or antidiabetic medications per ICD code for detailed list.
- Statistical analysis:** Continuous variables were analyzed using t-tests or Mann-Whitney U tests, and categorical variables using chi-square tests or Fisher's exact tests, as appropriate. Multivariable logistic regression estimated adjusted odds ratios (AORs) for obesity controlling for covariates. All analyses were conducted with SPSS version 28.0 and statistical significance was set at p < 0.05.

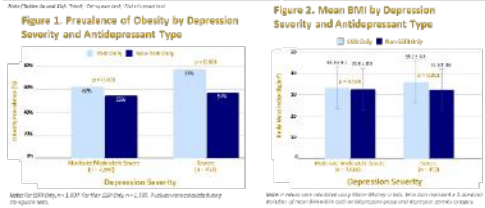
References

1. National Institute of Mental Health and U.S. Food and Drug Administration. *Depression: A Guide to Treatment*. Washington, DC: U.S. Government Printing Office; 2008. Accessed April 11, 2024. <https://pubmed.ncbi.nlm.nih.gov/24281001/>
2. Dulcan MK, Smith MR, Quillen NE, et al. Association of duration and intensity of weight gain during 30-day treatment of major depressive disorder with antidepressant medication. *Depression*. 2013;21(4):405-412. <https://doi.org/10.1007/s12288-013-9103-1>
3. Hervey A, Hartley M, Hulsbeck LR, et al. Medication-induced weight change in large American Geriatric Psychiatry Research Network (GENE) cohort. *Alzheimer Dis Assoc Dis*. 2019;33(3):375-382. <https://doi.org/10.1093/alzdis/33.3.375>
4. Mousavizadeh M, Niazpour A, et al. Impact of Antidepressant on Weight Gain Underlying Mechanisms and Mitigation Strategies. *Journal of Clinical Pharmacy and Therapeutics*. 2023;48(6):817-829. <https://doi.org/10.1111/jcpt.12879>
5. Lee SH, Park H, Park S, et al. Clinical Use of SNRIs in Hospitalized Depression Inpatients with Substantive Weight Gain: A Retrospective Cohort Study. *Journal of Clinical Pharmacy and Therapeutics*. 2023;48(6):817-829. <https://doi.org/10.1111/jcpt.12879>
6. National Health and Medical Research Council. *Obesity: Clinical Guidelines for Identification, Evaluation, and Treatment of Overweight and Obesity Worldwide: International Survey of Body Mass Index*. 2004. Accessed April 11, 2024. <https://www.nhmrc.gov.au/about-us/publications/obesity>
7. Lopez MS, et al. The Role of Insulin Resistance, Hyperlipidemia, and Hypertension in the Pathogenesis of Depression. *Journal of Clinical Pharmacy and Therapeutics*. 2012;37(6):621-628. <https://doi.org/10.1111/j.1365-2796.2012.02571.x>
8. Kessler RC, et al. The PHQ-9: validity of a brief depression severity measure. *Journal of General Internal Medicine*. 2002;17(9):1022-1026. <https://doi.org/10.1093/gim/17.9.1022>

Results

Table 1. Comparison of Baseline Characteristics Between SSRI and Non-SSRI Groups			
a. Cohort with Moderate-to-Moderately Severe Depression		b. Cohort with Severe Depression	
Characteristics	SSRI Only (n = 1,385)	Non-SSRI Only (n = 1,725)	P value
Age (years), Mean ± SD	61.39 ± 14.73	58.27 ± 18.27	<0.001*
Gender			0.03*
Male	479 (35%)	396 (31%)	
Female	906 (65%)	879 (69%)	
Race/Ethnicity			<0.001*
Non-Hispanic White	748 (54%)	684 (54%)	
Non-Hispanic Black	321 (23%)	212 (17%)	
Mexican American	44 (3%)	104 (8%)	
Other Hispanic	132 (10%)	144 (11%)	
Other (e.g., multiracial)	140 (10%)	131 (10%)	
Vigorous Work Activity			<0.001*
No	1147 (82%)	941 (74%)	
Yes	238 (17%)	334 (26%)	
Smoking Status			<0.001*
No	459 (33%)	474 (37%)	
Yes	270 (20%)	296 (23%)	
Missing Data	856 (67%)	505 (40%)	
Self-Reported Hypertension Status			0.024*
No	397 (29%)	417 (31%)	
Yes	988 (71%)	858 (67%)	
Self-Reported Hyperlipidemia Status			<0.001*
No	500 (36%)	447 (35%)	
Yes	885 (64%)	808 (63%)	
Missing Data	0 (0%)	20 (2%)	
Self-Reported Diabetes Status			<0.001*
No	759 (56%)	867 (68%)	
Yes	266 (20%)	375 (29%)	
Borderline	30 (2%)	33 (3%)	
Antipsychotic Medication Use			0.003*
No	1369 (99%)	1240 (97%)	
Yes	16 (1%)	35 (3%)	
Hypothyroidism Medication Use			<0.001*
No	1345 (97%)	1244 (88%)	
Yes	40 (3%)	31 (2%)	
Antidiabetic Medication Use			0.028*
No	1281 (92%)	1206 (95%)	
Yes	104 (8%)	69 (5%)	

Table 2. Adjusted Odds Ratios for Obesity from Multivariable Logistic Regression Analysis			
a. Cohort with Moderate-to-Moderately Severe Depression		b. Cohort with Severe Depression	
Characteristics	Adjusted Odds Ratio	95% CI	P value
Antidepressant Type (Non-SSRI Only/SSRI Only)	Reference		
Age (years)	1.33	1.12 - 1.57	0.003
Gender	0.97	0.87 - 0.98	<0.001
Race/Ethnicity (Non-Hispanic White/Non-Hispanic Black/Mexican American/Other Hispanic/Other)	Reference		
Non-Hispanic White	1.23	1.03 - 1.47	0.025
Non-Hispanic Black	3.45	2.65 - 4.43	<0.001
Non-Hispanic Black	1.13	0.92 - 1.37	0.240
Vigorous Work Activity	Reference		
No	1.34	1.09 - 1.66	0.006
Smoking Status	Reference		
No	0.42	0.33 - 0.54	<0.001
Yes	0.70	0.58 - 0.84	<0.001
Self-Reported Hypertension Status	Reference		
No	1.80	1.47 - 2.19	<0.001
Self-Reported Hyperlipidemia Status	Reference		
No	0.81	0.68 - 0.98	0.030
Self-Reported Diabetes Status (No or Borderline/Yes)	Reference		
No or Borderline	1.97	1.60 - 2.42	<0.001
Antipsychotic Medication Use	Reference		
No	0.85	0.48 - 1.57	0.630
Hypothyroidism Medication Use	Reference		
No	1.18	0.72 - 1.96	0.512
Antidiabetic Medication Use	Reference		
No	1.02	0.70 - 1.48	0.936



Discussion & Conclusion

- Crude analyses** demonstrated an association between antidepressant class and obesity among both the moderate-to-moderately severe and severe depression cohorts (Figure 1). **After adjusting for covariates**, this association remained statistically significant in both groups. In the moderate-to-moderately severe cohort, SSRI use was associated with increased odds of obesity (AOR = 1.33, 95% CI 1.12 - 1.57, p = 0.003; Table 2), and in the severe cohort, SSRI use was associated with approximately 2.5-fold higher odds of obesity (AOR = 2.96, 95% CI 1.47 - 4.44, p < 0.001; Table 2). Significant covariates in both cohorts included self-reported hyperlipidemia and diabetes status.
- The models demonstrated **acceptable to good discrimination** by receiver operating characteristic analysis, with area under the curve values of 0.72 and 0.74 for the moderate-to-moderately severe and severe cohorts, respectively.
- Strengths:** Nationally representative NHANES sampling frame and exposure groups, binomially equivariable identification by PHQ-9 severity multivariable adjustment for covariates.
- Limitations:** Cross-sectional design precludes causal inference; potential confounding by diet, socioeconomic status, lifestyle, NHANES topographic age at 80 years, limiting analyses in older adults, overrepresentation of Non-Hispanic White limiting generalizability.
- Clinical Relevance:** These findings emphasize the importance of considering metabolic factors when selecting antidepressant therapy. SSRI use was associated with increased odds of obesity across both moderate-to-moderately severe and severe depression, with substantially higher odds observed in severe disease. This supports closer monitoring and more individualized treatment decisions.

Third Place - Association Between Antidepressant Class and Obesity Status Across Levels of Depressive Symptom Severity

Kayla Aquilante, Andrew Jones, Nicole Sagias, Sara Yahya

Group 6

Looks at whether the type of antidepressant a person takes is linked to obesity, and whether that relationship changes depending on how severe their depressive symptoms are. The background explains that different antidepressant classes can affect appetite, metabolism, and weight, and that obesity and depression often occur together. The objective is to compare obesity status between people taking SSRIs versus non-SSRIs while accounting for depression severity measured by PHQ-9. In the discussion and conclusion, the authors report that SSRI use was associated with higher odds of obesity in both the moderate-to-moderately severe and severe depression groups, with a much stronger association in the severe group. They conclude that antidepressant choice should consider metabolic risk and that closer monitoring and more individualized treatment may be especially important for patients with more severe depression.

Among Adults with Heart Failure, How do Selective Beta Blockers Compare with Nonselective Beta Blockers in Terms of Heart Failure Related Overnight Hospitalization Rates?

Sarah Alkinani, PharmD Candidate; Anna Carlino, PharmD Candidate; Kaitlyn Clavet, PharmD Candidate; Patrick Ward, PharmD Candidate;

University of Rhode Island, College of Pharmacy

Background

Heart failure (HF) is a major cause of morbidity and mortality worldwide, with hospitalizations representing a significant burden for patients as well as the healthcare system. Beta blockers, one of the most common pharmacological treatments for HF can be categorized as selective versus non-selective, which differs their pharmacologic properties. As selective and additional β -blocking effects¹. While beta blockers are a cornerstone of guideline directed heart failure therapy, it remains unclear whether selective versus non-selective beta blockers differ in effect on heart failure overnight hospitalization rates². Previous studies have evaluated beta blockers as a class in HF treatment, but have not directly compared selective versus nonselective beta blockers in relation to overnight hospitalization in HF patients, representing an important research gap³.

Objectives

Evaluate whether treatment with selective beta blockers compared to non-selective beta blockers is associated with differences in heart failure related overnight hospitalization rates among adults with heart failure.

Methods

- Cross-sectional data was collected from the National Health and Nutrition Examination Survey (NHANES) dataset from 2017 to March 2020. A binary logistic regression was performed to evaluate the association between beta-blocker type and heart failure-related overnight hospitalization. In addition, chi-square tests and independent sample t-tests were used to compare baseline characteristics and outcomes between exposure groups. Analyses were conducted using SPSS 29.0.
- **Inclusion criteria:** Adults 18 years of age or older with heart failure who were using a beta blocker medication (oral and ophthalmic).
- **Exclusion criteria:** Patients who reported use of both selective and nonselective beta blockers, and patients with missing exposure or outcome data.
- **Covariates:** Age, gender, LDL cholesterol, body mass index (BMI), history of heart failure, and other clinical characteristics that could act as confounding variables.
- **Exposure:** Use of a selective beta blocker (atenolol, acebutolol, metoprolol, nebivolol, bisoprolol) compared to nonselective beta blockers (propranolol, nadolol, sotalol, labetalol, carvedilol).
- **Outcome (binary logistic regression):** Presence of overnight hospitalization in patients with HF (defined as patient-reported overnight hospital stay among individuals meeting heart failure symptom criteria based on ICD-10 codes).
- **H₀:** There is no difference in overnight hospitalization between patients using selective beta blockers and nonselective beta blockers.
- **H_a:** There is a statistically significant difference in overnight hospitalization between patients using selective beta blockers and nonselective beta blockers.

Results

Table 1. Patient Demographics and Clinical Characteristics by Exposure Group

Characteristic	Nonselective Beta Blockers (N=363)	Selective Beta Blockers (N=565)	P Value
Age, Years, Mean ± SD	64.69 ± 13.01	67.36 ± 11.21	<0.0001*
Gender			
Female, N (%)	191 (52.6%)	428 (89.4%)	0.0001*
Male, N (%)	172 (47.4%)	418 (90.6%)	
LDL, mg/dL, Median (75%, 75%)	90.20 ± 31.80	90.72 ± 37.06	0.8817
Race			
White, N (%)	186 (80.2%)	428 (89.4%)	
Black, N (%)	122 (33.6%)	116 (24.4%)	
Others, N (%)	10 (2.8%)	22 (2.8%)	0.0881*
BMI, kg/m ² , Mean ± SD	31.87 ± 6.09	31.86 ± 7.18	0.9822
Indications for Prescribing Beta-Blockers			
Hypertension	206 (56.5%)	389 (72.2%)	
Cardiac Arrhythmias and Heart Failure	99 (27.3%)	199 (42.3%)	<0.0001*
Others	56 (15.2%)	76 (15.5%)	

Figure 1 and Table 2. Unadjusted Comparison of Overnight Hospitalization Between Selective and Nonselective Beta-Blocker Groups.

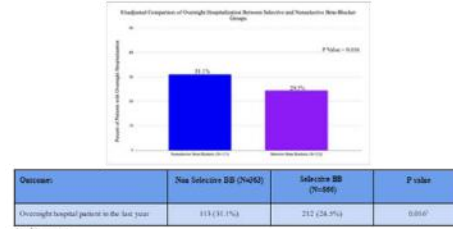


Table 3. Multivariable Logistic Regression Analysis for Overnight Hospitalization

Characteristic	Adjusted Odds Ratio	95% CI	P Value
Nonselective Beta Blockers vs. Selective Beta Blockers	0.78	(0.52-1.08)	0.24
Age, every 10 years older	0.97	(0.91-1.03)	0.71
Female vs. Male	0.83	(0.56-1.23)	0.32
LDL, mg/dL, every 10 mg/dL increase	0.96	(0.90-1.02)	0.68
Race			
Black vs. White	1.47	(0.66-3.29)	0.34
Others vs. White	1.28	(0.46-2.83)	0.32
BMI, every 10 kg/m ²	1.03	(0.93-1.08)	0.60
Indications for Prescribing Beta-Blockers			
Hypertension	Reference		Reference
Cardiac Arrhythmias and Heart Failure	1.38	(0.62-2.98)	0.48
Others	1.32	(0.62-2.98)	0.41

Note: *Statistically Significant (p < 0.05), Unadjusted Comparison

Discussion/Conclusion

- The results suggest that there was a significant difference in overnight hospitalization rates between patients taking nonselective and selective beta blockers in the unadjusted analysis, with higher hospitalization rates observed in the nonselective beta blocker group.
- However, after adjusting for demographic and clinical variables including age, gender, LDL, BMI, race, and heart failure severity, beta blocker selectivity was not significantly associated with overnight hospitalization, suggesting that other patient characteristics may explain the difference seen in the unadjusted analysis.
- Limitations of this study include the cross-sectional study design with no temporality and residual confounding. Overall, beta blocker selectivity did not appear to be an independent predictor of overnight hospitalization, and patient clinical factors may play a larger role in hospitalization risk⁴.

References

1. Braunholtz H, Gattuso J, Gattuso M, et al. Beta-blockers in patients with heart failure and newly diagnosed atrial fibrillation. *Am J Cardiol*. 2018;121(10):1501-1506.
2. National Center for Biotechnology Information. The National Health and Nutrition Examination Survey. <https://www.cdc.gov/nhanes/>
3. Kannel WB, Castelli WP, Castelli WP, et al. Effect of beta-blockers on survival and hospitalization in patients with heart failure and preserved ejection fraction. *Health Aff (Millwood)*. 2018;37(12):2007-2014.
4. Wang H, Wang H, Wang H, et al. Association between beta-blocker selectivity and overnight hospitalization rates in patients with heart failure and preserved ejection fraction. *Circulation*. 2018;138(10):1101-1109.

Among Adults with Heart Failure, How do Selective Beta Blockers Compare with Nonselective Beta Blockers in Terms of Heart Failure Related Overnight Hospitalization Rates?

Sarah Alkinani, Anna Carlino, Kaitlyn Clavet, Patrick Ward

Group 1

Examines whether adults with heart failure who take selective beta blockers have different rates of heart-failure-related overnight hospital stays compared with those taking nonselective beta blockers. The background notes beta blockers are a key treatment for heart failure, but it is unclear if selectivity changes hospitalization risk. In the discussion/conclusion, the authors report that nonselective beta blockers appeared linked to higher hospitalization in the unadjusted comparison, but after accounting for patient differences, beta-blocker selectivity was not an independent predictor; they conclude other clinical factors likely play a larger role.

Association Between Serum Cotinine Levels and Systemic Inflammation Among Self-Reported Non-Smoking Adults

Ava Scarpaci, PharmD Candidate, Griffin Geist, PharmD Candidate, Hailey Joo, PharmD Candidate, Ramez Rizk, PharmD/MS Candidate
University of Rhode Island College of Pharmacy, Kingston, RI



Background

Cotinine, the primary metabolite of nicotine, is the gold standard biomarker of recent nicotine exposure from active or secondhand smoke.¹ Smoking status is often measured by self-report, but self-report may underestimate true exposure.² Prior studies have mainly focused on validating self-reported smoking or on inflammation in smokers and secondhand smoke exposure more broadly. Less is known about whether self-reported non-smoking adults with detectable cotinine also have higher high-sensitivity C-reactive protein (hs-CRP), a biomarker of systemic inflammation linked to future cardiovascular risk.³ This subgroup may represent a hidden at-risk population that is missed when smoking status is based on self-report alone.

Objectives

To examine whether elevated serum cotinine levels among self-reported non-smoking adults are associated with elevated hs-CRP compared with those with undetectable cotinine.

Methods

Design and Data Source: Cross-sectional study using data from the National Health and Nutrition Examination Survey (NHANES), a nationally representative survey of the U.S. civilian, noninstitutionalized population (2017 to March 2020).⁴

Inclusion Criteria: Adults aged ≥18 years who self-reported not smoking and had available serum cotinine and hs-CRP data.

Exclusion: Participants reporting current smoking or with missing data on serum cotinine levels or hs-CRP.

Exposure: Serum cotinine categorized as undetectable (<0.05 ng/mL) and detectable cotinine (>0.05 ng/mL), which was classified as low/moderate (0.05-0.215 ng/mL), and high (>0.215 ng/mL), with undetectable cotinine as reference group.

Outcome: Elevated high-sensitivity C-reactive protein (hs-CRP), defined as >3 mg/L, a clinically established threshold indicating higher systemic inflammation and cardiovascular risk.⁵

Covariates: Age, sex, race/ethnicity, body mass index, diabetes mellitus, high cholesterol, and hypertension were included as adjustment variables in regression models. Education level and ratio of family income to poverty were also included to examine differences in socioeconomic characteristics.

Statistical analysis: Baseline characteristics were compared using independent-samples t-tests for continuous variables and chi-square tests for categorical variables (Table 1). Elevated hs-CRP across cotinine exposure groups was compared using chi-square tests, and the Cochran-Armitage trend test assessed linear trend across ordered exposure levels (Table 2, Figure 1). Multivariable logistic regression estimated adjusted odds ratios with 95% confidence intervals while controlling for confounders (Table 3). All analyses were conducted using SPSS version 29.0. P-value < 0.05 was considered statistically significant.

Results

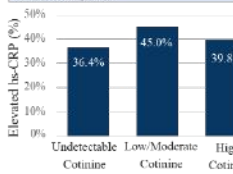
Table 1: Baseline Demographic and Clinical Characteristics: Undetectable vs Low/Moderate vs High Cotinine*

Variable	Undetectable	Low/Moderate	High	p-value
Age, mean ± SD	61.69 ± 15.42	57.73 ± 15.87	50.69 ± 17.83	<0.001 [†]
Sex, n (%)				0.021 [†]
Male	684 (60.1%)	147 (55.9%)	337 (65.5%)	
Female	454 (39.9%)	116 (44.1%)	177 (34.4%)	
Race, n (%)				<0.001 [†]
Mexican American	157 (13.8%)	23 (8.7%)	43 (8.4%)	
Other Hispanic	128 (11.2%)	24 (9.1%)	25 (4.9%)	
Non-hispanic White	568 (49.9%)	102 (38.8%)	228 (44.4%)	
Non-hispanic Black	155 (13.6%)	81(30.8%)	146 (28.4%)	
Other race	130 (11.4%)	33 (12.5%)	72 (14.0%)	
BMI, mean ± SD	30.63 ± 7.00	32.87 ± 8.02	30.58 ± 7.38	<0.001 [†]
Hypertension n (%)	592 (52.0%)	133 (50.6%)	211 (41.1%)	<0.001 [†]
Diabetes n (%)	266 (22.8%)	64 (24.3%)	90 (17.5%)	0.011 [†]
High Cholesterol n (%)	591 (51.9%)	117 (44.5%)	178 (34.6%)	<0.001 [†]
Education level, n (%)				<0.001 [†]
Less than 12 th grade or without diploma	217 (19.1%)	58 (22.1%)	104 (20.2%)	
High school graduate/GED or equivalent	247 (21.7%)	70 (26.6%)	158 (30.7%)	
Some college or AA degree	375 (33.0%)	99 (37.6%)	187 (36.4%)	
College graduate or above	296 (26.0%)	34 (12.9%)	58 (11.3%)	
Ratio of family income to poverty, mean ± SD	2.97 ± 1.57	2.22 ± 1.48	2.37 ± 1.53	<0.001 [†]

*Undetectable, low/moderate, and high cotinine were defined as <0.05 ng/mL, 0.05-0.215 ng/mL, and >0.215 ng/mL, serum cotinine, respectively.
[†]Variables from one-way ANOVA for continuous variables. [†]P-values from chi-square test for categorical variables.
 Results: Participants with higher cotinine exposure were younger (p<0.001). Most differed significantly across groups (p<0.001), with the highest values observed in the low-to-moderate exposure group. Cotinine exposure also differed significantly by sex, race/ethnicity, education level, hypertension, diabetes, high cholesterol, and family income to poverty rate.

Table 2/Figure 1: Unadjusted Comparison of Elevated hs-CRP by Cotinine Exposure Levels

Cotinine Exposure	Elevated hs-CRP*	Non-Elevated hs-CRP*	Total	p-value
Undetectable Cotinine (<0.05 ng/mL)	410 (36.4%)	716 (63.6%)	1126	0.011 [†]
Low/moderate Cotinine levels (0.05-0.215 ng/mL)	116 (45.0%)	142 (55.0%)	258	0.17 [†]
High Cotinine Levels (>0.215 ng/mL)	203 (39.8%)	307 (60.2%)	510	0.19 [†]
Overall Comparison			1894	0.03 [†]



*Elevated and non-elevated hs-CRP is defined as >3 mg/L and ≤3 mg/L, respectively.
 1. Pairwise chi-square test: undetectable vs low/moderate cotinine.
 2. Pairwise chi-square test: low/moderate vs high cotinine.
 3. Pairwise chi-square test: undetectable vs high cotinine.
 4. Overall chi-square test across all cotinine groups: $\chi^2(2) = 6.99, p = 0.03$

Results: The prevalence of elevated hs-CRP differed across cotinine groups: undetectable (36.4%, n=410), low/moderate (45.0%, n=116), and high (39.8%, n=203). The overall chi-square test was significant ($\chi^2(2) = 6.99, p = 0.03$). Pairwise comparisons showed that only the difference between the undetectable and low/moderate cotinine groups was statistically significant ($p = 0.011$). The Cochran-Armitage trend test was not significant ($Z = 1.62, p = 0.11$), indicating no significant linear trend across ordered cotinine exposure levels.

Table 3: Results of Multivariable Logistic Regression Analyses for Elevated hs-CRP

Cotinine Exposure	Adjusted* odds ratio (95% CI)	p-value
Undetectable Cotinine (<0.05 ng/mL)	Reference	—
Detectable Cotinine (>0.05 ng/mL)	1.261 (1.006-1.581)	0.044
Undetectable Cotinine (<0.05 ng/mL)	Reference	—
Low/moderate Cotinine levels (0.05-0.215 ng/mL)	1.159 (0.845 - 1.589)	0.360
High Cotinine Levels (>0.215 ng/mL)	1.325 (1.022 - 1.719)	0.034

*Adjusted for age, sex, race/ethnicity, body mass index, diabetes mellitus, high cholesterol, and hypertension.
 Results: Detectable cotinine was associated with higher adjusted odds of elevated hs-CRP compared with no detectable cotinine (aOR=1.261). High cotinine was associated with higher adjusted odds of elevated hs-CRP compared with no detectable cotinine (aOR=1.325), whereas low/moderate cotinine was not significantly associated with elevated hs-CRP compared with no detectable cotinine (aOR=1.159). Both logistic regression models demonstrated acceptable fit based on the Hosmer-Lemeshow goodness-of-fit test, with $\chi^2=535, df=8, p=0.960$ and $\chi^2=5.882, df=8, p=0.694$, respectively.

Discussion

In the unadjusted comparisons, the pattern was not strictly linear, since the only significant pairwise difference was between the undetectable and low/moderate groups and the Cochran-Armitage trend test was not significant. However, after adjustment for key covariates, detectable cotinine was associated with higher odds of elevated hs-CRP, and the strongest adjusted association was observed in the high-cotinine group.

These findings are supported by related, though not directly comparable, studies showing that secondhand smoke exposure has been associated with higher inflammatory markers in other populations, including never-smokers, nonsmoking youth, and occupational cohorts. There are also prior reports of higher CRP among never-smokers exposed to secondhand smoke, as well as elevated inflammatory biomarkers in cotinine-exposed workers and youth.

The association is biologically plausible because tobacco-smoke exposure, including secondhand exposure, has been linked to inflammation, oxidative stress, and endothelial dysfunction.⁶ Cotinine should be interpreted primarily as an objective exposure biomarker that identifies recent nicotine exposure rather than the sole causal mediator.

Strengths include use of different levels of serum cotinine rather than a binary comparison alone, use of a clinically significant measure of inflammation (hs-CRP), a large nationally representative NHANES sample, and multivariable adjustment for major demographic and clinical covariates.

Limitations include the cross-sectional design, possible residual confounding (exposure duration, environment, stress), no separate classification of former smokers, possible influence of recent acute inflammatory illness on hs-CRP, and reliance on a single cotinine measurement that reflects recent rather than long-term exposure.

Conclusion

Among self-reported non-smoking adults, detectable cotinine was associated with elevated hs-CRP, with the strongest association observed in the high cotinine group. These findings suggest a potential concentration-response relationship that should be further investigated and indicate that objective nicotine exposure assessment may identify hidden inflammatory risk not captured by self-report alone.

References

1. Benowitz NL. Cotinine as a biomarker of environmental tobacco smoke exposure. *Epidemiol Rev*. 1996;18(2):188-204. doi:10.1093/epir/kw075
2. Vandenberg E, Seegal T, Blumstein P, Pech P. Validation of self-reported smoking by urine cotinine measurement in a community-based study. *J Epidemiol Community Health*. 2002;56(1):67-70. doi:10.1093/epk/c1187
3. Pransky GA, Mrazek DA, Alexander EW, et al. Median of inflammation and cardiovascular disease: application to chronic and periodic health practice. *J Intern Med*. 2010;267(1):1-10. doi:10.1111/j.1365-2796.2009.02407.x
4. Vennart S, Oishi J, Corral JC, et al. National Health and Nutrition Examination Survey 2007 March 2009 representative data file development of files and procedure manuals for selected health outcomes. *Natl Health Stat Report*. 2012;11(8):1-23.
5. U.S. Department of Health and Human Services. The Health Consequences of Smoking: 40 Years of Progress: A Report of the Surgeon General. U.S. Department of Health and Human Services, Centers for Disease Control and Prevention, National Center for Chronic Disease Prevention and Health Promotion, Office on Smoking and Health, 2014.

Association Between Serum Cotinine Levels and Systemic Inflammation Among Self-Reported Non-Smoking Adults

Ava Scarpaci, Griffin Geist, Hailey Joo, Ramez Rizk

Group 2

Explores adults who say they do not smoke, but may still be exposed to nicotine (for example through secondhand smoke). The background explains that cotinine is a reliable blood marker of recent nicotine exposure, and that relying on self-reported non-smoking can miss people with real exposure. The objective is to see whether non-smokers with detectable cotinine also have higher levels of hs-CRP, a marker of body-wide inflammation linked to future cardiovascular risk. In the discussion and conclusion, the authors report that detectable cotinine was associated with higher odds of elevated hs-CRP, with the strongest association in the higher-cotinine group. They conclude that objective cotinine testing may help identify a “hidden” group of self-reported non-smokers with higher inflammation risk that would not be recognized using self-report alone.

Association Between SGLT2 Inhibitor or DPP-4 Inhibitor Use and PHQ-9-Measured Patient-Reported Depression Compared With Metformin in Adults With Type 2 Diabetes Mellitus

Authors: Ian Algozzine, Kierra Marcelino, Alyssa Perry, Victoria Silva
University of Rhode Island, College of Pharmacy

Background

Sodium-glucose co-transporter 2 inhibitors (SGLT2i's) and dipeptidyl peptidase-4 inhibitors (DPP-4i's) are commonly used in the treatment of type 2 diabetes mellitus (T2DM) after metformin; however, their effects on mental health remain unclear. This is an important area of study because T2DM is associated with an increased risk of depression, which may negatively impact medication adherence and glycemic control.¹⁻⁵

Objective

Evaluate the association between SGLT2i or DPP-4i use and patient-reported depression outcomes (PHQ-9 scores) compared to metformin in adults with T2DM.

Methods

Data Source: National Health and Nutrition Examination Survey (NHANES) 2017–2020 cycles, a nationally representative survey of U.S. adults conducted by the National Center for Health Statistics (NCHS).

Study Design & Cohort: Cross-sectional study including adult participants (>18 years) with T2DM. The final cohort consisted of 1,050 individuals, with 896 patients receiving metformin (reference group) and 164 patients receiving SGLT2i's or DPP-4i's. Patients using both exposure medications and metformin concurrently were excluded. Additional exclusions included missing PHQ-9 data where applicable.

Exposure: Exposure was defined as adult participants (>18 years) with T2DM taking SGLT2i's (canagliflozin, dapagliflozin, empagliflozin, ertugliflozin) or DPP-4i's (sitagliptin, saxagliptin, linagliptin, alogliptin), compared to those taking metformin alone.

Outcome Assessment: The primary outcome assessed was overall depression, defined as a Patient Health Questionnaire-9 (PHQ-9) score ≥ 5 .

Covariates included: Measured covariates included age, gender, body mass index (BMI), hypertension (HTN), and high low-density lipoprotein cholesterol (LDL-C).

Statistical Analysis:

- Continuous variables (PHQ-9, age, BMI) were analyzed using independent t-tests
- Categorical variables (depression, gender, HTN, LDL-C) were analyzed using chi-square tests
- Multivariable logistic regression was used to adjust for age, gender, BMI, HTN, and LDL-C

Conclusion/Discussion

Discussion: This study evaluated the association between SGLT2i's or DPP-4i's and depression compared to metformin in adults with T2DM. While PHQ-9 scores and depression prevalence showed no significant differences, the exposure group had slightly higher mean scores. Additionally, female sex and higher BMI were associated with increased odds of depression.

Biological Plausibility: Biologically, these findings are plausible. SGLT2i's and DPP-4i's may influence inflammatory and metabolic pathways linked to depression. Improved glycemic control may reduce systemic inflammation, but these effects may be limited. In contrast, patient-specific factors such as BMI and sex may play a larger role in depression risk.^{6,7}

Strengths: This study used a nationally representative NHANES dataset, improving generalizability. The use of validated PHQ-9 scoring strengthens assessment of depression outcomes, and regression models accounted for key confounders.

Limitations: Cross-sectional design limits causality. Residual confounding and self-reported depression may affect results. Residual confounders include smoking, statin use, antidepressant use, medication adherence, lifestyle factors, undiagnosed psychiatric illness, stress surrounding diabetes, race, ethnicity, serum blood glucose levels, A1c levels, and social support. Additionally, medication exposure was assessed at a single time point, and the smaller sample size in the SGLT2i's and DPP-4i's group may have limited statistical power.

Conclusion: SGLT2i's or DPP-4i's were not significantly associated with depression compared to metformin. Depression risk in this population may be more strongly influenced by patient characteristics such as sex and BMI. Further studies with larger sample sizes are needed to confirm these findings.

Results

Percentage of Depression by Treatment Group

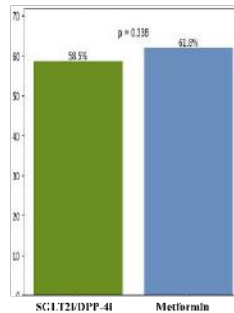


Table 1. Comparing Demographic and Clinical Characteristics between Exposure Groups

Characteristics	SGLT2* inhibitors or DPP-4* inhibitors N = 164	Metformin N = 896	P Value
Age, years	Mean \pm SD 63.95 \pm 11.45	61.62 \pm 12.91	0.031 [†]
Gender	Female, N 73 (44.5%) Male, N 91 (55.5%)	421 (47.0%) 475 (53.0%)	0.610 [‡]
Hypertension	Yes, N 116 (70.7%) No, N 48 (29.3%) Unknown, N 0 (0%)	608 (67.9%) 281 (31.4%) 4 (0.4%)	0.579 [‡]
High LDL-C*	Yes, N 0 (0%) No, N 72 (43.9%) Missing, N 92 (56.1%)	3 (0.3%) 422 (47.1%) 471 (52.6%)	0.60 [‡]
BMI ^{††} , kg/m ²	Mean \pm SD 32.01 \pm 7.71	32.90 \pm 7.70	0.192 [‡]

Note:
Student T-Test[†], Chi-square test[‡]
High LDL cholesterol was defined as values \geq 200 mg/dL
Normal LDL cholesterol was defined as values from 0-199 mg/dL
*SGLT2: Sodium-Glucose Co-Transporter 2
*DPP-4: Dipeptidyl peptidase-4
*LDL-C: Low Density Lipoprotein Cholesterol
*BMI: Body Mass Index

Table 2. Raw Comparison of Outcomes between Exposure Groups

Outcomes	SGLT2* inhibitors and DPP-4* inhibitors N = 164	Metformin N = 896	P Value
PHQ-9 Score	Mean \pm SD 4.13 \pm 4.65	3.74 \pm 4.80	0.270 [†]
PHQ-9 Level	Depression, N (%) 96 (58.5) No depression, N (%) 68 (41.5) Missing, N (%) 22 (13.4)	554 (61.8) 229 (24.9) 112 (12.3)	0.338 [‡]

Note:
Student T-Test[†], Chi-square test[‡]
*PHQ-9 Patient Health Questionnaire-9
*SGLT2: Sodium-Glucose Co-Transporter 2
*DPP-4: Dipeptidyl peptidase-4

Table 3. Results of Multivariable Logistic Regression Analyses for the Risk of Depression

Characteristics	Adjusted Odds Ratio	95% CI
SGLT2* inhibitors or DPP-4* inhibitors vs metformin	1.644	(0.907 - 2.981)
Age, years (per 1 year increase)	0.981	(0.963 - 1.000)
Female vs. Male	2.004	(1.287 - 3.120)
Presence of Hypertension	0.465	(0.276 - 0.784)
BMI ^{††} (per 1 kg/m ² increase)	1.063	(1.032 - 1.095)

Note:
*SGLT2: Sodium-Glucose Co-Transporter 2
*DPP-4: Dipeptidyl peptidase-4
*BMI: Body Mass Index

References

- Guo M, Salmeron JJ, Yankov N, et al. Investigating the Influence of Antidiabetic Medications and Psychosocial Factors. *Cureus*. 2024;16(5):e20270. Published 2024 May 14. doi:10.7759/cureus.60270
- Esokor SA, Mensah BO, Schmittlieb JA, et al. Comparative safety of glucose-lowering medications on depression in adults with type 2 diabetes. *Diabetes Obes Metab*. 2026;29(3):2215-2226. doi:10.1111/dsm.17815
- Gamble JM, Chikrov E, McFadden WK, Twiss LR, Majumder SR. Examining the risk of depression or self-harm associated with incretin-based therapies used to manage hyperglycemia in patients with type 2 diabetes: a cohort study using the UK Clinical Practice Research Datalink. *BMJ Open*. 2018;8(10):e023830. Published 2018 Oct 8. doi:10.1136/bmjopen-2018-023830
- Watts Anderson JK, Ockene JK, Sengstack M, Bingham J, Wilms-Anderson MK. Diabetes, antidiabetic medications and risk of depression - A population-based cohort and nested case-control study. *Psychosomatic Medicine*. 2022;140:105775. doi:10.1093/psyc/2022.105775
- Mansoor A, Dehdar Najm Abul A, Ezzam E, et al. Association of antidiabetic medications with psychiatric disorders in patients with type 2 diabetes: a cross-sectional study. *Int J Med Res*. 2023;52(1):675. Published 2023 May 22. doi:10.1186/s12916-025-02877-2

Association Between SGLT2 Inhibitor or DPP-4 Inhibitor Use and PHQ-9-Measured Patient-Reported Depression Compared With Metformin in Adults With Type 2 Diabetes Mellitus

Ian Algozzine, Kierra Marcelino, Alyssa Perry, Victoria Silva

Group 3

Analyzes adults with type 2 diabetes and examines whether taking an SGLT2 inhibitor or a DPP-4 inhibitor is linked to different patient-reported depression outcomes compared with taking metformin. The background explains that these diabetes medicines are commonly used after metformin, but their mental health effects are not clear, and depression is an important concern in type 2 diabetes because it can affect medication use and blood sugar control. In the discussion, the authors report that PHQ-9 scores and the overall rate of depression did not differ significantly between the treatment groups, although the SGLT2/DPP-4 group had slightly higher average scores. They also note that factors like being female and having a higher BMI were associated with higher odds of depression. The conclusion is that SGLT2 inhibitors or DPP-4 inhibitors were not significantly associated with depression compared with metformin, and that patient characteristics may matter more; they recommend larger studies to confirm the findings.

Background

Depression is a common comorbidity in individuals with diabetes and is associated with worse clinical outcomes, including reduced medication adherence and poorer glycemic control.¹ Prior literature demonstrates that depression is more prevalent in individuals with diabetes compared to those without,^{2,3} and that this relationship is likely bidirectional with each condition potentially exacerbating the other over time.⁴ While the coexistence of these conditions is well established, less is known about how different diabetes treatment strategies may influence depressive symptom burden.⁵ In particular, comparative data between insulin and metformin therapy remain limited. Understanding these differences may help inform treatment selection and improve both metabolic and mental health outcomes.

Objectives

To evaluate the association between diabetes treatment (insulin vs metformin) and depressive symptoms, measured as the odds of depression (PHQ-9 ≥5), among adults with comparable glycemic control.

Methods

Data Source: Data was obtained from National Health and Nutrition Examination Survey (NHANES) data from January 2017 to March 2020.

Study Design: Cross-sectional study of adults aged 18-65 with a self-reported diagnosis of diabetes.

Exposure: Diabetes treatment type, defined as patients taking insulin (rapid, biphasic, glargine, NPH, isophane, regular, glargine, detemir, or degludec) was compared to a comparison group of patients taking metformin to treat diabetes.

Inclusion Criteria: Adults aged 18-65 diagnosed with diabetes, as told by their doctor, taking either insulin or metformin with a hemoglobin A1c between 7-8%. An A1c range of 7-8% was selected to represent patients with moderately controlled diabetes, allowing for comparison between treatment groups while minimizing confounding from greater disease severity.

Exclusion Criteria: Patients taking both insulin and metformin, taking an antidepressant medication, or with incomplete PHQ-9 data were excluded. Sample sizes may vary due to missing data.

Outcome Assessment: The primary outcome was incidence of depression, which was assessed using a Patient Health Questionnaire (PHQ-9) score ≥5, which indicates mild depression.

Covariates: age, A1c level, antidepressant use, other medication use, depression diagnosis, BMI, sex, race.

Statistical Analysis: Differences in groups were assessed using chi-square tests for categorical variables and t-tests for continuous variables. Multivariable logistic regression was used to evaluate the association between treatment type and depressive symptoms, while adjusting for age, BMI, sex, and race. Results were reported as odds ratios with 95% confidence intervals, with statistical significance defined as p < 0.05. A1c was not retained in the final multivariable model due to lack of significance and model refinement. All analyses were conducted using SPSS version 29.0.

References

1. Lantieri PL, Chou SS. Depressive risks predict the relationship between mental and glycemic control. *Diabetes Care*. 2007; 30(12):2015-2016. doi:10.2337/dc07-1500
2. Wang J, Zhou F, Kishimoto M, et al. Prevalence of depression in patients with type 2 diabetes mellitus: a cross-sectional study. *Diabetes Care*. 2003; 26(12):2015-2016. doi:10.2337/dia2003-12-0900
3. Wang J, Zhou F, Kishimoto M, et al. Prevalence of depression in patients with type 2 diabetes mellitus: a cross-sectional study. *Diabetes Care*. 2003; 26(12):2015-2016. doi:10.2337/dia2003-12-0900
4. Wang J, Zhou F, Kishimoto M, et al. Prevalence of depression in patients with type 2 diabetes mellitus: a cross-sectional study. *Diabetes Care*. 2003; 26(12):2015-2016. doi:10.2337/dia2003-12-0900
5. Wang J, Zhou F, Kishimoto M, et al. Prevalence of depression in patients with type 2 diabetes mellitus: a cross-sectional study. *Diabetes Care*. 2003; 26(12):2015-2016. doi:10.2337/dia2003-12-0900

Results

Table 1. Comparing Demographic and Clinical Characteristics between Insulin and Metformin Users

Characteristic	Insulin (N=83)	Metformin (N=234)	P-value
Age (Mean ± SD)	55.22 ± 7.34	55.26 ± 7.62	0.96 ¹
Female N (%)	33 (39.8%)	94 (40.2%)	0.96 ²
BMI (Mean ± SD)	36.01 ± 5.22	33.41 ± 9.05	0.055 ¹
Hemoglobin A1c (%)	7.57 ± 0.36	7.43 ± 0.31	0.003 ¹
Race/Ethnicity N (%)			< 0.001 ²
White Non-Hispanic	24 (28.9%)	46 (19.7%)	
Black Non-Hispanic	41 (49.4%)	79 (33.8%)	
Mexican American			
Other Hispanic	15 (18%)	50 (21.4%)	
Other	3 (3.6%)	59 (25.2%)	
Education N (%)			< 0.001 ²
< 9th	0 (0%)	20 (8.5%)	
9th-11th	13 (15.7%)	22 (9.4%)	
HS/GED	37 (44.8%)	56 (23.8%)	
Some college	22 (26.5%)	78 (33.3%)	
College grad	11 (13.3%)	59 (25.2%)	

¹Independent T-test

²Chi-square test

Table 2. Comparing Frequencies of Depression between Insulin and Metformin Users

Outcome	Insulin (N=73)	Metformin (N=220)
Depression (PHQ-9 ≥ 5), N (%)		
Yes	24 (32.9%)	32 (14.5%)
No	49 (67.1%)	188 (85.5%)

Table 3. Results of Multivariable Logistic Regression Analysis

Characteristic	Adjusted Odds Ratio (95% CI)	P-value
Insulin vs Metformin (Reference)	2.22 (1.02-4.83)	0.044 ³
Age (per year)	0.98 (0.93-1.03)	0.387 ³
BMI	2.35 (1.15-4.80)	0.019 ³
Gender (Male vs Female)	2.47 (1.21-5.04)	0.011 ³
Race (Reference: White)		0.035 ³
Mexican American	0.21 (0.03-1.38)	
Other Hispanic	1.14 (0.15-8.85)	
Non-Hispanic Black	2.68 (0.84-8.55)	
Other	1.13 (0.37-3.44)	
Education Level (Reference: Highest)		
< 9th	8.89 (0.95-83.54)	0.056 ³
9th-11th	13.45 (2.32-77.99)	0.004 ³
HS/GED	4.76 (1.18-19.13)	0.028 ³
Some college	4.78 (1.21-18.85)	0.025 ³

³Wald's statistics. Reference (reference) = Fresh graduate. Adjusted Odds Ratio (95% confidence interval) = Adjusted Odds Ratio (95% confidence interval).

Figure 1: Unadjusted Prevalence of Depressive Symptoms by Diabetes Treatment

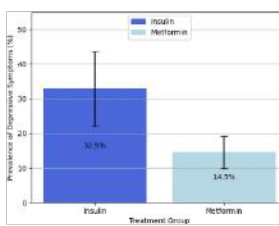
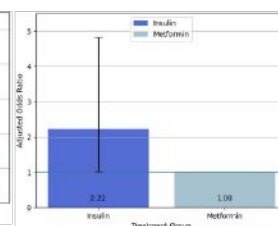


Figure 2: Adjusted Odds of Depressive Symptoms by Diabetes Treatment



Discussion/Conclusion

Consistency with prior literature: Our findings align with existing literature demonstrating a strong association between diabetes and depression. Insulin use was associated with higher adjusted odds of depressive symptoms compared with metformin use.

Biological plausibility: This association may reflect greater disease severity among insulin users, as well as increased treatment burden related to injectable therapy and risk of hypoglycemia, all of which may negatively impact mental health.

Strengths and limitations: Strengths include use of a large, nationally representative NHANES dataset, focusing on patients with similar A1c levels to improve comparability, and using the validated PHQ-9 tool to measure depression. We also adjusted for important factors like age, sex, BMI, and race. Limitations include the cross-sectional design, so we cannot say insulin causes higher depression risk, reliance on self-reported data which may not always be accurate, and missing factors like duration of diabetes, lifestyle, medication adherence, or socioeconomic status that could affect results. Excluding patients on antidepressants limit how well results apply to all patients. Insulin response was not limited to basal insulin due to NHANES data constraints.

Conclusions: Insulin use was associated with more than **two fold higher odds** of depressive symptoms compared to metformin among adults with diabetes and similar glycemic control. Baseline differences in race/ethnicity and education level were statistically significant between groups and were included as covariates. More research is needed to confirm this relationship and understand why it occurs.

Depressive Symptoms in Adults With Diabetes: Insulin vs Metformin

Jeff Draper, Alexa Roderick, Amanda Sherwood, Urba Uzzaman

Group 4

Investigates depression symptoms in adults with diabetes and compares people treated with insulin versus metformin. The background explains that depression is common in diabetes and can worsen outcomes, but it is less clear whether different diabetes treatments relate to differences in depression symptoms. The objective is to test whether treatment type (insulin vs metformin) is associated with depressive symptoms measured using the PHQ-9. In the discussion and conclusion, the authors report that insulin use was associated with higher odds of depressive symptoms compared with metformin among adults with similar blood sugar control. They suggest this may be related to greater illness severity and the added burden of injectable therapy and hypoglycemia risk. They note that the study cannot prove cause and effect and may miss other factors that influence depression, but conclude that insulin users may have higher risk and that more research is needed to confirm and explain the relationship.



Association Between Statin Type (Atorvastatin vs. Rosuvastatin) and Glycemic Status in U.S. Adults: A Cross-Sectional Analysis of NHANES

THE UNIVERSITY OF RHODE ISLAND COLLEGE OF PHARMACY

Jamie Brienza, Julia Ho, Amy LeBrun, Andrew Salama
University of Rhode Island, College of Pharmacy, Kingston, RI

Background

Status are widely prescribed for cardiovascular risk reduction but have been associated with dysglycemia and an increased risk of incident diabetes. Prior studies have primarily focused on binary outcomes such as new-onset diabetes or cardiovascular events rather than evaluating HbA1c across clinically relevant categories normal, prediabetes, and diabetes.¹⁻² Furthermore, existing studies often evaluate statins as a class rather than directly comparing individual agents, and glycemic outcomes are frequently not the primary focus.^{3,4} Hospital-based data also suggest increased diabetes risk with rosuvastatin exposure; however, HbA1c categories and statin comparisons were not assessed.⁵ Likewise, smaller cohort and non-U.S. studies suggest potential worsening glycemic control with statin use but lack generalizability and head-to-head comparisons between specific statins.⁶⁻⁸ Overall, there is limited nationally representative U.S. data examining whether glycemic status differs by statin type. Therefore, this study aims to evaluate differences in HbA1c category distribution between atorvastatin and rosuvastatin using NHANES data.

Objectives

Primary Objective:

To evaluate whether HbA1c category distribution of normal, prediabetes, or diabetes differs between atorvastatin and rosuvastatin users in a nationally representative U.S. sample (NHANES 2017–March 2020).

Null Hypothesis (H₀):

There is no difference in HbA1c category distribution between atorvastatin and rosuvastatin users.

Methods

Data Source

- Cross-sectional data from the 2017–March 2020 National Health and Nutrition Examination Survey (NHANES), a nationally representative survey of the U.S. civilian non-institutionalized population.
- Prescription medication files were used to identify statin exposure.

Study Design and Population

- Cross-sectional study comparing HbA1c category distribution between statin groups.
- Inclusion: Adults using atorvastatin or rosuvastatin with a valid HbA1c measurement.
- Exclusion: Non-statin users and participants with missing HbA1c or statin exposure data.

Exposure and Outcome

- **Exposure:** Statin type (rosuvastatin vs atorvastatin) identified from NHANES prescription data.
 - Rosuvastatin was used as the reference group in regression analyses.
 - **Outcome:** HbA1c categorized as: normal <5.7% (0), prediabetes 5.7–6.4% (1), and diabetes >6.5% (2)
- Covariates:** Age, sex, BMI (dichotomized as normal/underweight and overweight/obese), and race/ethnicity (Non-Hispanic White, Non-Hispanic Black, Other)

Statistical Analysis

- Baseline characteristics compared using chi-square or Fisher's exact test for categorical variables and Mann-Whitney U test for continuous variables.
- HbA1c category distribution compared using chi-square test.
- Two separate multivariable binary logistic regression models were conducted:
 - Pre-diabetes vs normal
 - Diabetes vs normal
- Models adjusted for age, sex, BMI, and race/ethnicity.
- Analyses performed using SPSS 29.0.
- Statistical significance set at p<0.05.

1. Tang ET, et al. Cardiovascular outcomes associated with statin therapy. *Cardiovasc Diabetol*. 2017;16(1):1-11.
 2. Gao H, et al. Association between statin use and incident diabetes: a meta-analysis. *Diabetologia*. 2018;61(10):1805-1814.
 3. Rosuvastatin vs atorvastatin: a randomized controlled trial of cardiovascular outcomes in patients with hypercholesterolemia. *Circulation*. 2017;135(10):1111-1121.
 4. Rosuvastatin vs atorvastatin: a randomized controlled trial of cardiovascular outcomes in patients with hypercholesterolemia. *Circulation*. 2017;135(10):1111-1121.
 5. Ho J, et al. Association between statin use and incident diabetes: a meta-analysis. *Diabetologia*. 2018;61(10):1805-1814.
 6. Ho J, et al. Association between statin use and incident diabetes: a meta-analysis. *Diabetologia*. 2018;61(10):1805-1814.
 7. Ho J, et al. Association between statin use and incident diabetes: a meta-analysis. *Diabetologia*. 2018;61(10):1805-1814.
 8. Ho J, et al. Association between statin use and incident diabetes: a meta-analysis. *Diabetologia*. 2018;61(10):1805-1814.

Results

Table 1. Comparing Demographic and Clinical Characteristics Between Statin Groups

Covariates	Rosuvastatin (n=188)	Atorvastatin (n=379)	P Value
BMI			0.621 ¹
Normal/Underweight, N (%)	114 (17.4%)	145 (16.2%)	
Overweight/Obese, N (%)	159 (82.4%)	752 (83.8%)	
Gender			0.396 ²
Male, N (%)	114 (33.8%)	169 (37.8%)	
Female, N (%)	99 (66.2%)	130 (33.9%)	
Race			0.556 ³
Non-Hispanic White, N (%)	90 (42.5%)	199 (39.9%)	
Non-Hispanic Black, N (%)	57 (26.9%)	25 (2.9%)	
Other, N (%)	65 (30.7%)	245 (34.5%)	
Age, years (Mean ± SD)	67.75 ± 6.724	65.20 ± 6.352	0.042 ⁴

Table 2. Comparing HbA1c Category Distribution Between Statin Groups

HbA1c Category	Rosuvastatin (n=188)	Atorvastatin (n=379)	P Value
Normal (<5.7%), N (%)	52 (27.7%)	214 (24.1%)	0.415
Prediabetes (5.7–6.4%), N (%)	75 (39.9%)	210 (31.7%)	
Diabetes (>6.5%), N (%)	61 (32.4%)	125 (37.0%)	

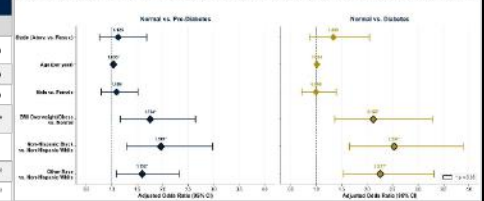
Table 3. Results of Multivariable Binary Logistic Regression

Characteristics	Pre-diabetes vs. Normal		Diabetes vs. Normal	
	Adj. OR	95% CI	Adj. OR	95% CI
Statin (Atorvastatin vs Rosuvastatin)	1.125	(0.751–1.687)	1.215	(0.872–2.014)
Age (years)	1.033	(1.018–1.049)*	1.014	(1.008–1.036)
Male vs. Female	1.189	(0.758–1.505)	0.998	(0.714–1.394)
BMI (Overweight/Obese vs. Normal/Underweight)	1.781	(1.161–2.699)*	2.122	(1.369–3.291)*
Race/Ethnicity (vs. Non-Hisp. White)				
Non-Hispanic Black	1.961	(1.208–2.964)*	2.510	(1.649–3.802)*
Other	1.592	(1.091–2.242)*	2.277	(1.516–3.319)*

Figure 1. HbA1c Category Distribution: Rosuvastatin vs. Atorvastatin



Figure 2. Forest Plot of Adjusted Odds Ratios from Multivariable Binary Logistic Regression



Discussion/Conclusion

Consistency of Results with Prior Literature

There was no statistically significant difference in HbA1c category distribution between atorvastatin and rosuvastatin users ($\chi^2=1.018$, $p=0.415$). After multivariable adjustment, statin type remained non-significant for both prediabetes (OR 1.125, 95% CI 0.751–1.687) and diabetes (OR 1.215, 95% CI 0.872–2.014), reinforcing comparable glycemic effects across statins. These findings align with prior literature suggesting that statins have similar glycemic effects as a class, although variability has been reported depending on study design and population. In contrast, BMI (overweight/obese) and race/ethnicity (Non-Hispanic Black and Other) were the strongest independent predictors of both prediabetes and diabetes, consistent with established epidemiologic risk factors.

Strengths and Limitations

Strengths of this study include the use of nationally representative NHANES data, laboratory-measured HbA1c outcomes, an adequate sample size ($N=1,067$), and multivariable logistic regression adjusting for key confounders including age, sex, BMI, and race/ethnicity. However, several limitations should be noted. The cross-sectional design precludes causal inference, and statin dose intensity (high vs moderate) and duration of therapy were not captured. Additionally, RXDDAYS reflects medication use within the past 30 days only, and there is potential for residual confounding from unmeasured variables such as dietary habits, family history of diabetes, concomitant medications, and medication adherence. Race/ethnicity categorization is a limitation, as smaller groups were combined into an "other" category instead of using the five standard NHANES categories (Mexican American, Other Hispanic, Non-Hispanic White, Non-Hispanic Black, Other Race), potentially obscuring subgroup differences.

Conclusions

Atorvastatin and rosuvastatin users demonstrated similar glycemic status in this nationally representative sample, suggesting that statin type is not independently associated with HbA1c category distribution. Overweight/obesity and race/ethnicity were the strongest predictors of prediabetes and diabetes, highlighting the importance of weight management and addressing racial health disparities in clinical practice. Further prospective/longitudinal studies are warranted to evaluate causal dose-response relationships between individual status and glycemic outcomes, particularly in patients with prediabetes who may benefit from tailored statin selection.

Association Between Statin Type (Atorvastatin vs. Rosuvastatin) and Glycemic Status in U.S. Adults: A Cross-Sectional Analysis of NHANES

Jamie Brienza, Julia Ho, Amy LeBrun, Andrew Salama

Group 5

Reviews whether two common statins—atorvastatin and rosuvastatin—are linked to different blood sugar status in U.S. adults. The background explains that statins have been associated with higher diabetes risk, but many studies focus on “new diabetes” as a yes/no outcome and often do not compare specific statins or look at HbA1c categories. The objective is to see if the distribution of HbA1c categories (normal, prediabetes, diabetes) differs between atorvastatin and rosuvastatin users using NHANES data. In the discussion and conclusion, the authors report no meaningful difference in HbA1c category distribution between the two statins, and statin type was not an independent predictor after adjustment. They note that factors such as overweight/obesity and race/ethnicity were stronger predictors of being in the prediabetes or diabetes categories. They conclude that atorvastatin and rosuvastatin users showed similar glycemic status in this sample, and suggest future studies to better understand whether dose and longer-term use could matter.

Among Adults Receiving Oral Anticoagulation Therapy, Is Use of a Direct Oral Anticoagulant (DOAC) Compared With Warfarin Associated With Lower Prevalence of Albuminuria (uACR ≥ 30 mg/g)?

Perla Albatal, PharmD Candidate, Jillian Caron, PharmD Candidate
University of Rhode Island College of Pharmacy, Kingston, RI



Background

❖ Anticoagulant-related kidney injury is a known complication of warfarin, driven by glomerular hemorrhage and tubular obstruction.¹ Direct oral anticoagulants (DOACs) may offer improved renal outcomes, but most studies focus on advanced kidney disease rather than early markers like albuminuria.^{2,3,5,6} This study examines whether DOAC use is associated with lower subclinical renal injury, measured by urine albumin-to-creatinine ratio (uACR), compared with warfarin.⁴

Objectives

❖ To determine whether adults receiving DOAC therapy exhibit a lower prevalence of albuminuria (uACR ≥ 30 mg/g) compared with those receiving warfarin.

Methods

- ❖ **Data Source:** National Health and Nutrition Examination Survey (NHANES), representing the U.S. population.
- ❖ **Study Design:** Cross sectional survey of participants between 2017 and 2020.
- ❖ **Population:** Adults ≥ 18 years with an active prescription for a DOAC or warfarin and a documented uACR were included. Exclusion criteria: age < 18 years, missing or extreme uACR values (≥ 1000 mg/g), diagnosis of chronic kidney disease and concurrent use of both DOAC and warfarin.
- ❖ **Exposure Definition:** Type of anticoagulant therapy (DOAC vs warfarin) at the time of uACR measurement.
- ❖ **Outcome Assessment:** The primary outcome was albuminuria, defined as uACR ≥ 30 mg/g (abnormal) versus < 30 mg/g (normal)
- ❖ **Covariates:** Age, sex, diabetes, and hypertension
- ❖ **Statistical analysis:** All analyses utilized SPSS version 29.0 where a p-value < 0.05 was considered statistically significant. Descriptive statistics were used to summarize baseline characteristics. Continuous variables were compared using Mann-Whitney U Test and categorical variables were compared using Chi-square tests. Multivariable logistic regression was performed to evaluate the association between anticoagulation type and albuminuria, adjusting for age, sex, diabetes, and hypertension. Results were reported as adjusted odds ratios (AORs) with 95% confidence intervals.

Results

Table 1. Comparing Demographic and Clinical Characteristics Between Comparison Groups

Characteristics	Warfarin N= 82	DOAC N= 136	Significance
Age, median (25%, 75%)	77 (67, 80)	74 (68, 80)	0.715 ¹
BMI (kg/m ²), Median (25%, 75%)	33.30 (25.80, 38.50)	30.10 (28.60, 35.50)	0.157 ¹
Sex	Male (N%)	82 (60.3)	0.798 ²
	Female (N%)	34 (41.5)	
Race	White (N%)	79 (58.1)	0.255 ⁴
	Other (N%)	28 (34.1)	
Diabetes (N%)	18 (22)	32 (23.5)	0.788 ³
Hypertension (N%)	46 (56.1)	87 (64)	0.248 ³

¹Mann-Whitney U Test; ²Chi-Square Test; ³DOAC= Direct Oral Anticoagulant

Table 2. Raw Comparison of uACR

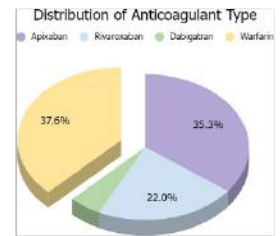
Outcomes	Warfarin N= 85	DOAC N= 140	Significance
uACR*, Median (25%, 75%)	14.78 (8.70, 46.74)	12.01 (7.84, 31.79)	0.264
uACR*	Normal (N%)	101 (74.3)	0.447
	Abnormal (N%)	35 (25.7)	

¹Mann-Whitney U Test; ²Chi-Square Test; *uACR = Urine Albumin-to-Creatinine Ratio

Table 3. Results of Multivariable Logistic Regression Analysis

Characteristics	Adjusted Odds Ratio	95% CI
DOAC vs. Warfarin	0.77	(0.41 - 1.44)
Age, every year older	1.04	(1.01 - 1.08)
Female vs. Male	0.89	(0.47 - 1.67)
History of T2DM*, Yes vs. History of T2DM*, No	2.76	(1.38-5.54)
History of Hypertension, Yes vs. History of Hypertension, No	0.83	(0.44 - 1.56)

*T2DM = Type 2 Diabetes Mellitus



Discussion/Conclusion

- ❖ Adjusted logistic regression of 218 patients showed no significant association between anticoagulant type and albuminuria (aOR 0.77, 95% CI 0.41–1.44)
- ❖ Older age and type 2 diabetes were independently associated with higher odds of albuminuria (age: aOR 1.04 per year, 95% CI 1.01–1.08; T2DM: aOR 2.76, 95% CI 1.38–5.54)
- ❖ Strengths of this study include use of a nationally representative dataset and evaluation of uACR as an early marker of renal injury. Limitations include the cross-sectional design, small sample size, potential residual confounding, and NHANES age top-coding at 80 years, which may reduce precision when assessing the effect of older age.
- ❖ Overall, while DOAC use demonstrated a lower frequency of albuminuria, no statistically significant association was observed. Larger longitudinal studies are needed to determine whether DOACs confer clinically meaningful renal benefit compared with warfarin.

References

1. Brodsky SV, Satoskar A, Hemminger J, et al. Anticoagulant-related nephropathy in kidney biopsy: a single-center report of 41 cases. *Kidney Med.* 2019;1(2):51-56.
2. Chan YH, Yeh YH, See LC, et al. Acute kidney injury in Asians with atrial fibrillation treated with non-vitamin K antagonist oral anticoagulants or warfarin. *J Am Coll Cardiol.* 2018;71(2):208-220.
3. Harrington J, Carnicelli AP, Hua K, et al. Direct oral anticoagulants versus warfarin across the spectrum of kidney function: patient-level network meta-analyses from COMBINE AF. *Circulation.* 2023;147(23):1748-1757.
4. Odutayo A, Serrano A, Chauhan A, et al. Association of albuminuria with 1-year risk of heart failure and other adverse outcomes in atrial fibrillation. *J Am Heart Assoc.* 2025;14(17):e041185.
5. Pastori D, Farcomeni A, Pignatelli P, Violi F, Lip GYH. ABC (Atrial fibrillation Better Care) pathway adherence and kidney function decline in patients with atrial fibrillation: the ATHERO-AF study. *Intern Emerg Med.* 2020;15(8):1417-1424.
6. Yao X, Tangri N, Gersh BJ, et al. Renal outcomes in anticoagulated patients with atrial fibrillation. *J Am Coll Cardiol.* 2017;70(21):2621-2632.

Among Adults Receiving Oral Anticoagulation Therapy, Is Use of a Direct Oral Anticoagulant (DOAC) Compared With Warfarin Associated With Lower Prevalence of Albuminuria (uACR ≥ 30 mg/g)?

Perla Albatal, Jillian Caron

Group 7

Tests whether adults taking a direct oral anticoagulant (DOAC) have a lower rate of early kidney injury compared with adults taking warfarin. The background explains that warfarin can cause kidney injury, and that prior research on DOACs often focuses on people with more advanced kidney disease rather than early warning signs like albumin in the urine. The objective is to compare albuminuria (based on the urine albumin-to-creatinine ratio) between DOAC and warfarin users. In the discussion and conclusion, the authors report that although albuminuria was less common in the DOAC group, the adjusted analysis did not find a statistically significant difference between DOACs and warfarin. They also note that older age and type 2 diabetes were linked to higher odds of albuminuria. They conclude that larger, longer-term studies are needed to determine whether DOACs provide meaningful kidney benefit compared with warfarin.

Association of Gabapentin and Serotonin-Norepinephrine Receptor Inhibitor Use with Elevated Blood Pressure: A Cross-Sectional Analysis of NHANES Data

Marc Cabral, Jina Im, Vanessa Oseghale, Julia Vorsa
 Doctor of Pharmacy (PharmD) Candidates
 University of Rhode Island - College of Pharmacy



Background

Cardiovascular disease is the leading cause of death worldwide, with modest increases in systolic blood pressure (SBP) associated with higher cardiovascular risk¹. Gabapentin and serotonin-norepinephrine reuptake inhibitors (SNRIs) share a common indication of neuropathic pain, with SNRIs associated with modest increases in blood pressure and gabapentin linked to cardiovascular events, though its impact on blood pressure remains less well characterized.²⁻⁵ Understanding gabapentin's effect on blood pressure may help inform medication selection for patients with neuropathic pain and pre-existing cardiovascular risk.

Objectives

To compare the prevalence of elevated systolic blood pressure (≥ 130 mmHg) between adults using gabapentin and those using SNRIs in a nationally representative sample of U.S. adults.

Methods

- Data Source:** The data was collected from National Health and Nutrition Examination Survey (NHANES) data between 2017-2020. NHANES is a nationally representative, cross-sectional survey designed to assess the health and nutritional status of the general U.S. population using a combination of interviews, physical examinations, and laboratory testing.
- Study Design & Cohort:** This cross-sectional study used NHANES data to identify and include individuals ≥ 18 years old with prior exposure to either gabapentin or SNRIs. Individuals were excluded from the study if they were less than 18 years old at the time of the NHANES data collection, had concomitant use of gabapentin and an SNRI, or were missing systolic blood pressure data.
- Exposure:** Exposure was defined as any prior use of gabapentin for any indication at the time of NHANES data collection. Only adults (≥ 18 years old) with systolic blood pressure data were included within the trial. The exposure group was compared to patients on SNRIs (duloxetine, venlafaxine, desvenlafaxine, levamisole, and milnacipran) for any length of exposure.
- Outcome:** The primary outcome systolic blood pressure with a dichotomized cut-off of 130 mmHg, chosen in accordance with the 2017 and 2025 ACC/AHA guidelines for hypertension management.^{6,7}
- Covariates:** Covariates included: age, gender, self-reported history of diabetes, self-reported history of kidney disease, self-reported hypertension, concomitant use of antihypertensive medications (defined by medication prescribed for ICD codes beginning with I10, I11, I12, I13 and I15), smoking history (> 100 cigarettes lifetime), income-to-poverty ratio, race, and PHQ-9 scores.⁸
- Statistical Analysis:** The difference in the risk of elevated SBP between gabapentin and SNRIs was assessed after adjusting for covariates using multivariable logistic regression using IBM SPSS 29.0. Baseline differences between groups were addressed using univariable logistic regression; however, residual confounding may remain. Continuous variables were compared either using independent student t-test or Wilcoxon rank-sum based on the normality test results. Categorical variables were compared using the Chi-squared test. Statistical significance was defined as $p < 0.05$.

References

1. World Health Organization. Cardiovascular diseases (CVDs). <https://www.who.int/news-room/fact-sheets/detail/cardiovascular-diseases-cvd-s>. 2017.
2. American Heart Association. High blood pressure facts. <https://www.heart.org/en/health-topics/high-blood-pressure/the-facts-about-high-blood-pressure>. 2019.
3. American Heart Association. Stroke facts and statistics. <https://www.heart.org/en/health-topics/stroke/the-facts-about-stroke>. 2019.
4. American Heart Association. Heart disease and stroke statistics: a report from the American Heart Association. <https://www.heart.org/en/health-topics/heart-disease/heart-disease-and-stroke-statistics>. 2019.
5. American Heart Association. Hypertension facts and statistics. <https://www.heart.org/en/health-topics/high-blood-pressure/the-facts-about-high-blood-pressure>. 2019.
6. Whellan DJ, et al. 2017 ACC/AHA guideline for the management of hypertension. *Circulation*. 2017;135:e151-103.
7. Whellan DJ, et al. 2025 ACC/AHA guideline for the management of hypertension. *Circulation*. 2025;151:e151-103.
8. Kroenke K, et al. A clinician rating scale for assessing current and worst ever pain: development and initial psychometric characteristics. *Medical Care*. 2002;40:1072-1083.

Results

Table 1. Demographic and Clinical Characteristics between Groups

Characteristics	Group 1: Gabapentin (n=283)	Group 2: SNRIs (n=125)	P value
Age (Years)	Mean \pm SD 64.0 \pm 14.0	58.7 \pm 14.0	< 0.001 [†]
Gender	Female, N (%) 112 (39.5%)	31 (24.8%)	< 0.001 [†]
	Male, N (%) 171 (60.5%)	94 (75.2%)	
Race	Non-Hispanic White, N (%) 123 (43.5%)	74 (59.2%)	0.01 [†]
	Non-Hispanic Black, N (%) 84 (29.7%)	24 (19.2%)	
	Hispanic/Other, N (%) 76 (26.9%)	27 (21.6%)	
BMI[†] (Body Mass Index kg/m²)	Mean \pm SD 32.8 \pm 8.4	32.9 \pm 8.1	0.935 [†]
PHQ-9[†] total score	Median (25%, 75%) 4 (2, 9)	7 (3, 12)	< 0.001 [†]
	Missing Cases 9	4	
Days on medication (Days)	Median (25%, 75%) 1460 (365, 2920)	1095 (365, 3376)	0.698 [†]
	Missing Cases 11	4	
Income-to-poverty ratio	Median (25%, 75%) 1.60 (0.99, 2.98)	2.19 (1.39, 4.45)	< 0.001 [†]
	Missing Cases 43	8	
Alcohol	Less than weekly / none, N (%) 88 (31.0%)	49 (39.2%)	0.740 [†]
	Weekly or more, N (%) 85 (30.0%)	33 (26.4%)	
	Missing, N (%) 110 (45.9%)	43 (34.4%)	
Self-reported kidney disease	Yes, N (%) 46 (16.3%)	21 (16.8%)	0.888 [†]
	No, N (%) 223 (83.4%)	103 (83.2%)	
	Missing, N (%) 2 (0.8%)	1 (0.8%)	
Self-reported diabetes	Yes, N (%) 131 (46.3%)	35 (28.0%)	< 0.001 [†]
	No, N (%) 152 (53.7%)	90 (72.0%)	
Self-reported hypertension	Yes, N (%) 291 (71.0%)	72 (57.6%)	0.003 [†]
	No, N (%) 80 (28.3%)	53 (42.4%)	
	Missing, N (%) 2 (0.7%)	0 (0.0%)	
Antihypertensive medication use	Yes, N (%) 38 (13.4%)	20 (16.0%)	0.518 [†]
	No, N (%) 245 (86.6%)	105 (84.0%)	
Self-reported high cholesterol	Yes, N (%) 162 (57.2%)	69 (55.2%)	0.618 [†]
	No, N (%) 118 (41.7%)	56 (44.8%)	
	Missing, N (%) 3 (1.1%)	0 (0.0%)	
Smoking status	Not currently smoking, N (%) 109 (38.2%)	47 (37.6%)	0.186 [†]
	Currently smoking, N (%) 83 (29.3%)	19 (15.2%)	
	Missing, N (%) 112 (39.6%)	59 (47.2%)	
Self-reported physical activity	Yes, N (%) 37 (20.1%)	25 (20.0%)	0.974 [†]
	No, N (%) 226 (79.9%)	100 (80.0%)	
Self-reported cardiac pain	Yes, N (%) 125 (44.2%)	52 (41.6%)	0.781 [†]
	No, N (%) 140 (49.5%)	62 (49.9%)	
	Missing, N (%) 18 (6.4%)	11 (8.8%)	

[†]Notes: [†] Wilcoxon rank-sum test; [†] Chi-square test

Table 2. Raw Outcomes between Exposure Groups

Outcomes	Group 1: Gabapentin (n = 283)	Group 2: SNRIs (n = 125)	P-value
Systolic Blood Pressure (mmHg) Median (25%, 75%)	126 (114, 142)	124 (115, 137)	0.283 [†]
SBP \geq 130 mmHg N (%)	124 (43.8%)	47 (37.6%)	0.241 [†]

[†]Notes: [†] Wilcoxon rank-sum test; [†] Chi-square test

Table 3. Multivariable Analysis of Elevated Systolic Blood Pressure

Characteristic	Adjusted Odds Ratio	95% CI	P-value	
Drug group	SNRI Reference	Reference	—	
	Gabapentin	1.34	0.75 – 2.42	0.336
Age (per one-year increase)	Reference	1.05	1.05 – 1.09	<0.001
Gender	Male Reference	Reference	—	
	Female	1.16	0.67 – 1.94	0.629
Self-reported diabetes	No Reference	Reference	—	
	Yes	1.21	0.76 – 2.08	0.464
Self-reported kidney disease	No Reference	Reference	—	
	Yes	0.83	0.42 – 1.64	0.592
Hypertension medication use	No Reference	Reference	—	
	Yes	1.09	0.61 – 1.98	0.164
Self-reported hypertension	No Reference	Reference	—	
	Yes	1.37	0.76 – 2.47	0.297
Race	Non-Hispanic White Reference	Reference	—	
	Non-Hispanic Black	2.33	1.24 – 4.38	0.009
	Hispanic/Other	1.38	0.64 – 2.47	0.460
Smoking Status	Not currently smoker Reference	Reference	—	
	Current smoker	0.82	0.40 – 1.28	0.197
Income-to-Poverty Ratio (per unit increase)	Reference	1.05	0.76 – 1.41	0.423
PHQ-9 Total Score (per 1-point increase)	Reference	1.00	0.96 – 1.05	0.954

Discussion/Conclusion

- Discussion:** The final study cohort consisted of 408 participants, 283 (69.4%) taking gabapentin and 125 (30.6%) taking SNRIs. Systolic blood pressure did not differ significantly between gabapentin and SNRI users (adjusted OR 1.34, 95% CI 0.75–2.42, $p = 0.326$).
- Biological Plausibility:** Compared with gabapentin, SNRIs may increase blood pressure through enhanced sympathetic activity⁹; however, this difference may be attenuated in a population-based analysis due to concurrent antihypertensive use, variability among SNRI agents, and residual confounding.
- Strengths:** This study uses nationally representative NHANES data with standardized blood pressure measurements and multivariable adjustment, enhancing the generalizability of the study.
- Limitations:** The small sample size limits statistical power, the cross-sectional design precludes causal inference, and residual confounding from unmeasured variables including medication dose, adherence, pain severity, diet, and non-cardiovascular comorbidities may have influenced the results. Potential misclassification from variable reporting and reliance on self-reported medication use further limit the precision. Diastolic blood pressure was not evaluated in this analysis; further studies are needed to assess its potential association.
- Conclusions:** Gabapentin use was not associated with a significant difference in the prevalence of elevated SBP compared to SNRI use. Larger prospective studies with dose-specific analyses and objective outcome measures are needed to clarify gabapentin's effects on blood pressure and guide prescribing in patients with neuropathic pain and pre-existing cardiovascular risk.

Association of Gabapentin and Serotonin-Norepinephrine Receptor Inhibitor Use with Elevated Blood Pressure: A Cross-Sectional Analysis of NHANES Data

Marc Cabral, Jina Im, Vanessa Oseghale, Julia Vorsa

Group 8

Summarizes the difference in blood pressure in adults using gabapentin versus adults using SNRIs, using NHANES data. The background explains that even modest increases in systolic blood pressure can raise cardiovascular risk, that gabapentin and SNRIs are both used for neuropathic pain, and that SNRIs are known to raise blood pressure slightly while gabapentin's effect on blood pressure is less clear. The objective is to compare how common elevated systolic blood pressure (at or above 130 mmHg) is in gabapentin users versus SNRI users. In the discussion and conclusion, the authors report that systolic blood pressure did not differ significantly between the two groups after adjustment. They note possible reasons this difference might be hard to detect in a population sample (such as other medications and differences among SNRI drugs) and point out limits such as cross-sectional design and possible confounding. They conclude that gabapentin was not associated with a meaningful difference in elevated systolic blood pressure compared with SNRIs, and that larger future studies are needed to clarify gabapentin's effect on blood pressure.

To determine whether the prevalence of prior kidney stone history differs among adults with hypertension treated with an angiotensin-converting enzyme inhibitor (ACEI) or an angiotensin receptor blocker (ARB)

Madalyn Bray, Stanley Cho, Grace Kimball, and Kyle Whitwell
University of Rhode Island / College of Pharmacy

Background

Hypertension and nephrolithiasis commonly coexist in adults, and certain antihypertensive medications may influence kidney stone formation through effects on renal calcium handling and urinary composition. Alterations in calcium excretion and renal hemodynamics may theoretically impact stone risk.

However, limited research has evaluated whether kidney stone history differs across antihypertensive medication classes in real-world populations^{1,2}. Understanding this relationship is clinically relevant, as it may reflect prescribing patterns or inform treatment decisions in patients at risk for nephrolithiasis.

Prior studies suggest that some antihypertensive classes, particularly thiazide diuretics, may reduce kidney stone risk, while ACE inhibitors and ARBs are not strongly associated with increased stone formation. However, real-world evidence comparing these classes remains limited.

Objectives

To determine whether the prevalence of prior kidney stone history differs among adults with hypertension treated with an angiotensin-converting enzyme inhibitor (ACEI) or an angiotensin receptor blocker (ARB)

Methods

Data Sources: National Health and Nutritional Examination Survey (NHANES), 2017 - March, 2020

Study Design: Cross-sectional study

Inclusion Criteria:

- Adults ≥ 18 years
- Diagnosis of hypertension. Hypertension was defined based on self-reported diagnosis.
- Reported current use of an ACE inhibitor (candesartan, lisinopril, ramipril, quinapril, fosinopril or perindopril) or ARB (losartan, valsartan, irbesartan, candesartan, telmisartan, olmesartan or azilsartan)
- Available data on kidney stone history

Exclusion Criteria:

- Missing or incomplete data on medication use
- Missing kidney stone history data
- Use of both ACE inhibitor and ARB concurrently
- Missing key covariate data (age, sex, BMI, diabetes, CKD, hyperlipidemia)

Exposure Definition: Current use of an ACE inhibitor or ARB

Outcome Assessment: Kidney stone history was assessed using the NHANES questionnaire item: "Have you ever had kidney stones?" (Yes/No)

Covariates: Age, sex, BMI, diabetes, chronic kidney disease (CKD), hyperlipidemia

Statistical Analysis:

- Means ± standard deviations (SD) for continuous variables and frequencies (%) for categorical variables
- Student's t-tests were used for continuous variables (e.g., age, BMI)
- Chi-square tests were used for categorical variables
- Multivariable logistic regression to assess association between medication class and kidney stone history
- Results reported as odds ratios (OR) with 95% confidence intervals (CI)
- p < 0.05 considered statistically significant

Results

Table 1. Baseline Characteristics

Characteristics	ACEI (1036)	ARB (884)	P-value	
BMI (Mean ± SD)	32.09 ± 7.49	31.99 ± 7.68	0.101	
Age (Mean ± SD)	63.34 ± 12.257	66.55 ± 11.753	<0.001	
Gender, N (%)	Female	605 (58.18%)	290 (42.30%)	<0.001
	Male	427 (41.82%)	394 (57.70%)	<0.001
Been told they have diabetes (DQ0018)	428 (44.00%)	249 (36.30%)	0.006	
Been told they have hypertension (DQ0020)	902 (86.70%)	622 (90.70%)	0.019	
Been told they have chronic kidney disease (DQ0022)	92 (8.80%)	58 (8.20%)	0.646	
Been told they have high cholesterol (DQ0040)	618 (59.40%)	466 (58.90%)	0.793	

Table 2. Kidney Stone Outcomes by Medication Class

Outcomes	ACEI (1036)	ARB (684)	P-value
Number of Patients with Kidney Stones	Abnormal N (%)	78 (11.40%)	0.004
	Normal N (%)	147 (14.20%)	
	889 (85.8)	606 (88.0%)	

Abnormal was defined as having a kidney stone and normal was defined as not ever having a kidney stone. All cells rounded to nearest whole number.

Table 3. Multivariable Logistic Regression Analysis

Characteristics	Adjusted Odds Ratio	95% CI	P-value
ACEI vs ARB	1.15	0.84 - 1.57	0.393
Female vs male	1.69	1.23 - 2.31	0.001
Age in years	0.10	0.99 - 1.01	0.007
BMI	0.99	0.97 - 1.01	0.163
Ever been told you had chronic kidney disease	2.31	1.49 - 3.67	<0.001
Ever been told you had high cholesterol	1.02	0.74 - 1.39	0.925
Ever been told you have diabetes	1.13	0.82 - 1.55	0.452
Ever been told you have hypertension	0.73	0.47 - 1.13	0.157

95% confidence intervals reported as 95% percentile to midline adjusted associations, odds ratios derived from Wald statistics. Model fit was assessed using the Hosmer-Lemeshow test.

Discussion/Conclusion

- No statistically significant association was observed between ACEI inhibitor and ARB use and kidney stone history after adjustment for demographic and clinical confounders.
- Baseline differences between groups, including age, sex, diabetes, and chronic kidney disease (CKD), indicate the presence of confounding. These findings suggest that observed unadjusted associations may be influenced by underlying clinical indications and patient characteristics influencing medication selection (channeling bias) rather than true medication effects.
- In adjusted analyses, antihypertensive class was not independently associated with kidney stone history, suggesting that ACE inhibitors and ARBs have similar risk profiles with respect to nephrolithiasis.
- Unlike thiazide diuretics, which are known to reduce urinary calcium excretion, ACE inhibitors and ARBs are not strongly associated with changes in calcium handling, which may explain the lack of observed association.
- Other variables, including sex and chronic kidney disease, were significantly associated with kidney stone history, suggesting these factors may play a more important role in risk than medication class.
- From a clinical perspective, these findings suggest that ACE inhibitors and ARBs can be selected based on standard indications (e.g., diabetes, CKD, medication tolerance) without concern for differential kidney stone risk.
- Strengths of this study include the use of a large, nationally representative dataset and adjustment for multiple clinically relevant confounders, improving generalizability.
- Limitations include the cross-sectional design, which precludes causal inference, reliance on self-reported kidney stone history, potential residual and unmeasured confounding from unmeasured variables such as diet, fluid intake, and medication adherence. Additionally, the temporal relationship between medication use and kidney stone history cannot be determined.
- Conclusion: Kidney stone history was not significantly associated with antihypertensive medication class. ACE inhibitors and ARBs appear to have similar clinical profiles in patients with prior nephrolithiasis, and medication selection is unlikely to be influenced by stone history. Future longitudinal studies are needed to evaluate incident kidney stone risk and better assess causal relationships.

To determine whether the prevalence of prior kidney stone history differs among adults with hypertension treated with an angiotensin-converting enzyme inhibitor (ACEI) or an angiotensin receptor blocker (ARB)

Madalyn Bray, Stanley Cho, Grace Kimball, Kyle Whitwell

Group 9

Studies adults with hypertension and examines whether having a history of kidney stones differs between people taking ACE inhibitors and people taking ARBs. The background explains that hypertension and kidney stones often occur together, and some blood pressure medicines may affect stone risk, but there is limited real-world research comparing ACE inhibitors and ARBs for kidney stone history. In the discussion and conclusion, the authors report that after accounting for patient differences, there was no significant association between ACE inhibitor versus ARB use and kidney stone history. They conclude that ACE inhibitors and ARBs appear to have similar kidney stone risk profiles, so medication choice can be based on usual clinical reasons rather than concern about different stone risk, and they recommend future longitudinal studies to better assess cause-and-effect.

Association Between Family Income-to-Poverty Ratio and Current Antipsychotic Medication Use Among U.S. Adults: A Cross-Sectional NHANES Analysis



Ryan Kay, Sarah Martidis, Mariah Ramos, Sydney Reyome
University of Rhode Island



Background

Socioeconomic disparities may influence access to mental health treatment, including antipsychotic medications. However, it remains unclear whether family income independently predicts antipsychotic use after accounting for clinical and demographic factors, specifically in the United States¹. If an association between lower income and increased antipsychotic use is identified, this may suggest socioeconomic disparities in mental health treatment or underlying psychiatric burden².

Objectives

The objective of this study was to determine whether family income level to poverty ratio (INDFMPIR) is associated with current increased antipsychotic medication use (AMU) among U.S. adults after adjusting for demographic characteristics, depression, smoking status, and medical comorbidities. Other psychiatric conditions were not accounted for, as this data was not available.

- **Null Hypothesis:** There is no association between family income level and increased antipsychotic use

Methods

Data Sources: National Health and Nutrition Examination Survey from 2017 to March 2020
Study Design: Cross-sectional study
Inclusion Criteria: U.S. adults 18 years and older
Exclusion Criteria: Any individuals with missing/incomplete data (missing exposure, outcome, or covariate data) needed for assessment of INDFMPIR associated with AMU, such as demographic variables (age), income level, or missing antipsychotic medication use data.
Exposure Definition: Family income-to-poverty ratio (INDFMPIR), categorized as (Family income to poverty is based on the US HHS poverty guidelines depending on the number of people in the household³):

- Low (<1)
- Middle (1-3)
- High (>3)

Population for adjusted analysis was 2,383 participants.
Outcome Assessment: Current antipsychotic medication use (yes/no) defined as self-reported use in the past 30 days of antipsychotic medications

- Haloperidol, aripiprazole, risperidone, quetiapine, olanzapine, ziprasidone or clozapine

Covariates: Age, sex, BMI, smoking status, hypertension, diabetes, depression
Statistical Analysis: Chi-square tests were used to compare categorical variables, while multivariable logistic regression estimated adjusted odds ratio and 95% confidence intervals for the independent association between INDFMPIR and AMU, adjusting for the covariates.

Results

Table 1. Baseline Characteristics by Income Level

Characteristic	Low (<1) (n=1281)	Middle (1-3) (n=2589)	High (>3) (n=1854)	P-value
Age, Mean ± SD	49.03 ± 16.26	55.22 ± 17.76	51.17 ± 16.30	<0.001*
BMI, Mean ± SD	32.31 ± 9.69	30.92 ± 7.89	29.87 ± 6.60	<0.001*
Depression, n (%)	444 (39.5%)	596 (27.4%)	281 (17.3%)	<0.001*
Female, n (%)	759 (59.3%)	1327 (52.9%)	948 (51.7%)	<0.001*
Smoking, n (%)	341 (46.2%)	382 (28.8%)	191 (26.2%)	<0.001*
Diabetes, n (%)	353 (27.6%)	774 (30.8%)	333 (18.2%)	<0.001*
Hypertension, n (%)	708 (60.0%)	1300 (51.8%)	813 (44.3%)	<0.001*

*ANOVA; *Chi-square test

Table 2. Unadjusted Association With Antipsychotic Use (n = 5,624)

Income level	No antipsychotic n (%)	Antipsychotic n (%)	P-value
Low	1245 (97.2%)	36 (2.8%)	<0.001
Middle	2447 (97.5%)	62 (2.5%)	
High	1815 (99.0%)	19 (1.0%)	

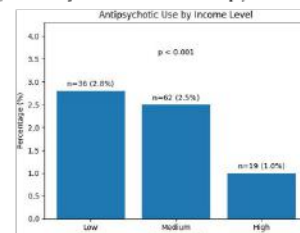
Values are presented as n (%). P-values were calculated using the chi-square test.

Table 3. Multivariable Logistic Regression Analysis of Factors Associated with Current Antipsychotic Use (n = 2,383)

Variable	aOR	95% CI	p
Low vs High income	0.51	(0.24-1.11)	0.088
Middle vs High income	0.67	(0.36-1.25)	0.208
Age (per year)	0.98	(0.96-0.999)	0.039
Female vs Male	0.73	(0.41-1.30)	0.285
BMI (kg/m ²)	1.01	(0.97-1.04)	0.766
Smoking (Yes vs No)	1.28	(0.71-2.31)	0.412
Hypertension (Yes vs No)	1.51	(0.78-2.95)	0.223
Diabetes (Yes vs No)	1.03	(0.54-1.97)	0.931
Depression (Yes vs No)	1.27	(0.72-2.26)	0.412

Abbreviations: aOR = adjusted odds ratio; CI = confidence interval; n = 2,383 | Reference groups: High income, Male, Non-smoker, No hypertension, No diabetes, Not depressed. Categorical variables (smoking, hypertension, diabetes, and depression) were dichotomized as yes vs no.

Figure 1. Unadjusted Association With Antipsychotic Use (n = 5,624)



P-values were calculated using the chi-square test

Discussion/Conclusion

Consistency of study results compared with previously published studies: Prior research suggests that socioeconomic status may influence mental health care. Although, our findings are consistent with studies showing that clinical factors, rather than income alone, are stronger predictors of antipsychotic use after adjustment.

Strengths: Nationally representative NHANES dataset, inclusion of multiple demographic and clinical covariates, use of multivariable logistic regression

Limitations: Cross sectional design limits causal inference, self reported medication use may introduce misclassification, missing data reduced sample size, residual confounding may be present

Conclusions: After adjustment for demographic and clinical factors, family income was not independently associated with increased antipsychotic medication use. Future research using simplified models, more covariates, or larger samples may improve statistical power and further clarify the relationship between income and AMU, as the current p-value is borderline significant. Due to the smaller sample of AMU in the low-income group, there may be an association of increased use. However, a larger sample size would be needed to confirm this association.

References

1. Fergusson, L., & Nicholson, O. (2019). The relationship between the duration of untreated psychosis and outcome in low- and middle-income countries: a systematic review and meta-analysis. *Schizophrenia Bulletin*, 45(1), 1-12. doi:10.1093/schbul/kby016
2. Wang, C. L., & Taylor, W. P. (2019). Prevalence and predictors of antipsychotic medication use among the U.S. population. *Frontiers in Behavioral Science*, 6(1), 1-10. doi:10.3389/fbeh.2019.00016
3. <https://www.hhs.gov/poverty-data/infographic>

Association Between Family Income-to-Poverty Ratio and Current Antipsychotic Medication Use Among U.S. Adults: A Cross-Sectional NHANES Analysis

Ryan Kay, Sarah Martidis, Mariah Ramos, Sydney Reyome

Group 11

Examines whether family income level (measured as the income-to-poverty ratio) is related to current antipsychotic medication use among U.S. adults. The background notes that socioeconomic differences may affect access to mental health treatment, but it is unclear whether income predicts antipsychotic use once other factors are considered. The objective is to test whether income-to-poverty ratio is associated with current antipsychotic use after adjusting for demographic and clinical factors such as depression, smoking, and medical conditions. In the discussion and conclusion, the authors report that after adjustment, family income was not independently associated with current antipsychotic medication use, and that clinical factors appeared to be stronger predictors. They note limitations such as the cross-sectional design and self-reported medication use, and they suggest that a larger sample or additional factors could help clarify whether there is a relationship.

Comparison of Systolic Blood Pressure Associated with Oral Semisynthetic Opioids and Oral Over-the-Counter NSAIDs

Dean Balcirak, Pharm.D. Candidate, Delaney Harrison, Pharm.D. Candidate
Michael Roy, Pharm.D. Candidate, Lauren Todd, Pharm.D. Candidate
University of Rhode Island College of Pharmacy, Kingston, RI

Background

- Hypertension is highly prevalent and frequently coexists with chronic pain conditions requiring analgesic therapy.
- Understanding how semi-synthetic opioids and oral over-the-counter (OTC) non-steroidal anti-inflammatory drugs (NSAIDs) are associated with blood pressure has important implications for patient safety, especially in populations with poorly controlled hypertension or at risk for cardiovascular events.
- Current contradictory evidence regarding opioid-mediated pressor versus depressor effects suggests an opportunity to clarify mechanisms and improve prescriber decisions.

Objectives

- To determine if systolic blood pressure readings, measured in mmHg, are elevated in patients receiving a semisynthetic opioid when compared to patients receiving an oral OTC NSAID.

Methods

- Data was collected from the United States National Health and Nutrition Examination Survey (NHANES) data from 2017 to March 2020.
- Cross-sectional survey design of participants receiving either an oral OTC NSAID or an oral semisynthetic opioid.
- Inclusion criteria: patients on naproxen or ibuprofen (n = 242) or hydrocodone +/- acetaminophen, oxycodone +/- acetaminophen, or hydromorphone (n = 242).
- The exposure of interest was oral semisynthetic opioid or oral OTC NSAID use.
- The outcome of interest was systolic blood pressure dichotomized as ≤ 129 mmHg (normal) or > 129 mmHg (abnormal).
- Covariates: Age, sex, BMI, smoking history, and reported pain
- Pearson Chi-Square tests (significance level of 0.05) were used to obtain P values for categorical data.
- Wilcoxon Rank-Sum tests (significance level of 0.05) were used to obtain P values for continuous variables, since our data is not normally distributed.
- A multivariable logistic regression analysis was performed to compare the exposures of interest while adjusting for multiple covariates. Results were reported as odds ratios (ORs) with 95% confidence intervals (CIs).

Discussion/Conclusion

- The semi-synthetic opioids group had 83 individuals (17.7%) with an abnormal blood pressure while the OTC NSAIDs group had 61 individuals (13.0%) with an abnormal blood pressure with a p-value of 0.008
- Our adjusted results suggest that there is a statistically significant relationship between semi-synthetic opioids and having an abnormal blood pressure when compared to OTC NSAIDs (OR = 1.67, 95% CI: 1.12-2.48).
- This study was limited by the inability to exclude patients on antihypertensive medications, the lack of analysis of pain severity, and the absence of a defined temporal relationship between medication administration and blood pressure measurement. Additionally, hypertension history was not included in the multivariable analysis due to the small sample size of that population.

Results

Table 1: Comparing Demographic and Clinical Characteristics Between Semi-Synthetic Opioid and OTC NSAID use

Characteristics	OTC NSAIDs n = 242	Semi-Synthetic Opioids n = 227	P value (n = 0.05)
Age, years	Mean \pm SD: 46.46 \pm 18.85	Mean \pm SD: 50.02 \pm 15.27	< 0.001*
Gender	Female, N (%) Male, N (%)	147 (66.7%) 80 (35.3%)	0.002*
Race	Mexican American, N (%) Other Hispanic, N (%) Non-Hispanic White, N (%) Non-Hispanic Black, N (%) Other race, N (%)	36 (7.7%) 29 (6.4%) 189 (83.7%) 77 (16.4%) 28 (6.4%)	< 0.002*
BMI/kg/m ²	Mean \pm SD: 32.2 kg/m ² \pm 8.74	31.0 kg/m ² \pm 7.90	0.29†
History of Hypertension	Yes, N (%) No, N (%)	2 (0.8%) 240 (106.2%)	0.002*
Smoking History	Yes, N (%) No, N (%)	56 (24.6%) 171 (75.4%)	< 0.002*
Reported Pain	Yes, N (%) No, N (%)	228 (102.5%) 17 (7.5%)	0.039†

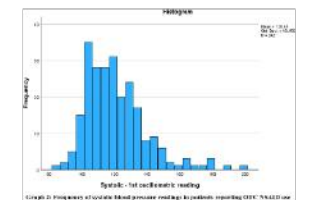
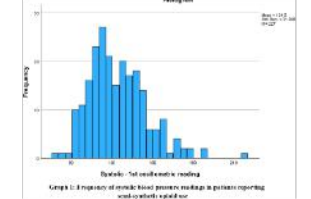
Table 3: Results of Multivariable Logistic Regression Analyses for Risk of Higher Systolic Blood Pressure

Characteristics	Adjusted Odds Ratio (OR)	95% Confidence Interval (CI)
Drug Class	NSAID (Ref) Semi-Synthetic Opioid	1 1.67
Age	< 50 years old (Ref) ≥ 50 years old	1 0.82
Gender	Male (Ref) Female	1 0.83
Race	Mexican American (Ref) Other Hispanic Non-Hispanic White Non-Hispanic Black Other race	1 1.04 1.04 2.28 1.13
BMI	< 25 (Underweight/Normal) (Ref) ≥ 25 (Overweight/Obese)	1 1.28
Smoking History	No (Ref) Yes	1 1.03
History of Pain	No (Ref) Yes	1 1.38

Table 2: Raw Comparison of Outcomes Between Exposure Groups

Outcome	OTC NSAIDs n = 242	Semi-Synthetic Opioids n = 227	P value (n = 0.05)
Systolic Blood Pressure, mmHg	Mean \pm SD: 128.46 \pm 15.46 mmHg	Mean \pm SD: 134.00 \pm 21.27 mmHg	0.008*
Systolic Blood Pressure	*Abnormal, N (%) *Normal, N (%)	83 (33.9%) 144 (63.6%)	0.008*

Abnormal defined as SBP > 129 mmHg
*Normal defined as SBP ≤ 129 mmHg
†Wilcoxon Rank-Sum test



References

- Carradino D, Savon FC, Cataldo D, et al. Acute pressor and hormonal effects of buprenorphine at high doses in healthy and hypertensive subjects: Role of opioid receptor agonism. *J Clin Endocrinol Metab*. 2005;90(9):5167-5174. doi:10.1210.2004-2254
- Figure 132, K218, Carroll MD, Afilalo J. Hypertension prevalence, awareness, treatment, and control among adults aged ≥18 years: United States, August 2011–August 2013. *MMWR Morbidity and Mortality Weekly Report*. 2014; doi:10.1093/mmwr/hru116
- Hirshy VJ, Smith CP, Deychman AI, et al. An antihypertensive, opioid: fentanyl, a synthetic non-addictive antiproliferative analog decreases blood pressure in spontaneously hypertensive rats. *Hypertension*. 2015;70:146. doi:10.1161/hypertension.2015.06
- Saha DK, Sazapanian P, Srinivasan SR, et al. Hypertensive effect of downregulation of the opioid system in a mouse model of diet-induced endogenous opioid activity. *Int J Obes*. 2012;36(10):1379-1386. doi:10.1038/sj.ijo.2011.179

Comparison of Systolic Blood Pressure Associated with Oral Semisynthetic Opioids and Oral Over-the-Counter NSAIDs

Dean Balcirak, Delaney Harrison, Michael Roy, Lauren Todd

Group 12

Explores people who need pain medicines and examines whether systolic blood pressure differs between those taking oral semisynthetic opioids and those taking oral over-the-counter NSAIDs. The background notes that high blood pressure is common and often occurs alongside chronic pain, so understanding how these medications relate to blood pressure is important for safety. The objective is to determine whether systolic blood pressure is higher in patients receiving a semisynthetic opioid compared with patients receiving an oral OTC NSAID. In the discussion and conclusion, the authors report that the semisynthetic opioid group had a higher proportion of abnormal systolic blood pressure than the OTC NSAID group, and that this association remained significant after adjusting for factors like age, sex, BMI, smoking history, and reported pain. They note limitations such as not being able to exclude people taking blood pressure medications, not analyzing pain severity, and the cross-sectional design, which makes it hard to know timing and cause-and-effect.

Findings of systemic inflammation burden by different opioid analgesic type in patients with pain

Abby Bullard, Hazel Moon, Matthew Potvin, Madison Ritzenhaler
University of Rhode Island/College of Pharmacy

Background

Opioid exposure has been associated with immune modulation and systemic inflammation, but existing studies are largely derived from opioid use disorder or long-term, high-dose exposure populations, where substantial confounding factors limit causal inference and reduce generalizability to routine clinical use. There has been limited evaluation of differences between opioid groups such as strong versus weak agents.¹⁻³ In contrast, direct comparisons of inflammatory burden across opioid analgesic types in the general chronic pain population remain limited. Therefore, we focused on individuals with pain, where opioid use is most common, to examine whether prescription opioid potency is associated with systemic inflammation.

Objectives

To compare the prevalence of elevated systemic inflammation, measured by high-sensitivity C-reactive protein (hs-CRP), among adults with pain diagnoses using weak versus strong opioid analgesics.

Methods

Data Sources and Study Design:

- We used National Health and Nutrition Examination Survey (NHANES) data from 2017 to 2020, a nationally representative, cross-sectional survey of U.S. adults. A cross-sectional design was selected to enable population-level prevalence estimation and exploratory analysis between opioid type and systemic inflammation, while adjusting for key covariates to minimize confounding and improve internal validity. This design is appropriate for generating one hypothesis regarding differential inflammatory burden by opioid use in real-world clinical settings.
- The study population included adults with pain-related diagnoses treated with opioid analgesics and available hs-CRP data (n = 300). Patients with hs-CRP > 10 mg/L, non-pain diagnoses, or reported substance use disorder were excluded to minimize confounding from acute inflammatory conditions, as hs-CRP > 10 mg/L typically indicates acute infection or inflammation.^{1,14}

Covariates:

- We adjusted for age, gender, race/ethnicity, obesity, diabetes, hypertension, hyperlipidemia, kidney impairment, and duration of opioid use.¹⁵ Covariates were selected a priori based on prior literature demonstrating associations with both opioid exposure and systemic inflammation.¹⁶ Additional exclusions further reduced confounding from acute inflammatory conditions and substance use disorder.

Statistical Analysis:

- We performed all analyses using IBM SPSS version 29.0, with statistical significance defined as a two-sided p-value < 0.05.
- Continuous variables were summarized as medians with interquartile ranges (IQR), and categorical variables as counts with percentages. Differences in median hs-CRP levels between opioid groups were assessed using the Wilcoxon rank-sum test, while category proportions were compared using the Pearson chi-square test or Fisher's exact test when expected cell counts were small.
- Binary logistic regression was performed to estimate odds ratios (ORs) for the association between opioid type and elevated hs-CRP, adjusting for demographic and clinical covariates to account for potential confounding. Due to limited sample size, covariate inclusion in multivariable logistic regression was constrained to maximum model parsimony and stability, consistent with recommended events-per-variable considerations.

References

1. Wang C, Tang Q, Tang Q. Association between chronic pain and elevated hs-CRP: A systematic review and meta-analysis. *PLoS One*. 2021;16(10):e0248099. doi:10.1371/journal.pone.0248099
2. Jain D, Patel DV, Gupta A. C-reactive protein. *Clinical Diabetes*. 2020;38(1):e123-129. doi:10.1093/cld/ciaa011
3. Torio AJ. High-sensitivity C-reactive protein. *StatPearls*. 2021; Available from: <https://www.ncbi.nlm.nih.gov/books/NBK537042/>
4. Pankovskiy CS, Kozlov M, Rubtsov CS, Pankovskiy CS, Pankovskiy CS, Pankovskiy CS, et al. hs-CRP, cardiovascular disease, and mortality. *Arterioscler Thromb Vasc Biol*. 2013;33(2):308-310. doi:10.1161/ATV.113.308310
5. Austin AA, Gornik SL, Hunter SK. U.S. trends in adult chronic pain. *Medical Care*. 2018;56(10):e18-23. doi:10.1097/MLR.0000000000000511

Results

Table 1-A. Baseline Demographic Between Comparison Groups

Characteristic	Weak Opioids (n=180)	Strong Opioids (n=120)	p-value
Age, mean (SD)	43 ± 11.1	51 ± 11.3	<0.001
Gender			0.949
Female, n (%)	81 (45.0%)	49 (40.8%)	
Male, n (%)	99 (55.0%)	71 (59.2%)	
Race/Ethnicity, n (%)			0.014
Non-Hispanic White	52 (28.9%)	47 (39.2%)	
Non-Hispanic Black	11 (6.1%)	22 (18.3%)	
Hispanic or Multiracial (combined)	17 (9.4%)	15 (12.5%)	
Educational attainment, n (%)			0.560
Less than High School	11 (6.1%)	10 (8.3%)	
High School Graduate	41 (22.8%)	28 (23.3%)	
Some College	41 (22.8%)	30 (25.0%)	
College Graduate	87 (48.3%)	52 (43.4%)	

Table 1-B. Clinical Characteristics Between Comparison Groups

Characteristic	Weak Opioids (n=180)	Strong Opioids (n=120)	p-value
Smoking Status, n (%)			0.002
Non-smoker	109 (60.6%)	71 (59.2%)	
Former/Current Smoker	71 (39.4%)	49 (40.8%)	
Model Interact			0.100
Non-Hispanic White	52 (28.9%)	47 (39.2%)	
Hispanic or Multiracial	18 (10.0%)	15 (12.5%)	
Obesity (Yes vs No)	71 (39.4%)	49 (40.8%)	
Diabetes (Yes vs No)	11 (6.1%)	22 (18.3%)	
Hypertension (Yes vs No)	41 (22.8%)	30 (25.0%)	
Hyperlipidemia (Yes vs No)	41 (22.8%)	30 (25.0%)	
Duration of Opioid Use (Months vs Less than 3 months)	1.04	0.84 ± 2.16	0.038
Obesity (Yes vs No)	2.80	0.82 ± 0.04	0.110
Diabetes (Yes vs No)	2.58	1.28 ± 0.15	<0.05
Hypertension (Yes vs No)	1.82	0.75 ± 0.08	0.210
Hyperlipidemia (Yes vs No)	1.82	0.81 ± 0.10	0.050
Kidney Impairment (Yes vs No)	1.77	0.52 ± 0.06	0.280
Duration of Opioid Use (Months vs Less than 3 months)	0.80	0.26 ± 0.04	0.047

Table 2. Raw Comparison of hs-CRP Levels Between Weak and Strong Opioid Users

Characteristic	Weak Opioids (n=180)	Strong Opioids (n=120)	p-value
hs-CRP Level, Mean ± SD	3.56 ± 0.51	3.46 ± 0.15	0.887
hs-CRP Level, Normal, n (%)	16 (8.9%)	10 (8.3%)	0.660
hs-CRP Level, Abnormal, n (%)	164 (91.1%)	110 (91.7%)	

Figure 1. Bar Graphs Demonstrating the Prevalence of Elevated hs-CRP among Patients using Opioid Analgesics for Pain

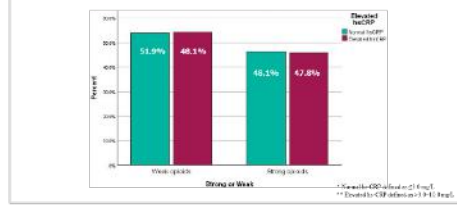


Table 3. Results of Multivariable Logistic Regression Analysis

Variable	AOR	95% CI	p-value
Opioid Type (Strong vs Weak)	0.72	0.37-1.40	0.337
Age (years)	0.95	0.96-1.01	0.208
Gender (male vs female)	0.91	0.48-1.72	0.787
Race/Ethnicity			
Non-Hispanic Black vs White	1.04	0.84-1.28	0.638
Hispanic and Multiracial vs White	2.80	0.82-9.04	0.110
Obesity (Yes vs No)	2.58	1.28-5.05	<0.05
Diabetes (Yes vs No)	1.12	0.46-2.72	0.800
Hypertension (Yes vs No)	1.82	0.75-4.38	0.210
Hyperlipidemia (Yes vs No)	1.82	0.81-4.10	0.150
Kidney Impairment (Yes vs No)	1.77	0.52-6.36	0.280
Duration of Opioid Use (Months vs Less than 3 months)	0.80	0.26-2.44	0.047

Discussion/Conclusion

- Strong opioid use was not a significant predictor of elevated hs-CRP (AOR 0.72, 95% CI 0.37-1.40, p=0.337). Consistently, no significant association was observed between opioid potency (weak vs strong) and hs-CRP in either unadjusted or adjusted analyses.
- These findings suggest that opioid potency alone may not significantly influence systemic inflammation in this population.
- Obesity was the only variable significantly associated with increased hs-CRP (AOR 2.51, 95% CI 1.28-4.93, p<0.007), indicating approximately 2.5-fold higher odds compared to non-obese patients. This is consistent with existing literature linking obesity to chronic low-grade inflammation.
- All other covariates were not significant, suggesting that these independent variables may have limited contributions to hs-CRP within this study.
- In conclusion, we suggest that opioid selection based on strength is unlikely to impact inflammatory risk. However, obesity may be a modifiable risk factor for systemic inflammation.
- Limitations include the cross-sectional design (precluding causal inference), potential recall bias from self-reported data, lack of dosage and adherence information, and relatively small sample size.
- Future studies should use longitudinal designs with objective and repeated inflammatory biomarkers to better assess temporal relationships and clarify the link between opioid use and systemic inflammation.

Findings of systemic inflammation burden by different opioid analgesic type in patients with pain

Abby Bullard, Hazel Moon, Matthew Potvin, Madison Ritzenhaler

Group 13

Analyzes adults with pain who are taking prescription opioids and asks whether opioid strength (weak versus strong opioids) is linked to higher levels of systemic inflammation. The background notes that opioids have been connected with immune effects and inflammation, but much of the past research comes from opioid use disorder or long-term high-dose exposure, and there has been limited direct comparison of different opioid types in typical pain patients. The objective is to compare how often high-sensitivity C-reactive protein (hs-CRP), a marker of inflammation, is elevated among people using weak versus strong opioid analgesics. In the discussion and conclusion, the authors report that opioid potency was not significantly associated with elevated hs-CRP in either unadjusted or adjusted analyses. They note that obesity was the main factor associated with higher hs-CRP, suggesting it may be a more important and modifiable driver of inflammation in this population. They conclude that choosing an opioid based on strength alone is unlikely to change inflammation risk, and recommend larger, longitudinal studies with repeated biomarker measurements.

Comparative Analysis of Liver Enzyme Elevations (AST/ALT) in Patients Treated with SSRIs Versus Other Antidepressants

Taylor Albanese, Emily Dwyer, Leah Seeram, Jack Sullivan
University of Rhode Island, College of Pharmacy

Background

Antidepressants are widely prescribed and generally well tolerated, but some have been associated with liver enzyme elevations and drug induced liver injury (DILI).^{1,2} Although rare, DILI can be clinically significant, particularly in patients with underlying liver disease or polypharmacy.³ Selective serotonin reuptake inhibitors (SSRIs) are often considered safer than other antidepressants, yet comparative data on their hepatic risk remain limited.¹ Understanding differences in liver enzyme elevation between antidepressant classes may help guide safer treatment decisions.

Objectives

To evaluate whether adult patients taking SSRIs have a higher risk of elevated Aspartate Aminotransferase (AST) and/or Alanine Aminotransferase (ALT) compared with patients taking non-SSRI antidepressants.

Methods

- Data Source:** collected from 2017-2020 National Health and Nutrition Examination Survey (NHANES).
- Study Design:** A cross-sectional design was used due to availability of nationally representative data, allowing assessment of population-level associations
 - Inclusion Criteria:** U.S. adults ≥18 years using SSRI or non-SSRI at the time of being surveyed used for any indication
 - Exclusion Criteria:** Individuals taking both SSRI and non-SSRI medications
- Exposure:**
 - SSRI Group:** sertraline, citalopram, fluvoxamine, vilazodone, fluoxetine, escitalopram, paroxetine
 - Non-SSRI Group:** SNRIs (31.0%), TCAs (16.8%), atypical antidepressants (51.8%), MAO inhibitors (0.4%)
- Primary outcome:** Elevated AST (>48 U/L) and/or ALT (>55 U/L)
- Covariates:** age, sex, race, BMI, alcohol use, number of prescription medications, and diabetes diagnosis
- Statistical Analysis** ($\alpha = 0.05$ for all tests)
 - Categorical Data: Pearson's Chi-Square test used to obtain P-values
 - Continuous Data: Independent T-test and Mann-Whitney U used to obtain P-values
 - Logistic regression was used to estimate adjusted odd ratios (ORs) and 95% confidence intervals (CIs) for the association between the exposure and outcome, controlling for relevant covariates to account for potential confounding

References

1. Valtierra C, et al. *Antidepressant-induced liver injury: a review of the literature*. *The American Journal of Psychiatry*. 171(9): 1104-1110. 2014.
2. Chikara S, et al. *Association of antidepressant drug-induced liver injury*. *The American Journal of Gastroenterology*. 112(12): 1800-1806. 2017.
3. Spivey C, et al. *Drug-induced liver injury: An overview*. *The American Journal of Gastroenterology*. 117(12): 2014-2024. 2012.

Results

Table 1. Comparing Demographic and Clinical Characteristics Between SSRI and Non-SSRI Use

Characteristic	Group 1: SSRI (n=738)	Group 2: Non-SSRI (n=701)	p-value
Age (years), Mean ± SD	33.9 ± 14.9	33.4 ± 14.9	0.819
Sex/Gender (%)			0.312
Male, N (%)	341 (32.7%)	225 (31.8%)	
Female, N (%)	407 (67.3%)	476 (68.2%)	
Race/Ethnicity/Origin (%)			0.144
White, N (%)	422 (57.2%)	334 (53.4%)	
Non-White, N (%)	316 (42.8%)	377 (53.6%)	
Number of Prescription Medications	5.2 ± 3.8	4.9 ± 3.8	<.001
BMI (Body Mass Index kg/m ²)	27.0 ± 5.2	27.0 ± 5.2	0.903
Diabetes (Yes/No, %)	11.0 (28.1%)	10.6 (28.0%)	0.381
Yes, N (%)	263 (35.7%)	207 (42.4%)	
No, N (%)	475 (64.3%)	494 (57.6%)	
Ever Had Alcohol (%)	131 (17.8%)	93 (13.3%)	0.179
Yes, N (%)	575 (77.8%)	582 (83.0%)	
No, N (%)	163 (22.2%)	119 (17.0%)	
Alcohol Use (past year) (%)			0.812
None, N (%)	171 (23.2%)	184 (26.2%)	
Everyday, N (%)	20 (2.7%)	21 (3.0%)	
Weekly or more, N (%)	37 (5.0%)	36 (5.1%)	
1-3 times per week, N (%)	43 (5.8%)	38 (5.4%)	
2 times per week, N (%)	37 (5.0%)	27 (3.9%)	
Once a month, N (%)	31 (4.2%)	27 (3.9%)	
3-11 times per year, N (%)	34 (4.6%)	32 (4.6%)	
1-2 times per year, N (%)	45 (6.1%)	42 (6.0%)	
Monthly, N (%)	183 (24.8%)	139 (19.8%)	
Alcohol Use Restriction (%)			0.489
Former Drinkers, N (%)	171 (23.2%)	184 (26.2%)	
Current Drinkers, N (%)	464 (62.8%)	582 (83.0%)	
Diabetes Medication (%)			0.312
Yes, N (%)	172 (23.2%)	175 (25.0%)	
No, N (%)	566 (76.8%)	526 (75.0%)	
Smoking Status (%)			0.151
Smoker, N (%)	117 (15.9%)	115 (16.4%)	
Nonsmoker, N (%)	621 (84.1%)	586 (83.6%)	

Table 2. Comparing Frequencies of the Outcome Variables Between Comparison Groups

Liver Enzymes Levels	Group 1: SSRI (n=738)	Group 2: Non-SSRI (n=701)	p-value
No Elevation in AST or ALT (AST <48.0 and ALT <55.0)	707 (95.8%)	678 (96.7%)	0.359
Elevated AST and/or ALT (AST >48.0 and ALT >55.0)	31 (4.2%)	23 (3.3%)	

Note: Statistical analysis was performed using the Chi-Square test. The result yielded a p-value of 0.359, indicating no statistically significant difference between liver enzyme elevations when comparing SSRI and Non-SSRI antidepressants.

Table 3. Results of Multivariable Binary Logistic Regression

Characteristics	Odds Ratio	95% CI	p-value
SSRI vs. Non-SSRI	1.22	(0.67 – 2.23)	0.511
Age (per 1-year increase)	0.98	(0.96 – 0.99)	0.014
Sex (Female vs. Male)	0.32	(0.18 – 0.59)	<.001
Race (Non-White vs. White)	1.58	(0.86 – 2.87)	0.139
Number of Prescription Medications (per additional med)	1.01	(0.92 – 1.11)	0.847
BMI (>30 vs. <30)	1.11	(0.60 – 2.05)	0.740
Current Drinkers vs Former Drinkers	2.00	(0.90 – 4.44)	0.090
Diabetes (No vs. Yes)	1.64	(0.65 – 4.13)	0.296

Note: Hosmer and Lemeshow Test P-value is 0.018

Discussion/Conclusion

Consistency of Study Results

- SSRI use was not associated with a statistically significant increase in liver enzyme elevations compared with other antidepressant classes ($p = 0.359$). The overall prevalence of AST/ALT elevation was low, with 31 (4.2%) events among SSRI users and 23 (3.3%) events among non-SSRI users, suggesting that clinically significant hepatotoxicity is uncommon.
- These findings are consistent with prior studies suggesting that antidepressant-induced liver injury is rare and typically idiosyncratic rather than class dependent. Existing literature indicates that while certain antidepressants can cause hepatotoxicity, the absolute risk remains low.

Biological plausibility

- Antidepressant induced liver injury is thought to occur via idiosyncratic mechanisms, including metabolic and immune-mediated pathways rather than predictable dose dependent toxicity, which may explain similar risk across drug classes.
- Strengths:** Inclusion of multiple antidepressant classes, adjustment for important confounders, cost-effectiveness, and real-world population increases generalizability
- Limitations:** Single time point liver enzyme measurement, possible unmeasured confounding (e.g., NAFLD, viral hepatitis), and small number of outcome events ($n = 54$)

Conclusion

- SSRI use was not associated with a statistically significant increase in AST/ALT elevation compared with non-SSRI antidepressants. Therefore, antidepressant class alone may not be a major determinant of liver enzyme abnormalities.

Comparative Analysis of Liver Enzyme Elevations (AST/ALT) in Patients Treated with SSRIs Versus Other Antidepressants

Taylor Albanese, Emily Dwyer, Leah Seeram, Jack Sullivan

Group 14

Investigates whether people taking SSRIs have a higher risk of elevated liver enzymes compared with people taking other types of antidepressants. The background explains that antidepressants are generally safe but can sometimes be linked to liver enzyme elevations and drug-induced liver injury, which can be important in people with liver disease or those taking many medications. The objective is to compare the risk of elevated AST and/or ALT in adults using SSRIs versus non-SSRI antidepressants using NHANES data. In the discussion and conclusion, the authors report that SSRI use was not associated with a statistically significant increase in liver enzyme elevations compared with other antidepressant classes, and that overall enzyme elevations were uncommon. They conclude that antidepressant class alone may not be a major driver of liver enzyme abnormalities, and note limitations such as having only one measurement time point and the possibility of unmeasured liver-related factors.



Background

- P2Y12 inhibitors, including clopidogrel, prasugrel, and ticagrelor, are widely used in the treatment of patients with acute coronary syndrome and those undergoing percutaneous coronary intervention. These medications reduce thrombotic events but also increase the risk of bleeding, which may lead to hospitalization, therapy discontinuation, and increased morbidity and mortality.
- Prior research has examined sex differences in major bleeding outcomes, limited attention has been given to subclinical markers such as hematocrit, which may indicate early bleeding, and assessing its relationship with biological sex may enhance risk stratification and support personalized, patient centered care.

Objectives

- The objective is to evaluate whether biological sex is associated with the prevalence of abnormal hematocrit among adult patients receiving P2Y12 inhibitor therapy, using hematocrit as a proxy marker for subclinical bleeding risk, and to assess whether this relationship may inform risk stratification and guide more individualized, patient-centered monitoring strategies.

Methods

Study Design:

- Cross-sectional study using data from NHANES database

Inclusion Criteria:

- Adults ≥18 years
- Available hematocrit laboratory data
- Current use of a P2Y12 inhibitor (clopidogrel, prasugrel, or ticagrelor)

Exclusion criteria

- Missing sex information or missing hematocrit values

Exposure Definition

- Biological sex (comparing females and males)

Outcomes:

- Primary: Abnormal hematocrit, defined using sex-specific thresholds (<41% for males, <36% for females)

Statistical Analysis

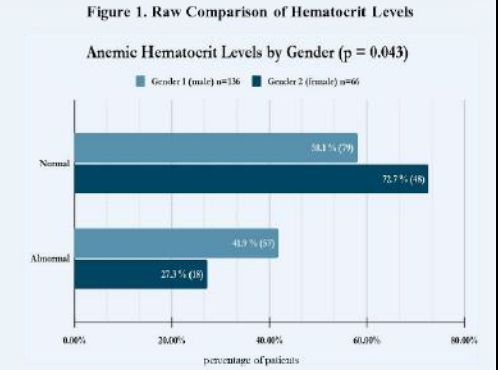
- Wilcoxon rank sum test ($\alpha = 0.05$) was used for continuous variables
- Chi-square tests, independent t-test, and multivariable logistic regression assessed risk adjusting for confounders (age, body mass index, comorbidities, renal function, and number of concomitant medications that could affect bleeding risk)

Results

Table 1. Demographic Comparison between Male and Female

Characteristics	Male n=136 (67.3 %)	Female n=66 (32.7 %)	P-value ($\alpha=0.05$)
Age (years), Mean ± SD	68.6 ± 9.8	68.8 ± 11.6	0.906 ^a
Number of Prescription medicines taken, Mean ± SD	7.53 ± 3.65	8.73 ± 3.96	0.020 ^b
Platelet Count (1,000 cells/uL), Mean ± SD	209.9 ± 57.2	247.8 ± 85.0	< .001 ^a
No Kidney Disease	139 (89.1%)	67 (83.7%)	0.191 ^b
Kidney Disease	17 (10.9%)	13 (16.3%)	
Non-smoking	75 (72.8%)	21 (58.3%)	0.451 ^b
Smoking	28 (27.2%)	15 (41.7%)	

^aIndependent t-test, ^bchi-square test



A Chi-square test was conducted to examine the relationship between gender and hematocrit levels. The results indicated a significant association (p = 0.043), with individuals in Gender 1 (male) exhibiting a higher prevalence of abnormal hematocrit (41.9%) compared to those in Gender 2 (female - 27.3%).

Table 2. Results of Multivariable Logistic Regression Analyses

Characteristics	Odds Ratio	95 % CI (Lower, Upper)	P-value
Gender (female)	(Ref)	(Ref)	
Gender (male)	0.339	(0.161, 0.712)	0.004
Age (every one year increase)	1.248	(0.829, 1.877)	0.289
No kidney disease	(Ref)	(Ref)	
Kidney Disease	0.553	(0.227, 1.345)	0.191
Number of Prescription medicines taken	1.037	(0.957, 1.123)	0.374
Platelet Count (1,000 cells/uL)	1.005	(1.001, 1.010)	0.018
Non-smoking	(Ref)	(Ref)	
Smoking	1.278	(0.675, 2.419)	0.451

Gender 1 (male) was associated with significantly lower odds of abnormal hematocrit (66% less risk, OR = 0.339), while increasing platelet count was associated with slightly increased odds. The model-data fit quality of multivariable logistic regression analysis was assessed with Hosmer and Lemeshow test (p = 0.592).

Discussion / Conclusion

- This study analyzed 202 adult patients (136 male, 66 female) receiving P2Y12 inhibitor therapy, identifying gender and platelet count as the only significant predictors of abnormal hematocrit. Initial Chi-square testing showed a significant association (p = 0.043), with males exhibiting a higher prevalence of abnormal hematocrit (41.9%) compared to females (27.3%).
- In the adjusted model, gender and platelet count remained statistically significant predictors. Males were associated with 66% reduced odds of abnormal hematocrit (OR=0.339, 95% CI: 0.161–0.712, p=0.004), while increasing platelet count slightly raised the odds (OR=1.005, 95% CI: 1.001–1.010, p=0.018). Other variables including age, smoking, kidney disease, and medication count were not significant (p=0.795).
- These findings align with previous research findings that gender and platelet count are significant determinants of hematological profiles in patients.
- The results suggest that gender and platelet count may be more important factors to consider when identifying patients at risk for abnormal hematocrit in this cohort. A primary strength is the use of both unadjusted and adjusted analyses to account for confounders, however, findings are limited by the study's observational nature, missing data, and relatively small sample size. While these results highlight useful predictors, larger studies are necessary to confirm these findings and improve generalizability.

References

- Lee EK, Borenstein E, Majeed SA, et al. Point P2Y12 Inhibitors in Men Versus Women: A Collaborative Meta-Analysis of Randomized Trials. *JAMA Cardiol.* 6(12):1949–55. <https://doi.org/10.1001/jama.2017.01803>
- Branan G, Rosengren J, Jackson CL, et al. Is There Sex-related Outcome Difference According to Oral P2Y12 Inhibitors in Patients with Acute Coronary Syndrome? A Systematic Review and Meta-Analysis of 107,126 Patients. *Curr Probl Pharmacol Clin Sci.* 116–213. https://doi.org/10.1007/978-94-007-6100-9_11
- Fry MF, Gens R, Jindal MM, et al. Sex-Related Bleeding Risk in Acute Coronary Syndrome: Patients Receiving Dual Antiplaquet Therapy with Aspirin and a P2Y12 Inhibitor. *Medicine (Baltimore).* 13(3):200–208. <https://doi.org/10.1097/MD.0000000000000282>
- Vogel H, Beyer C, Cohen RA, et al. Sex Differences Among Patients With High Risk Bleeding: Ticagrelor With or Without Aspirin After Percutaneous Coronary Intervention. *JAMA Cardiol.* 6(9):1032–1041. <https://doi.org/10.1001/jama.2017.1170>
- Schwartz ME, Dzau VJ, Brennan E, et al. Efficacy and Safety of High-Dose P2Y12 Inhibitors Prasugrel and Ticagrelor in Patients With Coronary Heart Disease Treated With Dual Antiplatelet Therapy: A Sex-Specific Systematic Review and Meta-Analysis. *Am Heart J.* 191:401–417. <https://doi.org/10.1016/j.ahj.2015.12.017>
- National Heart, Lung, and Blood Institute. (2012). Blood tests. U.S. Department of Health and Human Services. <https://www.nlm.nih.gov/health/bloodtests>

Biological Sex and Abnormal Hematocrit: Assessing Bleeding Risk in P2Y12 Inhibitor Therapy

Daniel He, Ava Conway, Shine Jeon, Brianna Meneve

Group 15

Reviews adults taking P2Y12 inhibitors and asks whether biological sex is associated with abnormal hematocrit, used as an early marker of possible bleeding risk. The background explains that these medications reduce clotting events but can increase bleeding risk, and that sex differences in major bleeding have been studied while earlier lab markers like hematocrit have been explored less. The objective is to evaluate whether abnormal hematocrit differs by sex in people using P2Y12 inhibitors and whether this could help with monitoring and risk assessment. In the discussion and conclusion, the authors report that sex and platelet count were the main factors related to abnormal hematocrit in their analysis. They note limitations such as the observational, cross-sectional design, missing data, and a relatively small sample size, and conclude that larger studies are needed to confirm these findings and improve how patients are stratified and monitored.

Among Adults Currently Taking Benzodiazepines, How Does Short-Acting Benzodiazepine Use Compare With Long-Acting Benzodiazepine Use in Their Association With Heart Rate?

Sydney Croly, Pharm.D. Candidate; Ava DiBiasio, Pharm.D. Candidate; Paul Kim, Pharm.D. Candidate; Deirdre McCaffrey, Pharm.D. Candidate
The University of Rhode Island College of Pharmacy, Kingston, RI

Objectives

- To compare the association between short-acting versus long-acting benzodiazepines on HR in adults, and to evaluate whether duration of action is associated with clinically meaningful differences in HR association.

Methods

- Study Design:** Cross-sectional study using 2017–2020 National Health and Nutrition Examination Survey (NHANES) data¹
- Population:** Adults ≥18 years reporting benzodiazepine use within the past year
- Excluded:** Individuals using both short- and long-acting benzodiazepines
- Exposure:** Benzodiazepine use categorized by duration of action:
 - Short-acting (t½ < 12 hrs): alprazolam, lorazepam, oxazepam, temazepam, triazolam
 - Long-acting (t½ > 24 hrs): diazepam, clonazepam, chlorthalidopoxide, flurazepam, clobazepam
- Outcome:** Heart rate (HR) Categorized based on AHA guidelines:
 - Low: < 60 bpm
 - Normal/High: ≥ 60 bpm²
- Covariates (Measured Confounders):** Age, gender, race/ethnicity, anxiety status (measured by ICD 10 codes 41.0 & 41.9 for anxiety and panic disorders)
- Statistical Analysis:**
 - Chi-square test for unadjusted comparisons of HR between groups
 - Multivariate logistic regression (SPSS) to assess association between benzodiazepine duration and HR while adjusting for confounders
 - Statistical significance was set at p < 0.05.

Background

- Benzodiazepines are commonly prescribed medications for the management of conditions such as anxiety and insomnia. They are commonly categorized into two groups (short-acting or long-acting) based on their pharmacokinetic properties (i.e. t½/2). These differences in duration of action are thought to influence their safety profiles, including potential cardiovascular association.
- Prior research for benzodiazepines has focused on associations in the realm of sedation, cognitive impairment, and risk of dependence^{3,4}. Existing literature that looks at the relationship between benzodiazepine use and heart rate (HR) is very limited, particularly with respect to pharmacokinetic properties (i.e. t½/2).
- HR is an important clinical marker for cardiovascular function and can fluctuate by central nervous system depressants, like benzodiazepines. Additionally, patient specific factors like age, sex, race, and anxiety may also influence HR and should be considered when evaluating the association. Current evidence and guidelines do not specify whether duration of action should be considered in when prescribing benzodiazepines in these populations.
- Even with the heavy use of benzodiazepines, limited data is out comparing HR outcomes across the class's pharmacokinetic properties. Further investigation is needed to better understand the potential cardiovascular implications associated with benzodiazepine duration of action.

Results

Table 1: Comparing Demographic and Clinical Characteristics between Exposure Groups.

Characteristic	Short-Acting Benzodiazepines (n = 159)	Long-Acting Benzodiazepines (n = 81)	P value
Race			0.704
- White, N (%)	97 (61.0%)	52 (64.2%)	
- Hispanic, N (%)	27 (17.0%)	17 (21.0%)	
- Black, N (%)	16 (10.1%)	6 (7.4%)	
Age			0.865
- 18-50, N (%)	51 (32.1%)	27 (33.3%)	
- 51+, N (%)	107 (67.9%)	53 (66.6%)	
Gender			0.473
- Female, N (%)	96 (60.4%)	45 (55.6%)	
- Male, N (%)	63 (39.6%)	36 (44.4%)	
Anxiety			0.137
- Yes, N (%)	104 (65.4%)	45 (55.6%)	
- No, N (%)	55 (34.6%)	36 (44.4%)	
CV comorbidities			0.354
- Yes, N (%)	2 (1.3%)	0 (0.0%)	
- No, N (%)	104 (66.1%)	45 (55.6%)	

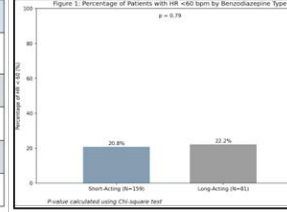


Table 2: Results of Multivariable Logistic Regressions Analyses

Characteristics	Adjusted Odds Ratio	95% CI
Duration of Action		
- Short-Acting	Reference	Reference
- Long-Acting	1.05	0.54-2.05
Race		
- White, N (%)	Reference	Reference
- Hispanic, N (%)	0.83	0.18-2.03
- Black, N (%)	0.19	0.04-0.99
Age		
- 18-50, N (%)	Reference	Reference
- 51+, N (%)	2.05	0.98-4.25
Gender		
- Female, N (%)	Reference	Reference
- Male, N (%)	0.74	0.39-1.41
Anxiety		
- No, N (%)	Reference	Reference
- Yes, N (%)	0.70	0.36-1.33

Discussion & Conclusion

- This study found no significant difference in heart rate between adults using short-versus long-acting benzodiazepines. These findings suggest that heart rate alone is unlikely to be a primary factor in selecting benzodiazepine duration; however, clinical decisions should still consider the broader patient context, including comorbid cardiovascular conditions and concurrent medications that may influence heart rate. **Benzodiazepine duration of action is not a clinically important determinant of HR and should not be an independent factor driving prescriber decision-making.**
- Strengths: Cost effective study, using a large, nationally representative dataset (NHANES), supporting generalizability and population-level insights.
- Limitations: Small sample size, residual confounding factors (healthcare access, substance use), and inability to adjust for HR-affecting medications, opioids, and cardiovascular comorbidities are all limitations of this study. The cross-sectional design precludes conclusions about causality. Also, reliance on self-reported data may introduce recall or misclassification bias. Information on dose, duration, and adherence was unavailable. Unable to run multivariable logistic regression for CV comorbidities due to lack of sample size. Potential for misclassification bias, measurement error, and unmeasured confounding with NHANES data.

References

1. Liu S, Soedamah-Muthu S.S, van Meenen S.C, Kromhout D, Geleijnse J.M, Gibney E.J. (2023). Use of benzodiazepines and 2-drugs and mortality in older adults after myocardial infarction. *International Journal of Geriatric Psychiatry*, 38(1). <https://doi.org/10.1002/gps.5861>

2. Jagelink MW, Majewski TB, Andrich J, Mueck-Weymann M. Short-term effects of intravenous benzodiazepines on autonomic neurocardiac regulation in humans: a comparison between midazolam, diazepam, and lorazepam. *Crit Care Med*. 2002 May;30(5):997-1006. doi: 10.1097/00003246-200205000-00008

3. Centers for Disease Control and Prevention. (2026). *National Health and Nutrition Examination Survey (NHANES)*. Retrieved March 30, 2026, from <https://www.cdc.gov/nchs/nhanes/>

4. Shacter, R. I., & Greenblatt, D. J. (1993). Use of benzodiazepines in anxiety disorders. *New England Journal of Medicine*, 328(19), 1399-1405.

5. Kusumoto, K. M., Schoenfeld, M. H., Barnert, C., Edgerton, J. R., Erlenbogen, K. A., Gold, M. R., Goldschlager, N. F., Hamilton, R. M., Jogger, J. A., Kim, R. J., Lee, R., Marine, J. E., McLeod, C. J., Oken, K. R., Patton, K. K., Pellegrini, C. N., Selzman, K. A., Thompson, A., Vavrosy, P. D., & American College of Cardiology/American Heart Association Task Force on Clinical Practice Guidelines. (2019). *2018 ACC/AHA/HRS guideline on the evaluation and management of patients with bradycardia and cardiac conduction delay*. *Journal of the American College of Cardiology*, 74(7), e51-e156. <https://doi.org/10.1016/j.jacc.2018.10.044>

Among Adults Currently Taking Benzodiazepines, How Does Short-Acting Benzodiazepine Use Compare With Long-Acting Benzodiazepine Use in Their Association With Heart Rate?

Sydney Croly, Ava DiBiasio, Paul Kim, Deirdre McCaffrey

Group 16

Compares adults taking benzodiazepines and asks whether short-acting versus long-acting benzodiazepines are linked to different heart rate outcomes. The background explains that benzodiazepines are often grouped by how long they last in the body, and that these differences might affect safety, including possible cardiovascular effects, but there is limited evidence comparing heart rate by duration of action. The objective is to compare heart rate between short-acting and long-acting benzodiazepine users in adults. In the discussion and conclusion, the authors report that they did not find a meaningful difference in heart rate between the two groups. They conclude that duration of action alone is unlikely to be an important reason to choose one benzodiazepine type over another based on heart rate, although other patient factors and medications should still be considered.

Comparing Hospitalization Rates Among Patients Treated with Direct Oral Anticoagulants (DOACs) Versus Warfarin Across Multiple Indications for Anticoagulation

Emma Brouillette, Pharm.D. Candidate, Thomas Morrell, Pharm.D. Candidate, Matthew Pari, Pharm.D. Candidate, Delaney Umbrianna, Pharm.D. Candidate

The University of Rhode Island College of Pharmacy, Kingston, RI



Additional Information

Background

- Oral anticoagulants are used for the prevention and treatment of thromboembolic conditions.
- Warfarin has been the standard therapy but requires routine International Normalized Ratio (INR) monitoring and has numerous drug and dietary interactions.¹
- Direct Oral Anticoagulants (DOACs) offer predictable pharmacokinetics, fixed dosing, and no need for routine monitoring.²
- While clinical trials show comparable or improved safety of DOACs compared to warfarin, real-world outcomes may vary based on patient-specific factors such as renal function, age, body mass index, comorbidities, and adherence.³
- Anticoagulant-related adverse events, particularly bleeding complications, are a major cause of hospitalization and healthcare utilization, making hospitalization an important real-world safety outcome.

Objectives

- To compare hospitalization rates among adults treated with DOACs (apixaban, rivaroxaban, and dabigatran) versus warfarin across multiple indications for anticoagulation

Methods

- Data sources:** Publicly available National Health and Nutrition Examination Survey (NHANES) 2017-2020 pre-pandemic data
- Study design:** Cross-sectional study assessing hospital prevalence across indications. Indications were categorized using ICD-10 codes
- Cohort selection:** Non-institutionalized U.S. adults ≥ 18 years reporting DOAC or warfarin use
- Inclusion criteria:** Age ≥ 18 years, self-reported DOAC or warfarin use within the past 30 days, and hospitalizations occurring within the past 12 months as self-reported by participants
- Exclusion criteria:** Age < 18 years, concurrent DOAC and warfarin use, institutionalized individuals, and hospitalizations occurring more than 12 months ago as self-reported by participants
- Exposure:** Self-reported use of DOACs (apixaban, rivaroxaban, dabigatran) versus warfarin at the time of data collection
- Outcome:** All-cause hospitalization within the past 12 months, defined as self-reported overnight hospital stay
- Covariates:** Demographics (age, sex, race/ethnicity, income), anticoagulation indication, lifestyle factors (smoking status, alcohol use), and comorbidities (high cholesterol, high blood pressure, diabetes, history of weak/failing kidneys)
- Statistical analysis:** Continuous variables were analyzed using t-test or Wilcoxon rank-sum tests, and categorical variables using chi-square tests. Multivariable logistic regression was used to estimate adjusted odds ratios (aORs) for hospitalization while controlling for covariates. All analyses were conducted using SPSS version 29.0 and a p-value < 0.05 was considered statistically significant

References

- Warfarin. Lexi-Comp. UpToDate Learning. UpToDate Inc. <https://www.uptodate.com/lookup/warfarin>. Accessed March 5, 2020
- Ruff CT, et al. Comparison of the efficacy and safety of new oral anticoagulants with warfarin in patients with atrial fibrillation: a meta-analysis of randomized trials. *Lancet*. 2014;383(9925):955-965. doi:10.1016/S0140-6736(14)62530-5
- Centers for Disease Control and Prevention (CDC). National Health and Nutrition Examination Survey. 2017-March-2020 Pre-Pandemic Data Documentation. <https://www.cdc.gov/nhanes/>

© 2023 The University of Rhode Island. All rights reserved. This document is intended for educational purposes only. All other trademarks are the property of their respective owners.

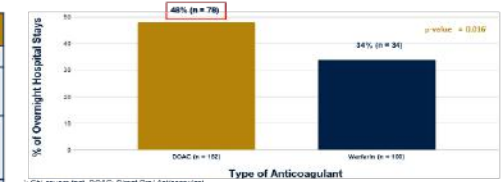
Results

Table 1. Comparing Demographic and Clinical Characteristics Between DOAC and Warfarin Users

Characteristics	DOAC (n = 162)	Warfarin (n = 100)	p-value (α = 0.05)
Age, years (mean ± SD)	71.05 ± 9.86	71.04 ± 11.73	0.992 [†]
Gender			0.583 [‡]
Male, N (%)	97 (60%)	50 (50%)	
Female, N (%)	65 (40%)	44 (44%)	
Race			0.038 [‡]
Non-Hispanic White, N (%)	92 (57%)	68 (68%)	
Non-Hispanic Black, N (%)	38 (22%)	10 (10%)	
Other Race, N (%)	34 (21%)	22 (22%)	
Current Smoker			0.792 [‡]
Yes, N (%)	12 (13%)	7 (12%)	
No, N (%)	78 (87%)	52 (88%)	
Indication			0.090 [‡]
Prevent Blood Clots, N (%)	75 (46%)	53 (53%)	
Atrial fibrillation/flutter, N (%)	35 (22%)	11 (11%)	
Other, N (%)	52 (32%)	38 (38%)	
Been Told You Had High Cholesterol			0.576 [‡]
Yes, N (%)	93 (56%)	54 (56%)	
No, N (%)	64 (41%)	43 (44.3%)	
Been Told You Had High Blood Pressure			0.090 [‡]
Yes, N (%)	122 (75%)	65 (65%)	
No, N (%)	40 (25%)	34 (34%)	
Been Told You Had Diabetes			0.021 [‡]
Yes, N (%)	50 (31%)	33 (33%)	
No, N (%)	103 (64%)	64 (63%)	
Unreported, N (%)	0 (0%)	4 (4%)	
History of Weak/Failing Kidneys			0.784 [‡]
Yes, N (%)	23 (14%)	13 (13%)	
No, N (%)	139 (86%)	87 (87%)	
Alcohol Use in the Past 12 Months			0.445 [‡]
None, N (%)	85 (49%)	37 (40%)	
Low (<11/year), N (%)	23 (17%)	12 (15%)	
Moderate (monthly), N (%)	13 (10%)	15 (18%)	
Frequent (weekly+), N (%)	31 (24%)	17 (21%)	
Income Ratio (Mean ± SD)	2.53 ± 1.56	2.73 ± 1.47	0.335 [†]

[†] Student's t test; [‡] Chi-square test. DOAC, Direct Oral Anticoagulant

Figure 1. Comparing Hospitalizations in the Past Year Between DOAC and Warfarin Users



[†] Chi-square test. DOAC, Direct Oral Anticoagulant

Table 2. Results of Multivariable Logistic Regression Analysis

Variable	Hospitalizations Adjusted OR	95% CI (Lower, Upper)	p-value (α = 0.05)
Drug			
Warfarin	Ref		
DOAC	2.78	1.05–7.38	0.040 [†]
Age (per 10 years)	Ref		
Age (per 10 years)	1.43	0.81–2.50	0.216 [†]
Gender			
Male	Ref		
Female	3.05	1.11–8.36	0.030 [†]
Current Alcohol Use			
No	Ref		
Yes	2.28	0.91–6.22	0.078 [†]
Been Told You Had Diabetes			
No	Ref		
Yes	1.58	0.60–4.13	0.364 [†]
Been Told You Had High Cholesterol			
No	Ref		
Yes	0.27	0.10–0.75	0.012 [†]
Been Told You Had High Blood Pressure			
No	Ref		
Yes	1.20	0.40–3.58	0.748 [†]
History of Weak/Failing Kidneys			
No	Ref		
Yes	1.76	0.52–6.02	0.361 [†]
Current Smoker			
No	Ref		
Yes	2.40	0.58–9.83	0.228 [†]
Non-Hispanic White			
No	Ref		
Yes	0.19	0.05–0.79	0.019 [†]
Below Poverty-Income Line			
Above (>1.2)	Ref		
Below (<1.2)	0.58	0.13–2.67	0.480 [†]
Indication			
Other	Ref		
Prevent Blood Clots	1.20	0.50–2.87	0.688 [†]

[†] Wald chi-square test. DOAC, Direct Oral Anticoagulant; Ref, Reference; p-value: 0.223

Discussion/Conclusion

- The only significant demographic difference between the groups was racial composition.
- In unadjusted analysis, DOAC users had a higher proportion of hospitalizations compared to warfarin users (48% vs 34%, $p = 0.016$).
- DOAC users had higher odds of all-cause hospitalization compared to warfarin users (aOR = 2.78; 95% CI: 1.05–7.38). Significant covariates affecting hospitalization rates were female sex (aOR 3.05; CI: 1.11–8.38), which was associated with higher odds, while hyperlipidemia (aOR 0.27; CI: 0.10–0.75) and non-Hispanic White race (aOR 0.19; CI: 0.05–0.79) were associated with lower odds (Table 2).
- Study Limitations/Potential Bias: cross-sectional design which cannot directly determine causality, data consisting of both self-reported medication use and self-reported hospitalizations, potential misclassification using ICD-10 codes, lack of adherence data, and small sample size.
- Findings suggest anticoagulant selection may influence hospitalization risk, supporting individualized therapy and risk stratification based on patient-specific factors.

Comparing Hospitalization Rates Among Patients Treated with Direct Oral Anticoagulants (DOACs) Versus Warfarin Across Multiple Indications for Anticoagulation

Emma Brouillette, Thomas Morrell, Matthew Pari, Delaney Umbrianna

Group 17

Considers hospitalization rates in adults using direct oral anticoagulants (DOACs) versus warfarin. The background explains that warfarin requires INR monitoring and has many interactions, while DOACs have more predictable dosing and typically do not require routine monitoring, but real-world outcomes can vary based on patient factors. The objective is to compare all-cause overnight hospitalization within the past year between adults using DOACs and those using warfarin, across multiple anticoagulation indications. In the discussion and conclusion, the authors report that DOAC users had a higher proportion of hospitalizations than warfarin users and higher odds of hospitalization after adjustment. They note limitations such as the cross-sectional design, self-reported medication use and hospitalizations, possible misclassification, lack of adherence data, and small sample size, and conclude that anticoagulant selection may relate to hospitalization risk and should be individualized using patient-specific factors and risk stratification.

The Comparative Prevalence of Anemia in Adults with Type II Diabetes Mellitus Receiving Metformin versus Sulfonylurea Therapy

Cailin McCaffrey, Willy Njeru, Elizabeth Orabona, Vanessa Varone
The University of Rhode Island College of Pharmacy

Background

Type 2 Diabetes Mellitus (T2DM) is a highly prevalent disease state with medication classes that influence glycemic control and complications, including insulin therapy.¹ Anemia in this population may arise from multiple medications, including long-term suppression, chronic disease processes, and vitamin B12 deficiencies, all of which are frequently observed in patients with chronic conditions such as T2DM. Prior studies have established that metformin use is associated with anemia and hematologic effects, primarily related to Vitamin B12 deficiency.^{2,3} Sulfonylureas such as glipizide, glimepiride, and glyburide are commonly prescribed alternative therapies that have not been consistently linked to hematologic abnormalities, though that evidence remains limited and heterogeneous.⁴ As the prevalence of patients with T2DM in the United States continues to rise, a direct comparison of the prevalence of anemia in patients taking these medications from a nationally representative sample is vital to developing individualized treatment plans that minimize any potential safety risks, establishing the clinical importance and applications of this study.

Objective

To determine the prevalence of anemia in patients with Type 2 Diabetes Mellitus receiving metformin versus glipizide, glimepiride, or glyburide (collectively referred to as "sulfonylurea") therapy.

Methods

- Data used was collected using the 2017-2020 National Health and Nutrition Examination Survey (NHANES).⁵ This is nationally representative data set and offers detailed demographic, medication use and laboratory data allowing for analysis of classification use and prevalence of anemia. Data to sample and variable restrictions complex survey weights were not studied.
- **Study Design:** This study utilized a cross-sectional analysis including adults ages 18 years and older with T2DM. Participants were categorized into treatment groups based on their reported use of metformin or sulfonylurea.
- **Inclusion Criteria:** U.S. adults >18 years with Type 2 Diabetes Mellitus (T2DM), identified using NHANES self-reported physician diagnosis of diabetes consistent with ICD-10 code E11 classification, and with available hemoglobin (Hb) laboratory data. Participants were included if they reported current use of either continuous or a combination (glipizide, glimepiride, or glyburide).
- **Exclusion Criteria:** Current use of metformin and a sulfonylurea, or if medication use or diabetes status data were missing or inconsistent with T2DM classification (ICD-10 E11).
- **Covariates:** Age, gender, body mass index (BMI), LDL cholesterol, history of hypertension, self-reported ever using alcohol, self-reported falling lifestyle status and the use of 9 or more concurrent medications were all included based on their clinical relevance and potential implications in patients with T2DM.
- **Exposure:** The primary exposure was antihyperglycemic medication class. Medication use was defined based on self-reported use in the past 30 days using NHANES data. NHANES does not provide specific dose, duration and exposure information therefore any self-reported users were included.
 - Metformin group: participants reporting use of metformin.
 - Sulfonylurea group: participants reporting use of glipizide, glimepiride, or glyburide.
 - Participants concurrently using metformin and a sulfonylurea were excluded.
- **Outcome:** The primary outcome was anemia, defined using hemoglobin threshold consistent with abnormal CDC criteria: Hemoglobin <13 g/dL in males and <12 g/dL in women. Anemia was analyzed as a binary variable.
 - Hb<13 will be no difference in anemia prevalence between metformin users and sulfonylurea users.
 - Hb<12 will have higher prevalence of anemia compared to sulfonylurea users.

References

1. Abbott RD, et al. Diabetes Care. 2002;25(4):625-632.
2. American Diabetes Association. 2018 Standards of Medical Care in Diabetes. 13.2. Anemia. https://doi.org/10.2337/s1366-3055-18-00000.
3. American Diabetes Association. 2018 Standards of Medical Care in Diabetes. 13.2. Anemia. https://doi.org/10.2337/s1366-3055-18-00000.
4. American Diabetes Association. 2018 Standards of Medical Care in Diabetes. 13.2. Anemia. https://doi.org/10.2337/s1366-3055-18-00000.
5. National Center for Health Statistics. 2018. National Health and Nutrition Examination Survey Data, 2017-2020. www.nhanes.gov. Accessed Feb 10, 2023.

Results

Table 1. Comparing Demographic and Clinical Characteristics Between Comparison Groups

Characteristic	Group 1: Metformin (N=11,412)	Group 2: Sulfonylurea (N=7,736)	P-value
Age (Mean ± SD)	62.14 ± 12.25	64.17 ± 11.28	<0.0001
Gender			
Male, N (%)	55,118 (70)	117,089 (76)	0.0002
Female, N (%)	59,014 (51)	144,047 (54)	
LDL (Mean ± SD)	160.00 (50.00)	163.00 (50.00)	0.1617
Body Mass Index (Mean ± SD)	27.84 ± 7.89	27.00 ± 7.87	<0.0001
Estimated Mean Hb (Mean ± SD)	13.14 (0.76)	12.96 (0.76)	0.0007
History of Hypertension (N (%))	59,014 (51)	144,047 (54)	
History of Diabetes (N (%))	59,014 (51)	144,047 (54)	<0.0001
History of Alcohol Use (N (%))	11,412 (51)	7,736 (54)	0.1967
History of Falling Lifestyle (N (%))	11,412 (51)	7,736 (54)	0.0007
History of 9+ Concurrent Medications (N (%))	11,412 (51)	7,736 (54)	<0.0001

Table 2. Comparing Frequencies of the Outcome Variables Between Comparison Groups

Outcome	Group 1: Metformin (N=11,412)	Group 2: Sulfonylurea (N=7,736)	P-value
Hemoglobin Level, mg/dL			
Mean ± SD	Mean = 13.19 SD = 1.19	Mean = 13.65 SD = 1.54	0.5607
Anemia** (N (%))	70 (14.4%)	47 (18.2%)	0.5607
Hb<12* (N (%))	415 (85.6%)	243 (89.8%)	

Table 3. Results of Multivariable Logistic Regression Analysis

Characteristic	Adjusted Odds Ratio	95% Confirmed Interval
Metformin vs. Sulfonylurea (reference)	1.06	(0.67-1.67)
Age, per 10 year increase	1.2	(0.97-1.49)
Female vs. Male (reference)	2.19	(0.76-6.48)
BMI (Obese/Overweight vs Normal Underweight) (reference)	0.68	(0.53-0.88)
Hypertension, yes vs no	1.57	(0.85-2.93)
Alcohol, ever vs no	2.14	(0.85-5.42)
History of Diabetes, yes vs no	2.90	(1.37-6.20)
Polypharmacy (≥ 9 medications), yes vs no	2.10	(1.25-3.76)

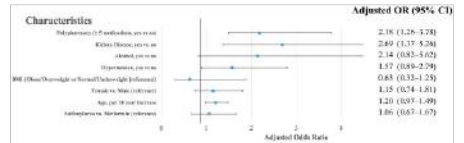
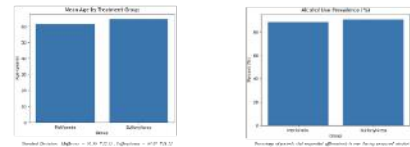


Figure 1: Forest Plot of Adjusted Odds Ratios From Multivariable Logistic Regression for Anemia in Adults with Type 2 Diabetes

Discussion/Conclusion

- The null hypothesis was confirmed, as no statistically significant difference in anemia prevalence was observed between patients taking metformin and glimepiride, glipizide, or glyburide as self-reported in the last 30 days. These findings support the initial hypothesis that there would be no difference in anemia prevalence between treatment groups.
- Age was not a significant confounder with sulfonylurea users >3 years older than metformin users.
- Also of note, LDL was excluded from the multivariable regression analysis due to more than 50% of data missing which could compromise power and increase bias/potential.
- A major limitation of this study was the small sample size of the NHANES data set, as well as the inability to establish causality using a cross-sectional study. Medication exposure was limited to self-reported use within the past 30 days and did not capture dose, duration, or cumulative exposure. Thus, misclassification of long-term metformin or sulfonylurea use is possible, potentially biasing results toward the null. Furthermore, the analysis did not adjust for concurrent medications which could independently affect hemoglobin parameters. These limitations introduce potential confounding and preclude attribution of observed anemia solely to the study drugs. Additionally, the inability to account for NHANES sampling design (strata, weights, and clustering) may limit generalizability.
- Other factors such as alcohol consumption metrics, medication indication, duration of medication use, and influence of other medications were unmeasured confounding factors and their influence on anemia prevalence in those with T2DM could not be assessed.
- A major strength of this study was that due to the fact it was retrospective and cross-sectional it was highly cost-effective.
- Despite the known potential of metformin to impact vitamin B12 and iron absorption, this effect did not result in a significantly higher incidence of anemia compared to sulfonylurea use. Clinically, these findings suggest short-term anemia risk may not differ between therapies, however, ongoing monitoring of hematologic parameters and vitamin B12 levels, especially with long-term metformin use, are worthy future considerations.
- Additional studies that take place over longer periods of time and include vitamin deficiencies, bone marrow suppression, and stratified comparisons of alcohol use with vitamin deficiencies, may better establish the true difference between glimepiride, glipizide, glyburide and metformin.
- Future studies should assess medication related anemia prevalence longitudinally accounting for variations in severity and glycemic control and further assess the implications of significant covariates such as kidney function and polypharmacy.

The Comparative Prevalence of Anemia in Adults with Type II Diabetes Mellitus Receiving Metformin versus Sulfonylurea Therapy

Cailin McCaffrey, Willy Njeru, Elizabeth Orabona, Vanessa Varone

Group 19

Compares adults with type 2 diabetes who are taking metformin versus those taking sulfonylureas (glipizide, glimepiride, or glyburide) to see whether anemia is more common in one group. The background explains that anemia can occur in people with type 2 diabetes for several reasons, and that metformin has been linked to anemia mainly through vitamin B12 deficiency, while evidence for sulfonylureas is more limited. The objective is to determine and compare the prevalence of anemia between these treatment groups using NHANES data. In the discussion and conclusion, the authors report that they did not find a statistically significant difference in anemia prevalence between metformin users and sulfonylurea users. They note important limitations such as small sample size, cross-sectional design, and self-reported short-term medication exposure, which could hide longer-term effects. They conclude that short-term anemia risk may not differ between therapies, but suggest continued monitoring—especially with long-term metformin use—and recommend longer-term studies that include vitamin deficiency measures.

Association Between Hydrochlorothiazide Use and Metabolic Syndrome Compared to Furosemide in U.S. Adults

Isabel Savinon, Ryan Min, Shakir Pike, Tyler Wallace
University of Rhode Island, College of Pharmacy

THE UNIVERSITY OF RHODE ISLAND COLLEGE OF PHARMACY

THINK BIG WE DO

Background

Diuretics such as hydrochlorothiazide and furosemide are commonly used in the management of hypertension and fluid-related conditions. Thiazide diuretics have been associated with metabolic abnormalities, including dyslipidemia, insulin resistance, and components of metabolic syndrome in U.S. adults. However, there is limited evidence directly comparing the association between hydrochlorothiazide and furosemide with metabolic syndrome in U.S. adults. Metabolic syndrome is a major risk factor for cardiovascular disease and mortality.

Objectives

To evaluate whether hydrochlorothiazide use is associated with metabolic syndrome compared to furosemide in U.S. adults

Methods

- ❖ A cross-sectional study was conducted using data from the 2017-2020 National Health and Nutrition Examination Survey (NHANES).
 - ▶ **Inclusion Criteria:** Adults ages ≥18 years reporting use of hydrochlorothiazide or furosemide and had sufficient data to assess metabolic syndrome status using ATP III criteria.
 - ▶ **Exclusion Criteria:** Participants were excluded for dual diuretic use, age <18 years, or missing data for metabolic syndrome or covariate data.
- ❖ **Exposure:** Self-reported use of hydrochlorothiazide or furosemide, with furosemide serving as the reference group.
- ❖ **Primary outcome** was dichotomized as presence or absence of metabolic syndrome. Metabolic syndrome was defined using ATP III criteria, requiring ≥3 of the following: abdominal obesity defined by waist circumference thresholds, elevated triglycerides, reduced HDL cholesterol, elevated blood pressure, or elevated fasting glucose.
- ❖ **Covariates:** Age (young <56 years vs. old ≥56 years per sample distribution), sex, race/ethnicity, alcohol use, smoking status, and heart failure ICD-10 code.
- ❖ All variables were categorized and were compared between exposure groups using chi-square tests; Fisher's exact test was used for heart failure due to small cell counts. Multivariable logistic regression was performed to estimate adjusted odds ratios (ORs) and 95% confidence intervals (CIs) for the association between hydrochlorothiazide use and metabolic syndrome, adjusting for covariates. Model fit was assessed using the Hosmer-Lemeshow goodness-of-fit test. Statistical significance was defined as $p < 0.05$. All analyses were conducted using SPSS 29.0.

References

1. Di Fulvio M, Rathod YD, Khader S. Diuretics: a review of the pharmacology and effects on glucose homeostasis. *Front Pharmacol*. 2025;16:1513125. Published 2025 Mar 28. doi:10.3389/fphar.2025.1513125
2. Preston RA, Alshartouf D, Cacoparla EV, et al. Thiazide-Sensitive Na^+Cl^- Cotransporter in Human Metabolic Syndrome: Sodium Sensitivity and Potassium-Induced Natriuresis. *Hypertension*. 2021;77(2):447-460. doi:10.1161/HYPERTENSIONAHA.120.15933
3. Sica DA, Carter B, Cushman W, Hamm L. Thiazide and loop diuretics. *J Clin Hypertens (Greenwich)*. 2011;13(9):639-643. doi:10.1111/j.1751-7178.2011.00572.x
4. Expert Panel on Detection, Evaluation, and Treatment of High Blood Cholesterol in Adults. Executive summary of the third report of the National Cholesterol Education Program (NCEP) Adult Treatment Panel III. *JAMA*. 2001;285(19):2486-2497.

Results

Table 1. Comparing Demographic and Clinical Characteristics between HCTZ and Furosemide Users

Characteristic	HCTZ N=114	Furosemide N=114	P value
Age	Young (<56 years), N (%) Old (≥56 years), N (%)	38 (33.4) 295 (28.1)	<0.001
Gender	Female, N (%) Male, N (%)	149 (49.1) 148 (29.3)	0.109
Race	Non-Hispanic White, N (%) Hispanic, N (%) Non-Hispanic Black, N (%) Other/Multi/Race, N (%)	27 (24.2) 39 (35.7) 120 (24.4) 156 (75.7)	<0.001
Ethnicity	Non-Hispanic, N (%) Hispanic, N (%)	103 (90.4) 11 (9.6)	<0.001
Current Smoking	Yes, N (%) No, N (%)	111 (97.4) 3 (2.6)	0.872
Heart Failure (ICD-10 E11)	Yes, N (%) No, N (%)	34 (29.8) 80 (70.2)	<0.001
Hypertension	Yes, N (%) No, N (%)	108 (94.7) 6 (5.3)	<0.001
BMI	Overweight (BMI ≥25 kg/m ²), N (%) Not Overweight (BMI <25 kg/m ²), N (%)	100 (88.1) 14 (12.4)	<0.001
Presence of T2DM**	Yes, N (%) No, N (%)	228 (20.1) 912 (80.9)	<0.001

Note: * Chi-square test; ** Fisher's exact test; *HCTZ = Hydrochlorothiazide; **T2DM = Type 2 diabetes mellitus.

Table 2. Raw Comparison of Metabolic Syndrome Between HCTZ and Furosemide Users

Outcomes	HCTZ N=114	Furosemide N=114	P value
Metabolic Syndrome Presence			
No Metabolic Syndrome, N (%)	26 (22.8)	26 (23.1)	0.513
Metabolic Syndrome, N (%)	121 (107.2)	99 (86.9)	

Note: * Chi-square test; *HCTZ = Hydrochlorothiazide. No statistically significant difference in metabolic syndrome was observed between groups ($p = 0.513$).

Table 3. Results of Multivariable Logistic Regression Analyses for the Risk of Metabolic Syndrome

Characteristics	Adjusted Odds Ratio	95% CI
HCTZ* vs. Furosemide	0.84	(0.38-2.06)
Age (Old ≥56 vs. Young <55)	1.23	(0.37-4.06)
Female vs. Male	0.99	(0.39-2.51)
Alcohol Use (Never vs. Frequent)	0.47	(0.14-1.59)
Alcohol Use (Infrequent vs. Frequent)	0.71	(0.24-2.06)
Current Smoking (Yes vs. No)	1.67	(0.61-4.55)
Non-Hispanic Black vs. White	0.69	(0.25-1.91)
Hispanic vs. White	0.51	(0.15-1.75)

Note: *HCTZ = Hydrochlorothiazide. Hypertension, BMI, and type 2 diabetes mellitus were excluded as covariates, as they are components of metabolic syndrome. Heart failure was excluded due to small sample size. No significant association was observed between HCTZ use and metabolic syndrome (OR 0.84, 95% CI 0.38-2.06). The Hosmer-Lemeshow goodness-of-fit test was not statistically significant ($p = 0.180$), indicating adequate model fit.

Discussion/Conclusion

- ❖ Prior studies suggest thiazide diuretics may contribute to metabolic abnormalities when compared with non-use or the general population. In contrast, the present analysis compares hydrochlorothiazide with furosemide, which are often used in different clinical populations, limiting direct comparability with prior findings. No statistically significant difference in metabolic syndrome was observed between groups ($p=0.513$).
- ❖ The lack of significant association in this study suggests that observed metabolic effects may be influenced by underlying comorbidities and patient characteristics rather than the medication itself.
- ❖ Utilizing a nationally representative dataset (NHANES) enhances generalizability to the U.S. adult population. The analysis adjusted for multiple demographic and clinical covariates, improving validity of the observed associations. Metabolic syndrome was defined using standardized ATP III criteria, ensuring consistency and reliability in outcome assessment.
- ❖ The cross-sectional study design limits the ability to establish causal relationships. The relatively small sample size may have reduced statistical power to detect significant associations. Residual confounding may be present due to unmeasured factors such as renal function and disease severity, which may influence both diuretic selection and metabolic risk. Co-medication use was not accounted for and may serve as a proxy for underlying metabolic syndrome risk. Medication use was self-reported, which may introduce misclassification bias.
- ❖ Hydrochlorothiazide use was not significantly associated with metabolic syndrome compared to furosemide after adjustment for covariates. Clinically, diuretic selection should continue to be individualized based on patient-specific factors and comorbidities. Further studies with larger sample sizes and longitudinal designs are needed to better evaluate this relationship.

Association Between Hydrochlorothiazide Use and Metabolic Syndrome Compared to Furosemide in U.S. Adults

Isabel Savinon, Ryan Min, Shakir Pike, Tyler Wallace

Group 20

Profiles two diuretics—hydrochlorothiazide and furosemide—and asks whether hydrochlorothiazide use is linked to metabolic syndrome in U.S. adults. The background explains that thiazide diuretics have been associated with metabolic problems, but there is limited evidence directly comparing hydrochlorothiazide with furosemide for metabolic syndrome risk. The objective is to evaluate whether hydrochlorothiazide use is associated with metabolic syndrome compared with furosemide. In the discussion and conclusion, the authors report that no statistically significant difference in metabolic syndrome was observed between the groups, and they suggest that underlying patient characteristics and comorbidities may influence observed metabolic effects more than the medication choice alone. They note limitations such as the cross-sectional design, relatively small sample size, and possible unmeasured confounding, and conclude that hydrochlorothiazide was not significantly associated with metabolic syndrome compared with furosemide after adjustment; they recommend larger, longitudinal studies.

Ratio of Family Income-to-Poverty and the Antidepressant Treatment Gap Among U.S. Adults Aged 18-74 with Moderate-to-Severe Depressive Symptoms: NHANES Cross-Sectional Analysis

Ari Cano, Reva Goyal, Flora Khoury, Cassidy Pepin
University of Rhode Island, College of Pharmacy

Background

Moderate-to-severe depressive symptoms are associated with substantial functional impairment and increased healthcare utilization¹. Although socioeconomic disparities in depression are well documented, it remains unclear whether antidepressant treatment engagement differs by income² among adults with clinically significant symptoms (Patient Health Questionnaire-9 score ≥ 10), a key health equity and managed-care issue³.

Objectives

To evaluate whether lower household income, measured by family income-to-poverty ratio (PIR), is associated with antidepressant non-use among U.S. adults with clinically significant depressive symptoms (Patient Health Questionnaire-9 [PHQ-9] score ≥ 10). We hypothesized that lower PIR would be associated with a greater likelihood of antidepressant non-use.

Methods

- Study design:** Retrospective cross-sectional analysis of the 2017-March 2020 National Health and Nutrition Examination Survey (NHANES) pre-pandemic cycle (United States). Analyses were conducted using SPSS 29.0
- Inclusion criteria:** U.S. adults 18-74 years with clinically significant symptoms (PHQ-9 ≥ 10 (moderate-to-severe depressive symptoms))⁴
- Exclusion criteria:** Missing family income-to-poverty ratio (PIR) or missing PHQ-9 data.
- Exposure:** Household income, categorized as PIR:
 - PIR < 1.00 (below poverty level)
 - PIR 1.00-1.99 (near poverty level)
 - PIR ≥ 2.00 (above poverty level; reference category)
- Rationale (design):** NHANES provides a nationally representative sample, appropriate for estimating income-related differences in treatment engagement at the population level
- Outcome (binary logistic regression):** Antidepressant non-use among participants with PHQ-9 ≥ 10 , defined as no antidepressant use in the past 30 days (NHANES prescription medication inventory, e.g., sertraline, fluoxetine, venlafaxine, duloxetine, bupropion)
 - Ha: There is no difference in antidepressant non-use across PIR categories
 - Hb: Antidepressant non-use differs across PIR categories (lower PIR is associated with higher antidepressant non-use)
- Rationale (outcomes):** PHQ-9 ≥ 10 is representative of major depression over the past 30 days where active treatment should be considered⁵; the NHANES 30-day medication inventory captures current antidepressant use
- Covariates:** Age, gender, race/ethnicity, smoking status, alcohol use, education level, total PIR score, and number of prescription medications
- Statistical analyses:** Baseline characteristics compared across PIR categories using ANOVA (continuous variables) and χ^2 tests (categorical variables)
 - Multivariable logistic regression estimated adjusted odds ratios (aORs) comparing PIR categories while controlling for covariates.
 - Statistical significance was defined as $\alpha = 0.05$

References

1. Kessler RC, et al. (2002) The burden of major depression. *Arch Gen Psychiatry* 59: 15-22.
2. Kessler RC, et al. (2006) The burden of major depression. *Arch Gen Psychiatry* 63: 15-22.
3. Kessler RC, et al. (2006) The burden of major depression. *Arch Gen Psychiatry* 63: 15-22.
4. Kessler RC, et al. (2006) The burden of major depression. *Arch Gen Psychiatry* 63: 15-22.
5. Kessler RC, et al. (2006) The burden of major depression. *Arch Gen Psychiatry* 63: 15-22.

Results

Figure 1. Mean PIR Relative to the Poverty Threshold by PIR Category Among U.S. Adults Aged 18-74 with PHQ-9 ≥ 10

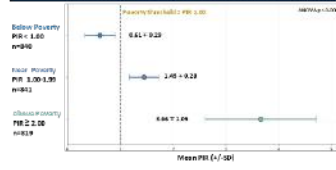


Figure 2. Mean PHQ-9 Score by PIR Category Among U.S. Adults Aged 18-74 with PHQ-9 ≥ 10

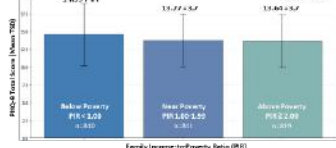


Table 2. Unadjusted Antidepressant Non-Use by PIR Category Among U.S. Adults Aged 18-74 with PHQ-9 ≥ 10

PIR Category	Non-Use (%)	n
Below Poverty (PIR < 1.00)	88.2%	101 (14.1%)
Near Poverty (PIR 1.00-1.99)	89.2%	214 (30.2%)
Above Poverty (PIR ≥ 2.00)	82.2%	222 (31.9%)

Figure 3. Adjusted Association Between PIR Category and Antidepressant Non-Use (Reference: PIR ≥ 2.00 ; Adults Aged 18-74 with PHQ-9 ≥ 10)

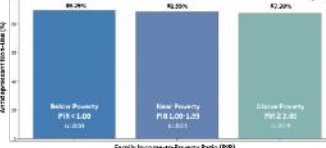


Table 3. Adjusted Association Between PIR and Antidepressant Non-Use Among U.S. Adults Aged 18-74 with PHQ-9 ≥ 10

Characteristic	Adjusted Odds Ratio	95% CI	P-Value
PIR < 1.00 (Below Poverty)	1.14	(0.63, 2.07)	0.666
PIR 1.00-1.99 (Near Poverty)	1.38	(0.79, 2.42)	0.258
Age (per 1-year increase)	1.02	(1.00, 1.04)	0.031
Total Patient Health Questionnaire-9 score (per 1-point increase)	1.09	(0.96, 1.23)	0.007
Male	Substance	—	—
Female	0.85	(0.61, 1.17)	0.320
Non-Hispanic White	Substance	—	—
Non-Hispanic Black	1.27	(0.68, 2.36)	0.455
Hispanic or Other Race	1.21	(0.74, 1.97)	0.433
Not current smoker	Substance	—	—
Current smoker	1.24	(0.79, 2.00)	0.367
Lower frequency alcohol use ^a	Substance	—	—
Higher frequency alcohol use ^b	0.91	(0.66, 1.25)	0.597
College degree	Substance	—	—
HS diploma/GED ^c	0.82	(0.64, 1.07)	0.173
No HS diploma/GED ^d	0.87	(0.62, 1.21)	0.397
Number of prescription medications (per 1 medication increase)	1.03	(0.98, 1.07)	0.006

Table 1. Baseline Characteristics of U.S. Adults Aged 18-74 with PHQ-9 ≥ 10 , by PIR Category (N=2500)

Characteristic	Non-Poverty (PIR < 1.00, n=842)	Near Poverty (PIR 1.00-1.99, n=882)	Above Poverty (PIR ≥ 2.00 , n=776)	P-Value
Age (Mean \pm SD)	52.02 \pm 12.8	52.08 \pm 12.8	52.02 \pm 12.2	0.087
Gender	Female, n=170; Male, n=170	Female, n=170; Male, n=170	Female, n=170; Male, n=170	0.004
Race	Non-Hispanic White, n=170; Non-Hispanic Black, n=170; Hispanic, n=170	Non-Hispanic White, n=170; Non-Hispanic Black, n=170; Hispanic, n=170	Non-Hispanic White, n=170; Non-Hispanic Black, n=170; Hispanic, n=170	0.004
Smoking	Current smoker, n=170; Not current smoker, n=170; Missing, n=170	Current smoker, n=170; Not current smoker, n=170; Missing, n=170	Current smoker, n=170; Not current smoker, n=170; Missing, n=170	0.007
Alcohol use	Lower alcohol use, n=170; Higher alcohol use, n=170; Missing, n=170	Lower alcohol use, n=170; Higher alcohol use, n=170; Missing, n=170	Lower alcohol use, n=170; Higher alcohol use, n=170; Missing, n=170	0.007
Education level (reference ≥ 2.0)	HS diploma/GED, n=170; HS diploma/GED, n=170; College degree, n=170; Missing/unknown, n=170	HS diploma/GED, n=170; HS diploma/GED, n=170; College degree, n=170; Missing/unknown, n=170	HS diploma/GED, n=170; HS diploma/GED, n=170; College degree, n=170; Missing/unknown, n=170	0.002
Number of prescription medications (reference ≥ 0)	0.62 \pm 0.3	0.79 \pm 0.4	0.75 \pm 0.4	0.007

Discussion & Conclusion

- After adjustment, PIR category was not significantly associated with antidepressant non-use among U.S. adults aged 18-74 with PHQ-9 ≥ 10 .
 - Below poverty vs. above poverty: aOR 1.14; 95% CI 0.63-2.07; $p = 0.666$
 - Near poverty vs. above poverty: aOR 1.38; 95% CI 0.79-2.42; $p = 0.258$
 - PIR alone may not fully explain antidepressant non-use; other clinical, access-related, and patient factors may influence treatment patterns
- Older age (each 1-year increase in age) was associated with slightly higher adjusted odds of antidepressant non-use.
 - Age: aOR 1.02 per 1-year increase; 95% CI 1.00-1.04; $p = 0.031$
- The wide confidence intervals around the adjusted odds ratios suggest limited precision and indicate that modest income-related differences may have gone undetected.
- Limitations:**
 - NHANES sampling weights and complex survey design were not incorporated, which may affect variance estimates and limit generalizability.
 - The cross-sectional study design limits causal inference and prevents assessment of temporality.
 - PHQ-9 ≥ 10 indicates clinically relevant depressive symptom burden, but is not a confirmed diagnosis of depression.
 - Antidepressant use was based on self-reported past 30-day medication inventory and may misclassify treatment status indication, adherence, dose, and duration were unavailable.
 - Complete case analysis may have introduced selection bias if excluded participants differed systematically from included participants.
 - Likely residual confounding remains, particularly related to healthcare access factors and socioeconomic context, such as insurance status, typical care, psychotherapy use, and out-of-pocket costs.
- Clinical Implication:** Even though PIR was not independently associated with antidepressant non-use in this analysis, treatment use remained low across income groups, suggesting that improving depression care may require strategies that extend beyond income-based risk stratification alone.
- Conclusion & Further Research:** In this NHANES-based sample of adults with moderate-to-severe depressive symptoms, PIR was not independently associated with antidepressant non-use after adjustment. Broader clinical and healthcare access barriers may better explain treatment gaps and should be examined in future research.

Ratio of Family Income-to-Poverty and the Antidepressant Treatment Gap Among U.S. Adults Aged 18-74 with Moderate-to-Severe Depressive Symptoms: NHANES Cross-Sectional Analysis

Ari Cano, Reva Goyal, Flora Khoury, Cassidy Pepin
Group 21

Examines whether household income is linked to a “treatment gap” in depression care among U.S. adults with moderate-to-severe depressive symptoms. The background explains that people with higher depression symptom burden often have significant impairment, and while lower income is linked to depression risk, it is less clear whether antidepressant treatment engagement differs by income among adults with PHQ-9 scores of 10 or higher. The objective is to test whether lower family income-to-poverty ratio (PIR) is associated with not taking antidepressants among adults aged 18–74 with PHQ-9 ≥ 10 . In the discussion and conclusion, the authors report that after adjustment, PIR category was not significantly associated with antidepressant non-use, and that treatment non-use was high across all income groups. They note limitations such as not incorporating survey weights, cross-sectional design, and limited medication details, and conclude that barriers beyond income alone may better explain antidepressant treatment gaps and should be explored in future research.

Comparing the Prevalence of Abnormal Kidney Function in Type 2 Diabetic Patients on SGLT2 Inhibitors versus Other Oral Antidiabetic Medications

Authors: Ben Cassellius, Annessa Mon, Zoe Plaisted, and Meghan Rigby
University of Rhode Island, College of Pharmacy

Background

Sodium-glucose cotransporter-2 (SGLT2) inhibitors have been extensively studied for renal outcomes in patients with type 2 diabetes mellitus (T2DM), with clinical trials and observational studies suggesting renal-protective effects^{1,2,4}. However, less is known about how these findings translate to broad population-level, cross-sectional datasets comparing SGLT2 inhibitor users with patients taking other oral antidiabetic medications^{5,6}. Because real-world comparator groups are often heterogeneous and may differ in important clinical characteristics, further evaluation in representative survey populations remains warranted^{1,4,5,7}.

Objective

To examine whether use of SGLT2 inhibitors, compared with use of other oral antidiabetic medications, was associated with lower prevalence of abnormal kidney function among adults with T2DM in NHANES 2017–2020.

Methods

- ❖ **Data Source:** Data collected from the 2017 to 2020 National Health and Nutrition Examination Survey; Prescription Medication Drug Information data files
- ❖ This cross-sectional study includes adults diagnosed with T2DM who were prescribed an SGLT2 inhibitor or any other oral antidiabetic agent.
- ❖ **Inclusion:** SGLT2 inhibitors including empagliflozin, dapagliflozin, canagliflozin, and ertugliflozin. Non-SGLT2 group of antidiabetic agents included several classes of drugs including first generation and second sulfonylureas, meglitinides, biguanides, thiazolidinediones, α-glucosidase inhibitors, DPP-4 inhibitors, cyclotols, amylin mimetic drugs, and bic acid sequestrants.
- ❖ **Exclusion:** Injectable diabetic therapies were not examined.
- ❖ **Exposure:** Was defined based on prescription records, with patients categorized into two groups: those prescribed SGLT2 inhibitors (defined as anyone with a prescription where RXDRUG contains an SGLT2 ingredient), and the comparison group was defined as patients on any other oral diabetic medication (excluding those with any SGLT2 ingredient).
- ❖ **Covariates:** Age, gender, and history of hypertension
- ❖ **Outcome:** The prevalence of abnormal kidney function, was assessed using multiple methods.
 - H₀ - There will be no difference in the prevalence of abnormal kidney function in T2DM patients taking SGLT2 inhibitors compared to other oral antidiabetics
 - H₁ - Patients taking SGLT2 inhibitors will have a lower prevalence of abnormal kidney function compared to patients on other oral antidiabetic medications
- ❖ These methods included measurements of abnormal urinary albumin levels, indicated by a URDACT >30 mg/g, as well self-reported kidney disease (KIQ022 “ever told you had weak or failing kidneys?”), along with ICD-10 codes indicative of kidney dysfunction, and lastly laboratory biomarkers including abnormal creatinine or estimated glomerular filtration rate.
- ❖ Albumin-creatinine ratio (ACR) was evaluated both as a continuous and categorical variable. Continuous values were used to assess overall distribution and variability, while a categorical definition (ACR >30 mg/g) was used to define clinically relevant abnormal kidney function based on established clinical thresholds.
- ❖ All analysis were conducted using SPSS version 29.0.
- ❖ P-value <0.05 was considered statistically significant.

Results

Table 1: Comparing Demographics and Clinical Characteristics between Comparison Groups

Characteristics	SGLT2 Inhibitors N= 74	Other Oral Anti-Diabetic Medications N= 938	P-value
AGE, Years, Mean ± SD	59.34 ± 10.27	63.33 ± 12.22	0.002 ¹
Gender, N(%)			0.075 ³
Female	26 (35.1%)	437 (46.6%)	
Male	48 (64.9%)	501 (53.4%)	
Ever told you had weak/failing kidneys? N (%)			0.412 ²
Yes	4 (5.4%)	83 (8.8%)	
No	70 (94.6%)	847 (90.3%)	
Kidney Related ICD-10 Codes, P(%)			0.340 ²
Yes	4 (5.4%)	33 (3.5%)	
No	70 (94.6%)	905 (96.5%)	

Note:
¹ Student t-test;
² Chi-square Test;
³ Fisher's exact test
 P values for continuous variables were calculated using the independent-samples t test. P values for categorical variables were calculated using the chi-square test or Fisher's exact test when expected cell counts were small. Values are presented as mean ± SD or N (%).
 Abbreviations: SD, standard deviation; ICD-10, International Classification of Disease, 10th Revision

Table 2: Comparison Frequencies of the Outcome Variable between Exposure Groups

Outcomes	SGLT2 N=74	Other Oral Anti-Diabetic Medications N=938	P-value
Albumin creatinine ratio (mg/g) Median (IQR)	11.20 (33.03)	14.74 (42.89)	0.440 ¹
Albumin creatinine ratio (mg/g) Abnormal, N (%)** Normal, N (%)**	22 (33.3%) 44 (66.7%)	405 (33.5%) 803 (66.5%)	0.974 ²

Note:
¹ Albumin ACR was defined as > 30 mg/g
² Normal ACR was defined as < 30 mg/g
³ Mann-Whitney U test
⁴ Chi-square test
 P values were calculated using the Mann-Whitney U test for continuous data and the chi-square test of independence for categorical data.

Table 3: Results of Multivariable Logistic Regression Analysis

Characteristics	Adjusted Odds Ratio	95%CI
Diabetic Medication		
Other Oral Anti-Diabetic Medications	(Ref.)	0.34-1.83
SGLT2 Inhibitors	0.79	
Age, every 10 years older	1.38	1.14-1.67
Gender		
Male	(Ref.)	0.63-1.41
Female	0.94	
History of Hypertension		
No	(Ref.)	1.53 - 5.62
Yes	2.93	

Note:
 Adjusted odds ratios (AORs) and 95% confidence intervals were estimated using multivariable binary logistic regression. Other oral anti-diabetic medications and male sex were used as reference categories. Age was modeled per 10-year increase. Hypertension was defined using the NHANES variable BPQ020 (ever told you had high blood pressure). Confidence intervals that do not include 1.00 were considered statistically significant.
 Hosmer-Lemeshow goodness-of-fit: p = 0.101

Conclusion/Discussion

- ❖ SGLT2 inhibitors were evaluated for their potential renal-protective effect compared with other oral antidiabetic medications
- ❖ In this cross-sectional NHANES analysis, SGLT2 inhibitor use was not associated with a statistically significant lower prevalence of abnormal kidney function compared to use of other oral antidiabetic medications after limited adjustment.
- ❖ Although prior trials support renal benefits with SGLT2 inhibitors, the benefits were not clearly demonstrated in this real-world dataset.
- ❖ Age emerged as the strongest predictor of abnormal kidney function.
- ❖ These findings should be interpreted cautiously. The small SGLT2 sample size, heterogeneous comparator group, potential residual confounding, and possible outcome misclassification may have limited the ability to detect differences between groups.
- ❖ These results should be considered hypothesis-generating rather than definitive.
- ❖ Larger real-world studies with more clinical covariates and longer follow-up are needed to better assess renal outcomes associated with SGLT2 inhibitors
- ❖ Larger Albumin-Creatinine ratio (ACR) shows high variability and a likely skewed distribution. Therefore, median and interquartile range may better represent the data than mean and standard deviation.
- ❖ Major Limitation: NHANES sampling weights and complex survey design were not incorporated into the analysis, which may limit the generalizability of findings to the broader U.S. population.

References

1. Tanne CD, Del Buono S, Avogaro A, Scialò A. Challenges and opportunities in real-world evidence on the renal effectiveness of sodium-glucose cotransporter 2 inhibitors. *Diabetes Care*. 2022;45(11):1899-1909.
2. Kishimoto T, Park H, et al. Effect of sodium-glucose cotransporter 2 inhibitors on kidney function in patients with type 2 diabetes: a meta-analysis of randomized controlled trials. *Pharmacotherapy*. 2023;43(5):222-230. doi:10.1093/ptp/ptac019
3. Kim H, Zhang H, Mannan M, et al. Lower risk of hospitalization for heart failure, kidney disease and death with sodium-glucose cotransporter 2 inhibitors compared with other antidiabetic medications in type 2 diabetes: evidence of renal and cardiovascular benefits. *A retrospective cohort study in the primary care database*. *Diabetologia*. 2023;66(11):2000-2007.
4. Kishimoto T, Langer M, Geyer H, et al. Trends in medication utilization over time among individuals with type 2 diabetes: a retrospective, population-based study. *Diabetes Care*. 2024;47(6):1086-1092. doi:10.2337/240422
5. Rigby M, Riddick A, Simon M, et al. Prevalence of kidney disease among type 2 diabetes patients in the United States: a cross-sectional study. *Diabetes Care*. 2023;46(10):1800-1807. doi:10.2337/230107
6. Kishimoto T, Langer M, Geyer H, et al. Trends in medication utilization over time among individuals with type 2 diabetes: a retrospective, population-based study. *Diabetes Care*. 2024;47(6):1086-1092. doi:10.2337/240422
7. Langer M, Kishimoto T, Geyer H, et al. Trends in medication utilization over time among individuals with type 2 diabetes: a retrospective, population-based study. *Diabetes Care*. 2024;47(6):1086-1092. doi:10.2337/240422

Comparing the Prevalence of Abnormal Kidney Function in Type 2 Diabetic Patients on SGLT2 Inhibitors versus Other Oral Antidiabetic Medications

Ben Cassellius, Annessa Mon, Zoe Plaisted, Meghan Rigby

Group 22

Explores adults with type 2 diabetes and asks whether people taking SGLT2 inhibitors have a lower prevalence of abnormal kidney function compared with people taking other oral diabetes medications. The background notes that clinical trials often show kidney-protective effects with SGLT2 inhibitors, but it is less clear how well this translates to broad population survey data where comparison groups can be very mixed. The objective is to test whether SGLT2 inhibitor use is associated with lower abnormal kidney function in NHANES 2017–2020. In the discussion and conclusion, the authors report that SGLT2 inhibitor use was not linked to a statistically significant lower prevalence of abnormal kidney function compared with other oral antidiabetic medications after limited adjustment. They note that age was the strongest predictor of abnormal kidney function, and emphasize limitations such as a small SGLT2 sample size, a heterogeneous comparison group, possible residual confounding and outcome misclassification, and not using NHANES survey weights. They conclude the results are best viewed as hypothesis-generating and that larger real-world studies with more covariates and longer follow-up are needed.

Association Between Long-Term Versus Short-Term Systemic Corticosteroid Use And Elevated HbA1c (> 5.7%)

Authors: Paige Fontes¹, Jonathan McArdle¹, Ola Omeike¹, and Anna Reilly¹
 1. PharmD Candidate 2027 University of Rhode Island College of Pharmacy

Background

Corticosteroids are widely prescribed medications used to manage a range of conditions, including asthma, chronic obstructive pulmonary disease (COPD), and other inflammatory disorders¹. Hyperglycemia is a well-established adverse effect of corticosteroid use², driven by increased insulin resistance and hepatic gluconeogenesis. Short-term therapy, which is commonly less than one month, often causes temporary elevations in blood glucose that may resolve after treatment ends, whereas long-term use, which can last many months or be chronic, may lead to more persistent metabolic changes, increasing the risk of impaired glucose tolerance and progression to diabetes. Distinguishing between short-term and long-term exposure is important because the duration of therapy may influence whether corticosteroid-related hyperglycemia is transient or contributes to sustained changes in hemoglobin A1c (HbA1c), a marker of chronic glycemic control. Despite this biological plausibility, the long-term impact of corticosteroid exposure on HbA1c across diverse patient populations remains incompletely characterized.

Objectives

To evaluate the association of higher HbA1c values ($\geq 5.7\%$) in long-term (>3 months) corticosteroid use vs short-term (<3 months) corticosteroid use, regardless of dosage form.

Methods

Data was obtained from the 2017-2020 National Health and Nutrition Examination Survey (NHANES), which includes 3 years worth of data from non-institutionalized resident populations within the United States, covering all ages. A total of 655 corticosteroid users were included; 483 long-term and 172 short-term, with HbA1c data available for 434 participants; 332 long-term and 102 short-term. Data was analyzed using SPSS. **Exposure:** Use of any of the following corticosteroids; beclomethasone; betamethasone; budesonide; dexamethasone; fluticasone; hydrocortisone; methylprednisolone; mometasone; prednisolone; prednisone; and triamcinolone.

Inclusion Criteria: Individuals living in the United States between the ages of 8 and 69 with recorded use of corticosteroids for any length of time with a recorded HbA1c value.

Exclusion Criteria: Individuals using corticosteroids without a recorded HbA1c.

Covariates: Age, gender, history of diabetes, BMI, race/ethnicity.

Outcomes:

- Primary:** HbA1c assessed as either $\geq 5.7\%$ or $< 5.7\%$ based on ADA criteria for prediabetes.
- Secondary:** BMI

Statistical Methods

- Wilcoxon Rank Sum Test: non-normal continuous variables
- Chi-Square Tests: categorical comparisons (e.g. abnormal HbA1c)
- Multivariate logistic regression: adjusted association between steroid duration and HbA1c

References

1. Jones RW, Hill G, Garmize-Harris JL, Rodriguez-Gutierrez R, Cozzani-Lopez J, et al. Systemic corticosteroids for asthma. *Cochrane Database of Systematic Reviews*. 2019;2019(12):CD012992. doi:10.1002/14651914.CD012992
2. Wilcox BJ. The risk for hyperglycemia and glucose intolerance in patients with rheumatoid arthritis. *Arthritis Rheum*. 2005;48(12):2244-2250. doi:10.1002/art.21444
3. Kivimäki M, Kivimäki M, Kivimäki M. Association between short-term corticosteroid use and risk of hyperglycemia in patients with rheumatoid arthritis. *Arthritis Rheum*. 2010;52(12):3955-3960. doi:10.1002/art.21944
4. Huh G, De Sa J, Bhatia R, et al. S. Bhatia S, Choudhry M, et al. The impact of corticosteroid treatment on HbA1c levels in patients with type 2 diabetes mellitus. *Diabetes Care*. 2014;37(12):1345-1348. doi:10.2337/1345
5. Fontes P, et al. Association of HbA1c levels and development of type 2 diabetes and prediabetes in non-diabetic rheumatoid arthritis patients. *Diabetes Care*. 2014;37(12):1345-1348. doi:10.2337/1345
6. Fontes P, et al. Association of HbA1c levels and development of type 2 diabetes and prediabetes in non-diabetic rheumatoid arthritis patients. *Diabetes Care*. 2014;37(12):1345-1348. doi:10.2337/1345

Results

Table 1: Comparing Demographic and Clinical Characteristics Between Long-Term and Short-Term Corticosteroid Exposure Groups

Characteristic	Steroid Use < 90 Days (N=172)	Steroid Use ≥ 90 Days (N=483)	P Value
Age (Years) Median (25%, 75%)	38.5 (21, 58)	55 (38, 69)	<0.001 ¹
Gender			0.989 ²
Female, N (%)	87 (50.6)	234 (50.5)	
Male, N (%)	85 (49.4)	239 (49.5)	
History of T2DM			0.127 ²
Yes, N (%)	16 (10.1)	73 (15.6)	
No, N (%)	142 (89.9)	398 (84.4)	
BMI, kg/m ² Median (25%, 75%)	28.8 (21.5, 34)	26 (20.9, 32.3)	<0.001 ¹
BMI, kg/m ² Normal/Underweight, N (%) Obese/Overweight, N (%)	81 (47.1) 91 (52.9)	246 (50.9) 237 (49.1)	0.387 ²
Family Income Median (25%, 75%)	1.9 (1, 3.9)	2 (1.2, 3.9)	< 0.001 ¹
Race / Ethnicity			0.774 ²
Mexican American, N (%)	16 (9.3)	45 (9.3)	
Other Hispanic, N (%)	14 (8.1)	39 (8.1)	
Non-Hispanic White, N (%)	79 (45.9)	204 (42.2)	
Non-Hispanic Black, N (%)	37 (21.5)	129 (26.5)	
Other Race - Including Multi-Racial, N (%)	26 (15.1)	67 (13.9)	

Table 1: ¹T2DM: Type 2 Diabetes Mellitus. 1. Wilcoxon rank-sum test; 2. Chi-square test; 3. Fisher's exact test

Table 2: Raw Comparison of Outcomes Between Two Exposure Groups

Outcomes	Steroid Use < 90 Days N=162	Steroid Use ≥ 90 Days N=332	P value
A1c, % Mean ± SD	6.2 ± (1.2)	5.8 ± (0.9)	0.134 ¹
A1c, % Abnormal, N (%) ^{**} Normal, N (%) ^{***}	56 (34.9) 96 (65.1)	159 (47.9) 173 (52.1)	0.216 ¹

Table 2: ^{*} Abnormal defined as $> 5.7\%$. ^{**} Normal defined as $< 5.7\%$. 1. Independent samples t test; 2. Chi-Squared test

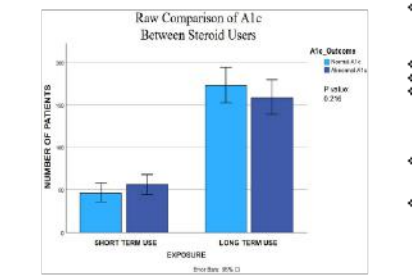


Table 3: Results of Multivariable Regression Analyses for the Risk of Abnormal HbA1c

Characteristics	Adjusted Odds Ratio	95% CI
Duration of Steroid Use Short term, Reference Long term	1 0.5	(0.3-0.9)
Waist Circumference	1.0	(1-1)
BMI Normal/Underweight ^{***} , Reference Obese/Overweight ^{**}	1 2.6	(1.6-4.3)
Age, every 10 years older	1.6	(1.4-1.8)
Gender Male, Reference Female	1 0.6	(0.4-0.9)
History of T2DM [#] No, Reference Yes	1 6.7	(3.3-13.5)
Race/Ethnicity Mexican American, reference Other Hispanic Non-Hispanic white Non-Hispanic Black Other Race - Including Multiracial	1 3.5 1.2 2.4 4.2	(0.9-13.6) (0.4-3.3) (0.8-13) (1.3-13.3)

Table 3: [#] Short term defined as < 90 days, long term defined as ≥ 90 days. ^{**} T2DM: Type 2 Diabetes Mellitus. ^{***} Normal/Underweight defined as < 25 kg/m² and Obese/Overweight defined as ≥ 25 kg/m².

Discussion/Conclusion

- Key Finding:** After adjustment long-term steroid use was associated with lower odds of abnormal HbA1c [aOR 0.5 (95% CI 0.3-0.9)].
- Interpretation:** The observed lower odds of abnormal HbA1c with long-term use may reflect confounding by indication, where patients on chronic steroids are more closely monitored or managed for glycemic control. Survivorship bias may also contribute, as patients tolerating long-term therapy may differ systematically from short-term users.
- Older age, history of T2DM, and BMI were also significant predictors of abnormal HbA1c.**
- Strengths:** This study was cost-effective, using available data from a reliable source.
- Limitations:** The cross-sectional design limits causal inference, as exposure and outcomes were measured at a single time point without capturing trends. Unmeasured confounders (such as diet and exercise habits) are unable to be adjusted for. Additionally, inclusion of a wide age range (8-69 years) may introduce heterogeneity in metabolic risk profiles, potentially affecting the interpretation of long-term effects.
- Comparison to Literature:** Findings are inconsistent with prior studies assessing HbA1c and steroid use. Difference may be due to variation in populations, steroid types, and duration definitions, as many prior studies focused on a single drug or disease state.
- Clinical Implications:** These findings highlight the importance of individualized monitoring of glycemic outcomes in patients receiving corticosteroids. Further studies are needed to evaluate the impact of long-term vs short-term use in broader patient populations.

Association Between Long-Term Versus Short-Term Systemic Corticosteroid Use And Elevated HbA1c (> 5.7%)

Paige Fontes, Jonathan McArdle, Ola Omeike, Anna Reilly

Group 23

Analyzes whether people who use systemic corticosteroids for a longer time are more likely to have an elevated HbA1c (above 5.7%), compared with people who use corticosteroids for a shorter time. The background explains that steroids can raise blood sugar, and that longer exposure could lead to more lasting effects on blood sugar control. The objective is to compare elevated HbA1c in long-term steroid users (more than 3 months) versus short-term users (less than 3 months). In the discussion and conclusion, the authors report that after adjustment, long-term steroid use was associated with lower odds of elevated HbA1c. They suggest this unexpected finding may be due to factors like closer monitoring and treatment of blood sugar in long-term users, or differences between people who remain on long-term therapy versus short-term users. They conclude that individualized monitoring of blood sugar remains important for patients on corticosteroids, and that more research is needed to better understand long-term versus short-term effects.

Evaluating Hidden Metabolic Risk: Elevated Fasting Glucose in Non-Obese Patients on Second-Generation Antipsychotics

Andrew Breneman, Emmie Parker, Julia Strife, Renee Popiel
University of Rhode Island

Background

- Second-generation antipsychotics (SGAs) are associated with clinically significant metabolic side effects, including weight gain and metabolic syndrome.
- Existing literature primarily focuses on overweight and obese populations, limiting applicability to patients with normal body mass index (BMI).
- Detection bias can occur, as hyperglycemia and metabolic abnormalities may be independent of baseline body weight. In turn, early metabolic changes may be underrecognized in lower-BMI patients, delaying intervention.
- Many real-world studies use incident diabetes as the primary endpoint, rather than assessing earlier markers (fasting glucose, HbA1c), limiting detection of early glycemic dysregulation associated with SGA use.
- Inconsistent outcome definitions (ICD-coded diagnoses, surrogate markers) further complicate interpretation.
- Together, these gaps highlight the need to better identify early glycemic changes across all BMI categories.

Objective

- The objective of the study is to compare the prevalence of elevated fasting plasma glucose (FPG) among non-obese adult patients treated with SGAs versus non-obese adults treated with SSRIs/SNRIs, in order to assess whether SGA use is associated with impaired glucose regulation independent of obesity.
- The null hypothesis is that there is no difference in the prevalence of elevated FPG in non-obese patients treated with SGAs vs those treated with SSRIs/SNRIs.

Methods

Study Design: A cross-sectional study was conducted, using a multivariable regression analysis of data from the 2017–2020 National Health and Nutrition Examination Survey. In psychiatric disorders, patients are often on either one of these drug classes, if not both. While SGAs have more data showing side effects compared to SSRIs/SNRIs, there is a lack of knowledge in effects of FPG independent of obesity in these classes of medications.

Cohort Selection: The target population is non-obese patients ages 18 and older that are being treated with a SGAs, while comparing those who are being treated with SSRIs/SNRIs. In this case, we are classifying "non-obese" as having a BMI less than 30. The comparison group will be patients taking SSRIs and SNRIs.

From our data set, SSRIs available for comparison are citalopram (Celexa), fluvoxamine (Luvox), escitalopram (Lexapro), paroxetine (Paxil), fluoxetine (Prozac) and sertraline (Zoloft). The SNRIs available are duloxetine (Cymbalta) and venlafaxine (Effexor).

Exposure Definition: The exposure will be the use of SGAs.

From our data set, the SGAs for exposure will be aripiprazole (Abilify), risperidone (Risperdal), quetiapine (Seroquel), olanzapine (Zyprexa), paliperidone (Invega), ziprasidone (Geodon) and clozapine (Clozaril).

Outcome Assessment: The outcome being measured is blood glucose, and elevations will be defined as a FPG level ≥ 5.6 mmol/L (LBDGLUS1 ≥ 5.6).

Covariates: Age, adults ≥ 18 are more likely to develop impaired FPG. They may also be more likely to receive SGAs. Psychiatric diagnosis (psych disorders can lead to poor diet, smoking, inflammation, low physical activity which could all affect glucose levels). Want to adjust for confounding to ensure association between FPG elevation is due to SGA use and not underlying illness severity.

Statistical Analysis:

- Continuous variables (e.g. fasting glucose, LDL) in Table 1 were compared between groups using independent samples t-tests, while categorical variables (e.g. sex, smoking status, hypertension) were compared using chi-square tests.
- In table 2, unadjusted outcomes were compared using independent samples t-tests (continuous glucose) and chi-square tests.
- Multivariable logistic regression was performed to evaluate the association between SGA use and abnormal FPG while controlling for potential confounders. The dependent variable was abnormal FPG (≥ 5.6 mmol/L), modeled as a binary outcome. Independent variables included medication exposure (SGA vs SSRI/SNRI) and covariates selected based on clinical relevance, including age, sex, smoking status, and hypertension. Adjusted odds ratios (aORs) with 95% confidence intervals (CIs) were calculated to estimate the strength and precision of associations. Statistical significance was assessed at $\alpha = 0.05$, with confidence intervals not crossing 1.0 considered statistically significant.

Results

Table 1. Comparing Demographic and Clinical Characteristics between Comparison Groups

Characteristic	SSRI/SNRI (n=10)	SGA (n=10)	P value
Age, mean (SD)	49.6 (21.1)	46.4 (9.1)	0.305
Female, n (%)	5 (50.0)	7 (70.0)	0.007
Female vs. Male	5 (50.0)	7 (70.0)	0.007
Smokers vs. Non-smokers	1 (10.0)	1 (10.0)	0.803
Hypertension vs. No hypertension	3 (30.0)	3 (30.0)	0.127
Weight (kg) (mean (SD))	68.4 (15.0)	68.5 (15.0)	0.987
Diabetes (yes or no) (n=10)	1 (10.0)	1 (10.0)	0.914

- Independent sample t-test
- Chi-square test
- Multivariable logistic regression

Notes: All variables are clinical characteristics. All variables were compared between groups using the statistical analyses above. Most chi-square tests were conducted using independent samples chi-square test, unless otherwise noted. The only exception being age that utilized significantly ($p = 0.005$).

Table 2. Comparing Frequencies of the Outcome Variables between Comparison Groups

Outcome	SSRI/SNRI (n=10)	SGA (n=10)	P value
Blood glucose level (mean (SD))	5.77 (1.04)	6.29 (2.07)	0.14
Blood glucose level (abnormal) (n=10)	1 (10.0%)	5 (50.0%)	0.099

Table 2 & Figure 1: Unadjusted outcomes were compared using independent samples t-tests (continuous glucose) and chi-square tests. No statistically significant differences were observed between groups for mean glucose levels ($p = 0.14$) or prevalence of abnormal blood glucose levels ($p = 0.09$).

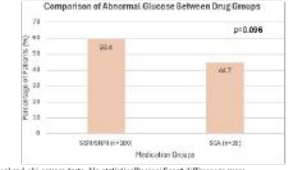
All statistical analyses were conducted using SPSS version 28 and p-values < 0.05 were considered statistically significant.

Table 3. Results of Multivariable Logistic Regression

Characteristic	Adjusted Odds Ratio	95% CI
SGA vs SSRI/SNRI	0.474	0.209-1.064
Age, every 1 year older	2.033	0.834-5.041
Female vs. Male	0.510	0.187-1.544
Smokers vs. Non-smokers	1.212	0.063-2.217
Hypertension vs. No hypertension	0.290	0.201-0.460

Multivariable logistic regression was performed to evaluate adjusted odds ratios for abnormal FPG, while controlling for age, sex, smoking, and hypertension. SGA use was not significantly associated with abnormal glucose levels (aOR 0.474, 95% CI 0.209-1.064). Female use was associated with lower odds of abnormal FPG (aOR 0.510, 95% CI 0.187-1.544), while age and smoking were not statistically significant based on the reported confidence intervals.

Figure 1. Interpreting Outcome Variables between Comparison Groups



Discussion/Conclusion

- Discussion:** Among non-obese adults in this NHANES-based analysis, SGA use was not significantly associated with elevated FPG compared with SSRI/SNRI use after adjustment for measured confounders.
- Limitations:** These findings should be interpreted cautiously given the cross-sectional design, inability to establish temporality, and potential for residual confounding from unmeasured factors such as psychiatric illness severity, diet, medication adherence, dose, and duration of therapy.
- Biological Plausibility:** The findings of this study are plausible, as the lack of significance is most likely due to the fact of limited sample size and limited exposure duration rather than the absence of a true effect. SGAs may be associated with glucose metabolism. Their mechanisms can contribute to increased insulin resistance and weight gain. They differ from previous literature, which has demonstrated an association between SGAs and increased metabolic risk. However, many previous studies included obese populations and evaluated long-term outcomes such as diabetes. This study shows that by reducing the population to non-obese individuals, the association may be less pronounced. In addition, hypertension was associated with lower odds of abnormal glucose (adjusted OR 0.290, 95% CI 0.201-0.460). This likely reflects confounding factors or differences in healthcare utilization rather than a true protective effect, as causality cannot be inferred given the cross-sectional design.
- Conclusion:** These results suggest that among non-obese individuals taking an SGA, impaired glucose regulation may not be solely driven by the medication alone. Although a statistically significant association was not observed, metabolic monitoring may still be appropriate regardless of BMI, and future longitudinal studies are needed to better define the relationship between second-generation antipsychotic exposure and hyperglycemia in non-obese patients.

References

1. Marder SR, Greenberg MR, Greenberg ME, et al. (2017) Second-generation antipsychotics and metabolic syndrome. *Journal of Clinical Psychiatry*, 78(10), 1303-1311.

2. Marder SR, Greenberg MR, Greenberg ME, et al. (2018) Second-generation antipsychotics and metabolic syndrome: A systematic review. *Journal of Clinical Psychiatry*, 79(10), 1303-1311.

3. Marder SR, Greenberg MR, Greenberg ME, et al. (2019) Second-generation antipsychotics and metabolic syndrome: A systematic review. *Journal of Clinical Psychiatry*, 80(10), 1303-1311.

4. Marder SR, Greenberg MR, Greenberg ME, et al. (2020) Second-generation antipsychotics and metabolic syndrome: A systematic review. *Journal of Clinical Psychiatry*, 81(10), 1303-1311.

5. Marder SR, Greenberg MR, Greenberg ME, et al. (2021) Second-generation antipsychotics and metabolic syndrome: A systematic review. *Journal of Clinical Psychiatry*, 82(10), 1303-1311.

Evaluating Hidden Metabolic Risk: Elevated Fasting Glucose in Non-Obese Patients on Second-Generation Antipsychotics

Andrew Breneman, Emmie Parker, Julia Strife, Renee Popiel

Group 24

Investigates whether non-obese adults taking second-generation antipsychotics (SGAs) have a higher prevalence of elevated fasting plasma glucose compared with non-obese adults taking SSRIs or SNRIs. The background explains that SGAs are known to cause metabolic side effects, but most research focuses on overweight or obese patients and often uses diabetes as the endpoint instead of earlier warning signs like fasting glucose. The objective is to see if elevated fasting glucose occurs more often in non-obese SGA users, which could indicate metabolic risk that might be missed when monitoring is based mainly on body weight. In the discussion and conclusion, the authors report that SGA use was not significantly associated with elevated fasting glucose compared with SSRI/SNRI use after adjusting for measured factors. They note the cross-sectional design, limited sample size, and possible unmeasured factors such as diet, psychiatric illness severity, medication dose and duration, and adherence. They conclude that metabolic monitoring may still be appropriate regardless of BMI, and larger longitudinal studies are needed.

Association of Angiotensin-Converting Enzyme Inhibitors vs. Angiotensin II Receptor Blockers Use With Albuminuria Among Adults with Hypertension

Sami Gangji, Nisha Kakwani, Elena Silva
The University of Rhode Island College of Pharmacy



Background

- Albuminuria is an important marker of kidney damage and is associated with progression and cardiovascular risk.^{1,2}
- Angiotensin-converting enzyme inhibitors (ACEi) and angiotensin II receptor blockers (ARBs) are widely used in hypertension management, but their comparative association with albuminuria in a broader hypertensive population remains unclear.^{3,4}
- Class-level comparisons have generally focused on effectiveness and safety outcomes rather than albuminuria as the primary endpoint, and many studies remain limited to selected high-risk populations.^{3,5}
- Prior studies largely focused on blood pressure control, cardiovascular outcomes, chronic kidney disease progression, or composite renal endpoints rather than albuminuria as a primary outcome.^{3,4,7}
- Together, these gaps support the need for a direct comparator analysis focused on albuminuria as the primary outcome in a broader hypertensive population.

Objectives

- To evaluate the association between ARB use versus ACEi use and albuminuria (urine albumin-creatinine ratio [uACR] ≥ 30 mg/g) among adults with hypertension.

Methods

- Data source: United States National Health and Nutrition Examination Survey (NHANES) from 2017 to March 2020.
- Study design: Cross-sectional analysis of adults with hypertension using prescription medication records and laboratory uACR data from NHANES.
- Study population: Adults aged ≥ 18 years with hypertension treated with either an ACEi or an ARB.
- Hypertension definition: Hypertension was identified using the medication-associated indication of primary "essential" hypertension in NHANES prescription records.
- Exposure group: ACEi users (benazepril, captopril, enalapril, enalaprilat, fosinopril, lisinopril, moexipril, perindopril, quinapril, ramipril, trandolapril).
- Comparison group: ARB users (azilsartan, candesartan, eprosartan, irbesartan, losartan, olmesartan, telmisartan, valsartan).
- Primary outcome: Albuminuria, defined as urine albumin-creatinine ratio (uACR) ≥ 30 mg/g; no albuminuria was defined as uACR < 30 mg/g. This aligns with the albuminuria definition and risk categories using 30 mg/g as a threshold.
- Covariates: Age, sex, body mass index (BMI), race, diabetes, kidney disease, smoking, and socioeconomic status.
- Statistical analysis: Pearson chi-square tests were used to compare categorical baseline characteristics and unadjusted albuminuria prevalence between groups. Multivariable logistic regression was used to estimate odds ratios (ORs) and 95% confidence intervals (CIs) for the association between medication class and albuminuria after adjustment for prespecified covariates.
- Software/significance: Analyses were conducted using SPSS version 29.0 and a p-value < 0.05 was considered statistically significant.

Results

Table 1: Demographic and Clinical Characteristics between ACE-I and ARB

Characteristics (N = 1450)	ACE-I (N = 866)	ARB (N = 584)	P-value [†]
Age, N (%)			
< 64 years	462 (53.3)	233 (39.9)	< 0.001
≥ 65 years	404 (46.7)	351 (60.1)	
Sex, N (%)			
Male	483 (55.8)	237 (40.6)	< 0.001
Female	383 (44.2)	347 (59.4)	
BMI (kg/m²), N (%)			
< 25	110 (14.0)	87 (18.4)	0.231
≥ 25	675 (86.0)	443 (88.6)	
Race, N (%)			
Non-Hispanic White	344 (39.7)	212 (36.3)	0.189
All Other	522 (60.3)	372 (63.7)	
Diabetes, N (%)			
HbA1c < 6.5	511 (65.7)	387 (75.1)	< 0.001
HbA1c ≥ 6.5	267 (34.3)	128 (24.9)	
Kidney Disease, N (%)			
Ever told had weak or failing kidneys [‡]			
No	797 (92.0)	532 (91.9)	0.918
Yes	69 (8.0)	47 (8.1)	
Smoking, N (%)			
Smoked at least 100 cigarettes/lifetime			
No	424 (49.0)	361 (61.9)	< 0.001
Yes	442 (51.0)	222 (38.1)	
Socioeconomic Status, N (%)			
Ratio of family income to poverty:			
≥ 1	607 (81.5)	409 (84.7)	0.147
< 1	138 (18.5)	74 (15.3)	

[†]††† values were derived from Pearson chi-square tests

Table 2: Comparing Frequencies of the Outcome Variables between ACE-I and ARB

Outcome (N = 1375)	ACE-I (N = 795)	ARB (N = 522)	P-value
No Albuminuria, N (%)	598 (76.2)	386 (72.6)	0.138 [†]
Normal: < 30 mg/g			
Albuminuria, N (%)			
Absnormal: ≥ 30 mg/g	187 (23.8)	146 (27.4)	

[†]The p-value was derived from Pearson chi-square test

Table 3: Results of Multivariable Logistic Regression Analysis of Factors Associated with Albuminuria

Variable	Adjusted OR	95% CI	P-value
Drug			
ACE-I	(Ref)		
ARB	1.25	0.916-1.702	0.139
Age			
64-65 years	0.64		
≥ 65 years	1.10	0.810-1.496	0.541
Sex			
Male	(Ref)		
Female	0.78	0.576-1.063	0.120
BMI (kg/m²)			
< 25	(Ref)		
≥ 25	0.80	0.526-1.203	0.278
Race			
Non-Hispanic White	(Ref)		
All Other	1.08	0.793-1.484	0.646
Diabetes (HbA1c)			
HbA1c < 6.5	(Ref)		
HbA1c ≥ 6.5	2.50	1.815-3.497	< 0.001
Kidney Disease: Ever told had weak or failing kidneys[‡]			
No	(Ref)		
Yes	4.77	3.826-7.765	< 0.001
Smoking: Smoked at least 100 cigarettes/lifetime			
No	(Ref)		
Yes	1.41	1.072-1.915	0.031
Socioeconomic Status: Ratio of family income to poverty:			
≥ 1	(Ref)		
< 1	1.67	1.148-2.429	0.007

[†]The p-value from the Pearson and Likelihood tests is 0.138

Discussion/Conclusion

- The baseline differences between treatment groups suggest confounding by patient characteristics, supporting the importance of adjusted analysis when comparing ACEi and ARB users.
- In the unadjusted analysis, ARB users had a numerically higher prevalence of albuminuria than ACEi users; however, the absolute difference was small and not statistically significant, suggesting limited evidence of a between-group difference.
- In the adjusted analysis, controlling for demographic and clinical covariates did not materially change the interpretation, as ARB use remained not significantly associated with albuminuria compared with ACEi use.
- Overall, ARB use was not significantly associated with albuminuria relative to ACEi use in this cross-sectional analysis of adults with hypertension.
- Strengths: Use of a large national dataset increasing generalizability, standardized laboratory measurement to support consistent outcome assessment, adjustment for clinically relevant covariates, and use of publicly available data as a cost-effective and reliable source for analysis.
- Limitations: Cross-sectional design does not allow assessment of causation, residual confounding may remain because variables such as eGFR and treatment duration were not available, and limited sample size may have reduced statistical power and constrained additional covariate adjustment.
- These findings are generally consistent with prior comparative literature showing similar class-level renal effectiveness outcomes between ACEi and ARBs, while extending the comparison specifically to albuminuria in a broader hypertensive population.
- Longitudinal studies are needed to further evaluate whether ACEi and ARBs differ in albuminuria progression or other renal outcomes over time.
- Additional analyses would be strengthened by data on medication dose and adherence, treatment duration, blood pressure control, eGFR/CKD stage, albumin levels, and baseline severity of albuminuria, which were not fully available in NHANES.

References

- Qiao Y, Shin J-I, Chen TK, et al. Association of Albuminuria Levels With the Prescription of Renin-Angiotensin System Blockade. *Hypertension*. 2020.
- Chiu CD, Powe NR, McCulloch CE, et al. Angiotensin-Converting Enzyme Inhibitor or Angiotensin Receptor Blocker Use Among Hypertensive US Adults With Albuminuria. *Hypertension*. 2021.
- Chen R, Suchard MA, Krumholz HM, et al. Comparative First-Line Effectiveness and Safety of ACE Inhibitors and ARBs: A Multinational Cohort Study. *Hypertension*. 2021.
- Wang K, Hu J, Luo T, et al. Effects of ACE Inhibitors and ARBs on Mortality and Renal Outcomes in Patients with Diabetes and Albuminuria: A Systematic Review and Meta-Analysis. *Kidney & Blood Pressure Research*. 2018.
- Mann JFE, Schmieder RE, McQueen M, et al. Renal outcomes with telmisartan, ramipril, or both, in people at high vascular risk (ONTARGET). *The Lancet*. 2008.

Association of Angiotensin-Converting Enzyme Inhibitors vs. Angiotensin II Receptor Blockers Use With Albuminuria Among Adults with Hypertension

Sami Gangji, Nisha Kakwani, Elena Silva

Group 25

Reviews adults with hypertension and examines whether people taking ARBs differ from people taking ACE inhibitors in how often they have albuminuria, which is a marker of kidney damage. The background explains that ACE inhibitors and ARBs are commonly used for hypertension, but direct comparisons focused on albuminuria in a broad hypertensive population are less common. The objective is to evaluate the association between ARB use versus ACE inhibitor use and albuminuria. In the discussion and conclusion, the authors report that although ARB users had a slightly higher albuminuria prevalence in the unadjusted comparison, the difference was small and not statistically significant, and the adjusted analysis did not change the interpretation. They conclude that ARB use was not significantly associated with albuminuria compared with ACE inhibitor use in this cross-sectional analysis, and that larger longitudinal studies are needed to assess changes in albuminuria and other kidney outcomes over time.

